

Univerzita Karlova

1. lékařská fakulta

Studijní program: Molekulární a buněčná biologie, genetika a virologie



UNIVERZITA KARLOVA
1. lékařská fakulta

Mgr. Pavel Horák

Regulace exprese markerů nádorových kmenových buněk (CSC) včetně epigenetických mechanismů, exprese/aktivita transkripčních faktorů GLI a cílený experimentální zásah proti CSC subpopulaci nádoru jako účinná protinádorová terapie u vybraných nádorových typů.

Regulation of expression of cancer stem cells (CSC) by epigenetic mechanisms and expression/activity of transcription factors GLI, and targeted experimental intervention against CSC tumor subpopulation as an effective anticancer therapy in selected tumor types.

Disertační práce

Školitel: doc. MUDr. Jiří Vachtenheim, CSc.

Praha, 2023

Prohlášení:

Prohlašuji, že jsem tuto závěrečnou práci sepsal samostatně a že jsem řádně odcitoval a uvedl všechny použité prameny a literaturu. Zároveň deklaruji, že práce nebyla využita k získání jiného nebo stejného titulu

Tímto také vyjadřuji souhlas s trvalým uložením elektronické verze mé práce v databázi systému meziuniverzitního projektu Theses.cz za účelem soustavné kontroly podobnosti kvalifikačních prací.

V Praze, 10.3.2024

Pavel Horák

Identifikační záznam:

HORÁK, Pavel. Regulace exprese markerů nádorových kmenových buněk (CSC) včetně epigenetických mechanismů, exprese/aktivita transkripčních faktorů GLI a cílený experimentální zásah proti CSC subpopulaci nádoru jako účinná protinádorová terapie u vybraných nádorových typů. [Regulation of expression of cancer stem cells (CSC) by epigenetic mechanisms and expression/activity of transcription factors GLI, and targeted experimental intervention against CSC tumor subpopulation as an effective anticancer therapy in selected tumor types.]. Praha, 2024, 184 stran. Disertační práce. Univerzita Karlova, 1. lékařská fakulta, Ústav Lékařské Biochemie a laboratorní diagnostiky. Školitel: doc. MUDr. Jiří Vachtenheim, CSc.

Acknowledgements

Here, I would like to express my gratitude to everyone who guided, helped, and supported me in my post gradual studies and thesis writing.

Primarily, I want to thank my tutor doc. MUDr. Jiří Vachtenheim, CSC, who gave me the opportunity to work in his laboratory, inspired me, motivated me, and helpfully guided me through my scientific journey.

Special acknowledgements also go to my lovely fiancée and to my family, who, albeit poignantly at times, kept pushing me forward. I would also like to thank to everyone, who did not disown me despite my prolonged unavailability during the pursuit of this degree.

List of Abbreviations

ABCG2	ATP-binding cassette subfamily G member 2
ALDH	Aldehyde dehydrogenase
AML	Acute myeloid leukemia
APC	Antigen-presenting cell
Apt1	Adenine phosphoribosyl transferase 1
Apt1-Lip	Apt1-conjugated liposomes
ATP	Adenosine triphosphate
BCL2	B-cell lymphoma 2
BCRP	Breast cancer resistance protein
BOC	Brother of CDO
bmi1	Polycomb complex protein BMI-1
BMP	Bone morphogenic protein
CD44ICD	CD44 intracellular domain
CDK	Cyclin-dependent kinase
CLL	Chronic lymphocytic leukemia
CSC	Cancer stem cell
CK1	Casein Kinase 1
TIL	Tumor initiating cell
DC	Dendritic cells
DFS	Disease-free survival
Dhh	Desert Hedgehog
DISP1	Dispatched RND Transporter Family Member 1
DNA	Deoxyribonucleic acid
DNMTi	DNA Methyltransferase Inhibitors
DOX	Doxycycline
EaOC	Endometriosis-associated ovarian cancer
EGFR	Epidermal growth factor receptor
EMT	Epithelial-to-mesenchymal transition
EpCAM	Epithelial cell adhesion molecule
EPR	Enhanced permeability and retention effect
ERK	Extracellular signal-regulated kinase

ESC	Epithelial stem cell
GLI	Glioma-associated oncogene
GSK-3	Glycogen Synthase Kinase-3
CTL	Cytotoxic T lymphocytes
HA	Hyaluronic acid
HCC	Hepatocellular carcinoma
HDACi	Histone Deacetylase Inhibitor
HIF	Hypoxia inducible factor
HH	Hedgehog signaling pathway
HHIP	Hedgehog-interacting protein
HSC	Hematopoietic stem cells
HSP	Heat Shock Protein
IAP	Inhibitor of apoptosis
IgG	Immunoglobulin G
iPSC	induced pluripotent stem cell
Ihh	Indian Hedgehog
ITP	Immune thrombocytopenic purpura
lncRNA	long non-coding RNA
m ⁶ A	N ⁶ -methyladenosine
mAb	Monoclonal antibody
MAPK	Mitogen-Activated Protein Kinase
MCL-1	Myeloid cell leukemia sequence 1
MDSC	myeloid-derived suppressor cell
MITF	Microphthalmia-associated transcription factor
miPSC	murine induced pluripotent stem cell
miRNA	microRNA
MM	Malignant melanoma
MSC	Mesenchymal stem cells
MSI	Musashi
NK	Natural killers
NTR	Nitroreductase
Oct4	Octamer-binding transcription factor 4
OS	Overall Survival

PDAC	Pancreatic ductal adenocarcinoma
PKA	Protein kinase A
PMM	Primary melanoma tumors
PRC1	Polycomb repressive complex 1
PTCH1	Patched1
PTEN	Phosphatase and Tensin Homolog deleted on Chromosome 10
PTM	Post-transcriptional modification
RA	Retinoic acid
RBP	RNA-binding protein
RNA	Ribonucleic acid
RSK	Ribosomal protein S6 kinase
SC	Stem cell
SCUBE	Signal peptide CUB and EGF-Like Domain-Containing Protein
SF	Melanosphere
Shh	Sonic Hedgehog
Shh-N	Shh N-terminal domain
Shh-P	Shh precursor protein
SMO	Smoothened
SOX2	SRY-box transcription factor 2
SUFU	Suppressor of Fused
SRY	Sex determining region Y gene
TGF- β	Transforming growth factor beta
TIC	Tumor initiating cells
TME	Tumor microenvironment
Tregs	regulatory T cells
UTR	Untranslated region
VT	Vertical tumor thickness
Wnt	Wingless Int-1
yCD:UPRT	yeast cytosine deaminase:uracil phosphoribosyltransferase

Abstrakt

Tato disertační práce se zabývá složitou rolí signální dráhy Hedgehog (HH) v melanomu s cílem napomoci pochopení její úlohy v melanomogenezi a jejího potenciálu jako terapeutického cíle. HH je klíčovým systémem buněčné komunikace, který reguluje různé vývojové procesy a homeostázu tkání. Odchytky v této dráze mohou vést k vývoji různých onemocnění, včetně rakovin, jako je melanom, což je agresivní a smrtelná forma kožního karcinomu, která je známá i tím, že obsahuje subpopulaci buněk známou jako rakovinné kmenové buňky (CSCs). Dle dostupných dat o CSCs se předpokládá, že významně podporují iniciaci, progresi a odolnost nádoru vůči terapii. V této práci se zaměřujeme na roli CSCs v progresi nádoru a na to, jak HH přispívá k udržení fenotypu kmenových buněk. Budou diskutovány současné analytické a terapeutické strategie zaměřené na CSCs a HH. Naše zjištění naznačují, že zaměření se na CSCs a HH signální dráhu může přinést naději pro vývoj účinných terapií pro léčbu melanomu.

Cílem práce bylo poskytnout nové poznatky o HH a jejích interakcích uvnitř buňky. Podařilo se nám identifikovat zcela nový transkripční cíl této dráhy – transkripční faktor Slug. Protein Slug je zapojen do vývoje neurální lišty a napomáhá udržování kmenového fenotypu rakovinných buněk. Zjistili jsme, jeho vnitrobuněčná koncentrace klesá při inhibici efektorových proteinů HH – transkripčních faktorů GLI – pomocí GANT61. Následně ukazujeme, že prvky signální dráhy HH jsou přítomny ve více než 50 liniích nádorových buněk.

Dále jsme ověřili platnost takzvaného “reostatového modelu” efektu MITF transkripčního faktoru na rakovinný fenotyp. V minulosti bylo dokumentováno, že vysoká koncentrace MITF se projevuje zrychlenou diferenciací a nízkou invazivitou. Naopak nízké hladiny MITF jsou provázeny pomalejší diferenciací, rychlým růstem a vysokou invazivitou. Naše data však tomuto protičeří, protože jsme zjistili opačné efekty snížení hladiny MITF. Také bylo ukázáno, že MITF přímo ovlivňuje podjednotku ligázového komplexu SCF E3 – FBXO32 a v souhře s dalšími chromatin remodelujícími komplexem hraje významnou roli v epigenetické regulaci ubikvitinace v melanomech.

Klíčová slova: Hedgehog signální dráha, Slug, CSC, marker

Abstract

This dissertation delves into the intricate role of the Hedgehog signaling pathway (HH) in melanoma, aiming to provide a comprehensive understanding of its involvement in melanomagenesis and its potential as a therapeutic target. Hedgehog signaling pathway is a crucial cellular communication system that regulates various developmental processes and tissue homeostasis. Aberrations in this pathway can lead to the development of various diseases, including cancers such as melanoma. This form of skin cancer is known to be aggressive and often deadly. It is also denoted by the presence a subpopulation of cells known as cancer stem cells (CSCs) within formed neoplasm. According to available data on CSCs, they are assumed to be crucial for tumor initiation, progression, and its resistance to therapy. In this work, we focus on the role of CSCs in tumor progression and how HH contributes to maintaining the stem cell phenotype. Current analytical and therapeutic strategies targeting CSCs and HH will be discussed. Our findings suggest that targeting CSCs and the Hedgehog pathway may hold promise for the development of effective therapies for melanoma.

We aim to provide novel insights to HH signaling pathway and its interactions within the cell. We have succeeded to identify a brand-new transcriptional target of this pathway – Slug transcription factor. Slug protein involved in development of the neural crest and maintenance of the CSC phenotype. We found out that its cellular levels decrease upon the inhibition of HH effector proteins – the GLI transcription factors – by GANT61. Furthermore, we demonstrate that elements of the HH signaling pathway are present in more than 50 cancer cell lines.

We also revisited the so-called “rheostat model” on Microphthalmia-associated transcription factor (MITF) influence on cancerous phenotype on cell lines with inducibly regulated MITF levels. In the past, it was documented that high-MITF levels are manifested by high differentiation rate and low invasiveness and the low-MITF level is associated with low differentiation and proliferation rates combined with high invasiveness. Our data disprove of this postulate as we report a contradictory effect of MITF decrease. Lastly, it was shown, that MITF directly targets a SCF E3 ligase complex subunit - FBXO32 and in concert with chromatin-remodeling complex plays a significant role in regulation of ubiquitination in melanoma cells on epigenetic level.

Key words: Hedgehog signaling pathway, Slug, CSC, marker

CONTENTS

I	INTRODUCTION	12
A	Regulation of expression of CSC markers	13
1	Cancer Stem Cells	13
2	CSC markers and their detection.....	19
3	CSC Markers and their regulation.....	26
B	Expression and activity of GLI transcription factors	34
1	Hedgehog signaling pathway	34
2	Hedgehog signaling pathway in CSC.....	40
3	Hedgehog signaling in melanoma	43
C	Therapeutic approaches against CSCs	43
1	Therapeutic interventions	43
2	GLI transcription factors as a focus of targeted experimental interference against CSC subpopulation	49
II	AIMS	51
III	METHODS.....	52
IV	RESULTS AND DISCUSSION	53
	Published research articles and author's contribution.	53
	Publication № 1	55
	Publication № 2	72
	Publication № 3	85
	Publication № 4	103
	Publication № 5	137
	Discussion of results.....	144
V	CONCLUSIONS	157
VI	REFERENCES	158
VII	APPENDIX	176

PERMISSIONS TO REPRINT PUBLICATIONS	176
Publication I:	176
Publication II:	178
Publication III:	180
Publication IV:	181
Publication V:	183

I INTRODUCTION

CSCs are a small subpopulation of cells within a tumor with the ability to self-renew and differentiate into various cell types found in the tumor (Clarke et al. 2006). They are thought to be responsible for initiating and driving tumor growth, metastasis, and resistance to conventional cancer treatments. CSCs are also characterized by their capacity to regenerate the tumor and are believed to lay foundation to their ability to act as a driving force of the progressive cancerous phenotype. (Wicha 2006).

Stem cells, in general, are defined as undifferentiated cells that are capable of proliferation and self-renewal. They also have the capacity to generate more than one type of cell within the body (Chagastelles and Nardi, 2011). Healthy stem cells are often found in a dormant state, resting inactive. As such, they are less susceptible to mutations and cellular damage, differentiating them from CSCs (Sottocornola and Lo Celso, 2012).

One of the characteristics that distinguishes CSCs from other cells is expression of a specific subset of markers on their surface. These markers are now pivotal in oncology research because they assist in the identification and isolation of CSCs. Commonly acknowledged CSC markers include CD44, CD133, and ALDH1, among others, and the rate of their expression fluctuates depending on the type of cancer (Walcher et al., 2020). Detection of these markers involves techniques such as flow cytometry, immunohistochemistry, and quantitative real-time PCR. Understanding the regulation of these markers is essential as it offers insights into the maintenance and survival of CSCs. The regulatory mechanisms involve intricate networks of genetic and epigenetic modifications, signaling pathways, and interactions with the tumor microenvironment. Targeting the regulation of these markers can provide therapeutic avenues to potentially eradicate CSCs, thereby improving cancer treatment outcomes (Walcher et al., 2020).

There is still an ongoing discussion regarding the validity of the CSC model. Some researchers question whether CSCs are truly a distinct subpopulation or a mere result of the tumor's microenvironment (Monroe et al., 2011). Opposed to the CSC model is the stochastic model (Metz et al., 1995). In this context, "stochastic" means random or probabilistic. This model accounts for the inherent randomness in biological processes (Wang et al, 2014). Tumor growth is a complex process influenced by numerous factors including cell proliferation, death rates, nutrient supply, and interactions with the immune system and stochastic model of its development is based around the theory, that any cell within a tumor has the potential to gain capacities to contribute to tumor growth and progression, depending on random genetic

mutations and environmental interactions. These are gained through at least one, but rather multiple DNA-altering events. These events and subsequent incorporation of the result into the genome, a mutation, might happen in any cell in the body, creating cancer stemness (Wang et al, 2014). This allows for any cancer to gain the ability of self-renewal and subsequently differentiate into multiple, heterogenous lineages co-existing within the tumor (Kreso and Dick., 2014).

A REGULATION OF EXPRESSION OF CSC MARKERS

1 Cancer Stem Cells

Cancer stem cells were identified for the first time by John Dick in the late 1990s. During his experiment, Dick reported observation of cells that were the foundation of three types of leukemia. He isolated leukemia cells that expressed CD34 surface marker, but not CD38. The resulting subset of cells was xenografted into NOD/SCID mice. Provided the donor and acceptor mice were histologically akin, these grafts were shown to induce tumor growth (Bonnet, 1997). This finding was later developed into the “cancer stem cell hypothesis”. It was later shown that CD34+/CD38- phenotype is similar to the human hematopoietic progenitor. This discovery led to formulation of the idea that leukemic stem cells originated either from an initial stem cell, or not fully differentiated progenitor. Further experiments analyzing various kinds of tissue, proved existence of cells that mimicked this behavior, described as self-renewal capacities and the ability to give rise to every other type of cell within the tumor, maintaining the high rate of neoplasm build up. These cells are also specific by their lengthy cell cycle, compared to the rest of the tumor cells. This novel point of view separated cellular population in the tumor into two subsets, which were then arranged into a hierarchy, in which the stem cell is the facilitator of both the formation and the expansion of cancer (Baker, 2009) and tumor cell is a fast dividing and proliferating mass of the tumor. In that time, this was considered a ground-breaking discovery (Baker, 2009).

The credibility of existence of CSCs was later further supported with finding of a clonogenic, sphere-forming adult human brain glioma cell (Ignatova, 2002). Then, adult human glioma CSCs were able to induce tumor like the parent one, when grafted into nude mice cranium (Wang, 2015). This theory also explains the ineffectiveness of conventional tumor therapies as they mostly target fast dividing cells, and do not present much of an interference for slowly dividing CSCs. This therapy eradicates the mass of fast proliferating cells, but the CSC population often remains viable and causes a relapse of the tumor (Clarke et al. 2006).

The identification and isolation of CSCs often rely on functional assays that assess their ability to form tumors when transplanted into immunodeficient mice. These assays help confirm the stem cell-like properties of these cells (Walcher et al., 2020).

CSCs differentiate into various cell types found within the tumor, which then becomes quite heterogeneous, containing both CSCs and non-CSCs. Heterogeneity in tumors amplifies over time as CSCs acquire more genetic or epigenetic alterations over time. Within the tumor microenvironment, CSCs presence leads to an uncontrolled formation of DNA mutation prone neoplasm. (Plaks et al., 2015)

CSCs are thought to be responsible for tumor initiation and maintenance. Non-CSCs make up the bulk of the tumor and do not possess the same self-renewal and tumorigenic properties. They have been linked to specific types of cancer, including acute myeloid leukemia, breast cancer, and central nervous system tumors. It was also proposed that cancer stem cells may play a specific role in tumor metastasis (Oskarsson et al., 2014).

Tumor cells are also able to undergo molecular and phenotypic changes during cancer progression, known as cellular plasticity. These changes can result from various factors, including microenvironmental cues, genetic and epigenetic alterations, and selective pressures from treatments. These alterations allow CSCs to differentiate into various cell types, contributing to the diversity of cells within the tumor. Recent research has revealed multiple other examples of cellular plasticity in cancer, each with its functional consequences (Thankamony et al., 2020). Historically, phenotypic plasticity in adult somatic cells has been associated with dedifferentiation and transdifferentiation, primarily in the context of tissue regeneration and wound healing. Dedifferentiation, a component of phenotypic plasticity, is essential for tissue repair and maintaining stemness but can also pose a risk of cancer initiation. Phenotypic plasticity represents a new paradigm for comprehending various aspects of cancer, including its initiation, progression, and resistance to therapeutic interventions (Thankamony et al., 2020).

Other cellular plasticity-related programs can involve changes in cell phenotype, behavior, and response to therapy. One of the examples is Epithelial-Mesenchymal Transition (EMT). EMT is a well-known manifestation of cellular plasticity in cancer. It involves transitions between epithelial and mesenchymal states and can contribute to tumor aggressiveness and metastasis. Understanding and targeting cellular plasticity holds promise for developing novel anticancer treatments. Strategies that inhibit or manipulate plasticity programs could enhance the effectiveness of therapies and reduce resistance (Wang et al., 2014).

1. Stem cell model

There are currently two models that are considered relevant in regard of description of tumor growth and heterogeneity. The former model, called the stochastic model is based on premise that all the tumor cells are equipotent, and it is through their random interactions that differentiation is achieved (Metz et al., 1995). This means that all the cells are collectively responsible for the tumor growth (Beck and Blanpain, 2013).

On the other hand, according to the CSC model, a small percentage of tumor cells, the CSCs, are responsible for the upkeep the tumor progression. Although the resulting cell lineages usually lack the self-renewal capacity, the result of extensive proliferation is that they make up most of the mass of the tumor (Shackleton et al., 2009). In this scenario, the selective clones compound genetic alterations both on primary structure and epigenetic levels. If these mutations

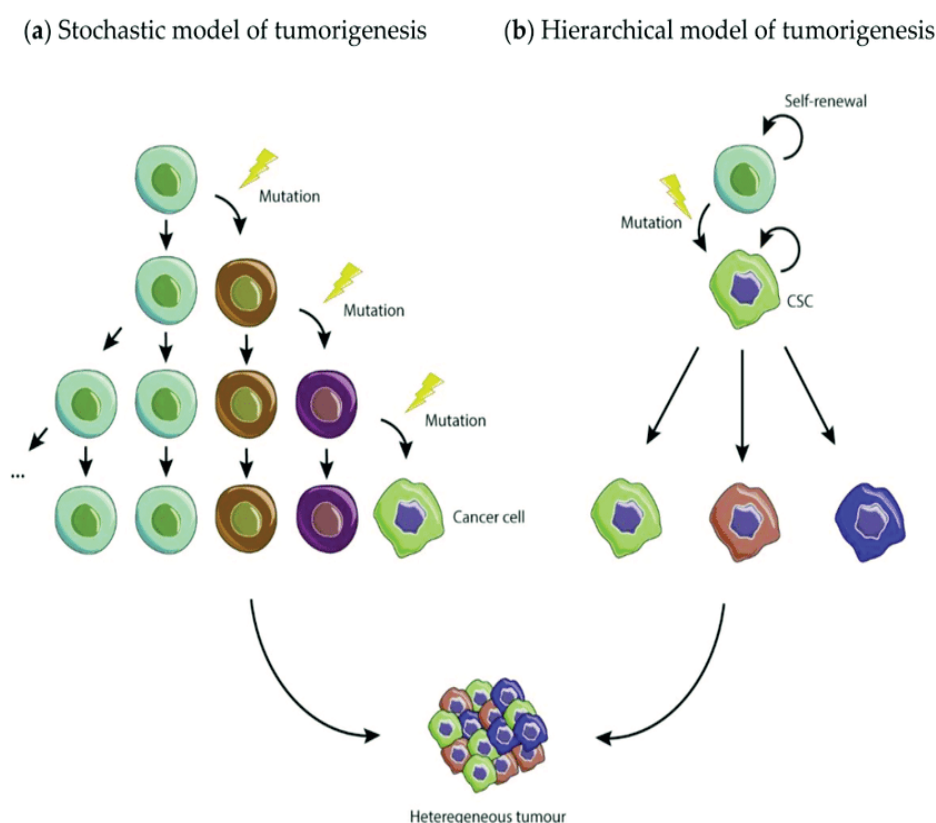


Figure 1 *Stochastic and hierarchical models of carcinogenesis*

(a) According to the stochastic model, all cancer cells have equal ability to initiate tumors and their evolution depends exclusively on stochastic influences. (b) The hierarchical model postulates that cancer stem cells (CSCs) are the only ones able to initiate, maintain and seed new tumors. (Carvalho et al., 2021, licensed under Creative Commons Attribution license (<http://creativecommons.org/licenses/by/4.0/>))

provide improvements of clone's "fitness" this might lead to a formation of a strong subpopulation (Greaves and Maley, 2012).

The abundance of tumor activity, which is on a steady rise for decades now, which does not correlate with a constant, relatively low occurrence of stem cells within an organism. Although this might be ascribed to the CSCs long lifespan and slow cell cycle, allowing the cumulation of mutations (Rajaraman et al., 2006), this suggests that there is supposedly a superposition of multiple modes of tumor origin, including one that initiates from fully differentiated, non-stem cell. These are, however, thought to be less aggressive tumors, which tend to be more responsive to conventional treatment (Martens et al., 2014).

2. Birth of cancer stem cell as a part of cancer onset

Various hypotheses have been proposed to explain the origin of CSCs, including events occurring in both stem cells and differentiated cells. These events may involve factors such as genomic instability, inflammatory microenvironments, cell fusion, and lateral gene transfer. Epigenetic changes and deregulation are key factors in the acquisition of CSC features, both in tumor initiation and maintenance. Epigenetic modifications can favor the transition of cancer cells into CSCs. Additionally, nontumorigenic cancer cells can dedifferentiate into CSCs, further contributing to tumor heterogeneity. However, the precise origin remains unclear. Various signaling pathways are implicated in the formation and maintenance of CSCs. These pathways can be influenced by external factors and contribute to CSC generation (Walcher et al., 2020).

The CSC tumor origin was observed during studies performed on epithelial SCs. Wnt pathway-induced tumor activity was correlated with the detection of myoepithelial and luminal cell markers, indicating that they are modified SCs. Contrarily, these epithelial markers are not found in tumors that are created by Neu, or H-Ras mutations. This is in accordance with the discovery of an increase of CD24⁺CD29^{hi} stem cell population in Wnt-1 transgene mice, not in Neu transgene mice. (Lynch et al., 2006).

A cell lineage hierarchy would be most of the time comprised of a limited number of spontaneously dividing pluripotent SCs, rapidly proliferating progenitor cells and lastly of terminally differentiated cells that have entered their postmitotic phase. This hierarchy ensures that any progenitor genetic mutation is eradicated from the tissue, as these cells do not possess self-renewal capacities. This suggests that most tumor-inducing mutations happen within a SC, rather than progenitor cell, although the latter case was also identified. (Jordan et al., 2006)

There are, however, theories that describe an event of tumorigenesis given rise from a progenitor cell. This might happen due to compounding progenitor mutations, which alter its genome to the extent that it is able to perform self-renewal. Or due to fact that the progenitor

cell contained a cancer predisposition inherited from its parent stem cell. This predisposition is then unleashed by subsequent mutation. As is the case of Acute myeloid leukemia (AML) M3, which is based off a progenitor cell, that regained the ability to self-renew via the expression of a fusion protein PML/RAR α (Lynch et al., 2006). This distinguishes this type of AML from the other ones, which are thought to be of a CSC origin. Last mode of incorporating a mutation through progenitor genotype is progenitor dedifferentiation to a SC. This phenomenon was observed in breast tissue during a repeated pregnancy, when differentiated cells that had been created during the first pregnancy regained their self-renewal abilities and the ability to differentiate into alveolar cells during the subsequent pregnancy. These dedifferentiated cells were observed to give rise to tumors in transgene mice. (Lynch et al., 2006)

3. *The Niche element*

Stem cell niches, or microenvironments are specialized surroundings found in adult somatic tissues. They provide essential signals to maintain normal stem cells and prevent tumorigenesis. These signals include both inhibitory and proliferative cues, which help regulate the balance between stem cell maintenance and tissue regeneration (Oskarsson et al., 2014).

A tumor microenvironment (TME) is the complex cellular and non-cellular milieu surrounding cancer cells. It consists of various cell types, extracellular matrix components, vesicles and signaling molecules. The TME plays a pivotal role in tumor progression and therapy response. Recent data suggest that targeting CSCs alone may not be sufficient for effective cancer therapy, especially in high-grade cancers. Instead, strategies that aim to disrupt the interplay between CSCs and the TME are proposed for achieving durable remission (Plaks et al., 2015).

Normal, healthy stem cells also rely on signals from their niches for regulation. The molecular mechanisms that normal stem cells use to interact with and respond to their niches can be exploited by cancer stem cells for invasion and metastasis. This hijacking of the niche machinery may facilitate cancer progression. Cancer stem cells that might arise through intrinsic mutations that result in self-sufficient proliferation, but also through alterations in the niche, such as the dominance of proliferation-promoting signals, may also contribute to the development of cancer stem cells (Hicks and Pyle, 2023).

Loss of the niche can lead to the loss of the respective stem cells, highlighting the dependence of these cells on niche signals. The interplay between CSCs and the TME is bidirectional and dynamic. The TME can influence the properties and behavior of CSCs, and CSCs can, in turn, shape the TME. This communication is partly mediated through the means

of exosomes. Exosomes, a type of extracellular vesicle, participate in cell-cell communication by transmitting signaling molecules, including proteins, nucleic acids, and lipids. They play critical roles in both physiological and pathological processes. This interaction contributes to tumor growth and therapeutic resistance (Kreso and Dick, 2014).

Scientists suspect the existence of a dynamic equilibrium between cancer stem cells and other cancer cells within the TME. This equilibrium suggests that targeting the transformation of cancer stem cells and cancer cells, rather than solely focusing on cancer stem cells, may be a more effective therapeutic strategy than conventional therapy. Exosomes engage in regulating the transformation of cancer cells within the dynamic equilibrium of cancer stem cells and other cancer cells. This marks them as a potential therapeutic target since their inhibition could potentially disrupt the formation of cancer stem cells (Cabarcas et al., 2011).

As was mentioned earlier tumors are not uniform masses of cells; instead, they exhibit dynamic heterogeneity. The cells at the tumor edge are described as more quiescent (less actively dividing), invasive (with the ability to spread to surrounding tissues), and resistant (less responsive to treatment). These features can make them challenging to target with therapies. In contrast, cells in the core of the tumor exhibit higher rates of proliferation (cell division), leading to increased cellular density. This increased rate contributes to the neoplasm growth of the tumor (Eun et al., 2017).

Hypoxia, or low oxygen levels, is a significant factor highlighting the difference between the two groups. Tumor growth often outpaces the ability of blood vessels to supply oxygen to all cells, leading to hypoxic regions within the tumor. Hypoxia-inducible factors (HIFs), including HIF-1 α and HIF-2 α , are proteins that play a leading role in cellular responses to low oxygen levels. Targeting these factors may hold promise for high-stage tumors, as they are associated with adaptation to hypoxic conditions. Combining therapies that target both HIF-1 α and HIF-2 α represents a potential strategy to address high-stage tumors. However, this hypothesis requires further research and validation to determine its efficacy and safety (Yun and Lin, 2013).

As our knowledge on CSCs deepened, it became increasingly apparent, that to establish a “prosperous” tumor lineage, its microenvironment must be regulated. It was then discovered that the tumor is comprised of a variety of stroma cells, like fibroblasts, vascular endothelial cells, or inflammation components. The presence of these cell types initially evaded scientific interest, but recently it was shown that their occurrence lays foundation for the niche and thus plays a vital role in tumor development. The importance of this niche foundation is now widely recognized. The niche provides a favorable environment for diffusion of specific factors, which

coordinate the disproportionation of life force put into self-renewal, differentiation and cellular junctions' construction. The existence of the niche microenvironment was further solidified, when it was discovered that niche cells, unlike the CSC, are responsible for the production of a differentiation factor BMP antagonist, Gremlin1 and thus preventing the differentiation of the SCs (Sneddon and Werb, 2007).

2 CSC markers and their detection

Various cell surface and enzymatic markers have been identified and characterized to help identify and isolate CSCs within the heterogeneous tumor cell population. Specific cell surface markers have been associated with CSCs in distinct types of cancer. For example, CD44, CD47, CD133, aldehyde dehydrogenases, EpCAM (Epithelial cell adhesion molecule), ATP-binding cassette subfamily G member 2, SOX2 (SRY-box transcription factor 2), or Nestin are commonly used markers. However, the markers can vary among different cancer types and even within the same cancer type (Walcher et al., 2020, Zhao et al., 2017)).

Many of the surface markers used to identify CSCs are derived from healthy stem cells, including human embryonic stem cells (hESCs) and adult stem cells. These markers are believed to be associated with self-renewal and tumorigenic potential. To properly decipher the code of cancer developments, it is essential to understanding their expression patterns in different cell types (Valent et al.,2019).

Approximately 70% of current CSC surface markers are also found on embryonic or adult stem cells. Especially the surface markers on hESCs serve as an attractive source for finding novel surface markers on CSCs. These markers may play a role in CSC identification and targeted therapies. Either of these Stem cell markers are rarely expressed on normal tissue cells (Monk and Holding, 2001).

Some CSC surface markers are expressed even in normal tissue cells. However, they have been extensively validated as specific CSC markers by research groups (Walcher et al., 2020).

CD44

CD44 is a cell surface glycoprotein that binds to hyaluronic acid (HA) and is found to be overexpressed in nearly all tumors of epithelial origin. Its significance lies in its involvement in tumor initiation and metastasis, making it a valuable marker for cancer stem cells in various solid malignancies. Moreover, the interaction between hyaluronic acid and CD44 can activate

pathways mediated by the epidermal growth factor receptor (EGFR), which contributes to tumor cell growth, migration, and resistance to chemotherapy in solid cancers. Research has shown that specific CD44 isoforms are particularly involved in the signaling pathways associated with HA-CD44 interactions, but the choice of isoform appears to depend on the type of tumor cells and the stage of cancer progression. CD44 is in the scope of scientists regarding the development of a potential drug delivery system for targeting cancer cells that overexpress marker, which is commonly found in various cancers, including colon, breast, pancreas, and head and neck cancers (Wang et al., 2017).

The actual cell type determines the CD44 isoform. For example, the cleaved intracellular domain (CD44ICD) is involved in regulating mammosphere formation and cancer stemness characteristics in breast cancer cells. The research found that CD44ICD plays an active role in regulating mammosphere formation, which is associated with cancer stem cells. The cleavage of CD44ICD is mediated by γ -secretase, allowing its translocation into the nucleus, where it regulates transcriptional activation through factors such as CBP/p300 and STAT3. CD44ICD was found to share characteristics with other stemness factors, like Nanog, Sox2, and Oct4, in maintaining pluripotency and preventing differentiation in stem cells (Weng et al., 2019).

Furthermore, the findings suggest that targeting CD44, particularly its cleaved intracellular domain, could have therapeutic potential in breast cancer treatment. Inhibition of the cleavage of CD44ICD, using for example γ -secretase inhibitors, could be explored as a strategy to target cancer stem cells (Weng et al., 2019).

Another study utilized a specific RNA aptamer called Apt1, which had previously been selected against CD44. Aptamers are single-stranded DNA or RNA molecules that can bind to specific target molecules with high affinity and specificity. Apt1 was successfully conjugated to the surface of PEGylated liposomes using the thiol-maleimide click reaction. This conjugation allowed Apt1 to attach to the liposome surface. The successful conjugation of Apt1 to liposomes was confirmed through several methods, including changes in liposome size and zeta potential, as well as migration in agarose gel electrophoresis. The binding affinity of Apt1 was found to be improved after conjugation to liposomes compared to free Apt1. This suggests that the conjugation process enhanced the ability of Apt1 to bind to its target, CD44. The study evaluated the cellular uptake of Apt1-conjugated liposomes (Apt1-Lip) using CD44-positive cell lines, such as human lung cancer cells (A549) and human breast cancer cells (MDA-MB-231), as well as a CD44-negative cell line, mouse embryonic fibroblast cells (NIH/3T3). The results demonstrated that Apt1-Lip exhibited higher sensitivity and selectivity for CD44-expressing cancer cells compared to blank liposomes (Mal-Lip). The findings suggest

that Apt1-Lip has the potential to serve as a specific drug delivery system for targeting CD44-expressing cancer cells. This approach could potentially improve the precision and effectiveness of cancer treatments by delivering therapeutic agents directly to cancer cells while minimizing damage to healthy tissues (Wei et al., 2022).

In conclusion, the successful conjugation of an anti-CD44 aptamer to the surface of liposomes holds promise as a potential strategy for targeted drug delivery in cancer therapy (Wei et al., 2022).

CD44 has also been implicated in the progression and metastasis of malignant melanoma (MM). In animal models, MM cell lines expressing high levels of CD44 have shown an increased capacity for hematogenous metastasis compared to those with low CD44 levels. Relation between the level of CD44 expressed by primary melanoma tumors (PMM) to their metastatic potential in vivo was assessed in a study conducted on 92 patients categorized by their metastatic risk based on the vertical tumor thickness (VT). Population was low-risk PMM ($VT \leq 0.7$ mm), intermediate-risk PMM ($VT = 0.71-1.4$ mm), and high-risk PMM ($VT > 1.4$ mm). Immunohistochemical staining with a panCD44 monoclonal antibody was used to analyze CD44 expression on PMM. The level of CD44 expression was assessed semi-quantitatively, using epidermal CD44 staining as an internal standard. Results showed that elevated levels of CD44 were detected in 58.3% of high-risk PMM, 40.6% of intermediate-risk PMM, 36.7% of low-risk PMM, and 16.7% of in situ PMM. 74% of patients who developed and/or died from MM metastasis had high CD44 expression, including some patients initially considered to have low metastatic risk based on VT measurements. Subsequent Kaplan-Meier analysis demonstrated that patients with high CD44 expression on PMM had a significantly reduced 5-year survival rate compared to those with low CD44 expression. In this patient population, high CD44 expression on PMM was associated with an increased risk of metastasis and reduced survival. These findings suggest that CD44 expression levels could serve as a useful indicator for assessing the metastatic potential and prognosis of malignant melanoma (Dietrich et al., 1997).

CD47

Integrin-associated protein, also known as CD47, is a widely expressed protein in the body. It plays several important roles, including stimulating T cells, aiding in the movement of white blood cells, and inhibiting the function of scavenger cells called macrophages. Macrophages play a crucial role in clearing pathogens and damaged or aging cells from the bloodstream through a process called phagocytosis. A key player in this process is a cell-surface

protein called CD47, which interacts with its receptor on macrophages, known as SIRP α , to prevent the phagocytosis of normal and healthy cells. The interaction between CD47, a protein on target cells, and the inhibitory receptor SIRP α on macrophages serves to prevent macrophage-mediated phagocytosis of host cells that express CD47 (Lian et al., 2019). This mechanism has implications for the regulation of platelet turnover and the clearance of platelets in a condition called immune thrombocytopenic purpura (ITP). Researchers conducted experiments in CD47 knockout (CD47^{-/-}) mice and found that these mice experienced mild spontaneous thrombocytopenia, a condition characterized by low platelet levels. Interestingly, the reduced platelet counts in CD47^{-/-} mice was not due to a decrease in platelet lifespan but rather related to increased expression of specific markers on the platelet surface, including P-selectin, CD61, and phosphatidylserine. When CD47^{-/-} platelets were transfused into CD47^{+/+} (normal) recipients, they were rapidly cleared from the circulation. However, CD47^{+/-} platelets, which have one functional CD47 allele, had a nearly normal lifespan in CD47^{+/+} mice under nonautoimmune conditions (Kaur et al., 2020; Lian et al., 2019).

In the context of ITP, CD47^{-/-} mice were more susceptible to the condition compared to CD47^{+/+} mice. In laboratory experiments, it was observed that macrophage phagocytosis of CD47^{-/-} platelets, which were opsonized with immunoglobulin G (IgG), was significantly higher than that of equally opsonized CD47^{+/+} platelets. However, when SIRP α , the receptor for CD47 on macrophages, was blocked, the phagocytosis of CD47^{+/+} platelets increased to a level like that of CD47^{-/-} platelets. Additionally, CD47^{+/-} platelets exhibited intermediate levels of phagocytosis compared to CD47^{+/+} and CD47^{-/-} platelets, suggesting a gene-dose effect of CD47 in this system (Willingham et al., 2012).

The level of CD47 expression appears to be a crucial indicator for determining whether immune cells will survive or be eliminated by the body's immune system. Comparison of the effects of T cells with normal CD47 levels (CD47^{+/+}) to those lacking CD47 (CD47^{-/-}) when transplanted into recipients with differing immune conditions. The results showed that CD47^{-/-} T cells significantly reduced the lethality of graft-versus-host disease, a condition where the transplanted immune cells attack the host. Interestingly, CD47^{-/-} T cells had difficulty engrafting in immunodeficient recipients. Similarly, CD47^{-/-} marrow cells could not effectively reconstitute the immune systems of heavily irradiated recipients. These findings suggested that CD47^{-/-} T cells and marrow cells were being eliminated by the innate immune system. This was confirmed when researchers labeled CD47^{-/-} and CD47^{+/+} immune cells and marrow cells with a dye and then tracked their clearance in vivo. They found that CD47^{-/-} cells were rapidly engulfed and cleared by splenic dendritic cells and macrophages, leading to the elimination of

nearly all CD47^{-/-} immune cells within one day after infusion. In contrast, when phagocytes (cells that engulf and digest other cells) were depleted in CD47^{+/+} recipients, they were more accepting of transplanted CD47^{-/-} T cells. This suggests that dendritic cells and macrophages play a critical role in clearing lymphohematopoietic cells that have reduced CD47 levels (Caras, 2020).

Another study suggests that CD47 may serve as a valuable surface marker in endometriosis-associated ovarian cancer (EAOC). Endometriosis is a condition that is known to increase the risk of developing ovarian carcinoma, particularly clear cell and endometrioid malignancies. The exact mechanism through which EAOC evades the body's immune surveillance by macrophages is not very well understood. However, CD47 is an important immune checkpoint that plays a role in preventing macrophage-mediated phagocytosis. Additionally, targeting CD47 could offer a novel therapeutic approach for the treatment of ovarian cancer. A study was conducted involving 36 clinical ovarian samples. The researchers assessed the expression of the CD47 protein using immunohistochemistry and analyzed its correlation with clinical and pathological features using statistical analysis. The study found that CD47 expression was notably higher in patients with EAOC compared to a normal control group. High CD47 expression was positively and significantly associated with specific histological characteristics ($P = 0.007$) and tumor grade ($P = 0.002$). Furthermore, the study explored the functional role of CD47 in cancer progression. It was discovered that the overexpression of CD47 promoted cancer cell growth and motility in the TOV-112D and TOV-21G cell lines. Conversely, when CD47 was silenced or targeted with anti-CD47 monoclonal antibodies (mAb), it inhibited cancer cell growth and motility in these cell lines (Luo et al., 2023).

The upregulation of CD47 is a critical mechanism that protects normal hematopoietic stem cells (HSCs) during inflammation-induced mobilization. Leukemic progenitor cells exploit this mechanism to evade destruction by macrophages, highlighting the significance of CD47 in the context of immune response and disease progression. Research has revealed that when certain cytokines and inflammatory stimuli are present, CD47 levels are temporarily increased on HSCs and their progenitors in mice. This upregulation occurs just before and during their migratory phase. Importantly, the level of CD47 on these cells influences the likelihood of them being engulfed by macrophages *in vivo*. Furthermore, CD47 is consistently upregulated on both mouse and human myeloid leukemias. When CD47 is overexpressed on a myeloid leukemia cell line, it enhances the disease's pathogenicity by allowing it to evade macrophage-mediated phagocytosis (Jaiswal et al., 2009).

CD133

CD133 (also labeled prominin-1), originally associated with hematopoietic precursor cells, has been found on the surface of various adult tissue cells, both epithelial and non-epithelial. In the context of solid tumors, including breast cancer, CD133 has garnered attention as a surface marker associated with CSCs. However, the significance of CD133 in breast cancer remains a subject of limited and sometimes conflicting research. Breast cancer is the most common malignancy among women in developed countries, making understanding CD133's role in this context crucial (Glumac and LeBeau, 2018).

In a study performed *in vitro* on a mouse model, the presence of neural CD133+Nestin+ cells, which are thought to harbor CSCs, is correlated with proximity of special type of endothelial cells that excrete factors responsible for self-renewal maintenance and differentiation reduction. (Neradil and Veselska, 2015)

Aldehyde dehydrogenase

ALDHs are a superfamily of enzymes that detoxify a variety of endogenous and exogenous aldehydes. They are also required for the biosynthesis of retinoic acid (RA) and other molecular regulators of cellular function. This detoxification role is essential for protecting cells from harmful substances, contributing to the survival and resilience of CSCs (Clark and Palle, 2016).

The ALDH family consists of 19 isozymes, each playing a role in the oxidation of aldehydes to carboxylic acids. ALDH enzymes have been identified as robust CSC markers in gynecologic and other types of malignancies. ALDHs are crucial for the maintenance and differentiation of stem cells, as well as for normal development. They are involved in vital biological processes and contribute to cellular and tissue homeostasis. There is growing evidence that ALDH expression increases in response to cancer therapy. This increase in expression is associated with the promotion of chemoresistance and survival mechanisms in CSCs, making it a challenging aspect of cancer treatment. Specifically, the ALDH1A1 enzyme has emerged as a useful therapeutic target in CSCs, especially in tissue types that normally do not express high levels of ALDH1A1. These tissue types include breast, lung, esophagus, colon, and stomach cancers (Toledo-Guzmán et al., 2019).

Epithelial cellular adhesion molecule

EpCAM is recognized for its significant role in cancer biology, particularly as a marker for CSCs. Recent research has made significant strides in understanding the structure, molecular functions, pathophysiological mechanisms, and clinical applications of EpCAM in cancer. This encompasses its role in cell adhesion, proliferation, and signaling in cancer cells. EpCAM expression is not exclusive to CSCs; however, its frequent expression in CSCs from cancers like breast, colon, pancreas, and prostate is noteworthy. This broad expression profile underscores the importance of EpCAM in different cancer types and stages (Gires et al., 2009).

In liver cancer cell lines, cells expressing EpCAM showed higher levels of certain proteins like ERK, RSK, and PEP-CTERM system histidine kinase, which are associated with cancer progression. This suggests a potential link between EpCAM expression and enhanced pro-oncogenic activities in these cells (Yamashita et al., 2013).

In primary hepatocellular carcinoma (HCC), EpCAM and CD90 are independently expressed. Gene-expression analysis indicated that EpCAM-positive cells had characteristics of epithelial cells, while CD90-positive cells resembled vascular endothelial cells. This finding highlights the distinct roles these markers play in liver cancer (Sun et al., 2016).

ATP-binding cassette subfamily G member 2

The ABCG2 plays a significant role in cancer biology, particularly as a marker for CSCs. ABCG2 serves as a key marker for CSCs in various cancers, contributing significantly to drug resistance mechanisms. Its role in different types of cancers, especially in lung and pancreatic cancers, makes it a vital focus in cancer research and treatment strategies. The ongoing research into its specific functions and mechanisms in different cancer types highlights the complexity and importance of this protein in oncology. ABCG2 is noted for its role in chemotherapy drugs efflux out of the cell, a characteristic of CSCs. This feature is utilized in selecting CSCs by flow cytometry, where side population cells that rapidly efflux DNA-binding fluorescent dyes are isolated. The widespread expression of ABCG2 in various cancers highlights its potential as a therapeutic target, especially in combating drug resistance (Ding et al., 2010).

ABCG2 expression is linked to tumorigenic CSCs in several types of cancers. However, its specific effects on CSC-related malignant characteristics in pancreatic ductal adenocarcinoma (PDAC) are still being explored. This indicates an ongoing effort to understand the complete role of ABCG2 in the context of different cancers (Sasaki et al., 2018).

Nestin

Nestin, a class VI intermediate filament protein, has been identified as a significant marker in the study of CSCs. Recent research has focused on understanding nestin expression in CSCs, particularly regarding its role in CSC phenotypes. This includes its potential involvement in the self-renewal capacity of CSCs, which is a hallmark trait of these cells. Such studies aim to elucidate the utility of nestin as a putative marker for identifying and characterizing CSCs in various malignancies (Neradil and Veselska, 2015).

Originally detected in neural stem cells during development, nestin has expanded its significance in the field of cancer research. Its crucial role in the pathology of malignant diseases, especially as a marker of CSCs, has been extensively studied over the past decade. This highlights the evolving understanding of nestin from a neural-specific marker to one that is broadly relevant in cancer biology (Zhao et al., 2017).

In addition to its role in CSCs, nestin is a specific marker of neural stem/progenitor cells. This indicates its relevance not only in cancer but also in developmental biology and neurobiology. Embryonic nestin-positive cells have the capability to differentiate into neurons and glial cells, underscoring its role in the nervous system's development (Macas et al., 2014).

Studies have also investigated the clinical value of nestin, especially in conjunction with other CSC markers like CD133. In the context of glioma, research has focused on determining the prognostic value of nestin, either independently or in combination with other markers. Such studies aim to integrate CSC markers like nestin into clinical decision-making processes, particularly in prognostic evaluations (Jin et al., 2013).

3 CSC Markers and their regulation

The expression of CSC markers is regulated at 4 main levels – transcriptional, epigenetic, posttranscriptional, and posttranslational (Bao et al., 2013). In this part of the thesis, I will elaborate on each of the modes of the control.

Transcriptional Regulation:

Transcriptional control of CSC marker expression is pivotal mean of their regulation, and is exercised in multiple ways, with various players and mechanisms contributing to the upkeep of the CSC phenotype. Understanding the transcriptional mechanisms that regulate CSC marker expression can offer insights into tumor heterogeneity, progression, and therapeutic resistance. This mode of regulation is facilitated by a variety of transcription factors and

signaling pathways. The activity of specific transcription factors can induce or repress the expression of CSC markers. Several transcription factors have been identified that directly or indirectly modulate the expression of CSC markers (Bao et al., 2013). Among identified factors, we list:

- **SOX2** (SRY-box transcription factor 2) is a member of the SOX family of transcription factors that play pivotal roles in embryonic development and cellular differentiation. SOX2, which is key factor in maintaining pluripotency, has been linked to the regulation of multiple CSC markers across various tumor types. SOX2 stands at the crossroads of stemness, tumorigenesis, and therapeutic resistance. Understanding its intricate regulation and its role in CSC marker expression is crucial for devising strategies to target CSCs more effectively, potentially leading to improved cancer treatment outcomes. In the context of cancer, SOX2 has emerged as a crucial regulator of stemness, aiding in the maintenance and function of CSCs (Al-Mamun et al., 2018).

SOX2 is considered a core factor in maintaining the pluripotency of embryonic stem cells alongside other transcription factors like OCT4 and NANOG. In cancer, SOX2 is often found overexpressed in various tumor types, where it contributes to stemness maintenance. Overexpression of SOX2 can enhance the self-renewal capacity of CSCs and maintain their undifferentiated state. Elevated SOX2 levels have been linked to tumorigenesis promotion, increased tumor initiation, growth, and metastasis. CSCs are often more resistant to chemotherapeutic and radiation therapies than their differentiated counterparts, an ability ascribed to the SOX2 overexpression (Lu et al., 2010).

SOX2 can directly or indirectly modulate the expression of CD44, a prominent CSC marker, thus affecting cell adhesion, migration, and the stem-like properties of cancer cells. SOX2 has also been linked to the expression of ALDH1, an enzyme associated with stemness and drug resistance in several cancer types. Apart from these, SOX2 can influence the expression of a range of other markers, either by direct transcriptional regulation or through its interaction with other signaling pathways and transcriptional regulators (Martinez-Cruzado et al., 2016).

The actual expression and activity of SOX2 can itself be regulated at various levels, like transcriptional Regulation via signaling pathways, such as the Notch, Wnt/ β -catenin, and Sonic Hedgehog pathways, can influence SOX2 transcription. Also, on epigenetic level when DNA methylation and histone modifications can affect the expression of the SOX2 gene. Further, various miRNAs have been identified that can target SOX2 mRNA, leading to its degradation

and thereby affecting SOX2 levels as a part of post-transcriptional regulation and finally – post-translational modifications - phosphorylation, ubiquitination, and other post-translational modifications can affect SOX2's stability and activity (He et al., 2017).

Targeting SOX2 directly or its associated pathways offers a promising avenue for cancer therapy. This is achieved through use of small molecule inhibitors or antagonists that target SOX2 or disrupt its interaction with other proteins leading to reduction of its function in CSCs. Employment of gene therapy approaches has also been recorded. These strategies knock down or modulate the expression of SOX2 using siRNA, shRNA, or CRISPR/Cas systems. Lastly, SOX2 upstream Pathways can also be targeted. Inhibiting these pathways regulate SOX2 expression and indirectly diminish CSC properties. For instance, the Wnt/ β -catenin signaling pathway is one of the examples of mode of this regulation. The Wnt signaling pathway is central to the maintenance of CSCs and the regulation of associated markers. Understanding the nuances of its regulation and its influence on CSC biology provides significant opportunities for therapeutic intervention, potentially transforming the landscape of cancer treatment (Lu et al., 2021).

- **OCT4** (Octamer-binding transcription factor 4), also known as POU5F1, is a POU domain transcription factor indispensable for maintaining the pluripotency and self-renewal of embryonic stem cells (ESCs). As such, it stands as a key player in the regulation of stemness, both in embryonic development and in the oncogenic domain. Its role in CSC marker regulation signifies its importance in tumor biology. Targeting OCT4 or its associated pathways offers a promising strategy for cancer therapeutics, potentially curbing tumor growth, metastasis, and recurrence (Zhang et al.,2020).

OCT4, in concert with other factors like SOX2 and NANOG, forms the core regulatory network ensuring the maintenance of ESC identity. OCT4's extensive transcriptional network means it can regulate a myriad of other proteins and pathways, potentially influencing the expression of multiple CSC-associated markers. It is also commonly overexpressed in various tumor types. Its elevated expression is often correlated with tumor initiation, progression, therapeutic resistance, and poor prognosis. OCT4 can enhance the expression of CD44, a discussed CSC marker, promoting the stem-like characteristics of cancer cells. Furthermore, the expression of ALDH1, a functional marker for CSCs in several cancer types, is influenced by OCT4. Enhanced ALDH activity is often associated with increased tumorigenicity and drug resistance. In some tumors, OCT4 regulates the expression of Nestin, a type VI intermediate

filament protein, which is a marker for neural stem cells and has been associated with CSCs in various malignancies (Zhang et al., 2020).

OCT4 expression can be modulated by upstream signaling pathways, including the JAK/STAT, PI3K/AKT, and TGF- β pathways. Its gene expression is regulated also on an epigenetic level by means of DNA methylation, histone modifications, and chromatin remodeling at the OCT4 promoter region. For the purposes of CSC phenotype maintenance, the epigenetic silencing of OCT4 is often reversed in CSCs, leading to gene activation. Once the gene is transcribed, miRNAs, such as miR-145 and miR-34a, have been shown to target OCT4, affecting its expression post-transcriptionally (Ruan et al., 2018; Zhang et al., 2020).

Epigenetic drugs or RNA interference techniques could be employed to downregulate OCT4 expression, affecting the CSC pool. Targeting OCT4 in combination with standard therapies might enhance therapeutic efficacy by targeting both the bulk tumor and the CSC population (Zeng et al., 2023).

- **NANOG:** Essential for self-renewal and pluripotency, NANOG also contributes to the transcriptional activation of certain CSC markers. NANOG is a homeobox-containing transcription factor that plays a fundamental role in the maintenance of pluripotency and self-renewal in ESCs. Beyond embryogenesis, NANOG has emerged as a key player in the field of oncology due to its association with the properties of CSCs (Gong et al., 2015).

In concert with transcription factors like OCT4 and SOX2, NANOG forms the core regulatory circuitry that upholds the pluripotent identity of ESCs. Owing to its extensive transcriptional network, NANOG may influence multiple proteins and pathways, indirectly modulating the expression of several CSC-associated markers. Increased levels of NANOG are found in various tumor types and are frequently linked with increased tumor initiation, aggressive progression, therapeutic resistance, and worse clinical outcomes (Zeng et al., 2023). NANOG has been shown to upregulate the expression of CD133, a widely acknowledged CSC marker, particularly in tumors such as glioblastoma and colorectal cancer (Ghorbani et al., 2023). Similarly to OCT4, NANOG regulates the expression of ALDH1 and CD44. By modulating ALDH1 expression, NANOG plays a role in the regulation of detoxifying enzymes associated with stemness and drug resistance in various malignancies. By regulating the expression of CD44, NANOG contributes to improvement of cell adhesion, migration, and the stem-like properties of cancer cells (Zhang et al., 2016).

Recent data report that signaling pathways like PI3K/AKT, MEK/ERK, and STAT3 have been associated with NANOG expression, influencing its transcriptional activity. Epigenetic alterations, such as DNA methylation and histone modifications, can dynamically regulate NANOG expression. In certain cancers, epigenetic reprogramming leads to NANOG gene reactivation. Several miRNAs have been shown to target NANOG mRNA, like miR-296 and miR-134, and are associated with post-transcriptional regulation of its expression (Yoon et al., 2021).

Employing small molecules, inhibitors, or antibodies to target NANOG directly could impede the function and maintenance of CSCs. Other therapeutic approaches include epigenetic modulators, RNA interference techniques, or CRISPR/Cas-based methods. Treating NANOG in cooperation with standard cancer therapies may enhance therapeutic outcomes by targeting both the differentiated tumor cells and the CSCs (Gong et al., 2015).

Epigenetic Regulation:

Epigenetics refers to heritable changes in gene expression that do not involve alterations to the underlying DNA sequence. In the context of cancer, epigenetic modifications play a crucial role in tumorigenesis, progression via the regulation of CSC markers. Modifications of DNA or histones, such as DNA methylation or histone acetylation, can influence their expression. For example, hypermethylation of promoter regions might silence genes associated with CSC characteristics. Unraveling these intricate layers of regulation offers a deeper understanding of tumor biology and unveils novel therapeutic targets for more effective cancer treatments as CSCs have been implicated in tumor initiation, metastasis, and resistance to therapy (French and Pauklin., 2020).

DNA Methylation which involves the addition of a methyl group to the 5-position of the cytosine ring, typically at CpG dinucleotides. DNA methylation usually leads to gene silencing. As such, hypomethylation can activate oncogenes or CSC markers, while hypermethylation can silence tumor suppressor genes or genes that inhibit CSC properties. DNA hypomethylation at the CD44 promoter is reported in association with CSC (Huang et al., 2020).

Histone Modifications impose various post-translational modifications to histones including acetylation, methylation, phosphorylation, and ubiquitination (Völker-Albert et al., 2020). The combination of these modifications creates a "histone code" that can activate or repress gene expression. This way, histone deacetylation and certain histone methylation patterns (e.g., trimethylation of histone H3 at lysine 27) are commonly associated with

repression of genes that suppress CSC properties (Witt et al., 2016). The promoters of pluripotency-associated genes, such as OCT4, SOX2, NANOG often undergo DNA demethylation and specific histone modifications to enhance their expression in CSCs. Histone modifications, especially histone deacetylation, around the ALDH1 gene locus can influence its expression in various malignancies (Toh et al., 2017).

Agents like azacitidine and decitabine can reverse aberrant DNA methylation patterns, reactivating silenced genes that counteract CSC properties (Zeng et al., 2023). Other therapeutics, like Histone Deacetylase Inhibitors (HDACi) can be employed. Drugs like vorinostat (Bubna et al., 2015) and romidepsin (Zeng et al., 2023) can modulate histone acetylation levels, affecting gene expression patterns in CSCs.

Epitranscriptomic changes, such as N6-methyladenosine (m⁶A) modifications, influence mRNA stability, splicing, and translation. The m⁶A “writers”, “readers”, and “erasers” have been associated with CSC marker regulation, indicating the complexity of RNA modification in stemness maintenance (Jiang et al., 2017).

Post-transcriptional Regulation:

Posttranscriptional regulation provides a rapid and efficient mechanism for cells to adjust protein levels in response to various cues. In the context of CSCs, this regulation ensures a fine balance between stemness and differentiation. Subcellular localization of CSC marker mRNAs can influence their translation efficiency, contributing to spatial heterogeneity within tumors (Berabez et al., 2019; Bryl et al., 2022).

Non-Coding RNAs, such as long non-coding RNAs (lncRNAs) and microRNAs (miRNAs) can regulate gene expression post-transcriptionally by targeting the transcripts of CSC markers, influencing their stability and translation (Chen et al., 2021). lncRNAs can modulate both transcriptional and post-transcriptional processes. Acting as sponges for miRNAs or interact with RBPs, indirectly modulating CSC marker expression. The lncRNA HOTAIR, for example, has been implicated in the posttranscriptional regulation of several CSC markers (Wang et al., 2022).

miRNAs typically function by binding to target mRNAs, leading to their degradation or translational inhibition thus regulating CSC marker expression rate (Divisato et al., 2021). These small non-coding RNAs can bind to the 3' untranslated region (UTR) of mRNAs, often leading to mRNA degradation or translational repression (Divisato et al., 2021). For instance, miR-34 has been found to target CD44 mRNA (Li et al., 2021). Certain miRNAs and lncRNAs

are differentially expressed in CSCs and can regulate the expression of CSC markers or modulate pathways that maintain CSC properties. Targeting posttranscriptional regulators presents a novel avenue for cancer therapy. For instance, miRNA mimics or inhibitors can modulate CSC marker levels, potentially impacting the CSC population (Divisato et al., 2021).

RNA-binding proteins (RBPs) are pivotal in mRNA stability, localization, and translation. RNA binding proteins provide an added layer of post-transcriptional regulation that significantly impacts the phenotype and marker expression of Cancer Stem Cells (Jiang et al., 2017). Recognizing the pivotal roles these RBPs play offers novel insights into tumor biology and opens the door to innovative therapeutic strategies that target the elusive CSC population. RBPs interact with RNA molecules to regulate their post-transcriptional fate, including splicing, transport, stability, and translation (Jiang et al., 2017). In the context of cancer, RBPs have emerged as critical regulators of tumor progression, metastasis, and the phenotypic attributes of CSCs. Their role in modulating the expression and function of CSC markers underscores their importance in tumor biology. RBPs can bind to specific sequences or structures on the target mRNA, leading to either stabilization or degradation. In other cases, through interacting with translation initiation complexes or modulating miRNA-binding, RBPs can enhance or inhibit the translation of specific mRNAs (Newman et al., 2015). RBPs can also alter alternative splicing patterns, producing isoforms that may have different, even opposing, functions in CSCs (Ebrahimie et al., 2021).

Musashi (MSI) is RBP, that is found in two isoforms - MSI1 and MSI2. Both are RBPs that have been implicated in various cancers and are known to maintain stemness. MSI proteins can regulate the translation of mRNAs encoding for pivotal factors like Notch and Phosphatase and Tensin Homolog deleted on Chromosome 10 (PTEN), influencing the CSC phenotype (Bley et al., 2021).

Lin28 along with its homolog Lin28B are associated with pluripotency and are overexpressed in numerous malignancies. Lin28 inhibits the biogenesis of the let-7 family of miRNAs, which are known to target multiple oncogenes and CSC markers (Balzeau et al., 2017).

Human antigen R (HuR) also called ELAVL1 stabilizes and modulates the translation of its target mRNAs. By stabilizing the mRNA of various oncogenes and cell cycle regulators, HuR can indirectly modulate the CSC phenotype (Schultz et al., 2020).

QKI has been recognized as a tumor suppressor in certain contexts. QKI can influence CSC marker expression through its role in mRNA splicing and stabilization (Chen et al., 2021).

RBPs, with their vast implications in CSC marker regulation present a promising target for therapeutic treatment. This can be achieved through the exposure to small molecules, peptides, or antisense oligonucleotides. All of these can be developed to inhibit the function of oncogenic RBPs or enhance the function of tumor suppressive RBPs (Hong., 2017). Given the interplay between RBPs and miRNAs, strategies to restore tumor-suppressive miRNAs like let-7 in the case of Lin28 can be employed to target CSCs (Ma et al., 2021).

Variants of CSC markers can arise due to alternative splicing, potentially leading to functionally distinct proteins. This adds another layer of complexity to the CSC phenotype. Given the role of RBPs in splicing, splicing modulators can be used to target aberrant splicing events promoted by RBPs in CSCs (Jiang et al., 2017).

Posttranscriptional regulation is a dynamic and intricate process governing CSC marker expression. Dissecting these mechanisms further can not only enhance our understanding of cancer biology but also pave the way for innovative therapeutic strategies.

Post-translational Regulation

Protein stability, degradation, and modifications can influence the levels and functionality of CSC markers at the protein level. Post-translational modifications provide fast and reversible mechanisms to regulate the function and stability of CSC markers. These modifications, driven by a complex network of enzymes, offer potential therapeutic targets in the battle against cancer by aiming at the very stemness properties that make CSCs so elusive and resilient (Wang et al., 2023). While transcriptional and post-transcriptional regulations play crucial roles in maintaining CSC attributes, post-translational modifications (PTMs) offer an additional, swift mode of regulating CSC marker functions and stability (Wang and Tong, 2023).

Addition of a phosphate group, generally by kinases, can activate or inactivate proteins. Phosphorylation can modulate ALDH1 enzymatic activity, influencing the detoxification pathways and thus, stemness (Clark et al., 2016). Phosphorylation modulates OCT4, SOX2, NANOG transcriptional activity and stability. For instance, phosphorylation can enhance the stability of OCT4, promoting stemness (Zhu et al., 2020).

Further, process of ubiquitination molecules to proteins, often targeting them for proteasomal degradation regulates the turnover and degradation of CD44, influencing cell adhesion and migration properties (Chen et al., 2018).

Attachment of an acetyl group, commonly influencing protein stability or interaction capabilities influences OCT4, SOX2, NANOG DNA-binding ability and interaction with other transcriptional regulators (Liu et al., 2022).

Attachment of sugar moieties can also affect protein stability, localization, and interactions. Variations in glycosylation patterns can influence CD44's interactions and functions, including its ability to bind hyaluronan (Liao et al., 2022).

Modulating the activity of kinases, ubiquitin ligases, or deacetylases can influence the post-translational landscape of CSC markers, presenting a potential therapeutic strategy (Wang and Tong, 2023).

Different approach involves interference peptides that mimic the PTM sites on proteins can be utilized to competitively inhibit the modification, thereby affecting the function of the target protein. Changes in the post-translational modification patterns of CSC markers can be utilized as potential diagnostic or prognostic biomarkers (Zhu et al., 2022).

B EXPRESSION AND ACTIVITY OF GLI TRANSCRIPTION FACTORS

1 Hedgehog signaling pathway

HH is a fundamental signaling cascade that is intertwined in the regulation of cell differentiation, tissue patterning, and organogenesis during embryonic development (Bürglin 2008). Initially discovered in *Drosophila*, its conservation across species underscores its importance in cell-to-cell communication, stem cell maintenance, and tissue repair. The pathway is named after its ligand, the Hedgehog protein, which, upon binding to its receptor, initiates a cascade of intracellular events crucial for proper cell fate determination (Ingham, 2022). Central to this pathway are the Hedgehog ligands, a family of secreted proteins that initiate and regulate HH signaling and the HH receptors to which they bind. To finish, intracellular components transduce the signal from the cell membrane to the nucleus, ensuring accurate gene expression responses (Bürglin 2008).

While the HH is well-known for its critical role in embryonic development, it continues to function in adult tissues, influencing cell proliferation, tissue maintenance, and regeneration (Jia et al., 2015).

Dysregulation of this pathway has been implicated in a variety of human diseases, including congenital disorders, and neurodegenerative conditions. Its aberrations are also linked to the initiation and progression of various cancers, with a particularly pronounced impact on

the behavior of CSCs. Thus, understanding the mechanisms that regulate this pathway is vital for developing therapeutic interventions (Neumann, 2005).

Components of the Hedgehog Signaling Pathway

Hedgehog ligands are a group of signaling proteins that share a conserved structure and function across various species. In mammals, there are three main types of Hedgehog ligands: Sonic Hedgehog (Shh), Indian Hedgehog (Ihh), and Desert Hedgehog (Dhh). Each has distinct and overlapping roles in development (Bürglin 2008).

Shh is the most widely studied and characterized member it plays crucial roles in neural development, limb patterning, and organogenesis. Ihh is essential for chondrocyte differentiation, endochondral ossification, and the regulation of stem cell niches. And lastly Dhh is involved in gonadal development and peripheral nerve sheath formation (Heussler, 2003).

Shh ligand is initially synthesized as precursor protein (Shh-P), comprising an N-terminal signaling domain and a C-terminal autoprocessing domain. This precursor then undergoes a series of PTMs to become an active signaling molecule. First PTM of this sequence is autoproteolysis, a process that splits Shh-P into two parts. This process generates the N-terminal signaling domain (Shh-N), to whose C-terminus is covalently attached a cholesterol molecule. This modification is essential for future activity and gradient formation. The N-terminal domain is also modified by means of palmitoylation, a modification where a palmitic acid molecule is added. Palmitoylation enhances the solubility and signaling potency of Shh. This dual lipidation of Shh is essential for its long-range signaling capabilities. These modifications also allow Shh to associate with lipoprotein particles, ensuring its distribution and concentration gradient creations, features essential for HH to be able to facilitate proper developmental patterning (Heussler, 2003).

Ligands then undergo the process of multimerization, which is a crucial one their release from producing cells. This complex formation with additional soluble proteins, and associations with components of the extracellular matrix such as heparan sulfate. These aspects of the pathway are essential for its proper functioning and regulation.

The PTMs of Shh are essential for its interaction with its receptor Patched-1 (PTCH1) and co-receptors, such as Cell adhesion molecule-related/down-regulated by oncogenes (CDO), Brother of CDO (BOC), and Hedgehog-interacting protein (HHIP). These interactions are critical for continuing the Hedgehog signaling cascade. PTCH1 is a 12-pass transmembrane protein that acts as the primary HH receptor. In the absence of HH ligands, PTCH1 inhibits the

activity of Smoothed (SMO), maintaining the pathway in a repressed state. Shh binding to the PTCH1 receptor triggers its conformational changes and relieves its inhibition on SMO, a seven-transmembrane protein and initiating intracellular signaling. SMO is a seven-pass transmembrane protein crucial for HH signal transduction. In its active state, SMO initiates a cascade of intracellular events leading to the activation of Gli transcription factors. Gli proteins are the final effectors of the HH pathway, modulating the expression of HH target genes. In response to HH signaling, Gli proteins undergo post-translational modifications that regulate their activity and localization. The activity and localization of SMO are tightly regulated by PTCH1, as well as by various post-translational modifications and interacting proteins. In the absence of HH ligands, PTCH1 keeps SMO in an inactive state, leading to the repression of HH target gene expression (Heussler, 2003).

Suppressor of Fused (SUFU), is another pivotal player in the cascade. This cytoplasmic protein binds Gli transcription factors in the repressed state, sequestering them in the cytoplasm and preventing their activation and nuclear translocation. Hedgehog signaling leads to the activation of Gli, converting it into a form that can enter the nucleus. Kinesin and dynein motors then play crucial roles in the intracellular trafficking of HH signaling components, including Gli proteins, ensuring their proper localization and function. Functionality is also largely modified by various protein kinases, including Protein Kinase A (PKA), Glycogen Synthase Kinase-3 (GSK-3), and Casein Kinase 1 (CK1), which engage in the phosphorylation of Gli proteins, influencing their stability, activity, and subcellular localization. Dispatched RND Transporter Family Member 1 (DISP1) and Signal peptide, CUB domain, EGF-like domain (SCUBE) proteins also come into play in the release and spread of Shh (Carballo et al., 2018).

The final effectors of the Hedgehog signaling pathway are the GLI family of transcription factors, consisting of Gli1, Gli2, and Gli3. Gli1 acts primarily as a transcriptional activator, while Gli2 and Gli3 can function as both activators and repressors, depending on their post-translational modifications and the cellular context. In response to Hedgehog signaling, GLI proteins translocate to the nucleus, where Gli binds to specific regions of DNA, regulating the transcription of target genes involved in cell proliferation, differentiation, and survival (Heussler, 2003).

Role in Development and Disease

The Hedgehog pathway is crucial for patterning and morphogenesis during embryonic development. This includes establishing the body plan of an organism, including limb development and neural patterning and segmentation. The latter is achieved by providing

guiding signals triggering the growth of nerve fibers during neural development. The pathway also plays a vital role in organogenesis, the formation of organs, such as the lungs, liver, and pancreas (Carballo et al., 2018).

HH retains its power to influence these tissues into adulthood, when it is involved in their cell type homeostasis and regeneration processes like following muscle injury, promoting the proliferation of hepatocytes and other liver cell types, or maintenance of lung tissue and the regulation of respiratory epithelial cells. Besides that, HH plays a role in tissue repair and regeneration, particularly in tissues with high turnover rates, such as the skin and gastrointestinal tract. HH is also involved the maintenance of hair follicles and sebaceous glands. Its relation to wound healing and the regeneration of the epidermis has also been reported. In the adult brain, Hedgehog signaling participates in maintaining neural stem cells, influencing their proliferation and differentiation. Involvement in the formation of blood vessels is also reported (Carballo et al., 2018).

Mutations in Hedgehog signaling components are associated with developmental disorders such as holoprosencephaly, a condition characterized by the failure of the forebrain to properly divide into two hemispheres, and ciliopathies, which are diseases related to defects in cilia (where Hedgehog signaling components are localized), impacting various organs and systems. Other developmental disorders related to HH mutations include fibrosis, in conditions like liver fibrosis (Klein et al., 2019).

Aberrant activation of the Hedgehog pathway has been linked to the development of several types of cancer, including basal cell carcinoma, which is the most common association off HH in relation with cancer. Next, medulloblastoma, glioblastoma, and pancreatic cancer. Mutations in pathway components, leading to constitutive activation of the pathway, are often implicated in these cancers. Recent data also suggest association with neurodegenerative diseases like Alzheimer's and Parkinson's (Klein et al., 2019).

Regulatory Mechanisms and the repressed state

The expression of Hedgehog ligands is tightly regulated at the transcriptional level, governed by a variety of transcription factors, and signaling pathways responsive to developmental cues and cellular context. The activity of the actual components in the HH pathway is regulated by various post-translational modifications, including phosphorylation, ubiquitination, and SUMOylation. These modifications influence the stability, localization, and activity of HH signaling proteins, impacting the repressed state of the pathway. HH also

employs negative feedback loops to fine-tune its activity. This loop consists of several components of the pathway, including PTCH1 and Gli proteins, being transcriptionally regulated by HH signaling itself. PTCH1 is a target gene of HH signaling, and its upregulation in the presence of HH ligands helps establish said negative feedback loop, ensuring that the pathway is tightly regulated. PTCH1 is a transmembrane protein that plays a central role in maintaining the repressed state of the HH pathway. In the absence of HH ligands, PTCH1 inhibits SMO, preventing the activation of downstream signaling components. Another interaction crucial for maintaining the repressed state of HH target genes is one between SUFU and GLI proteins. This binding restricts them in the cytoplasm and prevents their translocation to the nucleus. Kinases, such as PKA, GSK-3, and CK1 phosphorylate GLI proteins in the absence of HH signaling, targeting them for partial degradation and converting them into transcriptional repressors (Carballo et al., 2018).

The HH pathway does not operate in isolation; it interacts with other signaling pathways, such as Wnt, Notch, and BMP, to coordinate cellular responses. The interactions between the HH pathway and other signaling cascades are critical in embryonic development, organogenesis, and tissue repair. Dysregulation of these interactions can lead to developmental disorders and contribute to the pathogenesis of diseases, including cancer (Sigafoos et al., 2021).

The HH pathway often intersects with the Wnt signaling pathway, particularly in developmental processes and cancer. Both pathways can have synergistic or antagonistic interactions depending on the cellular context. For example, in some instances, HH signaling can enhance Wnt signaling by stabilizing β -catenin (Tang et al., 2010).

The interaction between the HH and Notch signaling pathways is crucial in the regulation of cell fate determination, stem cell maintenance, and differentiation. In many types of cancer, these pathways collaboratively promote tumor growth and survival (Tang et al., 2010).

The Transforming Growth Factor Beta (TGF- β) and Bone Morphogenetic Protein (BMP) pathways can either cooperate with or oppose HH signaling. This interaction is particularly important in embryonic development and in the maintenance of stem cell niches (Guo and Wang., 2008).

The crosstalk between HH signaling and the PI3K/AKT/mTOR pathway is significant in cancer biology. The HH pathway can activate the PI3K/AKT pathway, promoting cell survival and growth, and contributing to chemoresistance in cancer cells (Larsen and Møller., 2020).

The Mitogen-Activated Protein Kinase (MAPK)/Extracellular Signal-Regulated Kinase (ERK) pathway can be influenced by HH signaling. This interaction is often observed in the context of cancer, where it can contribute to uncontrolled cell proliferation and tumor progression (Liu et al., 2018).

HH signaling intersects with cell cycle regulators like cyclins and cyclin-dependent kinases (CDKs). This interaction can influence cell cycle progression and is a critical aspect of how HH signaling controls cell proliferation (Kenney and Rowitch., 2000).

Under hypoxic conditions, HH signaling can be modulated through HIF-1 α . This interaction is particularly relevant in the tumor microenvironment, affecting tumor growth and metastasis (Roy et al., 2020).

Therapeutic Interventions

Given its role in cancer and developmental disorders, the Hedgehog pathway is an attractive target for therapeutic intervention, particularly in regenerative medicine (Piccioni et al., 2014). Various inhibitors of the pathway have been developed, some of which have been approved for clinical use in treating specific types of cancer. However, vast roles in tissue homeostasis, therapeutic targeting of this pathway requires careful consideration and precise modulation (Carpenter et al., 2019).

On one hand, inducing a lagging Hedgehog signaling has potential in promoting tissue repair and regeneration in conditions such as neurodegenerative diseases, muscle degeneration, and liver cirrhosis (Edwards et al., 2004).

On the other side, inhibiting aberrantly hyperactive Hedgehog signaling is a strategy in treating cancers associated with this pathway. Several inhibitors targeting components of the Hedgehog pathway have been developed and approved for treating certain types of cancer (e.g., Smoothed inhibitors Sonidegib and Vismodegib for treatment of basal cell carcinoma) (Carpenter et al., 2019).

Outlook

The Hedgehog signaling pathway is a complex and highly regulated cascade that plays critical roles in development, tissue maintenance, and disease. Hedgehog signaling retains its importance well beyond embryonic development, playing crucial roles in the maintenance, repair, and regeneration of adult tissues. Its dysregulation is implicated in a wide array of diseases, particularly cancers, making it a critical target for therapeutic intervention (Bürglin

2008). Ongoing research continues to unravel its complexities, with the aim of developing more effective and precise therapies to modulate this pathway.

The influence of HH on regenerative processes positions it as a key player in the field of regenerative medicine, though its dual role in cancer necessitates a nuanced approach in therapeutic applications (Carballo et al., 2018). Hedgehog signaling plays a double-edged sword in human health, being crucial for normal development and tissue maintenance, while its dysregulation is implicated in a plethora of diseases. Understanding the intricacies of this pathway is vital for developing targeted therapies, offering hope for patients suffering from Hedgehog-related diseases and paving the way for precision medicine in these conditions. Research continues to unveil the complexities of Hedgehog signaling in disease, seeking safer and more effective therapeutic strategies (Giammona et al., 2023).

2 Hedgehog signaling pathway in CSC

Hedgehog signaling has gained attention for its association with CSCs, a subpopulation of cells within tumors that possess the ability to self-renew and differentiate, contributing to tumor heterogeneity and therapeutic resistance (Tang et al., 2011; Liu et al., 2022). The Hedgehog pathway is here reported to be crucial for maintaining the stemness of CSCs and their pluripotency (Tang et al., 2011). In CSCs, this pathway often becomes constitutively activated, either through mutations in pathway components or through external cues from the tumor microenvironment. HH is via its effect on CSCs implicated in promotion of tumorigenicity by supporting tumor initiation, progression, and metastasis in various types of cancer, including glioblastoma, breast cancer, and colorectal cancer. Inhibiting Hedgehog signaling in these cells has been shown to reduce their tumorigenic potential and stemness characteristics (Tang et al., 2011).

The Hedgehog signaling pathway also plays a crucial role in drug resistance of CSCs. Targeting this pathway represents a promising therapeutic strategy in oncology, though challenges remain in effectively and safely modulating Hedgehog signaling in the clinical setting. Further research is required to better understand the intricacies of this pathway in CSCs and to develop novel strategies to overcome the associated therapeutic challenges (Lu et al., 2021).

Mechanisms of Hedgehog Signaling in CSCs

Hedgehog signaling activates various survival and anti-apoptotic pathways in CSCs, which are central to the pathogenic success of the CSCs enhancing their viability. Not only does it promote the proliferation of CSCs, but it also enhances their survival capabilities (Cochrane et al., 2015). This is particularly alarming as CSCs are notoriously resistant to conventional therapies, contributing to treatment failure and cancer relapse. Activation of the HH pathway in CSCs upregulates the expression of anti-apoptotic genes such as BCL-2 (B-cell lymphoma 2) (Cochrane et al., 2015) and myeloid cell leukemia sequence 1 (MCL-1) (Barakat et al., 2010), which provide a survival advantage to CSCs in the hostile tumor microenvironment and under stress conditions such as chemotherapy.

BCL-2 and MCL-1 belong to the BCL-2 family of proteins, which includes both pro-apoptotic and anti-apoptotic members (Wu et al., 2017). By binding to and neutralizing pro-apoptotic proteins such as BAX and BAK, BCL-2 and MCL-1 prevent the release of cytochrome c from the mitochondria, thereby inhibiting the apoptotic cascade. In CSCs, the expression of these proteins is often dysregulated, contributing to the evasion of apoptosis and the facilitation of tumor progression. BCL-2 and MCL-1 are integral to the survival strategy of CSCs, conferring resistance to apoptosis and contributing to the daunting challenges of cancer treatment (Safa, 2022). Their roles in sustaining CSC populations and promoting therapeutic resistance underscore the potential benefit of developing targeted therapies against these proteins. CSCs exploit elevated levels of BCL-2 and MCL-1 to avoid cell death triggered by various stressors, including hypoxia, nutrient deprivation, and chemotherapy. By maintaining mitochondrial integrity and preventing the activation of the apoptotic machinery, BCL-2 and MCL-1 enable CSCs to survive and repopulate the tumor after treatment. These proteins are also implicated in the self-renewal and differentiation of CSCs, affecting the long-term dynamics of tumor cell populations. The HH pathway, through the action of Gli transcription factors, can directly or indirectly enhance the expression of BCL-2 and MCL-1, thus promoting cell survival and resistance to apoptosis. This regulation ensures the persistence of CSCs within the tumor niche, contributing to the challenge of eradicating cancers, particularly those resistant to conventional therapies (Safa, 2022).

As our understanding of the intricate networks regulating BCL-2 and MCL-1 in CSCs expands, so too will our capacity to design innovative approaches for the eradication of these resilient cells from the tumor hierarchy (Castelli et al., 2021). The interplay between HH signaling and apoptotic regulation presents an attractive target for cancer therapy, offering a potential route to undermine CSC resilience and improve patient outcomes. Ongoing research

into this interaction will be critical in guiding the development of more effective and durable cancer treatment strategies (Bisht et al., 2022). Targeting HH signaling may need to be combined with other targeted therapies to counteract compensatory. Additionally, the identification of biomarkers that can predict the response to HH inhibitors remains a significant challenge and an area for future research (Bisht et al., 2022).

The HH pathway contributes to the expression of stemness-related genes like SOX2, OCT4 and NANOG, which are crucial for maintaining the self-renewal capacity of CSCs (Lu et al., 2021).

HH also influences the tumor microenvironment, promoting a niche that supports CSC maintenance and activity. The TME plays a pivotal role in cancer progression, influencing the behavior of cancer cells, including CSCs. This crosstalk between CSCs and their niche is partially facilitated by the HH pathway, which is now recognized as a crucial regulator of multiple cellular and non-cellular components of the TME (Takabatake et al., 2019). It orchestrates a supportive tumor microenvironment by regulating the secretion of factors that foster angiogenesis and immune evasion. HH signaling can also induce the secretion of factors that promote angiogenesis, thus enhancing nutrient supply and CSC sustenance (Bausch et al., 2020). Furthermore, it can influence immune cells to adopt a tumor-promoting phenotype, contributing to immune evasion. This pathway influences CSCs directly by affecting their cell cycle and indirectly by shaping the TME to support CSC growth and survival (Takabatake et al., 2019).

Next, Hedgehog signaling is implicated in EMT, a process associated with increased stemness, migration, and invasion of cancer cells. EMT is a reversible cellular program that is critical for embryogenesis, tissue remodeling, and wound healing (Islam et al., 2015). When co-opted by cancer cells, it facilitates metastasis. This key event in cancer progression and metastasis endows epithelial (cancer stem) cells with mesenchymal features, enhancing their migratory and invasive abilities (May et al., 2011). The Hedgehog signaling pathway has been identified as a pivotal regulator of both EMT and CSC phenotypes, offering potential targets for therapeutic intervention. The HH signaling pathway influences EMT through its downstream effectors and transcription factors of the Gli family. The activation of HH signaling leads to the induction of EMT markers, such as N-cadherin, vimentin, and fibronectin, while downregulating epithelial markers like E-cadherin (Loh et al., 2019). Other EMT-associated transcription factors that also govern stemness properties, such as Snail (Fendrich et al., 2007), Slug (Horák et al., 2023), and Twist (Khales et al., 2022). These transcription factors not only promote EMT but also enhance the stemness characteristics of CSCs. Taken together, his shift

in marker expression is indicative of a transition to a more mesenchymal and stem-like state, contributing to increased tumor invasiveness and metastatic potential (Khales et al.,2022).

3 Hedgehog signaling in melanoma

The Hedgehog signaling pathway plays a significant role in melanoma progression (Li et al., 2011). A study explored the therapeutic potential of targeting this pathway in melanoma. They analyzed human melanoma cell lines and control melanocytes for changes in the expression of Hedgehog pathway members. The study found that over 40% of melanoma cell lines had significantly higher levels of Hedgehog pathway mediators, such as SMO, GLI2, and PTCH1, compared to melanocytes (Shamsoon et al., 2023).

The consequences of both genetic and pharmacological inhibition of SMO in melanoma were examined in vitro and in vivo. Inhibition of SMO, using siRNA and the small molecule inhibitor NVP-LDE225, suppressed melanoma growth, particularly in cell lines with moderate SMO and GLI2 expression (Jalili et al., 2013). NVP-LDE225 also induced apoptosis in vitro and inhibited melanoma growth in a xenograft model. Interestingly, gene expression data revealed compensatory up-regulation of other developmental pathways, Notch and WNT, in response to Hedgehog pathway inhibition. Additionally, pharmacological and genetic SMO inhibition downregulated genes involved in human embryonic stem cell pluripotency (Jalili et al., 2013).

The study also found a correlation between increased SMO expression, decreased expression of the Hedgehog pathway repressor GLI3, and shorter post-recurrence survival in metastatic melanoma patients (Jalili et al., 2013). These findings suggest that Hedgehog pathway inhibition might be a promising targeted therapy in appropriately selected metastatic melanoma patients.

C THERAPEUTIC APPROACHES AGAINST CSCS

1 Therapeutic interventions

Developing therapies that specifically target CSCs is an active area of research, as it has the potential to enhance the effectiveness of cancer treatments and overcome drug resistance. Strategies include disrupting CSC-specific signaling pathways, blocking surface markers, and developing immunotherapies that target CSC antigens (Dragu., 2015). To improve cancer treatments and overcome drug resistance, researchers are exploring innovative strategies for

targeting CSC-specific markers and their associated signaling pathways. Therapeutic approaches include:

Chemotherapy:

The use of chemotherapy in targeting CSCs is a complex and evolving area of cancer treatment. CSCs are a subpopulation of cancer cells that are inherently more resistant to chemotherapy than their differentiated counterparts (Phi et al., 2018). Traditional chemotherapy effectively reduces the tumor mass by targeting the bulk of differentiated cancer cells but tends to select for highly resistant CSCs that can regenerate the tumor. This resistance is attributed to the ability of CSCs to multiply indefinitely, making them a significant factor in relapse after therapy (Liu et al., 2018). Conventional chemotherapy drugs, like paclitaxel, mainly target rapidly proliferating cancer cells (Sharifi-Rad et al., 2021). Various strategies have been explored to target CSCs in different types of cancers. These strategies include blocking one or more self-renewal signaling pathways, reducing the expression of drug efflux and ATP-binding cassette efflux transporters, modulating epigenetic aberrations, and promoting CSC differentiation (Begicevic and Falasca, 2017). However, standard anti-tumor therapies, including conventional chemotherapy, radiation therapy, and molecularly targeted therapies, are not very effective against CSCs. Often, these therapies lead to an enrichment of CSCs, which can result in tumor relapse. This has led to the hypothesis that targeting CSCs is essential to increasing the efficacy of cancer therapies (Phi et al., 2018).

Immunotherapy:

Immunotherapeutic approaches aim to stimulate the immune system to recognize and attack CSCs. These strategies include the development of vaccines and immune checkpoint inhibitors that target CSC-specific antigens (Izadpanah et al., 2023). CSCs were found to be immunogenic and more effective as an antigen source compared to unselected tumor cells. This means that CSCs triggered a stronger immune response in the host. Also, cytotoxic T Lymphocytes (CTLs) generated from the blood or spleen cells of CSC-vaccinated hosts could kill CSCs in vitro (Ning et al., 2012). This suggests that the immune response induced by CSC vaccination included cytotoxic T cells that could target and eliminate CSCs.

Almost a century ago, German researcher Georg Schöne made seminal observations suggesting that vaccinating animals with fetal tissue could prevent the growth of transplantable tumors (Brewer et al., 2009). This early work hinted at the potential role of the immune system

in rejecting tumors. Subsequent research in the 1960s and 1970s explored the phenomenon of immunologic rejection of tumors and the prevention of carcinogenesis through vaccination with embryonic or fetal material. However, interest in this area of research appeared to decline in subsequent years. Data suggests that the earlier experimental work on vaccination against tumor growth with embryonic or fetal material may be particularly relevant in the context of current research on cancer stem cells (Barati et al., 2021). Further research in this area is warranted, including the exploration of using embryonic stem cells as immunogens. The results from earlier studies support the idea that vaccination against various types of cancers could be a realistic possibility (Hashemi et al., 2022). Using vaccination with embryonic or fetal material can prevent tumor growth and suggests that revisiting this concept, with modern approaches involving embryonic stem cells, could have implications for cancer prevention (Ouyang et al., 2019).

Construction of Melanoma Vaccines:

Advances have also been made in research of melanoma vaccines. The first vaccine was composed of cells derived from melanospheres (SFs) with CSC characteristics, which were admixed with B16F10 melanoma cells modified with a designer cytokine called Hyper-interleukin 6 (Gabka-Buszek et al., 2020). The second vaccine contained syngeneic murine induced pluripotent stem cells (miPSCs), again admixed with B16F10 cells modified with H6. Both vaccines were found to be effective in inhibiting tumor growth and increasing disease-free survival (DFS) and overall survival (OS) in C57BL/6 mice (Gabka-Buszek et al., 2020). This suggests that these vaccines triggered an immune response against melanoma cells, including CSCs. Mice treated with the SF vaccine or induced pluripotent stem cells (iPSCs) vaccine showed increased activation of the immune response at the vaccination site and within the tumor microenvironment (Gabka-Buszek et al., 2020). This included higher infiltration of dendritic cells (DCs), monocytes, and natural killer (NK) cells, as well as lower numbers of myeloid-derived suppressor cells (MDSCs) and regulatory T cells (Tregs). The vaccines were associated with higher levels of the cytokines IFN γ and IL-12, which engage in immune responses (Cheng et al., 2022). Splenocytes (immune cells) from mice immunized with the vaccines showed increased proliferation of CD4 $^{+}$ T helper lymphocytes and secretion of cytokines when restimulated in vitro. Mice immunized with the SF vaccine had increased serum antibody titers directed against B16F10 cells. The miPSC vaccine was found to be the most effective in extending DFS and OS (Hashemi et al., 2022).

Gene Therapy:

Gene-based therapies are being explored to selectively target CSCs. These approaches involve the delivery of genes or gene-modifying agents that inhibit CSC-specific pathways or promote their differentiation and elimination (Dragu et al., 2015). Tumors, especially those with high invasiveness and metastasis, need to evade the immune system once they detach from their primary site and establish metastatic sites. CD47 is a protein that sends a "self" signal to immune cells, preventing their clearance by macrophages and T cells, while PD-L1 suppresses immune responses. CD47 and PD-L1 expression is elevated in various cancer cells, including lung, breast, melanoma, and esophageal cancer, but not in normal cells (Leone et al., 2018). SiRNA molecules were used to inhibit CD47 and PD-L1 expression in cancer cells, and these molecules were incorporated into LPP-P4-Ep complexes modified with an EpCAM aptamer (Lian et al., 2019). The LPP-P4-Ep complexes effectively targeted cancer cells with high CD47 and PD-L1 expression, leading to decreased expression of immune-related proteins and increased cancer cell apoptosis when co-cultured with immune cells. In vitro experiments showed that inhibiting CD47 and PD-L1 proteins activated immune cells and increased cytokine secretion while reducing tumor growth and metastasis (Lian et al., 2019).

Nanotherapy:

Nanoparticles can be designed to specifically target CSCs by delivering therapeutic agents directly to these cells (Ertas et al., 2021). Nanoparticles are tiny particles with sizes on the nanometer scale, and they can be engineered to carry drugs, genes, or other therapeutic agents. The size of nanoparticles can significantly impact their biodistribution, cellular uptake and intracellular fate (Foroozandeh and Aziz, 2018). Nanoparticles are engineered in a way that they may enter cells more easily through various mechanisms, including endocytosis and compound in tumors through the enhanced permeability and retention (EPR) effect, making them valuable for delivering therapeutic payloads selectively to cancer cells. This approach enhances drug delivery to CSCs while minimizing exposure to healthy cells (Nie et al., 2023).

Nanoparticle-based combination therapies:

Nanoparticle-based combination therapies represent promising strategies for cancer treatment, particularly when targeting CSCs. These approaches have the potential to improve the precision, efficacy, and safety of cancer therapy, benefiting patients by reducing recurrence and metastasis. Nanoparticles can be engineered to target specific cell types, including CSCs,

minimizing damage to healthy tissue. Targeted drug delivery reduces systemic exposure to chemotherapeutic agents, reducing side effects (Nie et al., 2023).

Nanoparticulate approach can be combined with thermotherapy, which involves raising the temperature in the tumor region to induce cell death. When nanoparticles are designed to accumulate in tumors and absorb near-infrared light, they can convert this light into heat, selectively targeting and killing cancer cells while sparing healthy tissue. This approach, known as photothermal therapy, can be used to target CSCs within tumors (Chatterjee et al., 2011).

Nanoparticles can also be used to deliver chemotherapeutic agents directly to tumor sites (Yao et al., 2020). This targeted drug delivery minimizes the exposure of healthy tissues to the drug, reducing side effects. By designing nanoparticles that can specifically target CSCs, it is possible to enhance the effectiveness of chemotherapy against these critical cells. Nanoparticles are valuable tools for molecular imaging, allowing researchers to visualize and track specific molecules or processes in living organisms. The size of nanoparticles can impact their ability to target and bind to specific molecular targets in vivo (Wang et al., 2013).

Enzyme/prodrug systems:

Enzyme/prodrug systems represent a promising approach in cancer therapy with the potential to improve the efficacy and safety of conventional chemotherapies. This approach involves introducing a gene into cancer cells that can express an enzyme capable of converting a non-toxic prodrug into its active and cytotoxic form. As a result, when the prodrug is administered, it is selectively activated within the transfected cancer cells, leading to their destruction (Malekshah et al., 2016). Several enzyme/prodrug systems have been developed for this purpose. However, despite significant progress in preclinical studies and early clinical trials, enzyme/prodrug systems have faced challenges that have prevented their widespread clinical use. In some cases, the conversion of the prodrug into its active form may be slow, limiting the effectiveness of the treatment (Zhang et al., 2016). Efficient delivery of the therapeutic gene into cancer cells can be difficult to achieve, impacting the overall success of the therapy. Also, the delivery systems, plasmid DNA, enzymes, and prodrugs used in the therapy can sometimes result in nonspecific toxicity or immune responses, which may be harmful to the patient (Sheikh et al., 2021). Ongoing research has focused on addressing these challenges. New delivery systems and gene delivery techniques are being developed to improve transfection efficiency. Additionally, efforts are being made to enhance the specificity and safety of enzyme/prodrug systems. Despite the challenges, enzyme/prodrug systems have been evaluated in clinical studies (Poreba, 2020). These studies aim to assess the safety and efficacy

of this approach in human patients. Results from these trials can provide valuable insights into the feasibility of enzyme/prodrug systems in clinical settings. Mesenchymal stem cells (MSCs) were genetically modified to express four different suicide genes: thymidine kinase (TK), yeast cytosine deaminase:uracil phosphoribosyltransferase (yCD:UPRT), and nitroreductase (NTR) (Nouri et al., 2015). These stem cells were used as a delivery platform to compare the effectiveness of the different enzyme/prodrug systems. The study evaluated the anticancer efficacy of these genetically engineered MSCs both in vitro and in vivo using a sensitive cancer cell line (SKOV3) that is susceptible to all four enzyme/prodrug systems (Nouri et al., 2015). The researchers conducted experiments to determine the therapeutic impact of each system. The results indicated that the yCD:UPRT/5-FC enzyme/prodrug system was the most effective among the ones evaluated. This system demonstrated superior anticancer activity in the context of this study (Nouri et al., 2015). The MSCs used in this study were engineered to express the luciferase gene, allowing for quantitative imaging and dose-response studies in animals. This approach facilitated the side-by-side evaluation and screening of different enzyme/prodrug systems.

Hyperthermia:

The controlled application of heat to the body, has been investigated for its potential to enhance the body's natural immune response against cancer (Skitzki et al., 2009). Hyperthermia, particularly in the fever range (around 39-42°C), has been shown to enhance the body's anti-tumor immune response. Elevated temperatures can stimulate the immune system, leading to increased activity of immune cells like T cells, natural killer (NK) cells, and macrophages (Evans et al., 2015). This heightened immune response can help in recognizing and attacking cancer cells more effectively. Cells exposed to heat stress produce Heat Shock Proteins (hsps) in large quantities. These hsps serve as chaperone proteins, helping in the correct folding of other cellular proteins and preventing protein damage caused by stress. Importantly, hsps have been found to be potent immune modulators (Stetler et al., 2010). Hyperthermia can have direct effects on immune cells. For instance, it can increase the migration and infiltration of immune cells into the tumor microenvironment. Elevated temperatures can also enhance the cytotoxic activity of NK cells and T cells, making them better at killing cancer cells (Dayanc et al., 2008). Hsps released by heat-stressed cells can function as danger signals to the immune system. These hsps can be taken up by antigen-presenting cells (APCs), such as dendritic cells, which play a crucial role in initiating and regulating immune responses. Hsps can activate APCs, leading to the presentation of tumor-specific antigens to T cells, thereby initiating an

adaptive immune response against cancer. Hsps can be harnessed for the development of cancer vaccines (Setler et al., 2010). Tumor-associated antigens can be fused or associated with hsps to create vaccines that can stimulate an immune response against cancer cells. These vaccines can be administered as part of cancer immunotherapy strategies (Liu et al., 2022). Some therapeutic protocols combine hyperthermia with the administration of hsps or hsps-based vaccines to maximize the immune response against tumors. This combined approach aims to capitalize on both the direct effects of heat on immune cells and the immune-modulating properties of hsps.

2 GLI transcription factors as a focus of targeted experimental interference against CSC subpopulation

Targeting the HH signaling pathway in CSCs is a critical area of cancer research due to the pathway's significant roles in various cancer-related processes (Dusek and Hadden, 2021). Peripheral tumor cells, CSCs, and mesenchymal cells can initiate the transcription of stemness genes (such as NANOG, Oct4, Sox2, and Bmi1) in CSCs through Hedgehog signaling to maintain stem cell properties (Didiášová et al., 2018).

Early clinical trials with HH pathway antagonists have validated HH signaling as an anticancer target in a wide variety of human tumors. However, issues remain regarding the basic biology of the HH pathway in human cancers, such as the influence of specific oncogenic events on HH signal transduction and the best means to inhibit aberrant pathway activity in a clinical setting (Dusek and Hadden, 2020). Due to the diverse nature of HH signaling in human cancers, disease-specific factors must be carefully considered to optimize the use of novel pathway inhibitors.

To date, numerous agents have been developed to specifically target the HH pathway (glasdegib, sonidegib, vismodegib, ciclesonide) (Carpenter et al., 2019), along with other critical pathways like Wnt (niclosamide, TFP, DTX and SFN, PP, AD and Ts) and Notch (DAPT) signaling, for cancer treatment (Yang et al., 2020; Kumar et al., 2021). These treatments aim to inhibit the pathway's influence on cancer stem cells, potentially reducing tumor growth and spread, and overcoming drug resistance.

This ongoing research highlights the importance of the Hedgehog signaling pathway in cancer biology, especially in the context of cancer stem cells, and underscores the potential of targeted therapies in this area.

II AIMS

This doctoral thesis is focused on the functions of GLI transcription factors in cancer and is aimed to unveil their relation to further downstream genes, which are, in turn, linked tumor upkeep and prosperity.

- 1) The GLI transcription factors, the effectors of the Hedgehog signaling pathway, are known to target multiple genes associated with tumor development, progression, and metastasis. Our group already expanded the list of GLI targets while identifying Survivin as a GLI-regulated gene. Here we present data linking GLIs to Slug transcription factor, which engages in embryogenesis and tumor cell invasion. **Our aim is to define the relation between HH pathway and Slug, a known asset in EMT and anti-apoptotic activity.**
- 2) Recent years brought novel therapies based on SMO inhibition. This treatment was developed to help patients suffering from acute myeloid leukemia and basal cell carcinoma. Unfortunately, this therapy often leads to SMO acquired resistance. We understand that the signaling crosstalk between HH pathway and others is robust and can bridge over a singular interference, but **we aim to investigate the regulatory effect of GLI inhibition by GANT61 with outlook to clinical applications.**
- 3) Lastly, although the MiTF gene was isolated some 30 years ago and has been studied extensively for most of this period, we are far from describing its functions in its entirety. Its involvement in melanoma invasiveness has been reported, so **we aim to analyze how varying levels of MITF influence other key features of melanomas, such as, proliferation, differentiation, and ubiquitination.**

III METHODS

In this part I disclose the list of methods applied during my research. These are further elaborated in published papers.

Animal experimentation – See publication IV (p. 105)

Cell cultivating – see Publication I (p. 56), II (p. 78), III (p. 86) and IV (p. 104)

Cell migration assay – See publication IV (p. 104)

Cell proliferation assay – See publication II (p. 79) and IV (p. 105)

Chromatin Immunoprecipitation – see Publication I (p. 57) and IV (p. 105)

Colony outgrowth assay, growth curves – see Publication II (p. 79), III (p. 86) and IV (p. 105)

Detection of apoptosis – detection of apoptotic nuclei, TUNEL assay – see Publication II (p. 79, 80)

Flow cytometry- see Publication II (p. 79)

Gene expression profiling – see Publication IV (p. 106)

Immunofluorescence microscopy – see Publication I (p. 43), III (p. 86) and IV (p. 106)

Immunohistochemical analysis - see Publication I (p.58)

Invasivity assay - see Publication III (p. 87)

mRNA preparation and real-time/quantitative PCR - see Publication I (p. 57), III (p. 87) and IV (p. 105)

Plasmid engineering, expression vectors creation, promoter-reporter constructs transfection – see Publication I (p. 57) and II (p. 80)

Proteomics analysis and nano-HPLC-MALDI-TOF/TOF analysis - see Publication IV (p. 105)

shRNA knock-down, production of lentivirus, lentiviral infection - see Publication III (p. 86)

Statistical analysis – see Publication I, II (p. 80), III (p. 87) and IV (p. 106)

Transient transfection of siRNA – see Publication IV (p. 104)

Viability assay – see Publication III (p. 87)

Western blotting – see Publication I (p. 56 II, (p. 79), III (p. 87) and IV (p. 105)

Wound healing assay - see Publication III (p. 87)

IV RESULTS AND DISCUSSION

PUBLISHED RESEARCH ARTICLES AND AUTHOR'S CONTRIBUTION.

1. **Horák, P.**, Kreisingerová, K., Réda, J., Ondrušová, L., Balko, J., Vachtenheim Jr., J., Žáková, P. & Vachtenheim J. (2023) **The Hedgehog/GLI signaling pathway activates transcription of Slug (Snail2) in melanoma cells.** *Oncology reports*, 49(75).

doi: 10.3892/or.2023.8512

IF₂₀₂₃ = 4,136

Pavel Horák performer most of the experiments and is co-author of the manuscript.

2. Réda, J., Vachtenheim, J., Vlčková, K., **Horák, P.**, & Ondrušová, L. (2018). **Widespread expression of hedgehog pathway components in a large panel of human tumor cells and inhibition of tumor growth by GANT61: Implications for cancer therapy.** *International Journal of Molecular Sciences*, 19(9).

doi: 10.3390/ijms19092682.

IF₂₀₁₈ = 4,183

Pavel Horák performed GANT61 experiments.

3. Vlčková, K., Vachtenheim, J., Réda, J., **Horák, P.**, & Ondrušová, L. (2018). **Inducibly decreased MITF levels do not affect proliferation and phenotype switching but reduce differentiation of melanoma cells.** *Journal of Cellular and Molecular Medicine*, 22(4).

doi: 10.1111/jcmm.13506

IF₂₀₁₈ = 4,658

Pavel Horák performed growth curve and doxycycline experiments

4. Habel, N., El-Hachem, N., Soysouvanh, Hadhiri-Bziouche, Giuliano, S., Nguyen, **Horak, P.**, Gay, A.S., Debayle, D., Nottet, N., Beranger, G., Paillerets, B.B., Bertolotto, C. & Ballotti, R. (2021). **FBXO32 links ubiquitination to epigenetic reprogramming of melanoma cells.** *Cell Death and Differentiation* 28:1837–1848

doi: 10.1038/s41418-020-00710-x

IF₂₀₂₁ = 12,07

Pavel Horák performed western blot experiments.

Published review article (without impact factor)

5. Kreisingerová K, Ondrušová L., **Horák P**, Vachtenheim J. (2020) **Význam aberantně aktivované dráhy Hedgehog/Gli pro nádorovou progresi.** *Klinická Onkologie*, 33(3):177-183.

doi: 10.14735/amko2020177

IF₂₀₂₀ = N/A

Pavel Horák had minor contributions to the manuscript.

This article is not included to the discussion as it does not contain any original research data.

The Hedgehog/GLI signaling pathway activates transcription of Slug (Snail2) in melanoma cells

PAVEL HORÁK¹, KATEŘINA KREISINGEROVÁ¹, JIRI RÉDA¹, LUBICA ONDRUŠOVÁ¹, JAN BALKO²,
JIRI VACHTENHEIM Jr³, PETRA ŽÁKOVÁ¹ and JIRI VACHTENHEIM¹

¹Department of Transcription and Cell Signaling, Institute of Medical Biochemistry and Laboratory Diagnostics, First Faculty of Medicine, Charles University and General University Hospital in Prague, 12108 Prague;

²Department of Pathology and Molecular Medicine, Second Faculty of Medicine and ³3rd Department of Surgery, First Faculty of Medicine, Charles University and University Hospital Motol, 15006 Prague, Czech Republic

Received October 12, 2022; Accepted January 27, 2023

DOI: 10.3892/or.2023.8512

Abstract. In melanoma and other cancers, invasion, epithelial-to-mesenchymal transition, metastasis and cancer stem cell maintenance are regulated by transcription factors including the Snail family. Slug (Snail2) protein generally supports migration and apoptosis resistance. However, its role in melanoma is not completely understood. The present study investigated the transcriptional regulation of the *SLUG* gene in melanoma. It demonstrated that *SLUG* is under the control of the Hedgehog/GLI signaling pathway and is activated predominantly by the transcription factor GLI2. The *SLUG* gene promoter contains a high number of GLI-binding sites. Slug expression is activated by GLI factors in reporter assays and inhibited by GANT61 (GLI inhibitor) and cyclopamine (SMO inhibitor). *SLUG* mRNA levels are lowered by GANT61 as assessed by reverse transcription-quantitative PCR. Chromatin immunoprecipitation revealed abundant binding of factors GLI1-3 in the four subregions of the proximal *SLUG* promoter. Notably, melanoma-associated transcription factor (MITF) is an imperfect activator of the *SLUG* promoter in reporter assays, and downregulation of MITF had no effect on endogenous Slug protein levels. Immunohistochemical analysis confirmed the above findings and showed MITF-negative

regions in metastatic melanoma that were positive for GLI2 and Slug. Taken together, the results demonstrated a previously unrecognized transcriptional activation mechanism of the *SLUG* gene, which may represent its main regulation of expression in melanoma cells.

Introduction

Hedgehog (HH) signaling is a developmentally conserved pathway in numerous embryonic tissues and has been shown to be dysregulated in multiple cancers (1,2). The Sonic Hedgehog cascade involves the Sonic hedgehog (Shh) ligand binding to Patched (PTCH), a 12-pass transmembrane protein. When the ligand is absent, PTCH represses the activity of the neighboring 7-pass membrane protein Smoothened (SMO). This inhibition is released upon Shh binding. The ensuing activation of SMO triggers a chain of events that lead to the release of GLI1-3 effector proteins from the Suppressor of Fused (SuFu) and their subsequent translocation to the nucleus (2). The activated HH/GLI pathway has been linked to a number of types of human cancers and causes accelerated proliferation and survival and an enhanced rate of metastasis. HH also supports the self-renewal of cancer stem cells (CSCs), a subpopulation of tumor cells with inherent resistance to therapy (3,4). HH activity can be regulated in a noncanonical manner, and does not require the initial Shh binding to the receptor. A number of pathways, such as RAS (5), MAPK (6), AKT (7) and EGFR (8), have been shown to activate GLI factors directly in tumor cells.

The HH pathway has been shown to be essential for the oncogenic properties of melanoma (6). Moreover, blunting GLI1 and GLI2 restores sensitivity to vemurafenib in vemurafenib-resistant melanoma cells harboring BRAF mutations (9). SOX2 is crucial for the self-renewal of CSCs in melanoma and is regulated by GLI1 and GLI2, thus mediating HH signaling (10). GLI1 and GLI2 also transcriptionally regulate several genes involved in positive regulation of the cell cycle, such as E2F1, cdk1 and cyclin B (11).

The transcription factor Slug, the protein product of the *SNAIL2* gene, belongs to the Snail family of zinc-finger transcription factors (12). As early as 1998, the human Slug

Correspondence to: Dr Jiri Vachtenheim, Department of Transcription and Cell Signaling, Institute of Medical Biochemistry and Laboratory Diagnostics, First Faculty of Medicine, Charles University and General University Hospital in Prague, Katerinska 32, 12108 Prague, Czech Republic
E-mail: jiri.vachtenheim@lfl.cuni.cz

Abbreviations: Slug (Snai2, Snail2), snail family zinc finger 2; Snail1, snail family zinc finger 1; EMT, epithelial-to-mesenchymal transition; ALDH1A1, aldehyde dehydrogenase 1 family member A1; Klf4, Krüppel-like transcription factor 4; GLI, GLI family zinc finger; CSC, cancer stem cells; HH, Hedgehog signaling pathway; MITF, melanoma-associated transcription factor

Key words: Slug, Hedgehog signaling, GLI family zinc finger, melanoma-associated transcription factor, melanoma

protein was described to contain 268 amino acids and its molecular weight is ~30 kDa (13). Slug is expressed during embryogenesis and is critical for the development of the neural crest (14). Notably, Slug and Snail significantly contribute to the maintenance of CSCs (15). Slug is an antiapoptotic protein that contributes to the transcriptional repression of E-cadherin in epithelial tumors, thus contributing to epithelial-to-mesenchymal transition (EMT) in tumor cells (16). This is achieved by upregulating the expression of Zeb1, which is then engaged in repressing E-cadherin (17). Furthermore, Twist1 upregulates Slug which mediates Twist1-induced changes during EMT (18). Cooperatively, these transcription factors repress epithelial markers, enabling cell detachment and migration during early stages of EMT, which is a key phenomenon underlying cancer progression and invasion (19). Moreover, increased Slug expression is found in patients suffering from a number of types of cancers (20). Increased Slug levels are linked to metastasis, tumor recurrence and poor prognosis and play a role in the maintenance of CSCs (21). The CSC-like properties of tumor cells promote tumor initiation, expansion, EMT, metastasis, and tumor relapse and confer resistance to chemotherapy and radiotherapy in multiple types of cancer (22). Downregulation of Slug results in inhibition of the proliferation of cancer cell lines, and its overexpression leads to accelerated proliferation (21).

In melanoma, *SLUG* has been considered to be a pro-oncogenic gene contributing to EMT (17). Slug expression in melanoma cells has been reported to be regulated by osteonectin (SPARC). PI3/Akt kinase signaling acts upstream of SPARC, as its blockade hinders induction of the *SLUG* gene by SPARC, cell migration, and EMT-like changes (23). The protein Nodal is involved in the expression of *SNAIL* and *SLUG* genes and activation of ALK/Smads and PI3K/AKT pathways (24,25). Slug silencing has also been shown to increase the radiosensitivity of melanoma cells (26).

Despite these findings, the precise mechanisms of Slug expression and its role in EMT remain to be elucidated in melanoma. Gupta *et al* (27) described the necessity of Slug for the development of melanoma metastases in a mouse model. By contrast, Slug protein expression has been observed to be diminished in human metastases (28). Slug, together with Zeb2, was notably found to be downregulated during EMT in melanoma. Slug and Zeb2 transcription factors have been reported to drive a melanocytic differentiation program and behave as oncosuppressive proteins, whereas Zeb1 and Twist1 repress differentiation and have oncogenic properties (29). Similar conclusions were reported by Gunarta *et al* (30) after ablating GLI1 function in melanoma. GLI1-knockdown cells exhibited reduced invasion ability accompanied by downregulation of the EMT factors Snail1, Zeb1 and Twist1 but not Snail2 or Zeb2. As *SLUG* is one of the genes contributing to CSC maintenance, a central question for understanding the acquisition of the mesenchymal state and CSC renewal is how the expression of genes involved in EMT is regulated. In brief, inconsistent results have been reported regarding *SLUG* gene function in melanoma cells, and the mechanisms of its expression have not been extensively studied. The present study investigated the transcriptional regulation of *SLUG* in human melanoma cells and observed that Slug expression is controlled by the HH/GLI pathway, particularly the GLI2 transcription factor.

Materials and methods

Cell culture. The present study used eight melanoma cell lines (listed in Table SI). Their mutational status (BRAF and NRAS mutations) is shown in Table SII. The origin of cells has been described previously (31,32). Cells were cultivated in RPMI medium (MilliporeSigma) supplemented with 10% FCS (Thermo Fisher Scientific, Inc.), glutamine and antibiotics (MilliporeSigma) at 37°C and 5% CO₂ in 100% humidity. All cell lines were authenticated and tested for mycoplasma using a mycoplasma detection kit (MP0035; MilliporeSigma). Cells were passaged every 72-96 h using a trypsin-EDTA solution. When plated, cells (5x10⁵) were seeded from a stable culture into 12-well plates and incubated for 24 h at 37°C prior to inhibitor treatment or transfection, unless specified otherwise. Normal human melanocytes were purchased from Cascade Biologics Inc. and cultivated according to the manufacturer's instructions. The generation of inducible melanoma cell lines in which melanoma-associated transcription factor (MITF) protein can be downregulated by the addition of doxycycline (Tet-on system) has been previously described (32).

Chemical inhibitors. GANT61 (stock prepared in DMSO) and cyclopamine (stock prepared by dissolving in ethanol) were purchased from Selleck Chemicals LLC. The chemicals were applied to cells as indicated in the appropriate figures for 20 h before cell harvesting if not stated otherwise. The addition of 20 μM GANT61 for 20 h was used after the optimization of both the concentration and time to follow the changes in expression of GLI-dependent genes, when no signs of apoptosis had been yet detected in cells.

Western blot analysis. To obtain whole-cell extracts for immunoblotting analysis, cells were lysed in RIPA buffer (1% NP-40, 150 mM NaCl, 5 mM EDTA, 0.5% sodium deoxycholate, 50 mM Tris-HCl pH 7.5 and 0.1% SDS) with the addition of the protease and phosphatase inhibitors aprotinin, pepstatin and leupeptin at 1 mg/ml each. cOmplete (Roche Diagnostics) was added as recommended by the supplier. Then, 1 mM phenylmethylsulfonyl fluoride (MilliporeSigma) and phosphatase inhibitor PhosSTOP (Roche Diagnostics) were added. Equal amounts of protein (30 μg; concentration determined by Bradford's assay) were loaded on 10-12% SDS-polyacrylamide gels, separated by electrophoresis and transferred onto PVDF membranes. Blots were blocked in 5% non-fat dry milk Blotto (cat. no. sc-2325, Santa Cruz Biotechnology, Inc.), and incubated with 1:1,000 diluted primary antibodies for 2 h, washed, and then incubated at room temperature for 1 h with 1:4,000 diluted secondary anti-mouse or anti-rabbit horseradish peroxidase-conjugated antibodies (cat. no. sc-2055 or cat. no. sc-2030; Santa Cruz Biotechnology, Inc.). Chemiluminescent detection was used. For western blotting shown in Fig. 5A and B, cells were lysed in PLB buffer (Promega Corporation), used in dual luciferase measurements and these extracts were then directly utilized. Primary antibodies for western blotting were: GLI1 (cat. no. 3538; Cell Signaling Technology, Inc.), GLI2 (cat. no. TX46056; GeneTex, Inc.), and GLI3 (cat. no. AF3690; R&D Systems, Inc.). Anti-Slug (cat. no. sc-166476) was purchased from Santa Cruz Biotechnology, Inc. Klf4 (cat. no. LS-C415468) and ALDH1A1 (cat. no. LS-B10149) from LSBio. Anti-FLAG

(M2; cat. no. F1804) and anti- β -actin (A5316) antibodies were purchased from MilliporeSigma. Anti-livin antibody (cat. no. sc-30161) was from Santa Cruz Biotechnology, Inc. and MITF (D5) antibody (cat. no. NBP2451590) was from Thermo Fisher Scientific, Inc. Brn-2 (cat. no. sc-514295) was from Santa Cruz Biotechnology, Inc. E- and N-cadherins, vimentin, Zeb1, and Zeb2 antibodies were from Cell Signaling Technology (cat. no. 9782). Western blot bands were quantified using ImageJ (v. 1.52j) software (National Institutes of Health; data not shown).

Plasmids. The 12xGLI-TK-Luc plasmid was obtained from Professor R Toftgard, Karolinska Institute, Sweden. pGL3-PTCH1 was kindly donated by Professor Aberger, University of Salzburg, Austria. The *PATCHED* gene promoter contains one active GLI-binding site responsible for its activity (data not shown). The pGL3-sluc-prom-full-length promoter (-5216+112) and pGL3-sluc-prom- Δ middle (-5216-4635, -2092+112) were cloned as *XhoI-HindIII* (New England Biolabs, Inc.) inserts in the pGL3-basic plasmid (Promega Corporation). pGL3-sluc-prom- Δ proximal (-5216-2092) was cloned as the *XhoI-HindIII* insert. The -4635+112 promoter was cloned as the *NheI-HindIII* insert. pGL3-sluc-prom-middle (-4635-2092) was cloned as the *NheI-NheI* (New England Biolabs, Inc.) insert and the pGL3-sluc-proximal promoter (-2092+112) was cloned as the *NheI-HindIII* insert. Cloning of all GLI expression vectors has been described previously (31). Briefly, original GLI1 (GL1; cat. no. 16419), GLI2 (pCS2-MT GLI2 FL; cat. no. 17648), Δ GLI2 (pCS2-MT GLI2 delta N; cat. no. #17649) and GLI3 (GLI3 bs-2; cat. no. 16420) were acquired from the nonprofit plasmid repository Addgene, Inc. Respective coding sequences were amplified by PCR and subsequently cloned into the pcDNA3 expression vector or into the pFLAG-CMV-4 plasmid (MilliporeSigma) background to obtain FLAG-tagged GLI proteins. The types of GLI expression plasmids were similarly effective in promoter activation. The melastatin promoter plasmid with the three MITF-binding sites was constructed as previously described (33). The construction of the short hairpin plasmid directed to MITF has been previously described (32). All final plasmid inserts were verified by sequencing on both strands (GATC Biotech).

Transfection and promoter-reporter assays. Transient cell transfections of the promoter reporters were performed using 12-well plates at 37°C, seeded and incubated for 24 h before transfections, and the transfection reagent Mirus TransIT-2020 (Mirus Bio LLC) following the manufacturer's instructions and harvested 48 h after transfection. For detection, a dual luciferase system (Promega Corporation) was used according to the manufacturer's instructions. The pGL3-basic vector was used as a negative control. Expression vectors or controls (pcDNA3 or pFLAG-CMV-4) were cotransfected together with the reporter plasmids. Cell lysates were used for dual luciferase assays performed as recommended by the manufacturer's instructions. The luciferase values were acquired on a Turner Designs 20/20 luminometer (Promega Corporation). Data were normalized to *Renilla* luciferase activity (internal control) as arbitrary units. Statistical analysis of luciferase assay results was performed using a two-tailed unpaired Student's t test and SigmaPlot software V10.0 (Systat Software Inc.). Where indicated, cells were treated with GANT61 or

cyclopamine 20 h at 37°C before harvesting. Tomatidine, a compound inactive in the HH pathway but structurally similar to cyclopamine, was tested as a negative control and revealed similar results as vehicle (data not shown).

Reverse transcription-quantitative (RT-q) PCR. Total RNA was isolated using TRIzol® (Invitrogen; Thermo Fisher Scientific, Inc.) according to the supplier's instructions (3x10⁵ cells per 30 mm well). Then 2 μ g of RNA was reverse transcribed using SuperScript IV reverse transcriptase (Thermo Fisher Scientific, Inc.), and qPCR was performed using a TaqMan QuantiTect Probe PCR kit (Qiagen GmbH) on a ViiA7 Real-Time PCR system (Thermo Fisher Scientific, Inc.) following the manufacturer's instructions (cycling: 30 sec at 94°C and 1 min at 60°C). Data analysis was performed by QuantStudio 6 Software (Thermo Fisher Scientific, Inc.). Concurrent results were obtained in three independent experiments with the following PCR primers and probe for *SLUG*: Forward, 5'-AGA ACTCACACGGGGGAGAAG-3'; reverse, 5'-CTCAGATTT GACCTGTCTGCAA-3'; probe, 5'-6-FAM-TTTTCTTG CCCTCACTGCAACAGAGC-TAMRA-3'. β -Actin was utilized as an internal standard control: Forward, 5'-ATTGCCGAC AGGATGCAGAA, reverse, 5'-GCTGATCCACATCTGCTG GAA; probe, 6-FAM-CAAGATCATTGCTCCTCCTGA GCGCA-TAMRA. Fluorescent probes were purchased from Thermo Fisher Scientific, Inc.

Chromatin immunoprecipitation. 501mel cell cultures were transfected using Mirus TransIT-2020 (Mirus Bio LLC) with the pcDNA3-GLI1, pcDNA3-GLI2 or pcDNA3-GLI3 expression plasmids in 90 mm plates. After 24 h of treatment, fresh medium was applied. After another 24 h, cells were crosslinked with 1% formaldehyde for 10 min at room temperature and incubated with glycine solution, and chromatin immunoprecipitation was performed by using the ChIP-IT High Sensitivity kit (Active Motif, Inc.) in accordance with the manufacturer's protocols. Anti-acetylated histone H3 antibody (MilliporeSigma) was used as the positive control, and rabbit nonimmune IgG (MilliporeSigma) was used as a negative control. To detect GLI1 bound to the promoter, a rabbit anti-GLI1 antibody (cat. no. sc-20687; Santa Cruz Biotechnology, Inc.) was used. Rabbit anti-GLI2 (cat. no. ab26056; Abcam) was used to precipitate GLI2. For GLI3, a rabbit anti-GLI3 antibody (cat. no. 3538; Cell Signaling Technology, Inc.) was used and 2 μ g of each antibody was added in each reaction. To assess the amount of ChIP-generated DNA, PCR was performed using Phusion High-Fidelity DNA polymerase (Thermo Fisher Scientific, Inc.). The amplification of the regions of the proximal SLUG promoter was performed with four alternative primer pairs: Region A (-2108-1766): sense, 5'-GCATACGTGTTACTC GCTAGCAC-3', antisense, 5'-TCCTTGTTTCACTCTACA CAGTCTATTCAC-3'; region B (-1769-1163): sense, 5'-AGG AAATAATAGCCATGGCGATA-3', antisense, 5'-CAT CTCTGTCCATTGCAGAC-3'; region C (-1182-490): sense, 5'-GTCTGCAATGGACAGAGATGC-3', antisense, 5'-GGG AAGCGGAAGACAAAG-3'; and region D: (-509+112): sense, 5'-CCTTTGTCTTCCCGCTTCCCCCTTCC-3', antisense, 5'-ACACGGCGGTCCCTACAGCATCG-3'. PCR products were resolved on 1% agarose gels. The intensity of

the final PCR bands was quantified using ImageJ (v. 1.52j) software (National Institutes of Health).

Immunofluorescence. For immunofluorescence, four cell lines (501mel, Hbl, SK-MEL-5 and SK-MEL-28) were seeded into 8-well Lab-Tek II Chamber Slides (Thermo Fisher Scientific, Inc.). After 48 h, 20 μ M GANT61 was added for 20 h at 37°C. Vehicle (DMSO) alone was added to the controls. The cells were fixed with 3% paraformaldehyde at room temperature for 10 min, washed, permeabilized with 0.1% Triton X-100, and blocked with 5% goat serum. Slides were then stained with Slug primary antibody (1:1,000; cat. no. sc-166476; Santa Cruz Biotechnology, Inc.) at room temperature for 2 h followed by 1:1,000 secondary anti-mouse fluorescein-coupled antibody (cat. no. FI-2000-1.5, Vector Laboratories, Inc.) and mounted in medium with DAPI to stain nuclei. The visualization was performed using an Olympus IX70 microscope with cellSens software V2.2 (Olympus Corporation).

Immunohistochemical analysis. Formalin-fixed paraffin-embedded tissues (skin, nevus and melanoma) were retrieved from the archive of the Department of Pathology and Molecular Medicine, Second Faculty of Medicine, Charles University, University Hospital Motol, Prague. At least four samples of each tissue were processed and similar results were obtained. Deparaffinized, rehydrated in descending ethanol series, and blocked (with 3% H₂O₂) sections were stained with 1:1,000 primary antibodies. Immunohistochemistry for MITF was performed with the primary antibody MITF (cat. no. D5; cat. no. NBP2451590, Thermo Fisher Scientific, Inc.). GLI2 was stained with antibody cat. no. GTX46056 (GeneTex, Inc.) and Slug with anti-Slug (A-7) sc-166476 antibody (Santa Cruz Biotechnology, Inc.). Detection was performed using an EnVision+ avidin-biotin detection system (Dako; Agilent Technologies, Inc.). Each tissue was examined by two pathologists. Tissues were scored on a scale of 0 to 4 based on the combined extent and intensity of staining. The final score represented the predominant staining pattern of both combined parameters. Section fields were imaged using a BX51 microscope (Olympus Corporation) equipped with a PROMICAM 3-3CP 3.1 camera and QuickPHOTO CAMERA 3.2 software (Olympus Corporation).

Statistical analysis. Statistical significance (P-values) was assessed using a two-tailed Student's t test and Mann-Whitney test. Standard error of the mean values are depicted in graphs as bars within each column in the reporters and RT-qPCR. Data not significant (P>0.05) were not labeled, values of 0.01 <P<0.05 are marked by an asterisk, and values with P<0.01 are marked by two asterisks. SigmaPlot software V10.0 (Systat Software Inc.) and GraphPad Prism v.8.4.3 software (Dotmatics) were used to perform statistical analysis. Statistical analysis was verified using one-way ANOVA followed by post hoc tests as specified in figure legends. P<0.05 was considered to indicate a statistically significant difference.

Results

Slug expression in melanomas is inhibited by the Hedgehog pathway inhibitor GANT61. Snail1 and Snail2 (Slug) are among the main players in the tumorigenic program of EMT (19).

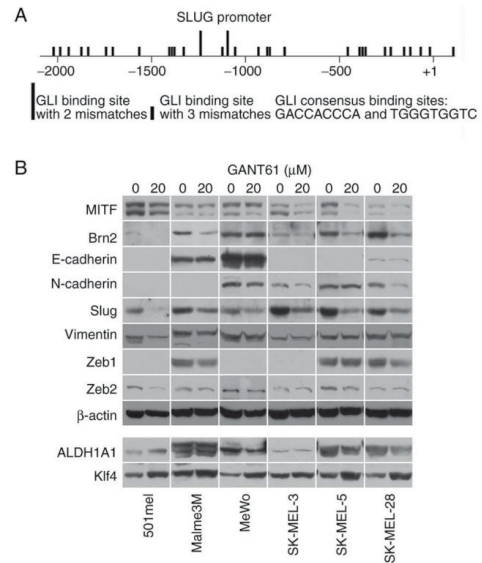


Figure 1. Distribution of GLI-binding sites in the *SLUG* proximal promoter and inhibition of Slug protein expression by GANT61 treatment. (A) Human *SLUG* promoter (proximal region -2092+112), where the +1 nucleotide denotes the start of translation, is depicted. A total of 31 GLI-binding sites are present in this promoter portion, of which two sites contain two mismatched nucleotides (longer bars) and all other sites harbor three mismatches (shorter bars). (B) Immunoblot analyses of several EMT-associated proteins after GANT61 treatment in 6 melanoma cell lines. Cells were treated with 0 μ M (vehicle) or 20 μ M GANT61 for 20 h and harvested for western blot analysis. The cancer stem cell markers ALDH1A1 and Klf4 were also analyzed. GLI, GLI family zinc finger.

SLUG gene deletions have been found in Waardenburg syndrome and piebaldism in humans (34,35), indicating the involvement of Slug in melanin pigmentation. The *SLUG* gene has long been thought to be under the transcriptional control of MITF (34). To further explore the regulation of Slug expression in melanoma, the present study examined the *SLUG* promoter and found 85 GLI-binding sites in the long *SLUG* promoter (-5216 +112; the start of translation is +1) and 31 sites in the proximal promoter (-2092 +112; Fig. 1A and Table SIII). Although none of the sites was a full consensus, GLI proteins, which are the final executive factors of the Hedgehog signaling pathway, bind to and are also active from sites with two or three mismatched nucleotides. This implies that *SLUG* gene expression could be controlled by the Hedgehog pathway.

To further investigate this hypothesis, Slug protein expression was examined in melanoma cell lines treated with GANT61, a potent and specific pan-GLI transcriptional inhibitor. It was found that GANT61 decreased Slug protein in all eight melanoma cell lines investigated as well as in normal melanocytes (Figs. 1B and SI). BRAF- or NRAS-mutated or wild-type cells for both oncogenes were present among the analyzed melanoma cell lines (Table SII). The levels of other proteins known to be involved in EMT, such as E- and N-cadherins, vimentin, Zeb1 and Zeb2, were not appreciably changed after GANT61 treatment in six melanoma cell lines.

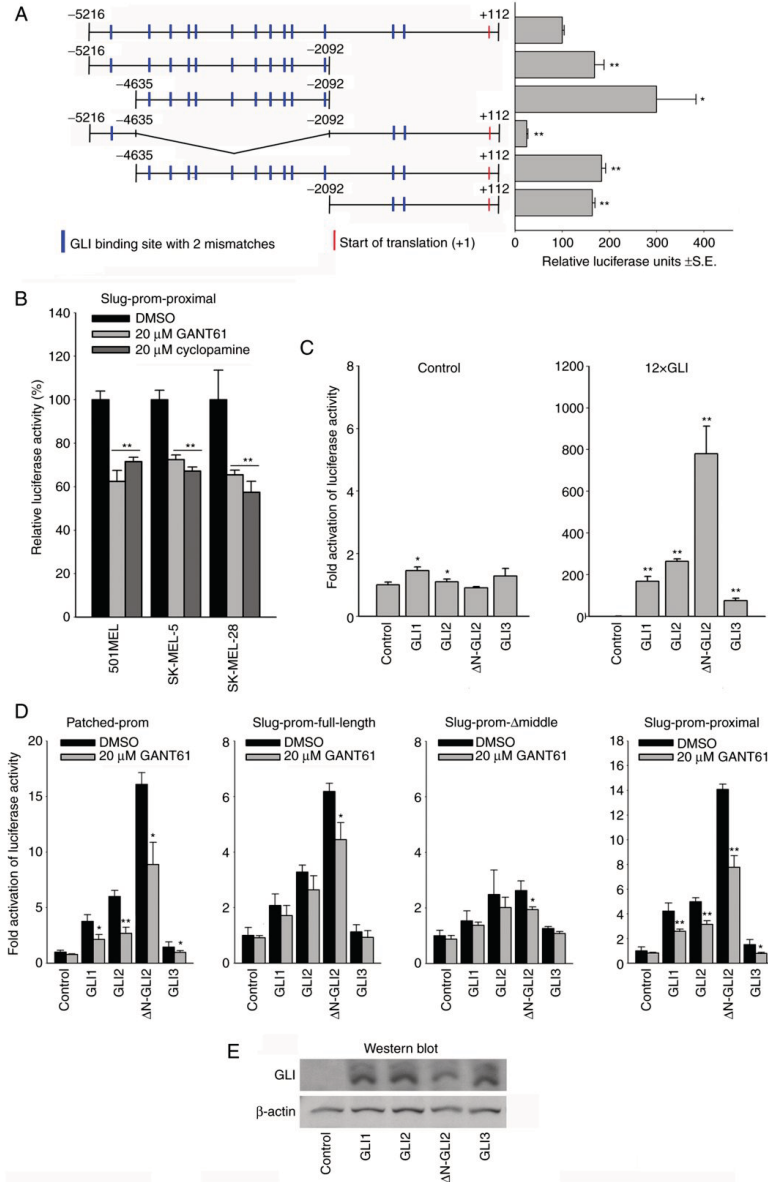


Figure 2. Promoter-reporter analysis of the *SLUG* gene promoter. (A) The long (full-length) *SLUG* promoter (-5216+112) and its truncated versions were assayed for activity in 501mel cells. Only two-mismatched consensus GLI-binding sites are shown as blue bars. pGL3-basic was used as a negative control and exhibited near zero activity (data not shown). The statistical significance of truncated promoters is related to the long promoter (100%). (B) Inhibition of the proximal *SLUG* promoter by GANT61 and cyclopamine in three cell lines. Bars are the mean \pm standard error of the mean. The statistical significance is related to the activity of the untreated proximal promoter. (C) Activation of the 12xGLI-site full consensus promoter by GLI transcription factors. Left, the control plasmid (pGL3-basic) had extremely low activity and was negligibly influenced by GLI factors; right, the massive effect of GLI expression vectors on a positive control reporter plasmid with 12 full consensus GLI sites. (D) Left, inhibition of the GLI-activated *PATCHED* promoter by GANT61; middle left, middle right and right graphs, GANT61 inhibited three versions of the *SLUG* promoter. The most significant inhibition was seen with the proximal promoter (right). The GLI-mediated effect is compared with the control (pGL3-basic) in (B-left) and (D). The significance of GANT61-mediated inhibition is related to the vehicle-treated control. Statistical analyses were performed using a Student's t test. Statistical analysis was verified using one-way ANOVA test, followed by Dunnett's post hoc test and equal results (P-values) were obtained. In all reporter assays, two or three independent experiments were performed (in triplicate) with similar results, and one representative experiment is shown. In all graphs, \pm standard error of the mean bars are shown. Statistical significance: no mark, not significant, *P<0.05, **P<0.01. (E) Western blotting showing similar levels of expression of all GLI proteins in (C) and (D). GLI, GLI family zinc finger.

Likewise, the CSC markers ALDH1A1 and Klf4 were generally only slightly affected (Fig. 1B). A mild increase in Klf4 was noted in the cell lines 501mel, MeWo, SK-MEL-5 and SK-MEL-28, while ALDH1A1 levels were somewhat increased in 501mel cells and slightly diminished in SK-MEL-28 cells after GANT61 treatment (Fig. 1B). Only Brn2 (N-Oct-3, POU3F2) protein, a known repressor of MITF (36), noticeably decreased in five of six cell lines, suggesting that its transcription may also be regulated by the HH pathway in most melanomas. MITF was slightly downregulated in three cell lines (Fig. 1B). Immunofluorescence staining confirmed blunting of Slug expression after the treatment of melanoma cells with GANT61 (Fig. S2).

SLUG promoter-reporter is activated by GLI2 and inhibited by GANT61 and cyclopamine. Since the transcriptional inhibitor of GLI factors GANT61 downregulated Slug protein expression, the activity of the *SLUG* promoter was analyzed in reporter assays. Examination of luciferase expression driven by the long (full-length) promoter (-5216+112) and its truncated versions revealed that the middle part of promoter (-4635-2092) was the most active fragment (Fig. 2A). Its deletion greatly decreased the activity of the full-length promoter. The short portion most upstream (-5216-4635) probably performs an inhibitory function because its presence in the contexts of the full-length promoter, middle part and proximal promoter (-2092+112) decreased the luciferase activity (Fig. 2A). As the proximal promoter also showed appreciable activity, it was used in the following experiments.

Next, to test whether the *SLUG* promoter-reporter is directly activated by cotransfected expression vectors for GLI factors and inhibited by GANT61, it was first investigated whether the proximal promoter activity decreased after the addition of HH pathway inhibitors. Indeed, both GANT61 and cyclopamine lowered the activity in all three melanoma cell lines tested (Fig. 2B). As a subsequent experiment, each of the expression vectors for GLI factors (GLI1-3) were cotransfected with the GLI-responsive promoter containing 12 canonical GLI-binding sites (12xGLI). First, it was ascertained that there was only a minimal difference between the cotransfected control (pcDNA3) and GLI vectors with the pGL3-basic empty control promoter (Fig. 2C, left). By contrast, all three GLIs greatly increased 12xGLI promoter activity compared with the negative control plasmid pcDNA3 (Fig. 2C, right). GLI3 showed the weakest activation of the canonical 12xGLI promoter (but still ~80-fold), whereas the highest activation (800-fold) was achieved by Δ GLI2, a truncated version of GLI2 in which the N-terminal repression domain was removed (37). The activity of the GLI factors was then tested on a known HH-responsive promoter of the *PATCHED* gene, also a component of the HH pathway. The results were similar to those obtained with the canonical promoter, but the extent of stimulation was substantially lower, ~6-fold in the case of the most active Δ GLI2 (Fig. 2D, first graph). Similar experiments were then conducted with the three types of *SLUG* promoters, the long (full-length), Dmiddle and proximal promoters (Fig. 2D, second, third and fourth graphs). In all cases, the Δ GLI2 construct again showed the best activation. In accordance with the results in Fig. 2A, the Dmiddle promoter exhibited the lowest overall activity. When the

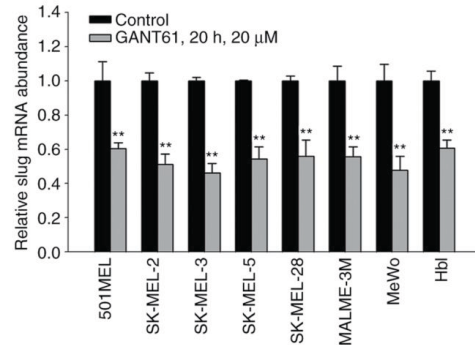


Figure 3. GANT61 decreases Slug RNA levels. mRNA levels of Slug were assessed by RT-qPCR quantification. A total of eight cell lines were treated with 20 μ M GANT61 for 20 h, and total RNA was isolated. After RT, RT mixes were analyzed by qPCR. The relative mRNA levels of Slug were normalized to those of β -actin. Values are presented as the mean \pm standard error of the mean. Three independent experiments were performed, each in triplicate. Similar results were obtained in all experiments, and one is depicted. The nontreated control (vehicle) was set as 1.0. All decreases in Slug RNA were statistically significant ($^{**}P < 0.01$) by Student's t test. RT-qPCR, reverse transcription-quantitative PCR.

PATCHED and *SLUG* promoters were tested, the addition of GANT61 more or less decreased the GLI-stimulated promoter activities (Fig. 2B and D). Western blotting verified that all GLI proteins were similarly expressed (Fig. 2E). These results together indicated that *SLUG* promoter activity is dependent mainly on GLI2 in reporter assays and that stimulation by GLI factors can be inhibited by GANT61.

Slug RNA levels are diminished after GANT61 treatment. To further evaluate the transcriptional regulation of Slug by HH/GLI, the present study examined the effect of GANT61 on Slug RNA levels using real-time PCR. RT-PCR was performed first, followed by qPCR. In all eight melanoma cell lines tested, 20 μ M GANT61 significantly ($P < 0.01$) lowered the mRNA level of Slug. This indicates that the positive effect of GLI factors on endogenous *SLUG* gene expression is mediated through the activation of transcription (Fig. 3).

ChIP assays show binding of GLI factors to the proximal SLUG promoter. The proximal *SLUG* promoter contains 31 GLI-binding sites, of which only two sites harbor two mismatches and all other sites have three mismatches (Fig. 2A and Table SIII). To investigate whether these sites are occupied by GLI proteins in cells, the 501mel cell line was used to chromatin immunoprecipitate DNA fragments bound to GLIs using specific anti-GLI1, GLI2 and GLI3 antibodies (Fig. 4). To obtain improved insight into whether the particular GLI binds to specific regions of the proximal promoter (-2092+112), the immunoprecipitated purified DNA was amplified by four primer pairs (see Materials and methods) that demarcated the four subregions A-D (Fig. 4) of the promoter. Each subregion contained several GLI-binding sequences. The most distal region A and a middle region C were bound by all three GLI factors. The middle region B was remarkably occupied only

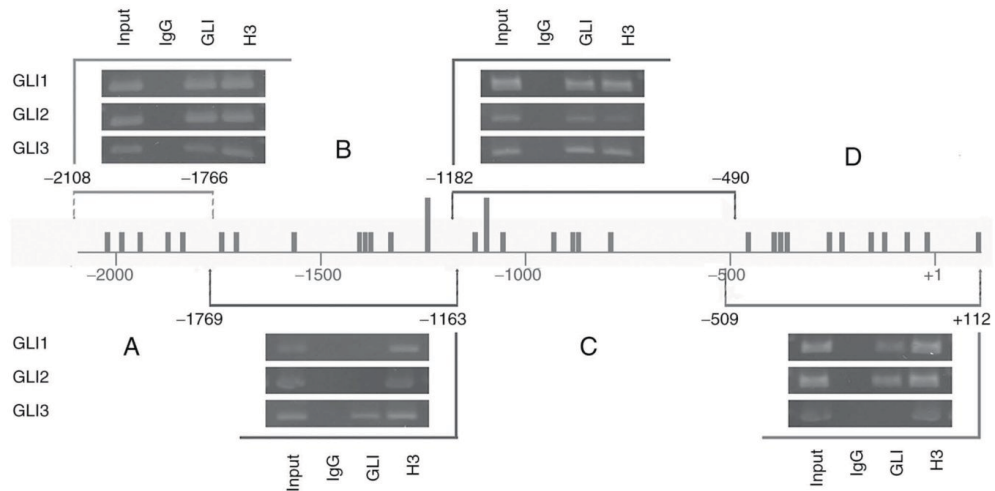


Figure 4. Binding of GLI factors to the proximal *SLUG* promoter. Chromatin immunoprecipitation was performed using the 501mel cell line. Cells were cultivated in 90 mm dishes and transfected with control vector (pCDNA3) or expression vectors for transcription factors GLI1, GLI2, or GLI3. Cells were harvested for immunoprecipitation 48 h after transfection. At 24 h before harvesting, new medium was applied to the cells. After crosslinking, the cells were processed by a ChIP High Sensitivity kit as described in the Materials and methods. Immunoprecipitation was performed with the respective specific anti-GLI antibody. The final isolated coprecipitated DNA was then amplified by a set of four primer pairs (see Materials and methods). Each portion of the promoter (denoted A-D) revealed a specific pattern of GLI factor binding. Inputs and a positive control (anti-acetylated histone H3) always showed a positive band. Nonimmune IgG used as a negative control gave no bands when compared with experimental samples. All bands of PCR products were quantified using ImageJ software and the results are summarized in Table SIV. The two longer bars indicate two mismatched sites and small bars represent three mismatches of the full consensus site. GLI, GLI family zinc finger.

by the GLI3 factor. The most proximal fragment D was bound by GLI1 and GLI2 but not GLI3 (Fig. 4). Thus, regions B and D showed some preference for GLI occupancy, whereas regions A and C clearly exhibited enrichment by all three GLI factors. Acetylated histone H3, which was precipitated by anti-acetylated H3 antibody as a positive control, showed occupancy at all four subregions. Nonimmune IgG as a negative control showed no binding in any experiment. Taken together, these data indicate that GLI transcription factors are abundantly present at their recognition DNA sites within the *SLUG* proximal promoter, further confirming their role in the transcriptional regulation of *Slug* expression through HH signaling. The data quantifying the final DNA amount formed through PCR are in Table SIV.

Slug is an imperfect target for MITF in melanoma cells. The *SLUG* gene has been demonstrated to be transcriptionally regulated by MITF in melanocytes (34) and during *Xenopus laevis* development (38). However, data relevant to a possible regulation of *Slug* expression by MITF in melanoma cells are lacking. To test whether MITF overexpression influences the activity of the *SLUG* gene promoter, we performed promoter-reporter assays in which the proximal promoter was cotransfected with the MITF expression construct into 501mel cells. Additionally, we compared activation by MITF-Vp16, a hyperactive MITF derivative in which the MITF N-terminal activation domain (AD) was replaced by a stronger Vp16 AD (39), with native MITF. While MITF had no effect on promoter activity, MITF-Vp16 increased it ~2-fold (Fig. 5A left). On the other hand, the

melastatin promoter, a known MITF target (33), was stimulated by both MITF and MITF-Vp16 ~4-fold and 10-fold, respectively (Fig. 5A middle). Western blotting verified the total MITF protein level (the control sample also showed the MITF protein signal because relatively high endogenous MITF protein is already present in nontransfected 501mel cells; Fig. 5A, right). Only transfected cells with ectopic MITF or MITF-Vp16 were measured for luciferase activity, which explained why promoter activity increased more compared with the overall MITF protein level. The same experiment was repeated with the FLAG-tagged vectors, and the same results were obtained. The expression of proteins expressed from transfected plasmids was verified with the anti-FLAG antibody (Fig. 5B).

To corroborate these results, doxycycline-regulatable melanoma cell lines, in which MITF could be downregulated by inducible expression of shRNA directed at MITF were used (32). Whereas a decrease in endogenous MITF protein was achieved after the addition of doxycycline in all cell lines, *Slug* expression remained unchanged. By contrast, the level of livin (ML-IAP), a known MITF target (40), mirrored the decrease in MITF protein (Fig. 5C). In agreement with this, overexpression of MITF did not change the endogenous level of *Slug* protein (data not shown). In a control experiment, inducible control nontargeting shRNA revealed no changes in the expression of all proteins tested. Thus, endogenous *Slug* seems to be expressed independently of MITF protein levels in human melanoma cells.

To further investigate the relationship between MITF and *Slug* and GLI2 vs. *Slug* protein expression in human samples, parallel sections of skin, nevus and melanoma metastasis were

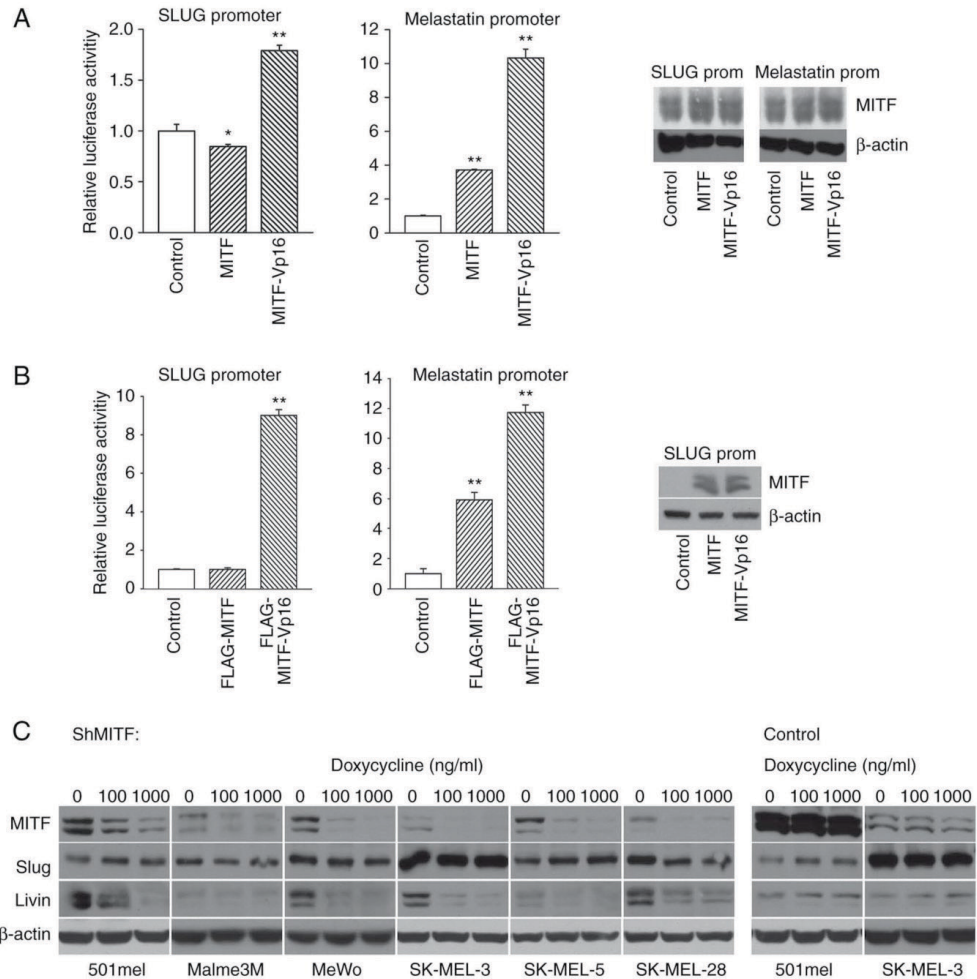


Figure 5. MIFF is an imperfect activator of Slug in 501mel melanoma cells. (A) Left, *SLUG* promoter activity is slightly decreased by cotransfection of the MIFF expression vector and activated ~twice by the MIFF-Vp16 chimeric hyperactive MIFF vector. Middle, the melastatin promoter is activated by both the MIFF and MIFF-Vp16 proteins. pcDNA3 plasmid served as a control. Three other melanoma cell lines likewise showed nonsignificant differences in the activity of the *SLUG* promoter compared with the control plasmid when cotransfected with the MIFF vector (not shown). Right, western blotting shows MIFF expression after transfection. The control sample also has a strong MIFF signal because the endogenous protein level is already present in naive 501mel cells. (B) Left, *SLUG* promoter activity after cotransfection of FLAG-tagged versions of the same plasmids as shown in (A). Middle, stimulation of melastatin promoter activity. Empty pFLAG-CMV-4 plasmid served as a control. Statistical analysis was as described in Materials and methods and verified using one-way ANOVA followed by Tukey's post hoc test and equal results (P-values) were obtained. Right, Western blotting performed with the anti-FLAG antibody show expression of FLAG-tagged proteins, the same pattern of expression was seen after the transfection of melastatin promoter (not shown). (C) Western blots depicting inducible knockdown of MIFF by tetracycline-regulatable shRNA repressing MIFF. Concomitant expression of Slug and livin proteins was observed in the same samples, whereas no change in Slug protein levels was observed. Six melanoma cell lines (left panel) and two control lines (right panel) were analyzed. β -actin detection served as a loading control for whole cell lysates (bottom). This figure is reprinted as a part of Figure 3 from our previously published paper Vlčková K *et al.*: Inducibly decreased MIFF levels do not affect proliferation and phenotype switching but reduce differentiation of melanoma cells (J. Cell. Mol. Med. 22, 2018, 2240-2251) (32), with the permission of the publisher (Wiley Global Permissions, permissions@wiley.com). MIFF, melanoma-associated transcription factor. * $P < 0.05$, ** $P < 0.01$.

compared by immunohistochemical staining (Fig. 6). Positive staining by anti-GLI2 and anti-Slug antibodies was observed in the epidermis of normal skin (scored 2-3), consistent with previous observations (41,42). Only a few strongly MIFF-positive (score 4) melanocytes were present in the epidermis.

GLI2 and Slug were also stained in nevus cells, albeit somewhat less intensively (score 2, rare cells scored 3 in Slug staining). The nevus showed abundant MIFF-positive cells (score 4). Epidermal keratinocytes were, as expected, MIFF-negative in the skin and nevus sections (score 0). In metastatic

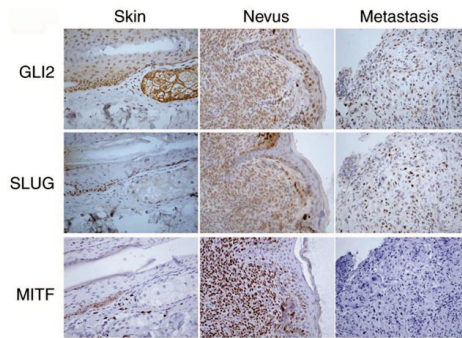


Figure 6. Slug and GLI2 expression correlate in serial sections of normal skin, nevus, and melanoma. Immunohistochemical staining was performed with antibodies against GLI2, Slug and MITF. For staining scores, see Results section (magnification, 400x). GLI, GLI family zinc finger; MITF, melanoma-associated transcription factor.

melanoma, both GLI2 and Slug staining was positive in ~half of the cell population (scored 2-4), with Slug staining slightly more positively than GLI2 staining. MITF-specific staining of metastatic melanoma was negative (score 0), with only a small number of positive cells (not shown in the picture). Sections that were negative or very slightly positive for MITF (scored 0-1) showed cells stained for both GLI2 and Slug (scores 2-3; Fig. 6). This is also consistent with the idea that invasive and metastatic cells have low or absent MITF (43). Notably, all three proteins were almost exclusively localized to the nucleus. Thus, Slug staining was associated with GLI2, but not MITF, positive staining in immunohistochemical sections of melanomas (Fig. 6). This result supports the aforementioned findings by demonstrating the positive regulation of Slug expression by GLI2, but not by MITF, in melanoma cells.

Discussion

The present study described the essential role of HH signaling and the transcription factor GLI2 in the transcription of the *SLUG* gene in human melanoma cells. The large number of GLI-binding sites present in the *SLUG* promoter led to the investigation of how GLI factors regulated *SLUG* gene expression. The presented data indicated that GLI factors activated the *SLUG* promoter in reporter assays and that the promoter was repressed by the HH signaling inhibitors GANT61 and cyclopamine. The most potent activator appeared to be GLI2. All GLI1-3 factors occupied the proximal *SLUG* promoter. Chromatin immunoprecipitation data revealed abundant and specific binding of GLI factors to four contiguous subregions of the proximal *SLUG* promoter. RT-qPCR, induced decrease of MITF and immunohistochemical experiments corroborated the foregoing data; GANT61 diminished Slug RNA abundance, decreased MITF and did not change Slug protein levels. In addition, the immunohistochemical analysis showed that MITF-negative portions of metastatic melanomas contained Slug-positive and GLI2-positive cells. Given that an extremely high number of GLI-binding sites are present in the *SLUG* promoter, the possibility that Slug

can also be upregulated by HH in other cancer cell types is worthy of further investigation. Of course, other transactivation mechanisms may also be plausible in different tumors beyond melanoma. For example, c-myc has been shown to regulate Slug expression in colon carcinoma, chronic myeloid leukemia, and neuroblastoma cells (44). C-myc-elicited EMT-like characteristics through *SLUG* gene activation in these cells. Homeobox C10 (HOXC10), which is a pro-oncogenic protein in cancer, has been shown to activate the *SLUG* promoter in melanoma through the YAP/TAZ signaling pathway (45). Das *et al* (46) reported that the oncogenic phenotype was induced by transcriptional upregulation of osteopontin through GLI1 in melanoma cells. Increased invasion, proliferation and migration was relieved by HH inhibitors. On the other hand, miR-33a-5p downregulates Slug in melanoma (47).

Previously, the essential role for HH signaling in melanoma has been demonstrated to occur mainly through the transcription factor GLI1 (6). Other signaling routes, such as RAS/MAPK and Akt/mTOR, regulate the nuclear localization of GLI1, not only in melanoma but also in other cancer cell types (6). Another report showed that GLI2 is capable of mediating the invasion and metastatic properties of melanoma (48). Furthermore, Slug is considered to be regulated by MITF, an essential transcription factor in melanoma (34). The present study showed that Slug expression depended mainly on the HH/GLI pathway. MITF probably does not serve any role in the endogenous expression of Slug because MITF downregulation had no effect on Slug protein levels in several melanoma cell lines. In the reporter assays, only the hyperactive MITF-Vp16 chimera, but not native MITF, activated the *SLUG* gene promoter (Fig. 5A).

It has been demonstrated that the oncogene *CRKL* is the downstream effector of GLI2 in lung adenocarcinoma cells (49). Crkl, which is oncogenic in several types of cancer, is activated by GLI2 through the binding of GLI2 to the site in the second intron of the *CRKL* gene. Blunting Crkl by shRNA or CRISPR-Cas9 knockout weakens the GLI2-elicited positive effect on cell viability, migration, invasion and colony formation. Thus, in lung adenocarcinoma, Crkl appears to be necessary for pro-oncogenic GLI2 effects and is itself regarded as an oncogene. For example, Crkl attenuates the therapeutic effect of several antioncogenic drugs (49) and has been found to be amplified in lung adenocarcinoma (50). It remains to be investigated whether Crkl is a general mediator of GLI factor activity in other tumor cell types. Although CRKL has been found to be amplified specifically in acral melanomas (51), no other data are available about the melanoma-specific role of the Crkl protein.

HH pathway and GLI factors are highly oncogenic and known to substantially contribute to the maintenance of CSC. In addition, GLIs are observed to be associated with EMT in various types of cancer (52-54). On the other hand, little data are available that GLI factors could be directly involved in the transcription of typical EMT-associated genes. In melanoma, GLI1 and GLI2 are reported to enhance transcription of Sox2, a stem cell marker (10). Furthermore, it was previously observed that EMT process is atypical in melanoma (55), as suggested in the present study. The present study clearly defined that GLIs, especially GLI2, are direct transcriptional regulators of Slug, a hallmark protein of EMT, in melanoma cells.

In melanoma, therapy is predominantly focused on targeting the mutated driver oncogenes BRAF and NRAS and/or kinases in the downstream MAPK signaling pathway. Unfortunately, therapies for advanced melanoma with low molecular weight inhibitors targeting these proteins result in acquired resistance. Despite advances in using a combination of drugs, the concept of targeting only the MAPK route remains questionable. As there are multiple mechanisms responsible for resistance to the inhibition of MAPK signaling in melanoma (56,57), alternative therapies should also be considered. Targeting HH and Bcl2 protein by the combination of GANT61 and obatoclox was effective in most melanoma cell lines tested previously (58). Taken together, the present study described a new mechanism of Slug transcription. It stressed the importance of the HH pathway for melanoma progression and suggested that targeting GLI2 in combination therapies could be beneficial for treatment, as GLI2 is a recognized transcriptional activator of a number of oncogenic proteins, including survivin (31). Although other mechanisms may play a role in Slug regulation in various types of cancer, the present study demonstrated that Slug is another HH/GLI target.

Acknowledgments

The authors thank Professor F. Aberger (University of Salzburg) for providing the PATCHED promoter plasmid and Professor R. Toftgard (Karolinska Institute) for the 12xGLI reporter plasmid.

Funding

The present study was supported by funding from the institutional programs PROGRESQ25 and Cooperatio (research areas SURG, MED BIOCHEM, METABOLISM, and ONCOLOGY) from Charles University Prague, from the League against Cancer Prague, and from the Conceptual Development of Research Organization, Motol University Hospital, Prague, funded by the Ministry of Health, Czech Republic (grant no. 6028). These funding organizations played no role in the analysis of the data or the preparation of this article.

Availability of data and materials

All data generated or analyzed during this study are included in this published article.

Authors' contributions

JV and PH conceived the project. JV and PH confirm the authenticity of all the raw data. PH, JR, KK, LO, JV and PZ performed the experiments. JB and JV Jr. performed the immunohistochemical experiments. PH and KK performed statistical analyses. PH and KK prepared the figures. PH and JV wrote the manuscript. All authors read and approved the manuscript.

Ethics approval and consent to participate

Immunohistochemical analysis of paraffin sections of human tissues was approved by the Ethical Committee of the

University Hospital Motol, Prague (approval no. EK-36/20). The study was carried out in accordance with the Declaration of Helsinki.

Patient consent for publication

Not applicable.

Competing interests

The authors declare that they have no competing interests.

References

1. Teglund S and Toftgård R: Hedgehog beyond medulloblastoma and basal cell carcinoma. *Biochim Biophys Acta* 1805: 181-208, 2010.
2. Varjosalo M and Taipale J: Hedgehog: Functions and mechanisms. *Genes Dev* 22: 2454-2472, 2008.
3. Marini KD, Payne BJ, Watkins DN and Martelotto LG: Mechanisms of Hedgehog signalling in cancer. *Growth Factors* 29: 221-234, 2011.
4. Jeng KS, Chang CF and Lin SS: Sonic Hedgehog signaling in organogenesis, tumors, and tumor microenvironments. *Int J Mol Sci* 21: 758, 2020.
5. Lauth M, Bergström A, Shimokawa T, Tostar U, Jin Q, Fendrich V, Guerra C, Barbacid M and Toftgård R: DYRK1B-dependent autocrine-to-paracrine shift of Hedgehog signaling by mutant RAS. *Nat Struct Mol Biol* 17: 718-725, 2010.
6. Stecca B, Mas C, Clement V, Zbinden M, Correa R, Piguet V, Beermann F, Ruiz JA and Altaba A: Melanomas require HEDGEHOG-GLI signaling regulated by interactions between GLI1 and the RAS-MEK/AKT pathways. *Proc Natl Acad Sci USA* 104: 5895-5900, 2007.
7. Riobó NA, Lu K, Ai X, Haines GM and Emerson CP Jr: Phosphoinositide 3-kinase and Akt are essential for Sonic Hedgehog signaling. *Proc Natl Acad Sci USA* 103: 4505-4510, 2006.
8. Mangelberger D, Kern D, Loipetzberger A, Eberl M and Aberger F: Cooperative Hedgehog-EGFR signaling. *Front Biosci (Landmark Ed)* 17: 90-99, 2012.
9. Faião-Flores F, Alves-Fernandes DK, Pennacchi PC, Sandri S, Vicente AL, Scapulatempo-Neto C, Vazquez VL, Reis RM, Chauhan J, Goding CR, *et al.*: Targeting the hedgehog transcription factors GLI1 and GLI2 restores sensitivity to vemurafenib-resistant human melanoma cells. *Oncogene* 36: 1849-1861, 2017.
10. Santini R, Pietrobono S, Pandolfi S, Montagnani V, D'Amico M, Penachioni JY, Vinci MC, Borgognoni L and Stecca B: SOX2 regulates self-renewal and tumorigenicity of human melanoma-initiating cells. *Oncogene* 33: 4697-4708, 2014.
11. Pandolfi S, Montagnani V, Lapucci A and Stecca B: HEDGEHOG/GLI-E2F1 axis modulates iASPP expression and function and regulates melanoma cell growth. *Cell Death Differ* 22: 2006-2019, 2015.
12. Nieto MA: The snail superfamily of zinc-finger transcription factors. *Nat Rev Mol Cell Biol* 3: 155-166, 2002.
13. Cohen ME, Yin M, Paznekas WA, Schertzer M, Wood S and Jabs EW: Human SLUG gene organization, expression, and chromosome map location on 8q. *Genomics* 51: 468-471, 1998.
14. Pérez-Mancera PA, González-Herrero I, Maclean K, Turner AM, Yip MY, Sánchez-Martín M, García JL, Robledo C, Flores T, Gutiérrez-Adán A, *et al.*: SLUG (SNAI2) overexpression in embryonic development. *Cytogenet Genome Res* 114: 24-29, 2006.
15. Wang Y, Shi J, Chai K, Ying X and Zhou BP: The role of snail in EMT and tumorigenesis. *Curr Cancer Drug Targets* 13: 963-972, 2013.
16. Bolós V, Peinado H, Pérez-Moreno MA, Fraga MF, Esteller M and Cano A: The transcription factor Slug represses E-cadherin expression and induces epithelial to mesenchymal transitions: A comparison with Snail and E47 repressors. *J Cell Sci* 116: 499-451, 2003.
17. Wels C, Joshi S, Koefinger P, Bergler H and Schaidt H: Transcriptional activation of ZEB1 by Slug leads to cooperative regulation of the epithelial-mesenchymal transition-like phenotype in melanoma. *J Invest Dermatol* 131: 1877-1885, 2011.

18. Casas E, Kim J, Bendesky A, Ohno-Machado L, Wolfe CJ and Yang J: Snail2 is an essential mediator of Twist1-induced epithelial mesenchymal transition and metastasis. *Cancer Res* 71: 245-254, 2011.
19. Brabletz S, Schuhwerk H, Brabletz T and Stemmler MP: Dynamic EMT: A multi-tool for tumor progression. *EMBO J* 40: e108647, 2021.
20. Pérez-Mancera PA, González-Herrero I, Pérez-Caro M, Gutiérrez-Cianca N, Flores T, Gutiérrez-Adán A, Pintado B, Sánchez-Martín M and Sánchez-García I: SLUG in cancer development. *Oncogene* 24: 3073-3082, 2005.
21. Cobaleda C, Pérez-Caro M, Vicente-Dueñas C and Sánchez-García I: Function of the zinc-finger transcription factor SNAI2 in cancer and development. *Annu Rev Genet* 41: 41-61, 2007.
22. Barbato L, Bocchetti M, Di Biase A and Regad T: Cancer stem cells and targeting strategies. *Cells* 8: 926, 2019.
23. Fenouille N, Tichet M, Dufies M, Pottier A, Mogha A, Soo JK, Rocchi S, Mallavialle A, Galibert MD, Khammari A, *et al*: The epithelial-mesenchymal transition (EMT) regulatory factor SLUG (SNAI2) is a downstream target of SPARC and AKT in promoting melanoma cell invasion. *PLoS One* 7: e40378, 2012.
24. Guo Q, Ning F, Fang R, Wang HS, Zhang G, Quan MY, Cai SH and Du J: Endogenous Nodal promotes melanoma undergoing epithelial-mesenchymal transition via Snail and Slug in vitro and in vivo. *Am J Cancer Res* 5: 2098-2112, 2015.
25. Pearlman RL, Montes de Oca MK, Pal HC and Afaq F: Potential therapeutic targets of epithelial-mesenchymal transition in melanoma. *Cancer Lett* 391: 125-140, 2017.
26. Arienti C, Tesei A, Carloni S, Ulivi P, Romeo A, Ghigi G, Menghi E, Sarnelli A, Parisi E, Silvestrini R and Zoli W: SLUG silencing increases radiosensitivity of melanoma cells in vitro. *Cell Oncol (Dordr)* 36: 131-139, 2013.
27. Gupta PB, Kuperwasser C, Brunet JP, Ramaswamy S, Kuo WL, Gray JW, Naber SP and Weinberg RA: The melanocyte differentiation program predisposes to metastasis after neoplastic transformation. *Nat Genet* 37: 1047-1054, 2005.
28. Shirley SH, Greene VR, Duncan LM, Torres Cabala CA, Grimm EA and Kusewitt DF: Slug expression during melanoma progression. *Am J Pathol* 180: 2479-2489, 2012.
29. Caramel J, Papadogeorgakis E, Hill L, Browne GJ, Richard G, Wierinckx A, Saldanha G, Osborne J, Hutchinson P, Tse G, *et al*: A switch in the expression of embryonic EMT-inducers drives the development of malignant melanoma. *Cancer Cell* 24: 466-480, 2013.
30. Gunarta IK, Li R, Nakazato R, Suzuki R, Boldbaatar J, Suzuki T and Yoshioka K: Critical role of glioma-associated oncogene homolog 1 in maintaining invasive and mesenchymal-like properties of melanoma cells. *Cancer Sci* 108: 1602-1611, 2017.
31. Vlčková K, Ondrušová L, Vachtenheim J, Réda J, Dundr P, Zadinová M, Žáková P and Poučková P: Survivin, a novel target of the Hedgehog/GLI signaling pathway in human tumor cells. *Cell Death Dis* 7: e2048, 2016.
32. Vlčková K, Vachtenheim J, Réda J, Horák P and Ondrušová L: Inducibly decreased MITF levels do not affect proliferation and phenotype switching but reduce differentiation of melanoma cells. *J Cell Mol Med* 22: 2240-2251, 2018.
33. Miller AJ, Du J, Rowan S, Hershey CL, Widlund HR and Fisher DE: Transcriptional regulation of the melanoma prognostic marker melastatin (TRPM1) by MITF in melanocytes and melanoma. *Cancer Res* 64: 509-516, 2004.
34. Sánchez-Martín M, Rodríguez-García A, Pérez-Losada J, Sgrera A, Read AP and Sánchez-García I: SLUG (SNAI2) deletions in patients with Waardenburg disease. *Hum Mol Genet* 11: 3231-3236, 2002.
35. Sánchez-Martín M, Pérez-Losada J, Rodríguez-García A, González-Sánchez B, Korf BR, Kuster W, Moss C, Spritz RA and Sánchez-García I: Deletion of the SLUG (SNAI2) gene results in human piebaldism. *Am J Med Genet A* 122A: 125-132, 2003.
36. Goodall J, Carreira S, Denat L, Kobi D, Davidson I, Nuciforo P, Sturm RA, Larue L and Goding CR: Brn-2 represses microphthalmia-associated transcription factor expression and marks a distinct subpopulation of microphthalmia-associated transcription factor-negative melanoma cells. *Cancer Res* 68: 7788-7794, 2008.
37. Roessler E, Ermilov AN, Grange DK, Wang A, Grachtchouk M, Dlugosz AA and Muenke M: A previously unidentified amino-terminal domain regulates transcriptional activity of wild-type and disease-associated human GLI2. *Hum Mol Genet* 14: 2181-2188, 2005.
38. Kumasaka M, Sato S, Yajima I, Goding CR and Yamamoto H: Regulation of melanoblast and retinal pigment epithelium development by *Xenopus laevis* Mitf. *Dev Dyn* 234: 523-534, 2005.
39. Vachtenheim J and Drdová B: A dominant negative mutant of microphthalmia transcription factor (MITF) lacking two transactivation domains suppresses transcription mediated by wild type MITF and a hyperactive MITF derivative. *Pigment Cell Res* 17: 43-50, 2004.
40. Dynek JN, Chan SM, Liu J, Zha J, Fairbrother WJ and Vucic D: Microphthalmia-associated transcription factor is a critical transcriptional regulator of melanoma inhibitor of apoptosis in melanomas. *Cancer Res* 68: 3124-3132, 2008.
41. Ikram MS, Neill GW, Regl G, Eichberger T, Frischauf AM, Aberger F, Quinn A and Philpott M: GLI2 is expressed in normal human epidermis and BCC and induces GLI1 expression by binding to its promoter. *J Invest Dermatol* 122: 1503-1509, 2004.
42. Parent AE, Choi C, Caudy K, Gridley T and Kusewitt DF: The developmental transcription factor slug is widely expressed in tissues of adult mice. *J Histochem Cytochem* 52: 959-965, 2004.
43. Müller J, Krijgsman O, Tsoi J, Robert L, Hugo W, Song C, Kong X, Possik PA, Cornelissen-Steijger PD, Geukes Foppen MH, *et al*: Low MITF/AXL ratio predicts early resistance to multiple targeted drugs in melanoma. *Nat Commun* 5: 5712, 2014.
44. Tanno B, Sesti F, Cesi V, Bossi G, Ferrari-Amorotti G, Bussolari R, Tirindelli D, Calabretta B and Raschella G: Expression of Slug is regulated by c-Myb and is required for invasion and bone marrow homing of cancer cells of different origin. *J Biol Chem* 285: 29434-29445, 2010.
45. Miao Y, Zhang W, Liu S, Leng X, Hu C and Sun H: HOXC10 promotes growth and migration of melanoma by regulating Slug to activate the YAP/TAZ signaling pathway. *Discov Oncol* 12: 12, 2021.
46. Das S, Harris LG, Metge BJ, Liu S, Riker AI, Samant RS and Shevde LA: The hedgehog pathway transcription factor GLI1 promotes malignant behavior of cancer cells by up-regulating osteopontin. *J Biol Chem* 284: 22888-22897, 2009.
47. Zhang ZR and Yang N: MiR-33a-5p inhibits the growth and metastasis of melanoma cells by targeting SNAI2. *Neoplasia* 67: 813-824, 2020.
48. Alexaki VI, Javelaud D, Van Kempen LC, Mohammad KS, Dennler S, Luciani F, Hoek KS, Hugé P, Goydos JS, Fournier PJ, *et al*: GLI2-mediated melanoma invasion and metastasis. *J Natl Cancer Inst* 102: 1148-1159, 2010.
49. Liu X, Hu Y, Yu B, Peng K and Gan X: CRKL is a critical target of Hh-GLI2 pathway in lung adenocarcinoma. *J Cell Mol Med* 25: 6280-6288, 2021.
50. Kim YH, Kwei KA, Girard L, Salari K, Kao J, Pacyna-Gengelbach M, Wang P, Hernandez-Boussard T, Gazdar AF, Petersen I, *et al*: Genomic and functional analysis identifies CRKL as an oncogene amplified in lung cancer. *Oncogene* 29: 1421-1430, 2010.
51. Weiss JM, Hunter MV, Cruz NM, Baggiolini A, Tagore M, Ma Y, Misale S, Marasco M, Simon-Vermot T, Campbell NR, *et al*: Anatomic position determines oncogenic specificity in melanoma. *Nature* 604: 354-361, 2022.
52. Jiang L, Huang J, Hu Y, Lu P, Luo Q and Wang L: Gli promotes tumor progression through regulating epithelial-mesenchymal transition in non-small-cell lung cancer. *J Cardiothorac Surg* 15: 18, 2020.
53. Chun HW and Hong R: Significance of the hedgehog pathway-associated proteins Gli-1 and Gli-2 and the epithelial-mesenchymal transition-associated proteins Twist and E-cadherin in hepatocellular carcinoma. *Oncol Lett* 3: 1753-1762, 2016.
54. Wang L, Jin JQ, Zhou Y, Tian Z, Jablons DM and He B: Gli is activated and promotes epithelial-mesenchymal transition in human esophageal adenocarcinoma. *Oncotarget* 9: 853-865, 2017.
55. Kim JE, Leung E, Baguley BC and Finlay GJ: Heterogeneity of expression of epithelial-mesenchymal transition markers in melanocytes and melanoma cell lines. *Front Oncol* 4: 97, 2013.
56. Davies MA and Kopetz S: Overcoming resistance to MAPK pathway inhibitors. *J Natl Cancer Inst* 105: 9-10, 2013.
57. Vachtenheim J and Ondrušová L: Many distinct ways lead to drug resistance in BRAF- and NRAS-mutated melanomas. *Life (Basel)* 11: 424, 2021.
58. Vlčková K, Réda J, Ondrušová L, Krayem M, Ghanem G and Vachtenheim J: GLI inhibitor GANT61 kills melanoma cells and acts in synergy with obatocax. *Int J Oncol* 49: 953-960, 2016.



This work is licensed under a Creative Commons Attribution-NonCommercial-NoDerivatives 4.0 International (CC BY-NC-ND 4.0) License.

Table SI. Melanoma cell lines used in the present study.

Cell line	Tumor type	Source
Hbl	Malignant melanoma	Dr. G. Ghanem-Free University of Brussels
Malme-3M	Malignant melanoma	American Type Culture Collection
MeWo	Malignant melanoma	American Type Culture Collection
SK-MEL-2	Malignant melanoma	American Type Culture Collection
SK-MEL-3	Malignant melanoma	American Type Culture Collection
SK-MEL-5	Malignant melanoma	American Type Culture Collection
SK-MEL-28	Malignant melanoma	American Type Culture Collection
501mel	Malignant melanoma	Dr. R. Halaban-Yale University

Table SII. Mutational status of cell lines.

Cell line	Mutation	Reference
Hbl	wt	Herraiz C et al.: <i>Int. J. Biochem. Cell. Biol.</i> 2012, 44:2244-2252.
Malme-3M	V600E amplified	Wajapeyee N et al.: <i>Cell</i> 2008, 132:363-364.
MeWo	wt	Domenzain-Reyna C et al.: <i>J. Biol. Chem.</i> 2009, 284:12306-12317.
SK-MEL-2	NRASQ61R	Singh S et al.: <i>Mol. Cancer Ther.</i> 2010, 9:3330-3341. Wajapeyee N et al.: <i>Cell</i> 2008, 132:363-364.
SK-MEL-3	BRAFV600E	Mazzio EA and Soliman KFA: <i>Cancer Genomics & Proteomics</i> 2018, 15:349-364.
SK-MEL-5	BRAFV600E heterozyg.	Singh S et al.: <i>Mol. Cancer Ther.</i> 2010, 9:3330-3341.
SK-MEL-28	BRAFV600E homozyg.	Smalley et al.: <i>Mol. Cancer Ther.</i> 2008, 7:2876-2883. Singh S et al.: <i>Mol. Cancer Ther.</i> 2010, 9:3330-3341. Wajapeyee N et al.: <i>Cell</i> 2008, 132:363-364.
501mel	BRAFV600E amplified	Packer LM et al.: <i>Pigment Cell & Melanoma Res.</i> 2009, 22:785-798.

wt, wild type (no BRAF or NRAS mutations).

Table SIII.31 GLI-binding sites in the proximal (-2092+112) SLUG promoter. Mismatched oligonucleotides are shown in bold and two mismatches are marked in green. All other sites contain three mismatches.

Position of GLI binding sites in SLUG promoter	Sequence	Position of GLI binding sites in SLUG promoter	Sequence
+102 to +110	GACCGCCGT	-1091 to -1099	GACCATACA
-15 to -23	ACCCTCCCA	-1119 to -1127	AACCACCTG
-64 to -72	AACCTCTCA	-1235 to -1243	AGGGTGATC
-119 to -127	GACAACAGA	-1325 to -1333	GACAATGCA
-152 to -160	AACAGCCCA	-1379 to -1387	AAACACACA
-223 to -231	GCTCACCGA	-1387 to -1395	CACCCTCCA
-254 to -262	TAGCTCCCA	-1401 to -1409	TGAGTGCCC
-363 to -371	AGGGCGGCC	-1561 to -1569	TGTGTGGAG
-373 to -381	GGTGTGGTG	-1702 to -1710	TGTGTGTTT
-383 to -391	AGGCTGGCC	-1738 to -1746	TGTGTTTTC
-452 to -460	TATTTGGTC	-1833 to -1841	TACCAGCAA
-788 to -796	CCGGTGGTT	-1869 to -1877	GAATACACA
-871 to -879	TACAACCCT	-1937 to -1945	TCTGTGATC
-880 to -888	AAAGACCCA	-1982 to -1990	GTGCACCCT
-927 to -935	CACCACATA	-2016 to -2024	GGTGTGGCC
-1051 to -1059	TGGGTCTT		

GLI consensus binding sites: GACCACCCA and TGGGTGGTC

Table SIV. Quantification of ChIP PCR bands (Fig. 4). The numbers are arbitrary units corresponding to the strength of each band. GLI1-3 were immunoprecipitated by a specific antibody for each protein (see Materials and methods). The quantification was performed by the ImageJ software.

Segment A	Input	IgG	GLI	H3
GLI1	13753	0	19068	20330
GLI2	12286	0	16124	19302
GLI3	11033	0	5866	6389
Segment B	Input	IgG	GLI	H3
GLI1	11814	0	0	28113
GLI2	21000	0	0	21956
GLI3	25998	0	15803	29607
Segment C	Input	IgG	GLI	H3
GLI1	29550	0	20561	23168
GLI2	19341	0	6356	4519
GLI3	16739	0	16613	11995
Segment D	Input	IgG	GLI	H3
GLI1	20843	0	11166	30365
GLI2	29220	0	16356	32008
GLI3	16984	0	0	23562

Figure S1. Decrease of Slug protein level in human melanocytes and two melanoma cell lines (SK-MEL-2 and Hbl) after the GANT61 treatment. GANT61 treatment and western blotting were performed as described in Fig. 1B. The same anti-Slug and anti- β -actin antibodies were used. He-MN-LP, normal human melanocytes (low pigmentation).

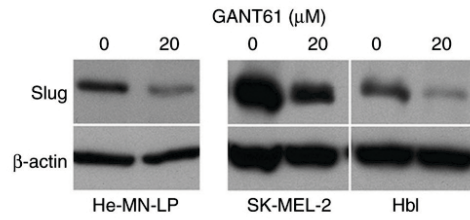
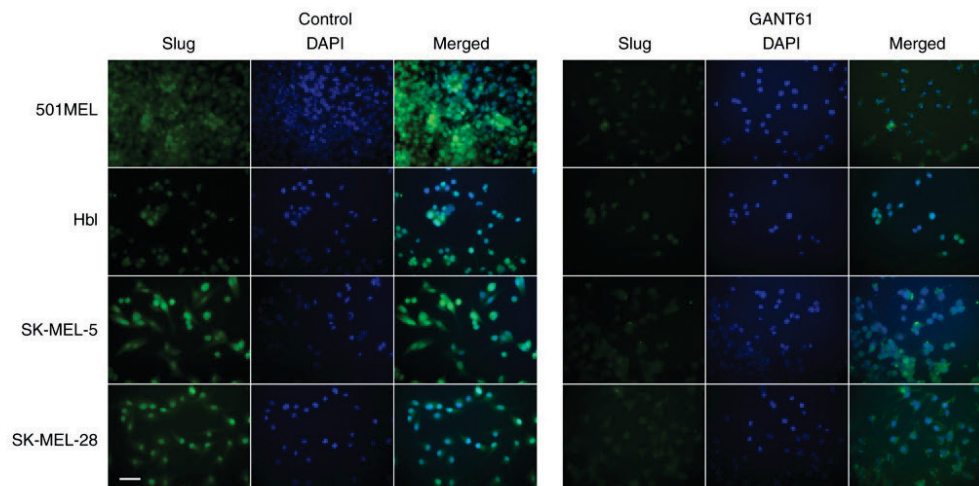


Figure S2. Representative immunofluorescent image indicating the decrease of Slug expression by GANT61 in four melanoma cell lines. Left panel shows the cells treated only by vehicle (DMSO), right panel depicts the low Slug expression after GANT61 application. Cells were treated with GANT61 for 20 h and processed for immunofluorescence. The left columns indicate staining with anti-Slug antibody. The same fields are visualized also by DAPI staining. Scale bar, 20 μ m.





Article

Widespread Expression of Hedgehog Pathway Components in a Large Panel of Human Tumor Cells and Inhibition of Tumor Growth by GANT61: Implications for Cancer Therapy

Jiri Réda ¹, Jiri Vachtenheim ^{1,*}, Kateřina Vlčková ¹, Pavel Horák ¹, Jiri Vachtenheim, Jr. ² and Lubica Ondrušová ¹

¹ Department of Transcription and Cell Signaling, Institute of Medical Biochemistry and Laboratory Diagnostics, Charles University Prague, 12108 Prague, Czech Republic; RedaJ@seznam.cz (J.R.); vlckova.katka@centrum.cz (K.V.); ppavel.horak@gmail.com (P.H.); lubica.ondrusova@gmail.com (L.O.)

² Third Department of Surgery, First Faculty of Medicine, Charles University Prague and University Hospital Motol, 15006 Prague, Czech Republic; jcdv@seznam.cz

* Correspondence: jiri.vachtenheim@lf1.cuni.cz

Received: 5 August 2018; Accepted: 6 September 2018; Published: 10 September 2018



Abstract: The sonic Hedgehog/GLI signaling pathway (HH) is critical for maintaining tissue polarity in development and contributes to tumor stemness. Transcription factors GLI1–3 are the downstream effectors of HH and activate oncogenic targets. To explore the completeness of the expression of HH components in tumor cells, we performed a screen for all HH proteins in a wide spectrum of 56 tumor cell lines of various origin using Western blot analysis. Generally, all HH proteins were expressed. Important factors GLI1 and GLI2 were always expressed, only exceptionally one of them was lowered, suggesting the functionality of HH in all tumors tested. We determined the effect of a GLI inhibitor GANT61 on proliferation in 16 chosen cell lines. More than half of tumor cells were sensitive to GANT61 to various extents. GANT61 killed the sensitive cells through apoptosis. The inhibition of reporter activity containing 12xGLI consensus sites by GANT61 and cyclopamine roughly correlated with cell proliferation influenced by GANT61. Our results recognize the sensitivity of tumor cell types to GANT61 in cell culture and support a critical role for GLI factors in tumor progression through restraining apoptosis. The use of GANT61 in combined targeted therapy of sensitive tumors, such as melanomas, seems to be immensely helpful.

Keywords: Hedgehog; GLI; tumor cell lines; GANT61; apoptosis

1. Introduction

The Hedgehog (HH) signaling pathway is a morphogenesis pathway crucial for the growth and patterning of various tissues during embryonic development [1,2]. The morphogen sonic Hedgehog binds the transmembrane receptor Patched (PTCH), which activates another transmembrane protein Smoothened (SMO) and triggers the HH pathway that influences the expression of many genes through the activation of transcription factors GLI1 and GLI2. GLI3 activates only exceptionally and behaves rather as a suppressor. HH components are highly conserved from fly to human [3]. Initially, the HH pathway was linked to the etiology of basal cell carcinoma and medulloblastoma [4–8]. The pathway transcriptionally upregulates the expression of survivin in more than half of analyzed cell lines [9]. Accumulating evidence suggests that the HH pathway is critical for almost all tumors. It has been found that HH signaling plays key roles in formation and maintenance of cancer stem cells (CSC), tumor stemness, and acquisition of epithelial-to-mesenchymal transition (EMT) in tumors. Since EMT

is important and responsible for cancer cell invasion, metastasis, drug resistance, and tumor recurrence, the HH signaling pathway is now believed to be an important target for cancer therapy [10–13]. The HH pathway and GLI factors thus appear to be promising targets for cancer therapy [14]. Several cancers were shown to be sensitive to HH inhibition, such as lung cancer (both non-small cell lung cancer (NSCLC) [15–18] and small cell lung cancer (SCLC) [19,20]). Many reports highlight the importance of the HH pathway in pancreatic cancer and the usefulness of its inhibition [21–24]. The HH pathway was described to be crucial for the pancreatic cancer development and HH inhibition caused autophagy in CFPAC-1 cells *in vivo* and in mouse xenografts [25]. GLI1 promoted EMT and metastasis in pancreatic cells in a genome-wide screening study [26]. In many other cancer types, the HH pathway inhibition decreases the oncogenicity and has been beneficial for the patients. Melanomas critically require HH signaling [27–29], presumably with activated RAS-MAPK and AKT signaling cascades [27]. HH has been described to promote oncogenesis in leukemias [30–34], bladder cancer [35], and prostate cancer [36–39].

Global significance of the HH pathway for tumor initiation, progression, and metastasis is documented by additional literature. Mounting evidence indicates that HH signaling is required for the maintenance of glioblastoma and its CSC population [40,41]. GLI2 has been identified as a target for the treatment of osteosarcoma [42] and the HH pathway has been reported to be important for osteosarcoma progression and metastasis [43]. HH signaling produces self-renewal in embryonal rhabdomyosarcoma [44], has a critical role in the growth of neuroblastoma [45], ovarian cancer [46,47], hepatocellular carcinoma [48], colon carcinoma [49,50], and is pivotal for forming breast cancer CSC [51] and bone metastases [52]. Rhabdoid tumors and cell lines lack INI1 (SMARCB1/SNF5) tumor suppressor. This is a causative event in these tumors. This protein is central in the nucleosome remodeling complex SWI/SNF and is also rarely absent in rhabdomyosarcomas. It was found that INI1 binds GLI1. In the presence of INI1, the HH pathway is silent and the loss of INI1 triggers the activation of the HH pathway in rhabdoid tumors [53]. Ectopic INI1 is able to rescue the nonmalignant phenotype in rhabdoid tumor cell lines. This implies that an activated HH cascade causes this tumor type. This is intriguing because INI1 is present in all other cells including tumor cells with an elevated HH pathway activity (above). This implies a very specific cell context in rhabdoid tumors and suggests the HH pathway as a target for their treatment.

Several studies have implicated a noncanonical activation of the HH route in tumors, thus abrogating the necessity of upstream ligand signaling. Through this mechanism, GLI factors can be activated directly by many different mechanisms upregulated in tumor cells, predominantly operating in RAS/MAPK, Wnt, or AKT pathways [38,54–57]. As an example, KRAS activates GLI1 in pancreatic cancer cells [58], an androgen receptor (AR) protects GLI3 from proteolytic cleavage [38], and HH can be activated by the mTOR/S6K1 signaling [59]. This allows the processing of the deregulated HH pathway without the membrane signaling through direct aberrant GLI factors stimulation with the consequent expression of their prooncogenic targets. Here, we present results showing that the main components of the HH pathway are invariably expressed across a large panel of tumor cells of various cancer types. The most potent HH inhibitor GANT61 suppressed proliferation more or less in about half of tumor cell lines (the sensitive cells were eradicated presumably through apoptosis) and is a prime candidate as a compound for the combined therapy in many tumor types.

2. Results

2.1. Broad Expression of HH Cascade Components in Human Tumor Cell Lines

We were interested in studying whether constituents of the HH pathway are invariably present in several tumor cell types or if some components are missing. It would potentially disable the activation of HH pathway in human cancer cell lines. A large screen has been performed and Western blots have shown complete expression of the main HH components in all tumor cells (Figure 1). Noteworthy, two lines expressed negligible GLI1 (G-401 and NCI H446), whereas GLI2 in them was

expressed abundantly. In some other cells, GLI2 was low but GLI1 sufficiently expressed (RPMI-7951, Calu-1, HeLa S3, H-209, H-345, and Jurkat). The SuFu level was low in Hbl and H69 cells. In some tumor cell lines, expression of GLI3 was lower (DOR, Saos-2, and H-196). GLI3 is nevertheless only exceptionally necessary for processing of HH signals, whereas either GLI1 or GLI2 are generally required. Patched was weak in Saos-2 and Jurkat cells, and SMO was weakly expressed only in H-69 cells.

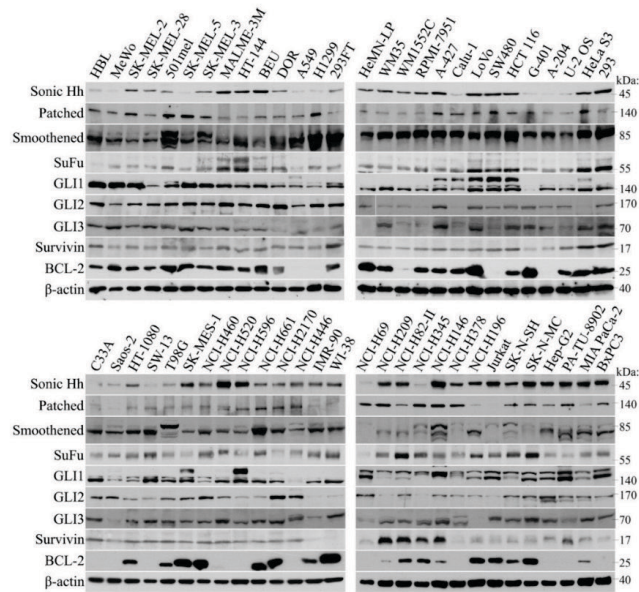


Figure 1. Panel of protein expression pattern of HH signaling components. Western blots made in RIPA extracts (30 µg) were probed with indicated antibodies. With some small exceptions, all HH proteins were expressed, although sometimes the expression level was weaker (see text). Survivin, an HH target, was invariably present in tumor cell lines. Notably, GLI3 was shown as a fragment that was cleaved off from the whole protein during sample preparation. However, its signals represent the true amount of intact GLI3 in the extract. The size of each protein is shown in kDa on the right.

Very peculiar was a varying expression of the ligand sonic Hedgehog among the cell lines, irrespective of the tumor type. This nevertheless does not preclude the efficient functioning of the HH pathway, since, in view of the fact that HH is frequently activated noncanonically at the GLI factors level, the production of the ligand itself (acting by an autocrine or paracrine manner in cell lines) is dispensable. Three cell lines were nontransformed and tested for comparison with tumor cells (HeMN-LP, IMR-90, and WI-38). HeMN-LP (melanocytes) expressed both GLI2 and GLI1, but the two fibroblast cell lines expressed very low GLI2, but retained their GLI1 level. Expression of other components was retained in these normal cell lines. Survivin was present in all tumor cell lines. Our previous results have shown that in IMR90 cells, transfected GLI2 plasmid is capable of evoking the expression of endogenous survivin [9], which underlies the necessity of HH signaling for the survivin expression even in normal cells. BCL-2, another important antiapoptotic protein, was abundantly present in the majority of cell lines, however, in some tumors its expression was completely lacking, independently of the tumor type. Together, the widespread abundance of HH components indirectly support the importance of the HH signaling in tumors and is in accord with the previous results.

2.2. Inhibition of Cell Proliferation by GLI Inhibitor GANT61

We next tested the sensitivity to a GLI inhibitor GANT61 in a panel of 16 tumor cell lines (Figure 2). The tumor types included melanomas, NSCLC and SCLC, osteosarcomas, neuroblastomas, rhabdoid tumors, hepatocellular carcinoma, and pancreatic cancers. Some cells were eradicated completely at the end of the experiment (SK-MEL-3, U-2 OS, MeWo, SK-N-MC, and H196). Another group of cells was only partially sensitive to GANT61 under the experimental conditions (Saos-2, SK-N-SH, G-401, and BxPC-3). The remaining cell lines did not reveal any sensitivity when cultured in GANT61 (A549, Calu-1, A-201, Hep-G2, and the three pancreatic cancer cell lines MIA PaCa-2, PANC-1, and PA-TU-8902). The pancreatic tumors were surprisingly most resistant to GANT61 treatment, although previous reports describe their sensitivity to the blocking of HH signaling [21,60].

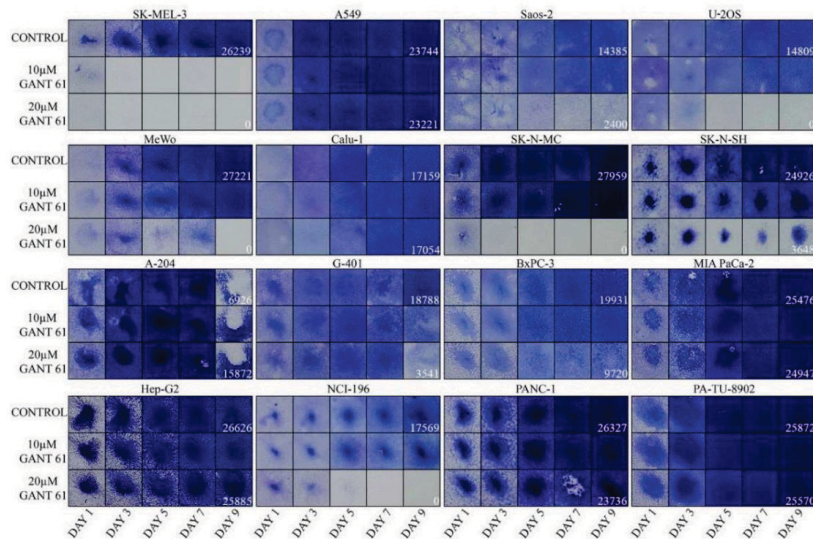


Figure 2. Proliferation assays showing the sensitivity to GANT61. The intensity of staining with crystal violet indicates the relative number of cells. The quantification numbers are given only for day 9 for controls and GANT61 (20 μ M) as these fields were the most important outcome of the experiment. Please note that the lower number of A-204 control cells at day 9 is caused by cell detachment. Two experiments with similar results were performed and one is presented. Results are shown as squares cut from the 12-well plate wells.

Expectedly, melanomas were sensitive to GANT61 (Figure 2). We have previously tested melanoma cells and found that GANT61 was variably effective in all tumors. The combination with obatoclax (a BCL-2 family inhibitor) revealed a better effect, showing clear synthetic lethality in six of nine melanoma lines [29] (Figure S1). The most sensitive cell line was SK-MEL-3. Here, less responsive were two osteosarcomas and one SCLC. Also, G-401 was sensitive, but only at day 9. Two neuroblastoma cell lines responded to GANT61 as well. Other cell lines did not reveal any GANT61 sensitivity even after day 9 (A-204, Hep-G2, NSCLC, and pancreatic cell lines from which only BxPC-3 reacted slightly, Figure 2). It is important to note that with the exception of the extremely sensitive SK-MEL-3, all other cells responded only to 20 μ M GANT61 and were insensitive to a 10 μ M concentration. We can speculate that higher doses of GANT61 or a prolonged time of treatment would have a better effect in eradicating tumor cells. In our assays, longer incubation time was precluded as untreated control cells would overgrow and detach. Our findings suggest that the testing of cancer

cell types might be useful for further consideration of therapy and show that more than half of tested tumors (when we include melanoma cells from Figure S1) were more or less sensitive to 20 μ M of GANT61 when observed up to 9 days.

2.3. GANT61 Eradicates Tumor Cells through Apoptosis

To gain insight into the mechanism underlying the eradication of cells in proliferation assays, we carried out the TUNEL assay that detects apoptosis. Many previous papers indicate that GANT61 kills the cells through apoptosis [29,49,57,61]. We have chosen two GANT61-sensitive tumors cell lines, SK-MEL-3 (see Figure 2) and SK-MEL-5 (see Figure S1). Cells were treated with 20 μ M GANT61 for 3 days and both detached and attached cells were combined and analyzed using flow cytometry. The extent of apoptosis was analyzed by a TUNEL assay (Figure 3A). The GANT61-treated cells revealed massive apoptosis (reflected by the FITC staining, about 60% of apoptotic cells in SK-MEL-3 and 50% in SK-MEL-5 cells, right peaks, left panels, Figure 3A), while negligible apoptosis was observed in control cells. No cell cycle alteration was seen. We thus presume that no stable blockade of the cell cycle occurred, as the cells stepwise disappeared, although sometimes slowly, which was caused by cell detachment. Since it has been reported that GANT61 may cause autophagy in some cell types [25,62], it can also be possible that in some cell lines, the elimination of cells could be brought about by autophagy. However, it is highly probable that most cells were eradicated by apoptosis as it is a well-known consequence of GANT61 treatment. To corroborate the results in Figure 3A, we left the same cells in a normal medium or medium with 20 μ M GANT61 for 3 days, fixed the cells, and mounted in DAPI-containing medium. Apoptotic figures were seen in both cell types, whereas no apoptotic nuclei were present in controls (Figure 3B).

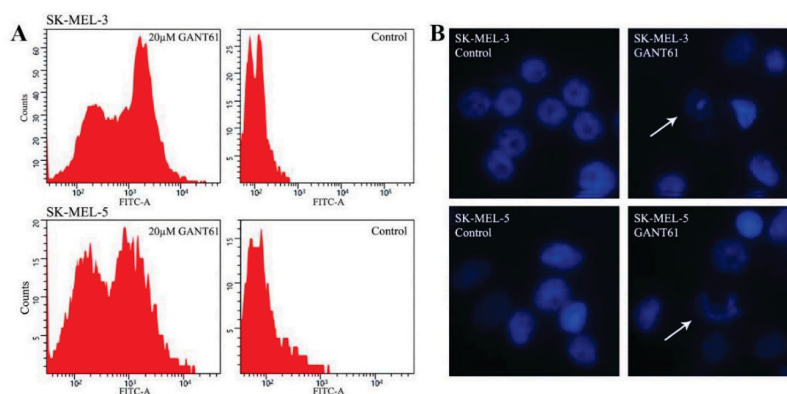


Figure 3. (A) TUNEL assay detecting apoptosis in two cell lines. Cells were seeded on 60-mm dishes, and the next day, 20 μ M GANT61 was added. The normal medium was replaced in controls. After three days, the majority of cells treated with GANT61 detached in both SK-MEL-3 and SK-MEL-5 cells. Both detached and remaining attached cells were used for analysis. FITC fluorescence clearly shows massive apoptosis in GANT61-treated cells. The percentage of the apoptotic and nonapoptotic cells were calculated using ImageJ software (National Institutes of Health, Bethesda, MD, USA). The results of cell quantification were as follows. SK-MEL-3 cells treated with GANT61: apoptotic cells 62.62%, nonapoptotic cells 37.38%; SK-MEL-3 controls: apoptotic cells 0.4%, nonapoptotic cells 99.6%. SK-MEL-5 cells treated with GANT61: apoptotic cells 51.97%, nonapoptotic cells 48.03%; SK-MEL-5 controls: apoptotic cells 4.18%, nonapoptotic cells 95.82%. No cell cycle blockade was observed. (B) Fluorescence showing apoptotic nuclei in the same cells as in (A), treated equally with GANT61 or untreated (control cells). Cells were mounted in a medium containing DAPI and documented by fluorescence. Magnification: 200 \times . Arrows show apoptotic nuclei.

2.4. Activity of the Promoter Containing 12xGLI Consensus Site

To study whether a GLI-responsive promoter-reporter is also affected by HH inhibitors GANT61 and cyclopamine, 12xGLI-luciferase reporter and a reference plasmid were cotransfected in several cell lines that were either variably responsive or nonresponsive to GANT61 in proliferation assays. As shown in Figure 4, the sensitive SK-MEL-3 cells were inhibited by cyclopamine and GANT61 extensively. To a lesser extent, reporter activity in G-401, A-204, and U-2 OS was also inhibited. Of these cells, U-2 OS were eradicated from day 5 onwards in the proliferation assay, G-401 were diminished only on day 9, and A-204 were resistant in the proliferation assay (Figure 2). The inhibition of the reporter by GANT61 or cyclopamine was insignificant in other cell lines (PANC-1, PA-TU-8902, MIA-PaCa-2, A-549, and Hep-G2). These cells were also completely resistant in the proliferation assay (Figure 2). The reporter activity thus approximately mimicked the sensitivity of cells to GANT61 (A-204 cells were only negligibly, though significantly, inhibited by cyclopamine, due to very low +SD, and were resistant to GANT61 in proliferation assay). Together, the results indicate a correlation between the sensitivity to inhibitors in the reporter assay and the sensitivity to GANT61 in longer proliferation analysis.

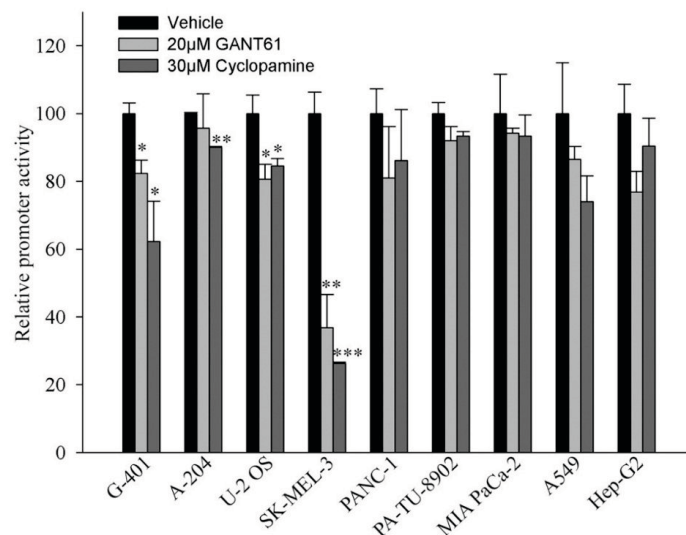


Figure 4. GANT61 and cyclopamine slightly reduced the 12xGLI reporter activity. Cells were seeded in 12-well plates and transfected the next day with the 12xGLI-luciferase plasmid together with a *Renilla luciferase* plasmid for the correction of transfection efficiency. The next day, inhibitors were added to the indicated concentration and cells were harvested 20 h later. No cell deterioration was observed after this period, even in sensitive SK-MEL-3 cells. The experiment was performed twice in triplicates with similar results and one experiment is presented. Data are presented as mean + SD. No mark means insignificant, statistical significance is: * $p < 0.05$, ** $p < 0.01$, *** $p < 0.001$.

3. Discussion

The HH signaling pathway, acting through transcription factors GLI1, GLI2, and GLI3, has been identified as critical for the initiation and progression of a number of cancers. Originally, it was believed to be important for only basal cell carcinoma (BCC) and medulloblastoma. Gradually, the pathway becomes a crucial signaling pathway for all frequent cancer types with the GLI family transcription factors being essential in tumor initiation, progression, EMT, CSC, and metastasis, dependent on the

tumor cell context. HH signaling is a network rather than as a simple linear pathway because of its cooperation with many other cell signaling pathways and its frequent noncanonical activation. GLI factors have several oncogenic targets [63]. Recently, using a large tumor panel, we identified survivin as another important GLI2 target in more than half of tumor cell types [9], suggesting a synergy in HH and survivin in forming tumors stemness and maintaining CSC. This implies more effective therapy by combining HH and survivin inhibitors.

Here, we have first analyzed the expression of HH cascade components across a panel of 56 tumor types using Western blot analysis. It was found that they are generally expressed (only exceptionally showing lower expression level). Importantly, either GLI1 or GLI2 were always present in all samples. In three normal control cell lines, the HH proteins were also present. HH signaling is emerging to be essential for the progression of nearly all tumors [12,13]. The presence of its components is therefore required for the proper progression of the pathway. In proliferation assays, GANT61 was active in melanoma cells (Figure 2 and Figure S1) and also in several other tumor cell lines. The most resistant seemed to be NSCLC and pancreatic cancer cells. This was rather surprising as many reports describe the blockage of the HH pathway in the treatment of pancreatic cancer in preclinical and clinical settings. In tumors, the dense impenetrable stroma is mixed with the pancreatic cancer cells *in vivo*, due to which, drugs cannot invade across this physical barrier, and that may cause a drug resistance [22,64–66]. Since in cell lines the stroma is missing, the drugs should have better access to tumor cells and the druggability might be more feasible. As GANT61 appeared to be nonfunctional in eradicating pancreatic tumor cells, the HH pathway possibly needs, e.g., a second agent to achieve cell killing. A possible explanation could also be that the cell lines used here have not been sensitive to GANT61, while other cell lines (not tested) might have been responsive. In pancreatic tumors, the situation might be even more complicated, e.g., because stromal cells themselves produce Hedgehog and HGF that support the tumor growth [67]. It requires further clarification why in pancreatic cancer the HH pathway sensitivity to drugs *in vivo* has specific requirements in which tumor stroma is determining, causing the known resilience and drug resistance of these tumors.

Our results suggest which type of cancer is resistant or sensitive to GANT61 when it is applied directly on cells in culture (Figure 2). Malignant melanomas are sensitive, when taken into account also our previous results (Figure S1). Thus, GLI factors are important to contribute to keeping their antiapoptotic status. It is believed that MITF (microphthalmia-associated transcription factor), a key factor in melanoma transcription circuitry, maintains antiapoptosis in melanomas [68]. It has been nevertheless demonstrated that low-MITF melanoma cell lines can also proliferate very fast, implicating sufficient antiapoptotic protection [29,69]. HH-GLI signaling has been recognized to keep melanoma stemness and maintain the presence of CSC [70]. Furthermore, the two neuroblastoma cell lines and one SCLC cell line were also relatively sensitive to GANT61, whereas two NSCLC were resistant. In GANT61-resistant cells, antiapoptotic signals ensuring tumor progression can maintain apoptosis by other pathways. Reporter assays measuring the sensitivity of the 12xGLI consensus promoter to GANT61 and cyclopamine roughly correlated with cell proliferation. Our results suggest that HH signaling participates in preventing cell death perhaps in more than half of all tumors cell lines. We speculate that the situation might be similar in other tumor cell lines as well. Taken together, HH signaling plays an important role in preventing tumors cell apoptosis in some cancer cell types.

4. Materials and Methods

4.1. Cell Cultivation

Cells were maintained in appropriate media (DMEM or RPMI1640) supplemented with 10% fetal calf serum (Gibco, Waltham, MA, USA), L-glutamine, streptomycin, and penicillin (Sigma, St. Louis, MO, USA). Some cells were cultured in EMEM medium supplemented also with essential amino acids and pyruvate (Sigma). Fresh media were replaced every third day. HH inhibitors GANT61 or cyclopamine were present in media as indicated in Figures and Figure legends. All melanoma

cell lines were maintained in RPMI1640 medium with the exception of lines WM35 and WM1552C that were kept in DMEM. NSCLC and SCLC cell lines cells were grown in RPMI1640 medium with the exception of Calu-1 (DMEM). SK-N-SH, SH-N-MC, HT-1080, and T98G cells were maintained in EMEM. The remaining cell lines were grown in DMEM medium.

4.2. Cell Lines

All cell lines were of human origin. Melanoma cell lines DOR, Beu, and Hbl were previously described [29]. Other melanoma cell lines (MeWo, SK-MEL-2, SK-MEL-28, SK-MEL-5, SK-MEL-3, Malme 3M, HT144, WM35, WM1552C, and RPMI-7931) were purchased from American Type Culture Collection (ATCC) (Manassas, VA, USA). Normal human melanocytes HeMN-LP were from Cascade Biologics (Portland, OR, USA). NSCLC lung cancer cell lines A549, HT1299, A-427, Calu-1, H-460, H-520, H596, H-661, H-2170, and SK-MES-1, and SCLC cell lines H-446, H-69, H-209, H-82, H-345, H-146, H-378, H-196 were purchased from ATCC. 293FT cells were from Invitrogen (Carlsbad, CA, USA). Colorectal cell lines LoVo, SW480, HCT116 were from ATCC. All other cell lines were purchased also from ATCC: G-401 and A-204 (rhabdoid tumors), U-2 OS and Saos-2 (osteosarcomas), HeLa S3 and C33A (cervical carcinomas), 293 (renal carcinoma), HT-1080 (connective tissue fibrosarcoma), SW-13 (adrenal gland carcinoma), T98G (glioblastoma), IMR90 and WI-38 (normal human fibroblasts), Jurkat (T-cell leukemia), Hep-G2 (hepatocellular carcinoma), SK-N-SH and SH-N-MC (neuroblastomas), PANC-1, PA-TU-8902, MIA PaCa-2, and BxPC-3 (pancreatic carcinomas).

4.3. Western Blots

Commercially available primary antibodies used were as follows: Sonic Hedgehog, Cell Signaling Technology #2207 (Danvers, MA, USA); Patched, Biorbyt #157169 (San Francisco, CA, USA); SMO, #ab72130 (Abcam, Cambridge, UK); SuFu, Cell Signaling #2520; Gli, Abcam #ab134906; Gli2, #sc-271786 (Santa Cruz Biotechnology, Dallas, TX, USA); Gli3, Biorbyt #157158; Survivin, Santa Cruz #sc-17779; BCL-2, BD Pharmingen #556354 (San Jose, CA, USA); β -actin, Sigma #A5316. HRP-labelled second antibodies were from Cell Signaling.

For Western blot analysis, cells were lysed in RIPA buffer (50 mM Tris-HCl pH 7.5, 150 mM NaCl, 5 mM EDTA, 1% NP-40, 0.5% sodium deoxycholate, 0.1% SDS), supplemented with aprotinin, leupeptin, pepstatin (Sigma), COMPLETE, and PhoStop (Roche, IN, USA). Total lysates containing 30 μ g of protein were separated on SDS-PAGE gels and subsequently transferred onto a PVDF membrane (Millipore, Billerica, MA, USA). Membranes were then subjected to probing with antibodies. Western blot signals were detected by using SuperSignal West Pico Chemiluminescent substrate (Fisher Scientific, Waltham, MA, USA) and exposed on films.

4.4. Proliferation Assays

To perform proliferation assays, colony outgrowth assays were carried out. Cells were trypsinized and seeded in about 40–50% confluency on 12-well plates (day 0). The next day (day 1), cell lines were treated with 10 μ M GANT61 or 20 μ M GANT61 (SelleckChem, München, Germany), for a maximum of 9 days. The medium was refreshed every third day. The plates were then fixed in 3% paraformaldehyde solution in 1 \times PBS and stained with 1% crystal violet and photodocumented. Two most important fields (day 9, control and 20 μ M GANT61) were quantitated using ImageJ software. Two experiments were performed in duplicate. Results of both experiments were similar.

4.5. Detection of Apoptosis

A TUNEL (terminal deoxynucleotidyltransferase-mediated dUTP nick-end labelling) assay was performed according to the manufacturer's instructions (BD Biosciences, San Jose, CA, USA). Results of FITC staining were analyzed on a flow cytometer BriCyte EA (Mindray, Shenzhen, China). A total of 50,000 cells were analyzed in each sample. The number of apoptotic cells was determined using ImageJ software.

4.6. Microscopic Detection of Apoptotic Nuclei

Immunofluorescence assays were performed as described previously [71]. Briefly, cells were seeded in NUNC (Roskilde, Denmark) chambers, 20 μ M GANT61 added next day and treated (or untreated, controls) for three days, and mounted in a DAPI-containing medium. Images of nuclear apoptosis figures and controls were there taken using a fluorescent microscope.

4.7. Reporter Assays

Luciferase Reporter Gene Assay: Luciferase reporter plasmid with luciferase gene under the transcriptional control of 12xGLI full consensus was obtained from Prof. R. Toftgard (Karolinska Institutet, Stockholm, Sweden). After transfection of the plasmid (1 μ g), together with the *Renilla luciferase* reporter plasmid (as a reference for transfection efficiency) on the 12-well plates in triplicates, the inhibitors GANT61 and cyclopamine were added at concentrations indicated in Figure 4 for 20 h. Cells were then harvested and the reporter activity was measured using a dual luciferase kit (Promega, Madison, WI, USA) according to the instructions of the manufacturer. Statistical significance is shown in the Figure 4. Two experiments were performed and one is presented. Results of both experiments were similar.

4.8. Statistical Analysis

To calculate the statistical significance of the reporter assays, a two-tailed Student test was used. The *p* values are listed in the corresponding figure legend. In all figures the error bars represent mean + SE. Proliferation assays and TUNEL assay were quantified by ImageJ software (National Institutes of Health, Bethesda, MD, USA).

Supplementary Materials: The following are available online at <http://www.mdpi.com/1422-0067/19/9/2682/s1>.

Author Contributions: J.R. performed most experiments; J.V. and K.V. conceived and designed the experiments and analyzed the data; P.H., J.V., L.O. and J.V.J. performed the experiments; J.V. wrote the paper.

Funding: This work was supported by the institutional research project PROGRES Q25 from Charles University Prague.

Acknowledgments: We thank R. Toftgard (Karolinska Institutet) for the 12xGLI-luciferase reporter plasmid.

Conflicts of Interest: The authors declare no conflict of interest.

Abbreviations

CSC	cancer stem cells
HRP	horseradish peroxidase
DAPI	40,6-Diamidino-2-Phenylindole, Dihydrochloride
SMARCB1	SWI/SNF related, matrix associated, actin dependent regulator of chromatin, subfamily b, member 1
EMT	epithelial-to-mesenchymal transition
TUNEL	terminal deoxynucleotidyl transferase-mediated d-UTP Nick End Labeling
AR	androgen receptor
BCC	basal cell carcinoma
GLI	glioma family zinc finger protein
MITF	microphthalmia-associated transcription factor
HGF	hepatocyte growth factor
PTCH	patched
SMO	smoothened, frizzled class receptor
NSCLC	Non-small cell lung cancer
SCLC	Small cell lung cancer
SWI/SNF	SWItch/Sucrose Non-Fermentable
mTOR	mechanistic target of rapamycin
FITC	fluorescein isothiocyanate

References

1. Cohen, M.M., Jr. The hedgehog signaling network. *Am. J. Med. Genet. A* **2003**, *123A*, 5–28. [[CrossRef](#)] [[PubMed](#)]
2. Robbins, D.J.; Fei, D.L.; Riobo, N.A. The Hedgehog signal transduction network. *Sci. Signal.* **2012**, *5*, re6. [[CrossRef](#)] [[PubMed](#)]
3. Ryan, K.E.; Chiang, C. Hedgehog secretion and signal transduction in vertebrates. *J. Biol. Chem.* **2012**, *287*, 17905–17913. [[CrossRef](#)] [[PubMed](#)]
4. Berman, D.M.; Karhadkar, S.S.; Hallahan, A.R.; Pritchard, J.I.; Eberhart, C.G.; Watkins, D.N.; Chen, J.K.; Cooper, M.K.; Taipale, J.; Olson, J.M.; et al. Medulloblastoma growth inhibition by hedgehog pathway blockade. *Science* **2002**, *297*, 1559–1561. [[CrossRef](#)] [[PubMed](#)]
5. Bar, E.E.; Chaudhry, A.; Farah, M.H.; Eberhart, C.G. Hedgehog signaling promotes medulloblastoma survival via Bc/II. *Am. J. Pathol.* **2007**, *170*, 347–355. [[CrossRef](#)] [[PubMed](#)]
6. Teglund, S.; Toftgard, R. Hedgehog beyond medulloblastoma and basal cell carcinoma. *Biochim. Biophys. Acta* **2010**, *1805*, 181–208. [[CrossRef](#)] [[PubMed](#)]
7. Li, C.; Chi, S.; Xie, J. Hedgehog signaling in skin cancers. *Cell Signal.* **2011**, *23*, 1235–1243. [[CrossRef](#)] [[PubMed](#)]
8. Archer, T.C.; Weeraratne, S.D.; Pomeroy, S.L. Hedgehog-GLI Pathway in Medulloblastoma. *J. Clin. Oncol.* **2012**, *30*, 2154–2156. [[CrossRef](#)] [[PubMed](#)]
9. Vlckova, K.; Ondrusova, L.; Vachtenheim, J.; Reda, J.; Dunder, P.; Zadinova, M.; Zakova, P.; Pouckova, P. Survivin, a novel target of the Hedgehog/GLI signaling pathway in human tumor cells. *Cell Death Dis.* **2016**, *7*, e2048. [[CrossRef](#)] [[PubMed](#)]
10. Varjosalo, M.; Taipale, J. Hedgehog: Functions and mechanisms. *Genes Dev.* **2008**, *22*, 2454–2472. [[CrossRef](#)] [[PubMed](#)]
11. Li, Y.; Maitah, M.Y.; Ahmad, A.; Kong, D.; Bao, B.; Sarkar, F.H. Targeting the Hedgehog signaling pathway for cancer therapy. *Expert Opin. Ther. Targets* **2012**, *16*, 49–66. [[CrossRef](#)] [[PubMed](#)]
12. Atwood, S.X.; Chang, A.L.; Oro, A.E. Hedgehog pathway inhibition and the race against tumor evolution. *J. Cell Biol.* **2012**, *199*, 193–197. [[CrossRef](#)] [[PubMed](#)]
13. Amakye, D.; Jagani, Z.; Dorsch, M. Unraveling the therapeutic potential of the Hedgehog pathway in cancer. *Nat. Med.* **2013**, *19*, 1410–1422. [[CrossRef](#)] [[PubMed](#)]
14. Onishi, H.; Katano, M. Hedgehog signaling pathway as a therapeutic target in various types of cancer. *Cancer Sci.* **2011**, *102*, 1756–1760. [[CrossRef](#)] [[PubMed](#)]
15. Shi, I.; Hashemi, S.N.; Duan, Z.H.; Shi, T. Aberrant signaling pathways in squamous cell lung carcinoma. *Cancer Inform.* **2011**, *10*, 273–285. [[CrossRef](#)] [[PubMed](#)]
16. Rodriguez-Blanco, J.; Schilling, N.S.; Tokhunts, R.; Giambelli, C.; Long, J.; Liang, F.D.; Singh, S.; Black, K.E.; Wang, Z.; Galimberti, F.; et al. The Hedgehog processing pathway is required for NSCLC growth and survival. *Oncogene* **2013**, *32*, 2335–2345. [[CrossRef](#)] [[PubMed](#)]
17. Justilien, V.; Walsh, M.P.; Ali, S.A.; Thompson, E.A.; Murray, N.R.; Fields, A.P. The PRKCI and SOX2 oncogenes are coamplified and cooperate to activate Hedgehog signaling in lung squamous cell carcinoma. *Cancer Cell* **2014**, *25*, 139–151. [[CrossRef](#)] [[PubMed](#)]
18. Abe, Y.; Tanaka, N. The Hedgehog Signaling Networks in Lung Cancer: The Mechanisms and Roles in Tumor Progression and Implications for Cancer Therapy. *BioMed Res. Int.* **2016**, *2016*, 7969286. [[CrossRef](#)] [[PubMed](#)]
19. Watkins, D.N.; Berman, D.M.; Baylin, S.B. Hedgehog signaling: Progenitor phenotype in small-cell lung cancer. *Cell Cycle* **2003**, *2*, 196–198. [[CrossRef](#)] [[PubMed](#)]
20. Park, K.S.; Martelotto, L.G.; Peifer, M.; Sos, M.L.; Karnezis, A.N.; Mahjoub, M.R.; Bernard, K.; Conklin, J.F.; Szczepny, A.; Yuan, J.; et al. A crucial requirement for Hedgehog signaling in small cell lung cancer. *Nat. Med.* **2011**, *17*, 1504–1508. [[CrossRef](#)] [[PubMed](#)]
21. Lauth, M.; Toftgard, R. Hedgehog signaling and pancreatic tumor development. *Adv. Cancer Res.* **2011**, *110*, 1–17. [[CrossRef](#)] [[PubMed](#)]
22. Hwang, R.F.; Moore, T.T.; Hattersley, M.M.; Scarpitti, M.; Yang, B.; Devereaux, E.; Ramachandran, V.; Arumugam, T.; Ji, B.; Logsdon, C.D.; et al. Inhibition of the Hedgehog pathway targets the tumor-associated stroma in pancreatic cancer. *Mol. Cancer Res.* **2012**, *10*, 1147–1157. [[CrossRef](#)] [[PubMed](#)]

23. Fu, J.; Rodova, M.; Roy, S.K.; Sharma, J.; Singh, K.P.; Srivastava, R.K.; Shankar, S. GANT-61 inhibits pancreatic cancer stem cell growth in vitro and in NOD/SCID/IL2R gamma null mice xenograft. *Cancer Lett.* **2013**, *330*, 22–32. [[CrossRef](#)] [[PubMed](#)]
24. Wang, F.; Ma, L.; Zhang, Z.; Liu, X.; Gao, H.; Zhuang, Y.; Yang, P.; Kornmann, M.; Tian, X.; Yang, Y. Hedgehog signaling regulates epithelial-mesenchymal transition in pancreatic cancer stem-like cells. *J. Cancer* **2016**, *7*, 408–417. [[CrossRef](#)] [[PubMed](#)]
25. Xu, Y.; An, Y.; Wang, X.; Zha, W.; Li, X. Inhibition of the Hedgehog pathway induces autophagy in pancreatic ductal adenocarcinoma cells. *Oncol. Rep.* **2014**, *31*, 707–712. [[CrossRef](#)] [[PubMed](#)]
26. Xu, X.; Zhou, Y.; Xie, C.; Wei, S.M.; Gan, H.; He, S.; Wang, F.; Xu, L.; Lu, J.; Dai, W.; et al. Genome-wide screening reveals an EMT molecular network mediated by Sonic Hedgehog-Gli1 signaling in pancreatic cancer cells. *PLoS ONE* **2012**, *7*, e43119. [[CrossRef](#)] [[PubMed](#)]
27. Stecca, B.; Mas, C.; Clement, V.; Zbinden, M.; Correa, R.; Piguat, V.; Beermann, F.; Ruiz, I.A. Melanomas require Hedgehog-Gli signaling regulated by interactions between GLI1 and the RAS-MEK/AKT pathways. *Proc. Natl. Acad. Sci. USA* **2007**, *104*, 5895–5900. [[CrossRef](#)] [[PubMed](#)]
28. Alexaki, V.I.; Javelaud, D.; Van Kempen, L.C.; Mohammad, K.S.; Dennler, S.; Luciani, F.; Hoek, K.S.; Juarez, P.; Goydos, J.S.; Fournier, P.J.; et al. GLI2-mediated melanoma invasion and metastasis. *J. Natl. Cancer Inst.* **2010**, *102*, 1148–1159. [[CrossRef](#)] [[PubMed](#)]
29. Vlckova, K.; Reda, J.; Ondrusova, L.; Krayem, M.; Ghanem, G.; Vachtenheim, J. GLI inhibitor GANT61 kills melanoma cells and acts in synergy with obatoclax. *Int. J. Oncol.* **2016**, *49*, 953–960. [[CrossRef](#)] [[PubMed](#)]
30. Ok, C.Y.; Singh, R.R.; Vega, F. Aberrant activation of the Hedgehog signaling pathway in malignant hematological neoplasms. *Am. J. Pathol.* **2012**, *180*, 2–11. [[CrossRef](#)] [[PubMed](#)]
31. Fukushima, N.; Minami, Y.; Kakiuchi, S.; Kuwatsuka, Y.; Hayakawa, F.; Jamieson, C.; Kiyoi, H.; Naoe, T. Small-molecule Hedgehog inhibitor attenuates the leukemia-initiation potential of acute myeloid leukemia cells. *Cancer Sci.* **2016**, *107*, 1422–1429. [[CrossRef](#)] [[PubMed](#)]
32. Kakiuchi, S.; Minami, Y.; Miyata, Y.; Mizutani, Y.; Goto, H.; Kawamoto, S.; Yakushijin, K.; Kurata, K.; Matsuoka, H.; Minami, H. NANOG expression as a responsive biomarker during treatment with Hedgehog signal inhibitor in acute myeloid leukemia. *Int. J. Mol. Sci.* **2017**, *18*, 486. [[CrossRef](#)] [[PubMed](#)]
33. Aberger, F.; Hutterer, E.; Sternberg, C.; del Burgo, P.J.; Hartmann, T.N. Acute myeloid leukemia—Strategies and challenges for targeting oncogenic Hedgehog/GLI signaling. *Cell Commun. Signal.* **2017**, *15*, 8. [[CrossRef](#)] [[PubMed](#)]
34. Burns, M.A.; Liao, Z.W.; Yamagata, N.; Pouliot, G.P.; Stevenson, K.E.; Neuberg, D.S.; Thorner, A.R.; Ducar, M.; Silverman, E.A.; Hunger, S.P.; et al. Hedgehog pathway mutations drive oncogenic transformation in high-risk T-cell acute lymphoblastic leukemia. *Leukemia* **2018**. [[CrossRef](#)] [[PubMed](#)]
35. Fei, D.L.; Sanchez-Mejias, A.; Wang, Z.; Flaveny, C.; Long, J.; Singh, S.; Rodriguez-Blanco, J.; Tokhunts, R.; Giambelli, C.; Briegel, K.J.; et al. Hedgehog signaling regulates bladder cancer growth and tumorigenicity. *Cancer Res.* **2012**, *72*, 4449–4458. [[CrossRef](#)] [[PubMed](#)]
36. Sanchez, P.; Clement, V.; Altaba, A. Therapeutic targeting of the Hedgehog-GLI pathway in prostate cancer. *Cancer Res.* **2005**, *65*, 2990–2992. [[CrossRef](#)] [[PubMed](#)]
37. Thiyagarajan, S.; Bhatia, N.; Reagan-Shaw, S.; Cozma, D.; Thomas-Tikhonenko, A.; Ahmad, N.; Spiegelman, V.S. Role of GLI2 transcription factor in growth and tumorigenicity of prostate cells. *Cancer Res.* **2007**, *67*, 10642–10646. [[CrossRef](#)] [[PubMed](#)]
38. Li, N.; Truong, S.; Nouri, M.; Moore, J.; Al Nakouzi, N.; Lubik, A.A.; Buttyan, R. Non-canonical activation of Hedgehog in prostate cancer cells mediated by the interaction of transcriptionally active androgen receptor proteins with Gli3. *Oncogene* **2018**, *37*, 2313–2325. [[CrossRef](#)] [[PubMed](#)]
39. Yang, H.; Hu, L.; Liu, Z.; Qin, Y.; Li, R.; Zhang, G.; Zhao, B.; Bi, C.; Lei, Y.; Bai, Y. Inhibition of Gli1-mediated prostate cancer cell proliferation by inhibiting the mTOR/S6K1 signaling pathway. *Oncol. Lett.* **2017**, *14*, 7970–7976. [[CrossRef](#)] [[PubMed](#)]
40. Clement, V.; Sanchez, P.; de Tribolet, N.; Radovanovic, I.; Altaba, A. Hedgehog-Gli1 signaling regulates human glioma growth, cancer stem cell self-renewal, and tumorigenicity. *Curr. Biol.* **2007**, *17*, 165–172. [[CrossRef](#)] [[PubMed](#)]
41. Takezaki, T.; Hide, T.; Takanaga, H.; Nakamura, H.; Kuratsu, J.; Kondo, T. Essential role of the Hedgehog signaling pathway in human glioma-initiating cells. *Cancer Sci.* **2011**, *102*, 1306–1312. [[CrossRef](#)] [[PubMed](#)]

42. Nagao-Kitamoto, H.; Nagata, M.; Nagano, S.; Kitamoto, S.; Ishidou, Y.; Yamamoto, T.; Nakamura, S.; Tsuru, A.; Abematsu, M.; Fujimoto, Y.; et al. GLI2 is a novel therapeutic target for metastasis of osteosarcoma. *Int. J. Cancer* **2015**, *136*, 1276–1284. [[CrossRef](#)] [[PubMed](#)]
43. Yao, Z.; Han, L.; Chen, Y.; He, F.; Sun, B.; Kamar, S.; Zhang, Y.; Yang, Y.; Wang, C.; Yang, Z. Hedgehog signalling in the tumorigenesis and metastasis of osteosarcoma, and its potential value in the clinical therapy of osteosarcoma. *Cell Death Dis.* **2018**, *9*, 701. [[CrossRef](#)] [[PubMed](#)]
44. Satheesha, S.; Manzella, G.; Bovay, A.; Casanova, E.A.; Bode, P.K.; Belle, R.; Feuchtgruber, S.; Jaaks, P.; Dogan, N.; Koscielniak, E.; et al. Targeting Hedgehog signaling reduces self-renewal in embryonal rhabdomyosarcoma. *Oncogene* **2016**, *35*, 2020–2030. [[CrossRef](#)] [[PubMed](#)]
45. Xu, L.; Wang, X.; Wan, J.; Li, T.; Gong, X.; Zhang, K.; Yi, L.; Xiang, Z.; Xu, M.; Cui, H. Sonic Hedgehog pathway is essential for neuroblastoma cell proliferation and tumor growth. *Mol. Cell Biochem.* **2012**, *364*, 235–241. [[CrossRef](#)] [[PubMed](#)]
46. Szkandera, J.; Kiesslich, T.; Haybaeck, J.; Gerger, A.; Pichler, M. Hedgehog signaling pathway in ovarian cancer. *Int. J. Mol. Sci.* **2013**, *14*, 1179–1196. [[CrossRef](#)] [[PubMed](#)]
47. Levanat, S.; Sabol, M.; Musani, V.; Ozretic, P.; Trnski, D. Hedgehog signaling pathway as genetic and epigenetic target in ovarian tumors. *Curr. Pharm. Des.* **2017**, *23*, 73–94. [[CrossRef](#)] [[PubMed](#)]
48. Kim, Y.; Yoon, J.W.; Xiao, X.; Dean, N.M.; Monia, B.P.; Marcussan, E.G. Selective down-regulation of glioma-associated oncogene 2 inhibits the proliferation of hepatocellular carcinoma cells. *Cancer Res.* **2007**, *6*, 73583–73593. [[CrossRef](#)] [[PubMed](#)]
49. Mazumdar, T.; Devecchio, J.; Shi, T.; Jones, J.; Agyeman, A.; Houghton, J.A. Hedgehog signaling drives cellular survival in human colon carcinoma cells. *Cancer Res.* **2011**, *71*, 1092–1102. [[CrossRef](#)] [[PubMed](#)]
50. Regan, J.L.; Schumacher, D.; Staudte, S.; Steffen, A.; Haybaeck, J.; Keilholz, U.; Schweiger, C.; Golob-Schwarzl, N.; Mumberg, D.; Henderson, D.; et al. Non-canonical Hedgehog signaling is a positive regulator of the WNT pathway and is required for the survival of colon cancer stem cells. *Cell Rep.* **2017**, *21*, 2813–2828. [[CrossRef](#)] [[PubMed](#)]
51. Jeng, K.S.; Jeng, C.J.; Sheen, I.S.; Wu, S.H.; Lu, S.J.; Wang, C.H.; Chang, C.F. Glioma-associated oncogene homolog inhibitors have the potential of suppressing cancer stem cells of breast cancer. *Int. J. Mol. Sci.* **2018**, *19*, 1375. [[CrossRef](#)] [[PubMed](#)]
52. Das, S.; Tucker, J.A.; Khullar, S.; Samant, R.S.; Shevde, L.A. Hedgehog signaling in tumor cells facilitates osteoblast-enhanced osteolytic metastases. *PLoS ONE* **2012**, *7*, e34374. [[CrossRef](#)] [[PubMed](#)]
53. Jagani, Z.; Mora-Blanco, E.L.; Sansam, C.G.; McKenna, E.S.; Wilson, B.; Chen, D.; Klekota, J.; Tamayo, P.; Nguyen, P.T.; Tolstorukov, M.; et al. Loss of the tumor suppressor SNF5 leads to aberrant activation of the Hedgehog-Gli pathway. *Nat. Med.* **2010**, *16*, 1429–1433. [[CrossRef](#)]
54. Riobo, N.A.; Lu, K.; Ai, X.; Haines, G.M.; Emerson, C.P., Jr. Phosphoinositide 3-kinase and Akt are essential for Sonic Hedgehog signaling. *Proc. Natl. Acad. Sci. USA* **2006**, *103*, 4505–4510. [[CrossRef](#)] [[PubMed](#)]
55. Lauth, M.; Toftgard, R. Non-canonical activation of GLI transcription factors: Implications for targeted anti-cancer therapy. *Cell Cycle* **2007**, *6*, 2458–2463. [[CrossRef](#)] [[PubMed](#)]
56. Shevde, L.A.; Samant, R.S. Nonclassical Hedgehog-Gli signaling and its clinical implications. *Int. J. Cancer* **2014**, *135*, 1–6. [[CrossRef](#)] [[PubMed](#)]
57. Po, A.; Silvano, M.; Miele, E.; Capalbo, C.; Eramo, A.; Salvati, V.; Todaro, M.; Besharat, Z.M.; Catanzaro, G.; Cucchi, D.; et al. Noncanonical GLI1 signaling promotes stemness features and in vivo growth in lung adenocarcinoma. *Oncogene* **2017**, *36*, 4641–4652. [[CrossRef](#)] [[PubMed](#)]
58. Ji, Z.; Mei, F.C.; Xie, J.; Cheng, X. Oncogenic KRAS activates Hedgehog signaling pathway in pancreatic cancer cells. *J. Biol. Chem.* **2007**, *282*, 14048–14055. [[CrossRef](#)] [[PubMed](#)]
59. Wang, Y.; Ding, Q.; Yen, C.J.; Xia, W.; Izzo, J.G.; Lang, J.Y.; Li, C.W.; Hsu, J.L.; Miller, S.A.; Wang, X.; et al. The crosstalk of mTOR/S6K1 and Hedgehog pathways. *Cancer Cell* **2012**, *21*, 374–387. [[CrossRef](#)] [[PubMed](#)]
60. Miyazaki, Y.; Matsubara, S.; Ding, Q.; Tsukasa, K.; Yoshimitsu, M.; Kosai, K.; Takao, S. Efficient elimination of pancreatic cancer stem cells by hedgehog/GLI inhibitor GANT61 in combination with mTOR inhibition. *Mol. Cancer* **2016**, *15*, 49. [[CrossRef](#)] [[PubMed](#)]
61. Desch, P.; Asslaber, D.; Kern, D.; Schnidar, H.; Mangelberger, D.; Alinger, B.; Stoecher, M.; Hofbauer, S.W.; Neureiter, D.; Tinhofer, I.; et al. Inhibition of GLI, but not Smoothened, induces apoptosis in chronic lymphocytic leukemia cells. *Oncogene* **2010**, *29*, 4885–4895. [[CrossRef](#)] [[PubMed](#)]

62. Wang, Y.; Han, C.; Lu, L.; Magliato, S.; Wu, T. Hedgehog signaling pathway regulates autophagy in human hepatocellular carcinoma cells. *Hepatology* **2013**, *58*, 995–1010. [[CrossRef](#)] [[PubMed](#)]
63. Katoh, Y.; Katoh, M. Hedgehog target genes: Mechanisms of carcinogenesis induced by aberrant Hedgehog signaling activation. *Curr. Mol. Med.* **2009**, *9*, 873–886. [[CrossRef](#)] [[PubMed](#)]
64. Li, X.; Ma, Q.; Duan, W.; Liu, H.; Xu, H.; Wu, E. Paracrine sonic Hedgehog signaling derived from tumor epithelial cells: A key regulator in the pancreatic tumor microenvironment. *Crit. Rev. Eukaryot. Gene Expr.* **2012**, *22*, 97–108. [[CrossRef](#)] [[PubMed](#)]
65. Lonardo, E.; Frias-Aldeguer, J.; Hermann, P.C.; Heeschen, C. Pancreatic stellate cells form a niche for cancer stem cells and promote their self-renewal and invasiveness. *Cell Cycle* **2012**, *11*, 1282–1290. [[CrossRef](#)] [[PubMed](#)]
66. Gu, J.; Saiyin, H.; Fu, D.; Li, J. Stroma—A double-edged sword in pancreatic cancer: A lesson from targeting stroma in pancreatic cancer with Hedgehog signaling inhibitors. *Pancreas* **2018**, *47*, 382–389. [[CrossRef](#)] [[PubMed](#)]
67. Rucki, A.A.; Foley, K.; Zhang, P.; Xiao, Q.; Kleponis, J.; Wu, A.A.; Sharma, R.; Mo, G.; Liu, A.; Van Eyk, J.; et al. Heterogeneous stromal signaling within the tumor microenvironment controls the metastasis of pancreatic cancer. *Cancer Res.* **2017**, *77*, 41–52. [[CrossRef](#)] [[PubMed](#)]
68. Levy, C.; Khaled, M.; Fisher, D.E. MITF: Master regulator of melanocyte development and melanoma oncogene. *Trends Mol. Med.* **2006**, *12*, 406–414. [[CrossRef](#)] [[PubMed](#)]
69. Vachtenheim, J.; Ondrusova, L. Microphthalmia-associated transcription factor expression levels in melanoma cells contribute to cell invasion and proliferation. *Exp. Dermatol.* **2015**, *24*, 481–484. [[CrossRef](#)] [[PubMed](#)]
70. Santini, R.; Vinci, M.C.; Pandolfi, S.; Penachioni, J.Y.; Montagnani, V.; Olivito, B.; Gattai, R.; Pimpinelli, N.; Gerlini, G.; Borgognoni, L.; et al. Hedgehog-Gli signaling drives self-renewal and tumorigenicity of human melanoma-initiating cells. *Stem Cells* **2012**, *30*, 1808–1818. [[CrossRef](#)] [[PubMed](#)]
71. Vlckova, K.; Vachtenheim, J.; Reda, J.; Horak, P.; Ondrusova, L. Inducibly decreased MITF levels do not affect proliferation and phenotype switching but reduce differentiation of melanoma cells. *J. Cell Mol. Med.* **2018**, *22*, 2240–2251. [[CrossRef](#)] [[PubMed](#)]



© 2018 by the authors. Licensee MDPI, Basel, Switzerland. This article is an open access article distributed under the terms and conditions of the Creative Commons Attribution (CC BY) license (<http://creativecommons.org/licenses/by/4.0/>).

Inducibly decreased MITF levels do not affect proliferation and phenotype switching but reduce differentiation of melanoma cells

Kateřina Vičková [#], Jiri Vachtenheim ^{#, *} , Jiri Réda, Pavel Horák, Lubica Ondrušová

Department of Transcription and Cell Signaling, Institute of Medical Biochemistry and Laboratory Diagnostics, First Faculty of Medicine, Charles University, Prague, Czech Republic

Received: September 2, 2017; Accepted: November 16, 2017

Abstract

Melanoma arises from neural crest-derived melanocytes which reside mostly in the skin in an adult organism. Epithelial–mesenchymal transition (EMT) is a tumorigenic programme through which cells acquire mesenchymal, more pro-oncogenic phenotype. The reversible phenotype switching is an event still not completely understood in melanoma. The EMT features and increased invasiveness are associated with lower levels of the pivotal lineage identity maintaining and melanoma-specific transcription factor MITF (microphthalmia-associated transcription factor), whereas increased proliferation is linked to higher MITF levels. However, the precise role of MITF in phenotype switching is still loosely characterized. To exclude the changes occurring upstream of MITF during MITF regulation *in vivo*, we employed a model whereby MITF expression was inducibly regulated by shRNA in melanoma cell lines. We found that the decrease in MITF caused only moderate attenuation of proliferation of the whole cell line population. Proliferation was decreased in five of 15 isolated clones, in three of them profoundly. Reduction in MITF levels alone did not generally produce EMT-like characteristics. The stem cell marker levels also did not change appreciably, only a sharp increase in SOX2 accompanied MITF down-regulation. Oppositely, the downstream differentiation markers and the MITF transcriptional targets melastatin and tyrosinase were profoundly decreased, as well as the downstream target livin. Surprisingly, after the MITF decline, invasiveness was not appreciably affected, independently of proliferation. The results suggest that low levels of MITF may still maintain relatively high proliferation and might reflect, rather than cause, the EMT-like changes occurring in melanoma.

Keywords: melanoma • MITF • phenotype switching • proliferation • invasiveness • differentiation

Introduction

Malignant melanoma is an aggressive tumour of neuroectodermal origin that has a dismal prognosis if it is not excised at an early stage. More than 50% of melanoma cases harbour the BRAF(V600E) mutation [1, 2]. However, singular targeted inhibition of BRAF leads invariably to acquired resistance (which can be also inherent) that can result in worsening of the patient's prognosis also through inducing the therapy-induced pro-oncogenic secretome [3]. Melanoma cells are very early phenotypically diversified and undergo phenotype switching resembling the EMT, through which they acquire considerable microheterogeneity resulting in plasticity, capability of invasion and migration. These properties lead to metastasis and poor prognosis [4–7]. EMT is mostly a reversible process through which undergoes epithelial

tumours to gain the mesenchymal phenotype and more oncogenic characteristics but occurs also in non-epithelial cancers [8, 9].

Melanocyte-specific isoform of MITF (microphthalmia-associated transcription factor) is a pivotal protein determining the melanocyte lineage identity and conferring a strong antiapoptotic activity to melanoma cells [10]. This is accomplished through the direct activation of expression of several antiapoptosis factors such as BCL2 [11], livin [12], BPTF [13] and others.

Two phenotypically distinct populations of melanoma cells were described related to MITF levels: High-MITF population is associated with differentiation and proliferation, whereas low-MITF cells, although they proliferate slowly, are endowed with the invasive and EMT-like characteristics [14], and they express pro-oncogenic genes such as Brn2 [15–19], GLI2 [20], JARID1B [21], Axl [22] and others. On the other hand, it has been found that a large proportion (over 25%) of melanoma cells derived directly from patients are capable of forming tumours in highly immunocompromised NOD/SCID

[#]Both the authors contributed equally.

*Correspondence to: Dr. Jiri VACHTENHEIM
E-mail: jiri.vachtenheim@lf1.cuni.cz

doi: 10.1111/jcmm.13506

© 2018 The Authors.

Journal of Cellular and Molecular Medicine published by John Wiley & Sons Ltd and Foundation for Cellular and Molecular Medicine.

This is an open access article under the terms of the Creative Commons Attribution License, which permits use, distribution and reproduction in any medium, provided the original work is properly cited.

interleukin-2 receptor gamma chain null (Il2rg^{-/-}), NSG mice [23]. Also, the phenotypic heterogeneity in melanoma is extremely reversible and not hierarchically organized [24]. These findings substantially challenge the concept of a small population of rare cancer initiating cells with stem cell (SC) properties [21, 25, 26] which are recruited from the invasive cells and have a high self-renewal potential and propensity to form metastasis.

When studying the phenotypic changes in melanoma, it is crucial to discern the effects of MITF alone from the effects of expression changes in many MITF transcriptional regulators and cofactors that operate upstream of MITF. They undoubtedly influence not only MITF but also many other targets involved in the phenotype outcome *in vivo*. Events caused purely by MITF down-regulation can be achieved through manipulating MITF levels alone, an approach that is not feasible to perform *in vivo*. It is thus highly desirable to understand precisely the mechanisms which MITF plays in modulating tumour cell invasiveness, plasticity, migration, proliferation and metastasis *in vitro* and *in vivo*.

We used here the doxycycline (DOX)-based inducible lentiviral system to stepwise decrease MITF level in six melanoma cell lines. In this setting, the expression of upstream genes regulating MITF expression remained intact, simplifying the interpretation of phenotype changes and evaluation of the effect of exclusive down-regulation of MITF. We found no profound changes in proliferation of whole cell populations, EMT gene expression pattern and invasiveness. In contrast, the expression of the downstream differentiation markers melastatin and tyrosinase and the antiapoptotic MITF target livin diminished after DOX-dependent reduction in MITF protein level. Based on these experiments with cell lines, we suggest slightly modified model concerning the role of MITF in proliferation and invasiveness of melanoma cells. The data further suggest that more complex events may occur during the phenotype switching in melanoma that might be a more non-uniform process than previously anticipated and may be a cause (rather than a result of) of the low-MITF levels in the invasive subpopulations.

Materials and methods

Cell culture

Melanoma cell lines SK-MEL-3, SK-MEL-5, SK-MEL-28, Malme 3M and MeWo were purchased from ATCC and were grown using EMEM complete medium with non-essential amino acids and pyruvate, or RPMI1640 medium (for Malme 3M). 501mel cells were generously provided by Dr. R. Halaban (Yale University) and maintained in RPMI1640 medium. All media were supplemented with 10% FCS and antibiotics. All cell lines harbour mutated BRAF(V600E), with the exception of MeWo cells which are BRAFwt; 293FT cells were purchased from Invitrogen (Carlsbad, CA, USA) and cultivated in DMEM with 10% FCS.

Proliferation assays

Colony outgrowth assay

After culturing the cells 6 days in appropriate concentration of DOX (Invitrogen), cells were seeded at low density in 12-well plates and

grown for 9 days. The medium with or without (as a control) DOX was changed every other day. Cells were then fixed, stained with crystal violet and quantified.

Growth curves

This experiment reflects the cell growth after previous long-term cultivation in DOX. Cells were first maintained for 5 weeks in appropriate DOX concentration, then plated in 24-well plates at low density and fixed on days 0, 3, 6 and 9. Medium was changed every other day. Cells were fixed, stained with crystal violet, destained and quantitated on a spectrophotometer. Growth curves were constructed using the triplicate data. The levels of MITF in DOX remained decreased all the time as assessed by Western blot. Curves are shown with a standard error for each point.

Western blot analysis and immunofluorescence

Cells were lysed in a complete RIPA buffer (1% NP-40, 150 mM NaCl, 5 mM EDTA, 0.5% sodium deoxycholate, 50 mM Tris-HCl pH 7.5, 0.1% SDS) with added protease and phosphatase inhibitors aprotinin, leupeptin, pepstatin, phenylmethylsulphonylfluoride and PhosStop (Roche, Indianapolis, IN, USA). After the electrophoresis on 10–12% SDS-polyacrylamide gels, the proteins were transferred onto PVDF membrane (Millipore, Billerica, MA, USA). Blots were incubated with primary and horseradish peroxidase-conjugated secondary antibodies and detected by chemiluminescent determination. The following commercially available antibodies were used for Western blots: antibody against MITF (cat. no. MS-772; Neomarkers, Fremont, CA, USA), BCL2 (556 354; Becton Dickinson, San Diego, CA, USA), livin (sc-30161; Santa Cruz Biotechnology, Dallas, TX, USA), Ax1 (sc-166269; Santa Cruz), β -catenin (8480; Cell Signaling, Danvers, MA, USA), SRC (2109; Cell Signaling), β -actin (A5316; Sigma-Aldrich, St Louis, MO, USA), E-cadherin (3195; Cell Signaling), N-cadherin (13116; Cell Signaling), SLUG (9585; Cell Signaling), SNAIL (Santa Cruz, sc-28199), vimentin (5741; Cell Signaling), ZEB1 (3396; Cell Signaling), ZEB2 (sc-271984; Santa Cruz), p27 (Santa Cruz, sc-528), KLF4 (LS-C415468; LSBiotechnologies, Seattle, WA, USA), ALDH1A1 (LS-B10149; LSBiotechnologies), Brn2 (sc-393324; Santa Cruz), SOX2 (5024; Cell Signaling), OCT4 (sc-514295; Santa Cruz). For immunofluorescence, cells were fixed in 3% paraformaldehyde the next day after seeding, permeabilized and stained with anti-MITF antibody followed by a FITC-labelled second antibody. Cell chambers were then mounted in the mounting medium with DAPI.

Lentivirus production and infection of target cells

ShRNA-coding hairpin sequence against MITF [27] was cloned in DOX-inducible (Tet-On) Tet-pLKO-puro plasmid [28] (Addgene plasmid no. 21915). This shRNA sequence has been previously verified and down-regulates MITF level best among other tested sequences. Lentiviruses were packaged in 293FT cells as described earlier [29]. Plasmid with scrambled shRNA sequence was used as a control. Six melanoma cell lines (above) were infected with the fresh virus overnight in the presence of 6 μ g/ml Polybrene (Sigma-Aldrich) and then briefly (4–5 days) selected in puromycin (Sigma-Aldrich) and maintained in low puromycin (0.25 μ g/ml) media.

Invasivity and wound-healing assay

For these assays, cells were grown for 6 days in medium without DOX and with 1 $\mu\text{g/ml}$ DOX (or in 0.5 $\mu\text{g/ml}$ DOX for wound-healing assay). Estimation of cell invasiveness has been made using the collagen invasivity kit (Millipore). For the wound scratch migration assays, cells were prepared in duplicates on 12-well plates. Next day, cells were near-confluent and wounded using 1-ml sterile pipette tip and photodocumented for control time zero, washed repeatedly and starved for 24 hrs in medium containing 0.5% FCS. Next day, cultivation medium containing 15% FCS was added (still keeping the cells with or without DOX), and invasion of cells in the same areas as at the time zero was photodocumented after next 24 and 48 hrs.

Viability

Cell viability was estimated on cells in duplicates. Cells bearing the inducible shRNA against MITF or control cells were treated for 6 days with the indicated concentrations of DOX, replated onto 12-well plates, and viability was determined next day by the MTT viability kit (Sigma-Aldrich) according to the manufacturer's instructions.

Real-time PCR

Estimation of melastatin mRNA levels was performed with primers and a labelled probe as described in the original procedure [12]. Primers for estimation of tyrosinase were as follows: forward, 5'-CCAGAAGCTGACAGGAGATG; reverse, 5'-AGGCATTGTGCATGCTGCTT; probe, 5'-FAM-ACGGCGTAATCCTGGAACCATGACA-TAMRA. After total RNA was isolated using TRIzol (Life Technologies, Carlsbad, CA, USA), 2 μg of RNA was reverse-transcribed using transcriptase reverse transcriptase (Roche), and cDNAs for melastatin and tyrosinase were quantitated using Taqman system QuantiTect Probe PCR Kit (Qiagen, Hilden, Germany). Data were acquired on a ViiA7 system (Life Technologies). Each experiment has been performed twice with similar results. Data are presented after the compensation to β -actin mRNA levels as a control gene.

Statistics

Each experiment was performed at least two times with consistent results. Data in graphs are presented as means and their standard errors. Statistical significance was determined using the Student's *t*-test. *P* value <0.05 or <0.01 was considered statistically significant as indicated. For quantification of proliferation assays, the ImageJ software (National Institutes of Health, Bethesda, MD, USA) was employed, and one of two experiments is presented.

Results

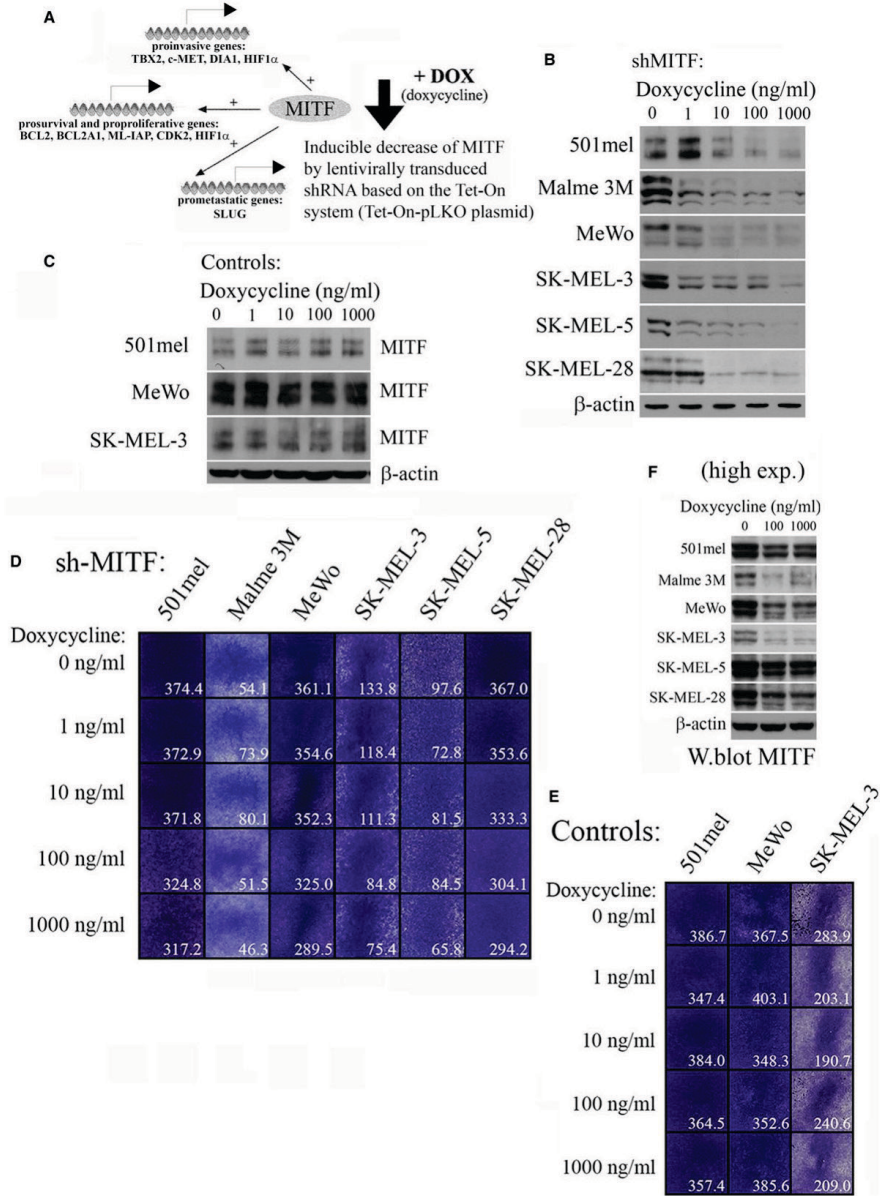
Reduced MITF levels do not cause halt of proliferation or cell cycle arrest

We generated lentivirus encoding shRNA-MITF enabling the regulatable decrease in MITF levels in cell lines. This approach enables the elimination of MITF upstream events that occur *in vivo*, which down-regulate MITF but can have many other activities which are MITF-independent. Thus, in our system, only MITF-regulated genes are participating in the resulting phenotype (schematic Fig. 1A).

Cells infected with the Tet-pLKO-puro-based produced virus were selected in puromycin and constituted DOX-responsive cell lines with gradually decreased MITF levels after increasing DOX doses. Six cell lines with high or average MITF levels were chosen to better follow the stepwise MITF depletion. We used 1 $\mu\text{g/ml}$ of DOX as the highest concentration because higher DOX began to cause a non-specific toxic effect to the cells. MITF levels decreased gradually with increasing DOX doses in all cell lines tested (Fig. 1B). No change in MITF level was seen in control virus-infected cells, as exemplified in three cell lines (Fig. 1C). Although MITF protein was substantially decreased (Fig. 1B), high exposures revealed still appreciable levels even in 1 $\mu\text{g/ml}$ of DOX (Fig. 1F). This is in contrast with our previous results where we were able to ablate MITF completely (targeting the same sequence) with transfected non-inducible pSUPER-puro-shMITF plasmid and puromycin selection [27] in 501mel cells (Fig. S1), which was followed by cell cycle arrest and subsequent apoptosis. The difference in results is apparently due to the different silencing system and a very effective block of MITF expression when shRNA was cloned in pSUPER plasmid and transfected. To substantiate the knockdown, we verified the decreased MITF levels and assessed the results by immunofluorescence. MITF staining was decreased in all DOX-treated cells but not in controls (Fig. S2).

Surprisingly, even the highest decrease in MITF had relatively little effect on cell proliferation in this study, as assessed by colony formation assay (Fig. 1D). Evidently, a smaller decrease in proliferation was seen in most cell lines at high DOX, but a very slight retardation of growth was visible also in some controls (Fig. 1E). Collectively, reduction in MITF levels had no dramatic effect on proliferation rate in melanoma cell lines, probably partly because the degree of knockdown left some MITF level which was sufficient for proliferation. Consistent with this, little or no changes in the cell cycle profiles were observed in cells without DOX or containing 1 $\mu\text{g/ml}$ of DOX (Fig. S3). The data thus show that even small

Fig. 1 Gradually decreased MITF protein in the inducible system causes minimal changes in proliferation. **(A)** A scheme of experimental setting with a view of groups of MITF-inducible genes. **(B)** Infection of six melanoma cell lines with a lentivirus carrying the shRNA sequence directed to MITF, followed by a brief puromycin selection. Incubation of cells in increasing concentrations of DOX leads to a stepwise disappearance of the MITF Western blot signal. The Western blot was performed 6 days after incubation without or with DOX. **(C)** No MITF level changes were seen in control virus-infected cultures. **(D)** Proliferation rates are determined in increasing DOX concentrations. Cells were maintained in DOX for 6 days, and then, the experiment was carried out and quantitated by ImageJ. Two experiments with consistent results were performed and one is presented. **(E)** Similar to **D**, control virus-infected cultures grew in all DOX concentrations. The setting of the experiment was the same as in **D**. **(F)** Longer exposure of the same Western blots as shown in **B**. Only two highest DOX concentrations are shown. In all cell lines, some residual MITF remains even in the highest DOX concentration.



amounts of MITF are capable of maintaining proliferation of melanoma cells.

To test the growth of established melanoma lines, we chose three low-MITF and three high-MITF cell lines and determined their proliferation rate. There was no relationship between the MITF level and proliferation (Fig. 2). The growth rate data of low-MITF cells (SK-MEL-2, Dor and A375) were completely mixed with the data of high-MITF cell lines (MeWo, 501mel, SK-MEL-28), indicating that even low level of MITF can sustain high proliferation rate in some melanomas, apparently dependent on the cellular context.

Inducible reduction in MITF protein generally does not induce the phenotype switching towards EMT changes or expression of SC markers

Although MITF levels are not critical for proliferation either in an artificial inducible system or in native cell lines (above), the presence of MITF is essential to prevent apoptosis in melanoma cells [10, 27, 30]. Furthermore, low-MITF populations of cells are believed to proliferate slowly but to be highly invasive, while high-MITF cells are proliferating rapidly and are not invasive. This 'rheostat model' has been proposed first in 501mel cells [14]. As invasive cells undergo EMT-like changes, we studied whether the inducible MITF decrease *per se* could induce EMT hallmarks. The EMT-like changes in melanoma are characterized by the increased expression of markers such as SNAIL, ZEB1, N-cadherin, vimentin and decreased E-cadherin [31, 32]. We first determined expression levels of proteins previously reported to be important for melanoma progression (Fig. 3A). We found no change in SRC and β -actin as controls. Also β -catenin did not display any changes. BCL2, a MITF target, did not decrease as well (only slightly in SK-MEL-28). Axl level increased in MeWo but remained unchanged in Malme 3M upon

DOX addition and was not present in other cell lines. On the other hand, livin perfectly mimicked the down-regulation of MITF (Fig. 3A) as it is a known MITF downstream target. P27 protein was found increased after increasing DOX levels in three cell lines, very slightly increased in two lines and remained unchanged in one line (Fig. 3A). This cdk inhibitor has been originally described to be the cause of inhibition of proliferation in pro-invasive subpopulations [14, 33]. Brn2 protein appeared increased in MITF-lowered samples in four cell lines, most prominently in 501mel cells (consistent with the original model [14]), while it remained unchanged in two cell lines (Fig. 3A).

As a next step, we have estimated markers which should undergo changes during the EMT-like process after the MITF decrease. We analysed protein levels of vimentin, E-cadherin, N-cadherin, SLUG, SNAIL, ZEB1 and ZEB2. ZEB2 and SLUG are mostly considered to be pro-proliferative and pro-differentiative markers, not involved in the EMT process in melanoma) and revealed a pattern showing only minimal changes (Fig. 3B). The only two characteristic pictures typically reflecting EMT were the decrease in E-cadherin in MeWo cells and increase in N-cadherin in SK-MEL-28 cells. Vimentin was uniformly expressed with increase in 501mel and SK-MEL-28 cells and a low decrease in SK-MEL-3 cells. Further, many EMT-related proteins were absent from cells at all DOX concentrations (*e.g.* E-cadherin and ZEB1 were absent in three different cell lines). In aggregate, lowering of MITF levels alone generally does not lead to EMT-like phenotype patterns on Western blots in six melanoma cell lines.

We examined also the pattern of cancer SC markers after MITF down-regulation. We found no change in the level of proteins ALDH1A1, KLF4 and OCT4 (Nanog was negative in all cell lines, not shown), whereas a profound increase in SOX2 was observed at both DOX concentration in SK-MEL-3, SK-MEL-5 and SK-MEL-28 cell lines. Other three lines did not express SOX2 (Fig. 3C). Thus, for a high expression of SC marker SOX2, which is critical for forming the tumour-initiating cells in melanoma [34], low-MITF level is required. This finding is consistent with the accepted model that the melanoma SC is recruited from the invasive low-MITF populations.

The growth rate of the whole cell population remains unchanged in low-MITF long-term cultures

As the proliferation assays after several days in DOX did not show any substantial growth diminution, we reasoned that longer cultivation of cells in DOX could be required to achieve the effect of more prominent growth deceleration. The cell lines were cultured for 5 weeks with or without DOX, and the proliferation curves were determined during next 9 days. The same experiment was also performed with control virus-infected cells to exclude the possible non-specific effect of DOX at the highest concentration. No substantial changes were observed when proliferation of pooled cultures cultivated in media -DOX and +DOX was estimated (Fig. S4A); 501mel

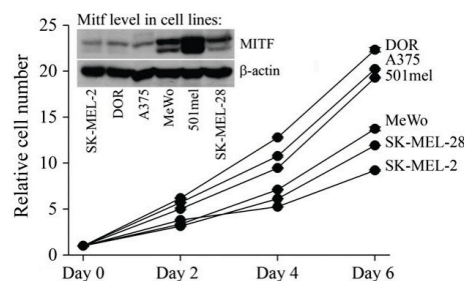


Fig. 2 The proliferation rates of native three low-MITF and three high-MITF melanoma cell lines are completely intermingled. Cells were seeded at lower density in triplicates and were fixed every other day. There were only minimal changes among triplicates, as demonstrated by extremely small S.E. values. Insert: Western blot stained with the anti-MITF antibody shows the MITF protein levels in cell lines analysed and equal loading (β -actin).

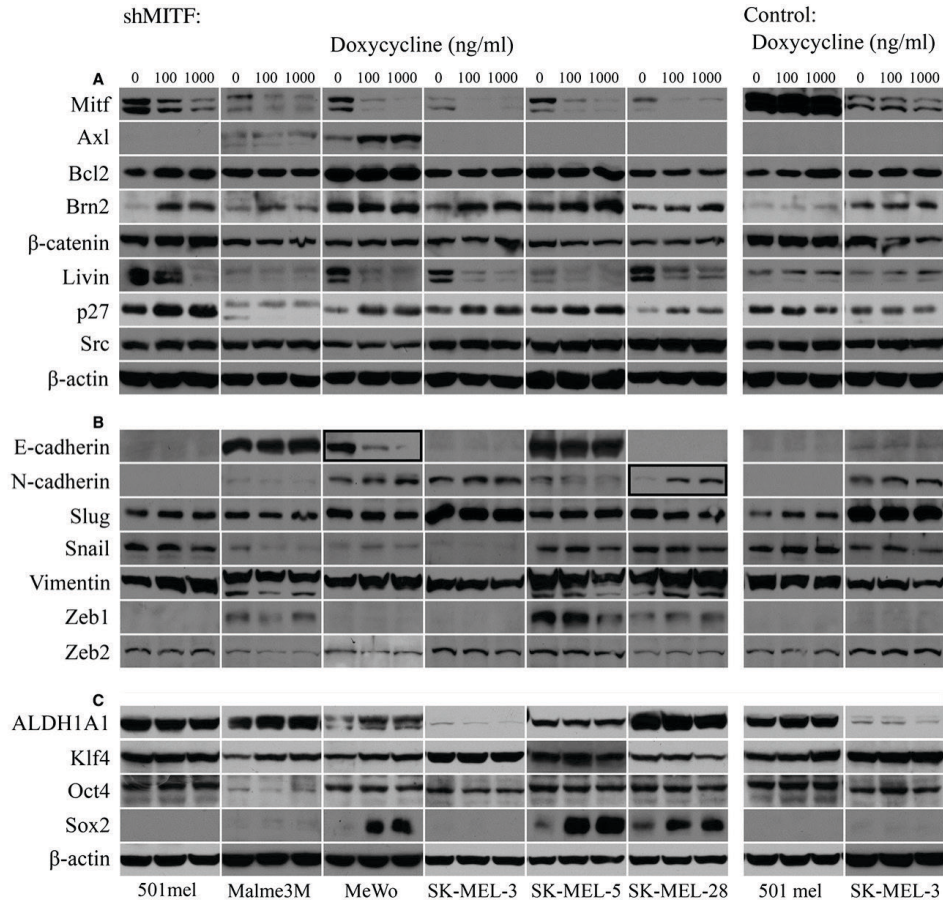


Fig. 3 Pattern of gene expression after down-regulating MITF by two highest DOX concentrations. **(A)** Western blot of proteins not directly connected with the EMT-like process. Livin is a MITF target and mirrors the decrease appearing in MITF samples. Axl is negatively correlated with MITF only in MeWo (the only BRAFwt cell line), where it is most prominently expressed. Actin control shows equal loading. **(B)** The proteins which are often associated with EMT. Two triplets of typical EMT changes (E-cadherin in MeWo and N-cadherin in SK-MEL-28) are framed. Loading and sample's integrity are demonstrated by expression by SLUG and vimentin expression. **(C)** Stem cell markers expression. Two control virus-infected cell lines are also shown (right). Some proteins (e.g. Axl or SOX2) were expressed only in some cell lines. All cells were maintained in DOX for 6 days before performing the Western blots.

cells +DOX ceased to grow at the end of the experiment, probably because their proliferation is highly dependent on MITF [27]. Proliferation of some cell lines was slower even from the day 3 onwards, but this phenomenon was seen also in controls (MeWo and MeWo control, SK-MEL-3 and SK-MEL-5 control). Control Western blots

confirmed lower MITF in DOX-containing cultures after the long-term cultivation (Fig. S4B). Together, the maintenance of melanoma cells in up to 1000 ng/ml DOX did not have any great deleterious effect on the rate of long-term proliferation in pools of infected cell lines.

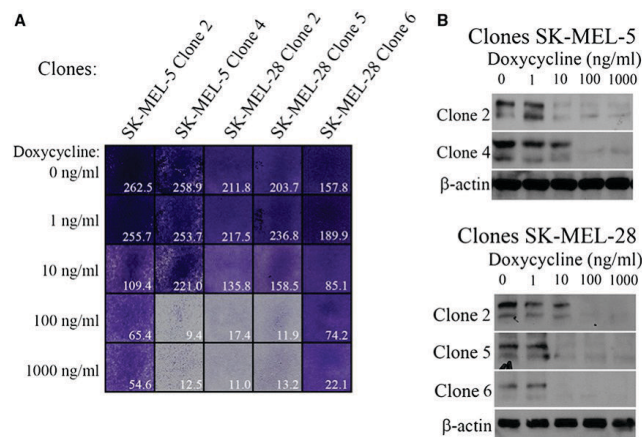


Fig. 4 Cell proliferation of five isolated and expanded clones. **(A)** Of 15 isolated clones from cell lines SK-MEL-5 or SK-MEL-28, maintained in DOX for 4–5 weeks required for expansion, only five clones (shown) revealed prominent decrease in growth in colony outgrowth assay. Two identical experiments gave similar results, and one experiment is depicted. Other 10 clones resembled minimal proliferation changes comparable to Figure 1D (not shown). Proliferation pictures were obtained during 9-day incubation in appropriate DOX concentration. After the removal of DOX, the slowdown clones recovered to near-to-normal proliferation rate. **(B)** Confirmation of stepwise MITF protein diminution on Western blots after DOX treatment in the five clones used in **A**, performed at the beginning of the proliferation experiment.

In long-term cultures, the minority of individual clones with reduced MITF reveals slow proliferation

Given the proliferation of the whole cell population was only slightly affected by MITF decrease, we investigated whether the growth of cultures raised from the individual cell clones could be retarded in DOX. To this end, we isolated and expanded 15 randomly chosen individual clones from SK-MEL-28 or SK-MEL-5 cell lines and maintained them in 0, 100 or 1000 ng/ml DOX concentrations for 5 weeks. The proliferation was determined thereafter by the colony outgrowth assay. We found five (of 15) clones that were substantially retarded in proliferation in these low-MITF cultures. The three most retarded clones were two SK-MEL-28 clones and one SK-MEL-5 clone (Fig. 4A). These three expanded clones retained less than about 15% of proliferation propensity compared the normal growth of the majority of clones. Besides these, other two clones showed decreased growth rate about fourfold to fivefold (Fig. 4A). The control Western blot revealed that MITF still remained gradually decreased at the time of the experiment in these clone-derived cultures maintained in DOX (Fig. 4B). Thus, some individual clones can indeed react to the lowered MITF by exclusive severe growth retardation. We hypothesize that this may happen by the absence of sufficient antiapoptotic signals that were probably almost entirely dependent on MITF in these clones. This experiment strengthens the enormous heterogeneity at the single cell level even in the relatively homologous cell line population.

Invasiveness and migration are not affected by reduced MITF levels

Because the low proliferation of melanoma cells has been reported to be associated with increased invasivity [14, 33], we have estimated invasiveness in the proliferating whole cell populations and in slowly proliferating clones. The collagen matrix invasion assay showed no significant changes between DOX-treated and non-treated cells in all cell lines (Fig. 5A) and clones (not shown). Similarly, the migration assay after cell scratches did not reveal any changes (Figs 5B and S5). Not unexpectedly, the very slow proliferation of the three clones (Fig. 4A) was accompanied with no increase in migration properties, as exemplified by the scratch assay in two clones (Fig. 5B). Next, the viability was tested in whole cell populations, and significant decrease was revealed in three cell lines (SK-MEL-3, SK-MEL-5 and SK-MEL-28) at high DOX concentrations (Fig. S6). This was in accord with the observation that these lines also revealed relatively higher growth retardation (Fig. 1D). These data indicate that viability was a sensitive assay for the detection of phenotype changes after lowering MITF and possibly reflects higher apoptosis in lower viable cells.

Reduction in MITF levels decreases expression of downstream MITF differentiation markers

MITF transcriptionally up-regulates dozens of downstream genes. Many of them are associated with the formation of the pigment

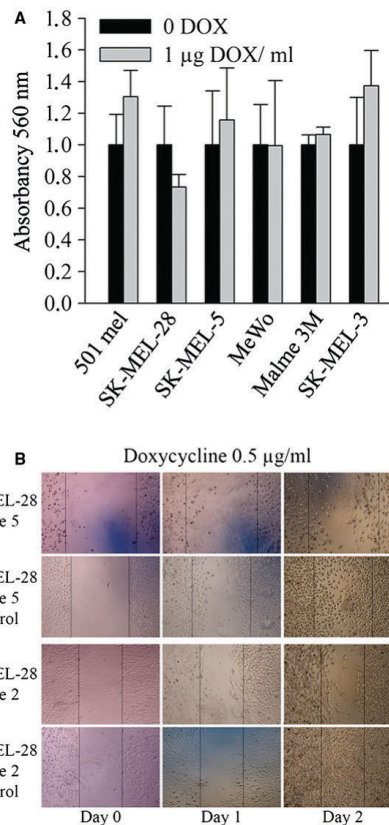


Fig. 5 Cell invasiveness of cell lines and migration assay of selected clones. **(A)** Collagen invasivity assay of six cell lines in medium without DOX and with the highest DOX concentration 1 µg/ml, performed after 6 days in appropriate medium. All results show insignificant changes in invasiveness. Two experiments with similar results were performed and one is presented. **(B)** Wound-healing assays of the two slowly proliferating clones. Note that migration in 0.5 µg/ml DOX is presented as concentrations 100 and 1000 nM produced similar results (not shown).

melanin [35]. Because melastatin, a MITF transcriptional target and a putative tumour suppressor, is sharply responding to MITF levels in melanocytes [36], we used real-time PCR to estimate the mRNA levels of melastatin, together with determining the mRNA levels of the *bona fide* MITF target tyrosinase. Maintaining cells for only 4 days in DOX caused profound decreases in melastatin and tyrosinase in 5 cell lines, while only in SK-MEL-3 cells the changes were less pronounced but significant

(Fig. 6A and B); this was possibly because the final MITF decrease was less dramatic compared to controls without DOX (Fig. 1B) in these cells. The antiapoptotic downstream MITF target livin has been also uniformly decreased in all cell lines, by Western blot (Fig. 3A). Together, differentiation has been reliably and quickly repressed by DOX-dependent down-regulation of MITF levels.

Discussion

Epithelial to mesenchymal transition is a key process associated with the invasive and metastatic disease in epithelial cancers, and EMT-like changes appear also during the phenotype switching in melanoma. Many genes change their expression during EMT-like process. The most characteristic is the down-regulation of E-cadherin and up-regulation of N-cadherin, together with the activation of SNAIL (SNAI1) and ZEB1 expression. EMT-like gene pattern has been induced in normal melanocytes by ectopic mutated BRAF [31]. Several authors have reported that melanoma has slightly atypical profile of protein expression in EMT, as SLUG (SNAI2) and ZEB2 have been presented as pro-differentiative genes coexpressed with high MITF, not participating in the EMT process [6, 29, 30, 37]. The expression of EMT markers has been found to be highly heterogeneous with the predominant EMT signature being high-N-cadherin/high-Axl/low-MITF, whereas the differentiation pattern was characterized mostly by high-E-cadherin/high-MITF in primary melanoma cell lines [38]. Even individual cells in tumours have shown different expression patterns of EMT proteins with SLUG expression weakening during tumour progression [39]. Our present results showed only two EMT-specific changes, each in other cell line (Fig. 3B), whereas the presence or changes in other EMT markers were inconsistent after the reduction in MITF expression.

We also observed no change in expression of three SC markers. Only SOX2, the expression of which was shown to require the Hedgehog signalling in melanoma and is crucial for the self-renewal and tumorigenicity of human melanoma-initiating cells [34], sharply increased in three cell lines with induced low MITF. In the remaining three cell lines, SOX2 was not expressed (Fig. 3C). Although OCT4 was found earlier increased in siRNA-MITF-transfected SK-MEL-28 cells [33], we did not observe any OCT4 changes (Fig. 3C). This discrepancy might be explained by possible more efficient reduction in MITF using siRNA-MITF. Formally, as MITF undergoes post-translational modifications that might have modulated the effect caused by MITF decrease.

Intriguingly, the highly pro-oncogenic and invasive Wnt/β-signalling pathway has been found to be anti-invasive in melanoma as β-catenin blocks invasiveness [40]. β-catenin pathway acts upstream of MITF and activates its transcription, and high-MITF levels are anti-invasive. MITF also suppresses the Rho-GTPase-regulated invading and interferes with β-catenin-induced expression of the pro-invasive enzyme membrane type 1 matrix metalloproteinase [40].

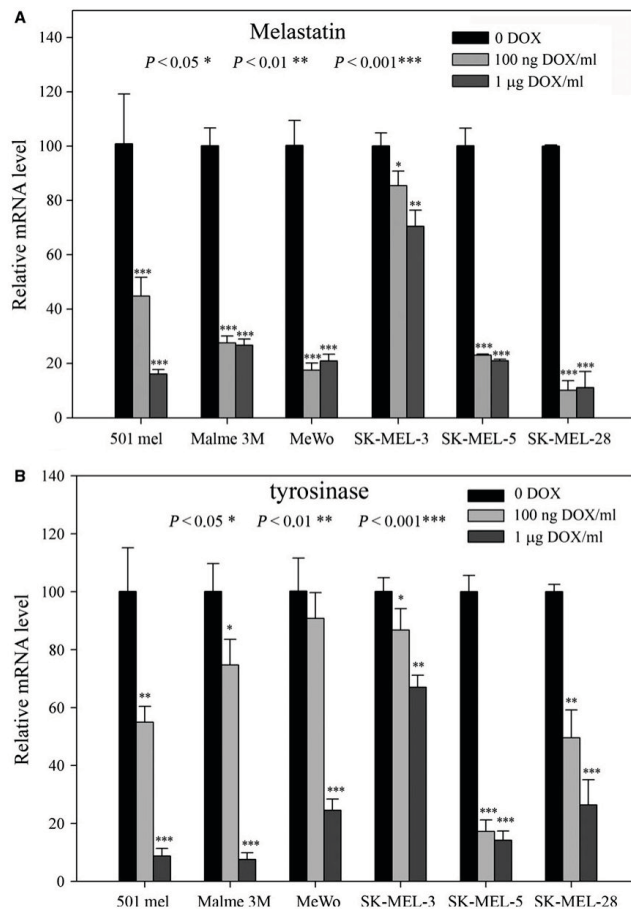


Fig. 6 Real-time PCR results detecting mRNA levels of MITF downstream differentiation markers. **(A)** The changes in melastatin mRNA levels after incubation of cells in DOX. **(B)** Levels of tyrosinase mRNA. All deviations from the -DOX controls (100 relative units) were statistically significant (with only one exception: tyrosinase in lower DOX concentration in one cell line), as depicted directly in the Figure. With the exception of SK-MEL-3 cells where the changes were small, strong decrease in RNA levels for these differentiation markers was observed.

Recently, two interesting studies which would at least partly explain the exclusive role of MITF in lowering invasiveness have implicated the expression of guanosine monophosphate reductase (GMPT), an enzyme of guanylate metabolism, in the regulation of invasiveness in melanoma cells. GMPT can deplete cellular GTP level, an event linked to lower melanoma invasiveness. The morphology of MITF-depleted invasive cells is accompanied by a larger number of invadopodia [41]. Subsequently, it has been shown that MITF is an upstream regulator of GMPT [42]. Due to the lower GTP levels in cells overexpressing MITF or GMPT, the invasiveness would be suppressed. Oppositely, when siRNA-mediated decrease in MITF was induced, with consequent declined levels of GMPT, even small increase in GTP (several per

cents) generated high increase in invasion, which was even eightfold in 501mel cells and about twofold to threefold in SK-MEL-28 cells [42]. High MITF concomitantly suppressed activity of RAC1, a kinase mutated in a subset of melanomas [43], and suppression of RAC1 activity was required to reduce invasiveness. Although we have also used clones from SK-MEL-28 and SK-MEL-5 cells displaying slower proliferation, no change in invasivity was recorded. Recently, glutamine depletion was shown to be sufficient to engender the decrease in MITF and invasiveness in melanoma cells. However, the MITF decrease could not be a cause of invasiveness, as glutamine starvation led to invasivity also in MITF-negative cells [44]. The transcription factor ATF4 alone down-regulated MITF but surprisingly did not induce

invasiveness. The authors suggested a mechanism of translation reprogramming whereby the eIF2B factor was found to be a crucial driver of melanoma invasiveness. Salubrinal, which inhibits dephosphorylation of complexes acting on p-eIF2 α , increased ATF4 and decreased MITF expression and induced invasiveness. Thus, as phosphorylated eIF2 α inhibits eIF2B, this global reprogramming of translation involving high expression of ATF4 leads to invasiveness in melanoma cells [44]. These findings where other factors besides sole MITF decrease are required to induce invasiveness are in conformity with the findings shown here.

The antiapoptotic role of MITF in melanomas is clearly established. However, some concern remains how the antiapoptotic signals are sustained in melanoma cell lines in which MITF expression is very low or in low-MITF (and more invasive) areas of tumours. First, apparently, highly different cell context may exist among tumour cell subpopulations, and possibly single cells, that ensure antiapoptosis within the low-MITF cells. Second, another one or more antiapoptotic genes, such as Axl or others ensure that low-MITF cells do not undergo apoptosis. Previously, we have discussed whether so-called 'MITF-negative' melanomas are still melanomas, as they must have lost all MITF downstream differentiation markers [45]. We argue that such cells either die due to the lack of MITF antiapoptotic function, as already documented in 501mel cells [27], or continue growing as an undifferentiated tumour if antiapoptosis is provided by other genes. The observed low-MITF/high-Axl populations in sections of human tumours [22] could serve as a possible example. What would be also conceivable is that in the course of cell line or tumour growth, cells might have adjusted MITF levels to amounts sufficient to promote proliferation, possibly with help of other pro-proliferative (and antiapoptosis) protein(s), a notion that would reconcile both the rheostat model and our results as discussed above.

Inducibly and gradually decreased MITF level in melanoma cell lines, as described here, incurred slightly diminished proliferation, but the decrease was much smaller than anticipated taking into account the previous results [14, 18, 33]. Low-MITF populations such as some cell lines or slightly pigmented areas of tumours presumably utilize other proteins to maintain proliferation. We have observed various proliferation levels among isolated cell clones from the same cell line, indicating that even single cells in a relatively homogenous original cell line population may gradually create quite different proliferation potential when cultured longer under low-MITF conditions; the growth of small number of clones almost halted proliferation while other clones proliferated at an unchanged rate (Fig. 4A and not shown). Consistent increase in the p27 protein, although slight, seems to be a more general hallmark of MITF down-regulation. It is questionable whether the increase in p27 protein alone can incur the deceleration of proliferation in all types of low-MITF cell lines and tumours subpopulations. Predictably, p27 protein might contribute to slow proliferation in some situations *in vitro* or *in vivo*. The *in vivo* effect of p27 has not been studied extensively.

The presented results bring more complexity to the phenotype switching process with the emphasis on the cell context and individual levels of MITF in cell lines and possibly even in single cells.

It is highly probable that the primary functions of MITF in melanoma are to maintain the lineage identity (by regulating the downstream differentiation markers) and to play the indisputable antiapoptotic role. We further suggest that diminution of MITF level may accompany rather than induce the invasive phenotype in tumours, and its lower level *in vivo* may then eventually participate in the slow proliferation of the invasive tumour subpopulations.

Acknowledgements

Funding source: The authors thank Dr. C. Goding (Ludwig Institute for Cancer Research, Oxford, UK) for reading the manuscript and critical remarks. This work was supported by grant GAUK no. 172214 from the Charles University Prague and by the institutional program PROGRES Q25 from the Charles University Prague.

Author contributions

J.V. and K.V. designed the study, cultured cells and carried out experiments; J.R. performed Western blots and most of other experiments; P.H. performed real-time PCR and invasivity assays; K.V. and L.O. prepared the Figures and performed statistical analysis; and J.V. wrote the manuscript. All authors have read and approved the manuscript.

Conflict of interest

The authors confirm that there is no conflict of interests.

Supporting information

Additional Supporting Information may be found online in the supporting information tab for this article:

Fig. S1 Complete blocking of MITF expression achieved by transfection of shRNA-MITF cloned in pSUPER-puro plasmid followed by a short 2 days puromycin selection.

Fig. S2 Immunofluorescence with the anti-MITF antibody confirming the knockdown of MITF.

Fig. S3 Cell cycle profiles of cell lines grown with or without DOX.

Fig. S4 Proliferation of long-term cultures of cell lines in media with or without DOX.

Fig. S5 Migration (wound-healing assay) of six cell lines in – DOX and + DOX.

Fig. S6 Viability of cell lines performed in the media with indicated concentrations of DOX.

References

- Davies H, Bignell GR, Cox C, *et al.* Mutations of the BRAF gene in human cancer. *Nature*. 2002; 417: 949–54.
- Wellbrock C, Rana S, Paterson H, *et al.* Oncogenic BRAF regulates melanoma proliferation through the lineage specific factor MITF. *PLoS One*. 2008; 3: e2734.
- Obenauf AC, Zou Y, Ji AL, *et al.* Therapy-induced tumour secretomes promote resistance and tumour progression. *Nature*. 2015; 520: 368–72.
- Roesch A. Tumor heterogeneity and plasticity as elusive drivers for resistance to MAPK pathway inhibition in melanoma. *Oncogene*. 2015; 34: 2951–7.
- Shannan B, Perego M, Somasundaram R, *et al.* Heterogeneity in Melanoma. *Cancer Treat Res*. 2016; 167: 1–15.
- Tulchinsky E, Pringle JH, Caramel J, *et al.* Plasticity of melanoma and EMT-TF reprogramming. *Oncotarget*. 2014; 5: 1–2.
- Roesch A, Paschen A, Landsberg J, *et al.* Phenotypic tumour cell plasticity as a resistance mechanism and therapeutic target in melanoma. *Eur J Cancer*. 2016; 59: 109–12.
- Meacham CE, Morrison SJ. Tumour heterogeneity and cancer cell plasticity. *Nature*. 2013; 501: 328–37.
- Jolly MK, Boareto M, Huang B, *et al.* Implications of the hybrid epithelial/Mesenchymal phenotype in metastasis. *Front Oncol*. 2015; 5: 155.
- Garraway LA, Widlund HR, Rubin MA, *et al.* Integrative genomic analyses identify MITF as a lineage survival oncogene amplified in malignant melanoma. *Nature*. 2005; 436: 117–22.
- McGill GG, Horstmann M, Widlund HR, *et al.* Bcl2 regulation by the melanocyte master regulator Mitf modulates lineage survival and melanoma cell viability. *Cell*. 2002; 109: 707–18.
- Dynek JN, Chan SM, Liu J, *et al.* Microphthalmia-associated transcription factor is a critical transcriptional regulator of melanoma inhibitor of apoptosis in melanomas. *Cancer Res*. 2008; 68: 3124–32.
- Dar AA, Majid S, Bezrookove V, *et al.* BPTF transduces MITF-driven pro-survival signals in melanoma cells. *Proc Natl Acad Sci USA*. 2016; 113: 6254–8.
- Carreira S, Goodall J, Denat L, *et al.* Mitf regulation of Dia1 controls melanoma proliferation and invasiveness. *Genes Dev*. 2006; 20: 3426–39.
- Goodall J, Carreira S, Denat L, *et al.* Brn-2 represses microphthalmia-associated transcription factor expression and marks a distinct subpopulation of microphthalmia-associated transcription factor-negative melanoma cells. *Cancer Res*. 2008; 68: 7788–94.
- Cook AL, Sturm RA. POU domain transcription factors: BRN2 as a regulator of melanocytic growth and tumorigenesis. *Pigment Cell Melanoma Res*. 2008; 21: 611–26.
- Pinner S, Jordan P, Sharrock K, *et al.* Intravital imaging reveals transient changes in pigment production and Brn2 expression during metastatic melanoma dissemination. *Cancer Res*. 2009; 69: 7969–77.
- Hoek KS, Goding CR. Cancer stem cells versus phenotype-switching in melanoma. *Pigment Cell Melanoma Res*. 2010; 23: 746–59.
- Thurber AE, Douglas G, Sturm EC, *et al.* Inverse expression states of the BRN2 and MITF transcription factors in melanoma spheres and tumour xenografts regulate the NOTCH pathway. *Oncogene*. 2011; 30: 3036–48.
- Javelaud D, Alexaki VI, Pierrat MJ, *et al.* GLI2 and M-MITF transcription factors control exclusive gene expression programs and inversely regulate invasion in human melanoma cells. *Pigment Cell Melanoma Res*. 2011; 24: 932–43.
- Roesch A, Fukunaga-Kalabis M, Schmidt EC, *et al.* A temporarily distinct subpopulation of slow-cycling melanoma cells is required for continuous tumor growth. *Cell*. 2010; 141: 583–94.
- Sensi M, Catani M, Castellano G, *et al.* Human cutaneous melanomas lacking MITF and melanocyte differentiation antigens express a functional Axl receptor kinase. *J Invest Dermatol*. 2011; 131: 2448–57.
- Quintana E, Shackleton M, Sabel MS, *et al.* Efficient tumour formation by single human melanoma cells. *Nature*. 2008; 456: 593–8.
- Quintana E, Shackleton M, Foster HR, *et al.* Phenotypic heterogeneity among tumorigenic melanoma cells from patients that is reversible and not hierarchically organized. *Cancer Cell*. 2010; 18: 510–23.
- Fang D, Nguyen TK, Leishear K, *et al.* A tumorigenic subpopulation with stem cell properties in melanomas. *Cancer Res*. 2005; 65: 9328–37.
- Parmiani G. Melanoma cancer stem cells: markers and functions. *Cancers*. 2016; 8: 34.
- Ondrusova L, Vachtenheim J, Reda J, *et al.* MITF-independent pro-survival role of BRG1-containing SWI/SNF complex in melanoma cells. *PLoS One*. 2013; 8: e54110.
- Wiederschain D, Wee S, Chen L, *et al.* Single-vector inducible lentiviral RNAi system for oncology target validation. *Cell Cycle*. 2009; 8: 498–504.
- Vachtenheim J, Ondrusova L, Borovansky J. SWI/SNF chromatin remodeling complex is critical for the expression of microphthalmia-associated transcription factor in melanoma cells. *Biochem Biophys Res Commun*. 2010; 392: 454–9.
- Hartman ML, Czyz M. Pro-survival role of MITF in melanoma. *J Invest Dermatol*. 2015; 135: 352–8.
- Caramel J, Papadogeorgakis E, Hill L, *et al.* A switch in the expression of embryonic EMT-inducers drives the development of malignant melanoma. *Cancer Cell*. 2013; 24: 466–80.
- Vandamme N, Berx G. Melanoma cells revive an embryonic transcriptional network to dictate phenotypic heterogeneity. *Front Oncol*. 2014; 4: 352.
- Cheli Y, Giuliano S, Botton T, *et al.* Mitf is the key molecular switch between mouse or human melanoma initiating cells and their differentiated progeny. *Oncogene*. 2011; 30: 2307–18.
- Santini R, Pietrobono S, Pandolfi S, *et al.* SOX2 regulates self-renewal and tumorigenicity of human melanoma-initiating cells. *Oncogene*. 2014; 33: 4697–708.
- Vachtenheim J, Borovansky J. “Transcription physiology” of pigment formation in melanocytes: central role of MITF. *Exp Dermatol*. 2010; 19: 617–27.
- Miller AJ, Du J, Rowan S, *et al.* Transcriptional regulation of the melanoma prognostic marker melastatin (TRPM1) by MITF in melanocytes and melanoma. *Cancer Res*. 2004; 64: 509–16.
- Denecker G, Vandamme N, Akay O, *et al.* Identification of a ZEB2-MITF-ZEB1 transcriptional network that controls melanogenesis and melanoma progression. *Cell Death Differ*. 2014; 21: 1250–61.
- Kim JE, Leung E, Baguley BC, *et al.* Heterogeneity of expression of epithelial-mesenchymal transition markers in melanocytes and melanoma cell lines. *Front Genet*. 2013; 4: 97.
- Shirley SH, Greene VR, Duncan LM, *et al.* Slug expression during melanoma progression. *Am J Pathol*. 2012; 180: 2479–89.
- Arozarena I, Bischof H, Gilby D, *et al.* In melanoma, beta-catenin is a suppressor of invasion. *Oncogene*. 2011; 30: 4531–43.

41. **Wawrzyniak JA, Bianchi-Smiraglia A, Bshara W, et al.** A purine nucleotide biosynthesis enzyme guanosine monophosphate reductase is a suppressor of melanoma invasion. *Cell Rep.* 2013; 5: 493–507.
42. **Bianchi-Smiraglia A, Bagati A, Fink EE, et al.** Microphthalmia-associated transcription factor suppresses invasion by reducing intracellular GTP pools. *Oncogene.* 2017; 36: 84–96.
43. **Krauthammer M, Kong Y, Ha BH, et al.** Exome sequencing identifies recurrent somatic RAC1 mutations in melanoma. *Nat Genet.* 2012; 44: 1006–14.
44. **Falletta P, Sanchez-Del-Campo L, Chauhan J, et al.** Translation reprogramming is an evolutionarily conserved driver of phenotypic plasticity and therapeutic resistance in melanoma. *Genes Dev.* 2017; 31: 18–33.
45. **Vachtenheim J, Ondrusova L.** Microphthalmia-associated transcription factor expression levels in melanoma cells contribute to cell invasion and proliferation. *Exp Dermatol.* 2015; 24: 481–4.

Supplementary Figure Legends.

Supplementary Figure Legends.

Fig. S1 Complete blocking of MITF expression achieved by a non-inducible transfection of shRNA-MITF used in this work. The target sequence was cloned in pSUPER-puro plasmid, transfected in 501mel cells, followed by a short 2 days puromycin selection. The RIPA extracts were prepared and Western blots performed. Control (scrambled) sequence did not have any effect on the MITF level. Actin has been used as a loading control confirming equal loading and the integrity of both samples.

Fig. S2 Immunofluorescence with the anti-MITF antibody confirming the knockdown of MITF. Immunofluorescence was performed with anti-MITF antibody (antibody dilution 1:200, left blocks) and DAPI (right blocks) in the identical image fields. Cells were left without DOX (upper blocks) or in 1 $\mu\text{g/ml}$ DOX (lower blocks) for one week, replated into IF chambers and processed for IF next day. Scale bar 25 μm . Control cells (only two cell lines are shown as controls, similar results were obtained with the remaining four controls) do not show any difference when - DOX and + DOX fields are compared.

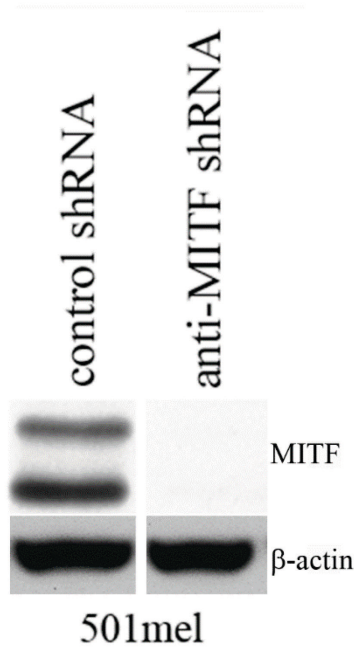
Fig. S3 Cell cycle profiles of cell lines grown with or without DOX. Cells were maintained in - DOX or + DOX media for one week and FACS profiles were then taken after staining DNA with propidium iodide. No appreciable changes were seen when - and + DOX cells were compared. Only in + DOX SK-MEL-28 cells the G2/S phase peak was (paradoxically) increased.

Fig. S4 Proliferation of long-term cultures of cell lines in media with or without DOX. (A) Whole cell populations including control cells (containing scrambled shRNA) were cultured for

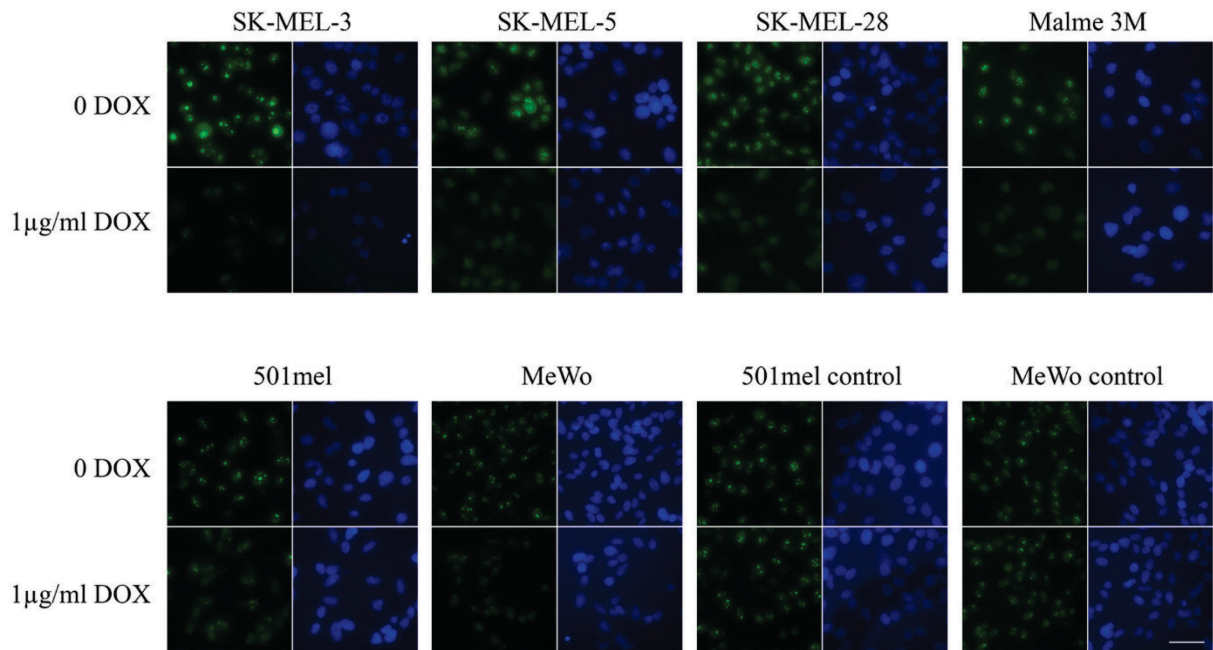
five weeks in the indicated DOX concentration and then the proliferation rate experiment was performed in 24-well plates in triplicates. All cell lines grew normally during the five week period. (B) Control Western blot indicating the decrease of MITF was done before the experiment.

Fig. S5 Migration (wound healing assay) of six cell lines in – DOX and + DOX. The migration of six cell lines was determined by the wound healing assay as described in Materials and Methods. No differences were observed between –DOX and + DOX cultures.

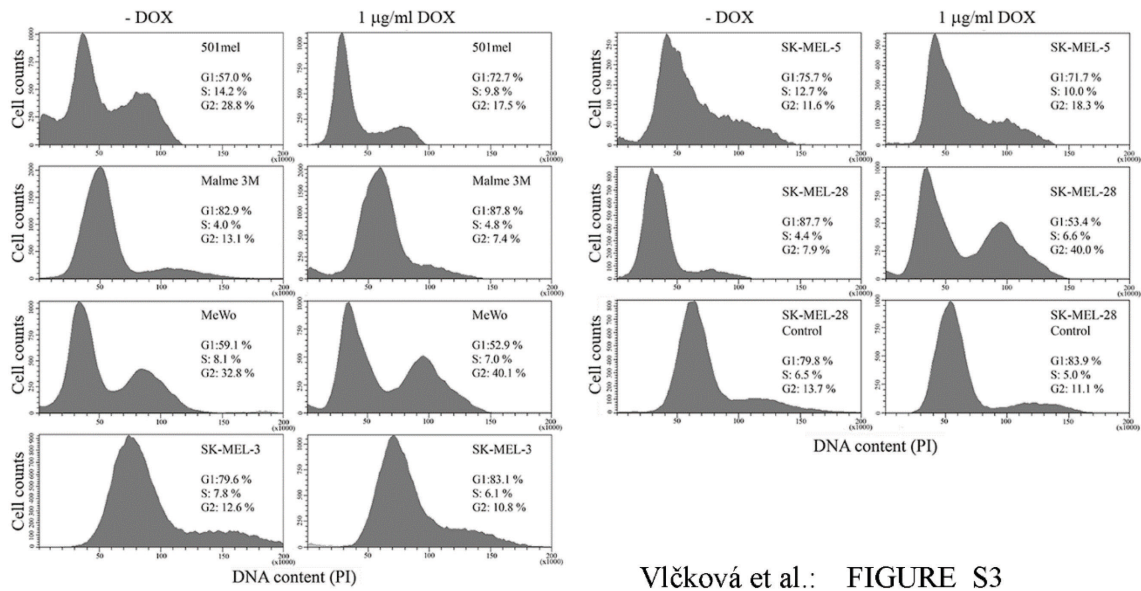
Fig. S6 Viability of cell lines performed in the media with indicated concentrations of DOX. All cell populations (including controls) were cultured for 6 days in media without or with the indicated concentration of DOX. Next day, the viability assay was performed. Cells more sensitive to MITF decrease seem to be SK-MEL-3, SK-MEL-5, and SK-MEL-28. It is a result which roughly corresponds to the slightly lowered proliferation in these cells (see Fig. 1). Predictably, lowered viability was caused by increased apoptosis in cells requiring higher MITF for proliferation.



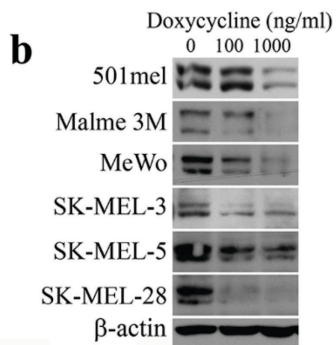
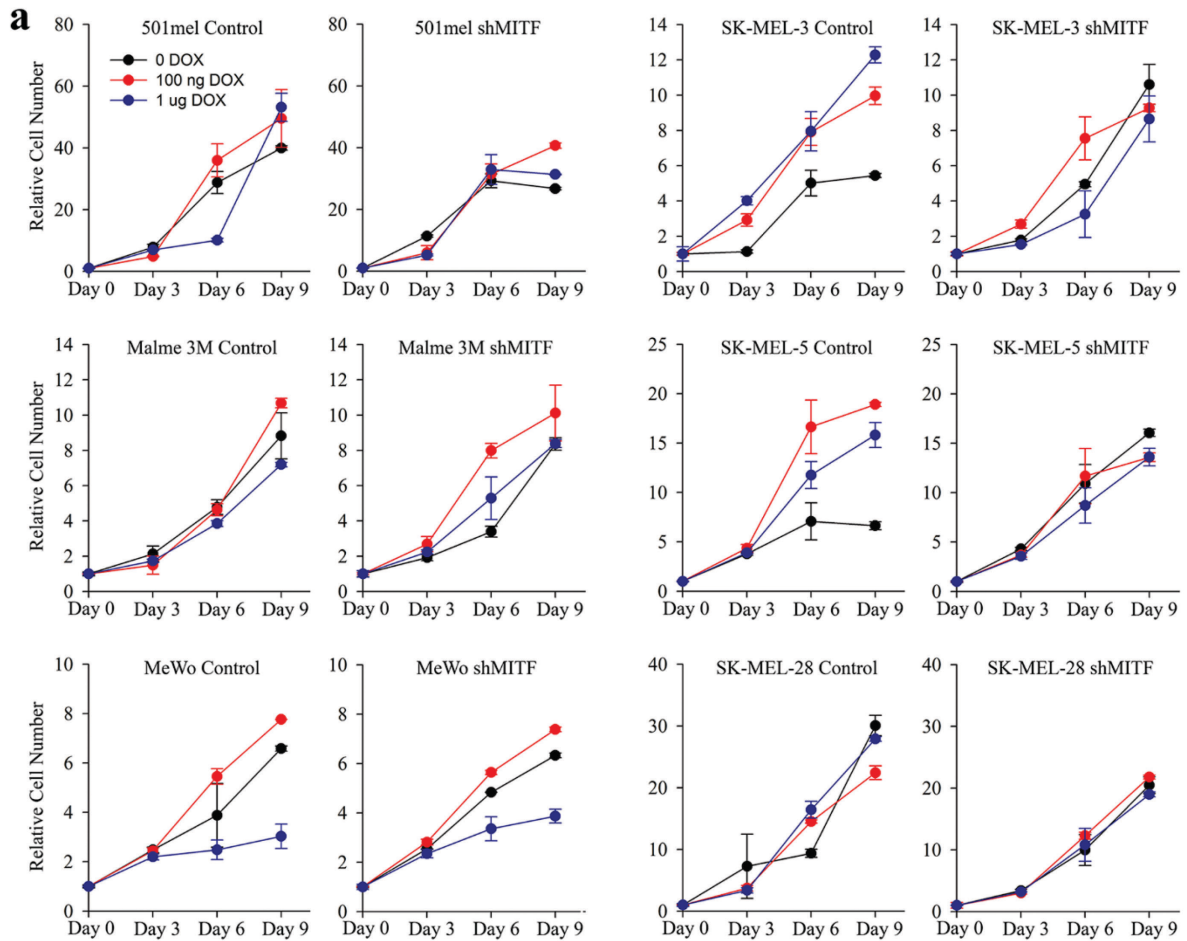
Vlčková et al.: FIGURE S1



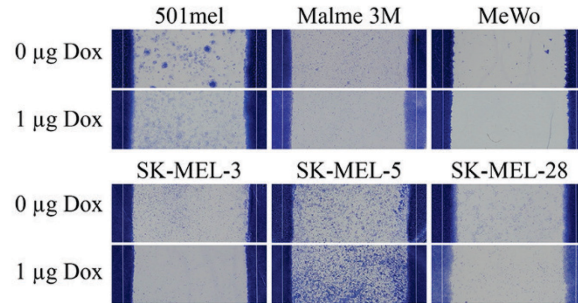
Vlčková et al.: FIGURE S2



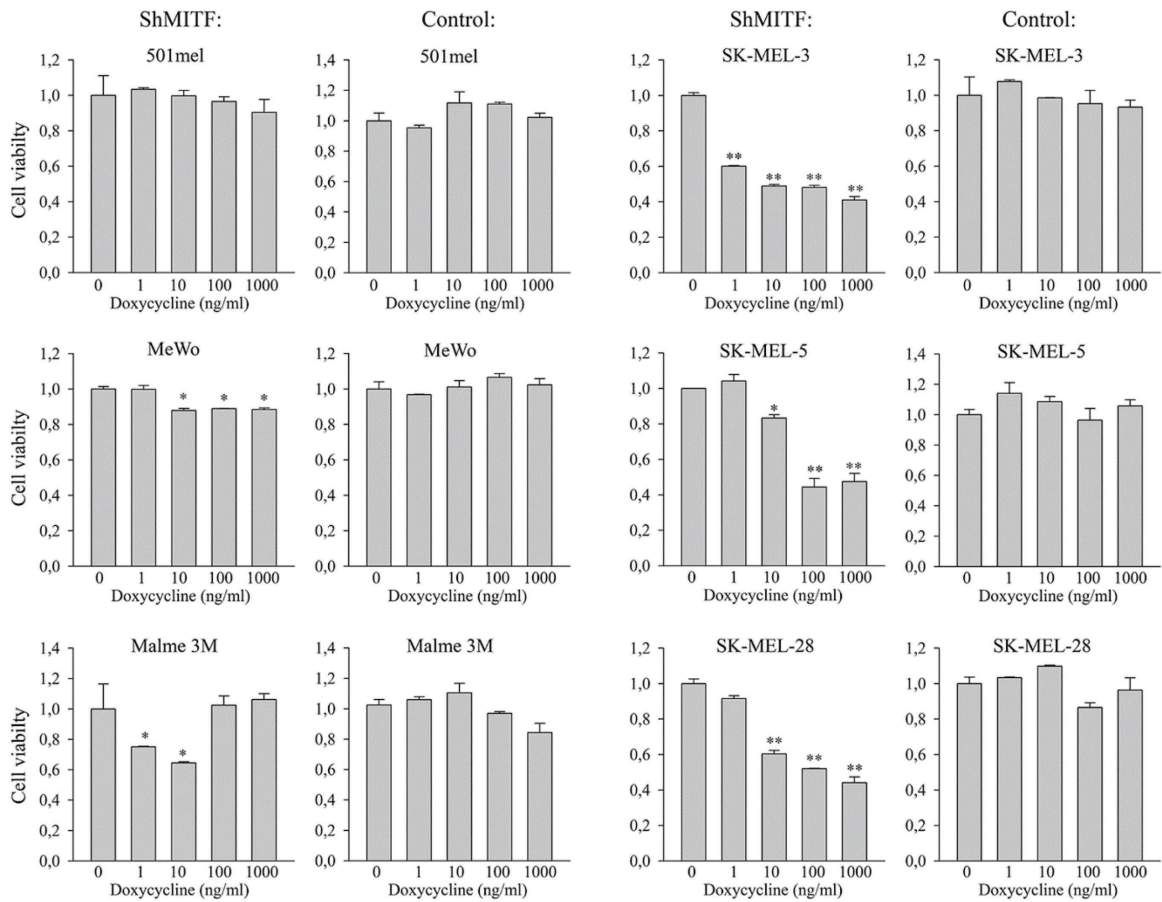
Vičková et al.: FIGURE S3



Vlčková et al. FIGURE S4



Vlčková et al: FIGURE S5



Vlčková et al.: FIGURE S6



FBXO32 links ubiquitination to epigenetic reprogramming of melanoma cells

Nadia Habel^{1,2} · Najla El-Hachem^{1,2} · Frédéric Soysouvanh^{1,2} · Hanene Hadhiri-Bziouche^{1,2} · Serena Giuliano^{1,2} · Sophie Nguyen^{1,2} · Pavel Horák^{1,2} · Anne-Sophie Gay³ · Delphine Debayle³ · Nicolas Nottet^{1,2} · Guillaume Béranger^{1,2} · Brigitte Bressac-de Paillerets⁴ · Corine Bertolotto^{1,2} · Robert Ballotti^{1,2}

Received: 25 May 2020 / Revised: 1 December 2020 / Accepted: 11 December 2020 / Published online: 18 January 2021

© The Author(s), under exclusive licence to ADMC Associazione Differenziamento e Morte Cellulare 2021. This article is published with open access

Abstract

Ubiquitination by serving as a major degradation signal of proteins, but also by controlling protein functioning and localization, plays critical roles in most key cellular processes. Here, we show that MITF, the master transcription factor in melanocytes, controls ubiquitination in melanoma cells. We identified FBXO32, a component of the SCF E3 ligase complex as a new MITF target gene. FBXO32 favors melanoma cell migration, proliferation, and tumor development *in vivo*. Transcriptomic analysis shows that FBXO32 knockdown induces a global change in melanoma gene expression profile. These include the inhibition of CDK6 in agreement with an inhibition of cell proliferation and invasion upon FBXO32 silencing. Furthermore, proteomic analysis identifies SMARCA4, a component of the chromatin remodeling complexes BAF/PBAF, as a FBXO32 partner. FBXO32 and SMARCA4 co-localize at loci regulated by FBXO32, such as CDK6 suggesting that FBXO32 controls transcription through the regulation of chromatin remodeling complex activity. FBXO32 and SMARCA4 are the components of a molecular cascade, linking MITF to epigenetics, in melanoma cells.

Introduction

Ubiquitination is a post-translational modification initially described to play a key role in protein homeostasis through subsequent degradation of targeted proteins by proteasome or lysosomes. Ubiquitination was also shown to regulate protein interaction, functioning, and localization. The specificity of the effects of ubiquitination is controlled by a complex ubiquitin code [1]. Ubiquitination controls a wide spectrum of cellular processes that includes NF-κB pathway activation, DNA damage repair, cell death, autophagy, or metabolism [2]. Therefore, it is not surprising that dysregulation of ubiquitination process has broad consequences in cellular biology, leading to numerous pathologies, including cancer. The characterization of the regulation of genes involved in ubiquitination, as well as the cellular processes regulated by ubiquitination are therefore of paramount importance to improve our knowledge on the associated diseases.

Cutaneous melanoma arises from melanocytes, neural crest-derived cells producing skin pigments. It is the most aggressive forms of skin cancer because of its high propensity to metastasize. Metastatic melanoma is the leading cause of skin cancer-related mortality. In the last decade, stunning

These authors contributed equally: Nadia Habel, Najla El-Hachem, Frédéric Soysouvanh

These authors jointly supervised this work: Corine Bertolotto, Robert Ballotti

Edited by D. Guardavaccaro

Supplementary information The online version of this article (<https://doi.org/10.1038/s41418-020-00710-x>) contains supplementary material, which is available to authorized users.

✉ Robert Ballotti
ballotti@unice.fr

¹ Université Nice Côte d'Azur, Nice, France

² Inserm U1065, C3M, Team 1, Biology and Pathologies of Melanocytes, Equipe labellisée ARC 2019, Nice, France

³ CNRS, Institut de Pharmacologie Moléculaire et Cellulaire, Sophia Antipolis, France

⁴ Département de Biopathologie et INSERM U1279, Gustave Roussy, Villejuif, France

improvement of metastatic melanoma treatment has been achieved by using therapies targeting *BRAF*^{V600E}, the most frequent somatic mutation in melanoma and most recently, with immunotherapies targeting the negative immune check points CTLA4 and PD1. Despite a huge response rate, the targeted therapies did not reach the initial expectations because of quasi systematic relapses, ensuing resistance acquisition. With immunotherapies, up to 40% of long-term responders have been described, but most of the patients are or become resistant to these therapies. Resistance can arise from genetic alterations, among which new mutations in *NRAS* or *MEK* for resistance to targeted therapies, and in *JAK* or *B2M* for resistance to immunotherapies [3].

In addition, melanoma cells are highly plastic, and resistance is also frequently caused by a switch from proliferative to invasive phenotype, ensuing epigenetic and transcriptional rewiring [4, 5].

Compelling data have been gathered showing the involvement of ubiquitination in melanoma development [6]. Among them, the deubiquitinase, BRCA-1-associated protein-1 is frequently mutated in uveal melanomas [7] and in a subset of cutaneous melanomas [8], where it functions as a tumor suppressor. FBXW7, a F-Box/WD repeat containing protein that constitutes a subunit of the ubiquitin protein ligase complex, SKP1-cullin-F-box (SCF), and PARKIN, an E3 ubiquitin ligase, also function as tumor suppressors and were found mutated in melanomas [9, 10]. More recently, HACE1, HECT domain and ankyrin repeat-containing E3 ubiquitin protein ligase that regulates RAC1 activity, was also reported to favor melanoma invasiveness [11].

Microphthalmia-associated transcription factor (MITF), the key transcription factor in melanocytes, is also known to play a crucial role in melanoma phenotypic switch [12–14] and therapy resistance [15–17].

MITF was initially described to control differentiation and pigmentation through the regulation of genes involved in melanogenesis [18], then MITF was also involved in melanoma cell survival and proliferation, while it represses motility and invasive capacities. The involvement of MITF in such a large array of biological processes makes of MITF a crucial player in melanoma development [19].

In this work, we sought to investigate the role of MITF in the ubiquitination processes in melanoma cells. We identified at least three distinct genes regulated by MITF that are also involved in the ubiquitination process. Among them, we focused our attention on *FBXO32* because it is located on chromosome 8q, a region frequently amplified in melanoma and its role in melanomas has never been studied. We performed a comprehensive analysis of the role of *FBXO32* in melanoma, showing that it regulates key biological processes and transcriptional programs of melanoma cells through epigenetics mechanisms.

Material and methods

Cell cultures and reagents

Human melanoma cell lines A375, MeWo, and SKMel 28 were from ATCC. 501Mel cell line was provided by Colin Goding (Oxford). All cell lines were used less than ten passages after STR profiling. Cells were cultured in Dulbecco's Modified Eagle's medium supplemented with 7% fetal bovine serum (FBS) and 1% penicillin-streptomycin. short-term cultures were isolated from metastatic malignant melanoma fresh sterile tissues obtained from the Nice CHU Hospital. Written informed consent was obtained from each patient included in this study, and the study was approved by the hospital ethics committee (Nice Hospital Center and University of Nice Sophia Antipolis, No. 210-2998). The study was performed in accordance with the Declaration of Helsinki. Cells were cultured in RPMI medium supplemented with 10% FBS and 1% penicillin-streptomycin. Cells were grown at 37 °C in a humidified atmosphere containing 5% CO₂. Melanocytes were obtained from children foreskin (5- and 7-year old) by overnight digestion in phosphate-buffered saline (PBS) containing 0.5% dispase grade II at 4 °C, followed by a 1-h digestion with trypsin/EDTA solution (0.05%:0.02% in PBS) at 37 °C. Cells were grown in MCDB 153 medium supplemented with FCS 2%, 0.4 µg/ml hydrocortisone, 5 µg/ml insulin, 16 nM PMA, 1 ng/ml b-FGF, and penicillin/streptomycin (100 U/ml:50 µg/ml).

FBXO32 lentivirus construction (RC223661L1) was from Origen.

Transient transfection of siRNA

Briefly, a single pulse of 25 nM of siRNA was administered to the cells at 50% confluency through transfection with 5 µl of LipofectamineTM RNAiMAX in Opti-MEM medium (Invitrogen). siRNA-mediated down-regulation of MITF was achieved with specific sequences 5'-GGUGAAUCGGAUCAUCAAGTT-3' and 5'-CUUGAUGAUCCGAUCCACCTT-3' from Invitrogen. FBXO32 (SI04366166, SI04317803), CDK6 (SI00024360, SI00605052), and SMAD7 (SI00082537, SI00082544) siRNAs were purchased from Qiagen.

Cell migration

Cell migration was carried out using a Boyden chamber assay with 8 µm pore filter inserts (BD Bioscience). Cells (100 × 10³) were seeded on the upper chamber of a trans-well and RPMI + 10% FBS placed into the lower chamber. Sixteen hours later, adherent cells to the underside of the filters were fixed with 4% paraformaldehyde, stained with

0.4% crystal violet, and counted. Results represent the average of triplicate samples from three independent experiments.

Cell proliferation

The cells were seeded onto 12-well dishes (1×10^4 cells), and at 48 h post-transfection, they were detached with trypsin from day 1 to 4 and counted in triplicate using a hemocytometer. The experiments were performed at least three times.

Colony formation assay

Human melanoma cells were seeded onto 6-well plates. The cells were subsequently placed in a 37 °C, 5% CO₂ incubator. Colonies were grown before being stained with 0.04% crystal violet/2% ethanol in PBS for 30 min. Photographs of the stained colonies were captured. The colony formation assay was performed in duplicate.

Western blot

Cytoplasmic fraction, nuclei fraction, and total cell lysates were separated by SDS-PAGE, transferred onto a polyvinylidene difluoride membrane and then probed with antibodies to FBXO32 (Abcam, Ab168372), MITF (Abcam, Ab12039), ubiquitin (Abcam, ab7254), CDK6 (DCS83, Cell Signaling Technology), SMAD7 (Santa Cruz Biotechnology, sc-11392), BRG1 (Abcam, ab10641), Baf60a (Santa Cruz Biotechnology, sc-51440), and HSP90 (Santa Cruz Biotechnology, sc-13119). Horseradish peroxidase-conjugated anti-rabbit or anti-mouse antibodies were from Dako. Proteins were visualized with the ECL system (Amersham).

mRNA preparation and real-time/quantitative PCR

mRNA isolation was carried out with TRIzol (Invitrogen) according to standard procedure. QRT-PCR was performed using SYBR[®] Green I (Eurogentec, Seraing, Belgium) and Multiscribe Reverse Transcriptase (Applied Biosystems) and subsequently monitored by the ABI Prism 7900 Sequence Detection System (Applied Biosystems, Foster City, CA). Primer sequences for each cDNA were designed using either Primer Express Software (Applied Biosystems) or qPrimer depot (<http://primerdepot.nci.nih.gov>) and are available upon request.

Detection of RPL0 gene was used to normalize the results. Primer sequences for each cDNA were designed using either Primer Express Software (Applied Biosystems) or qPrimer depot (<http://primerdepot.nci.nih.gov>), and these sequences are available upon request.

Proteomics analysis and nano-HPLC-MALDI-TOF/TOF analysis

Proteins from parental or MYC/DDK-FBXO32-expressing 501Mel melanoma cells were extracted in buffer containing TRIS-HCl pH7.5 50 mM, NaCl 15 mM, Triton X-100 1%, supplemented with protease and phosphatase inhibitors. Cell lysates (2 mg) were immunoprecipitated with anti-DDK antibody, washed and eluted with DDK peptide. Then, samples were immunoprecipitated again with anti-Myc antibody and separated by SDS-PAGE.

Proteins contained into gel slices were reduced/alkylated and digested by a treatment with DTT/IAA and trypsin. Peptides extracted were separated using a nano-HPLC (250 mm column, Ultimate 3000, ThermoFisherScientific). Nano-HPLC was coupled to Q-exactive plus mass spectrometer (ThermoFisherScientific). Data were reprocessed using Proteome Discoverer 2.2 equipped with Sequest HT. Files were searched against the Swissprot Homo sapiens FASTA database. Two separate experiments were performed, and all the proteins detected in one of the two immunoprecipitations from parental cells were considered as “non-specific.”

Chromatin immunoprecipitation (ChIP)

Cross-linked chromatin was prepared as previously described [20]. BRG1 ChIP was performed on 501Mel expressing or not Myc/DDK-tagged FBXO32 (5×10^7 cells per condition), using BRG1 or DDK antibody or an isotype matched control immunoglobulin, and analyzed by real-time PCR. Data are expressed as a percentage of enrichment compared to control immunoglobulin. Forward and reverse real-time PCR primers used for the human genomic DNA analysis are as follows. CDK6: 5'-AAGAACGGAGGCCGTTTCGTG-3'; 5'-TTTC TGGGCCTGAGGATTCCC-3' HDAC3: 5'-GTGCTGCG CAAGCACGTAGC-3'; 5'-CAAATGGCCCTCGCATCC TA-3'. As negative control, we used for CDK6, an intronic amplicon, chr7:92454544-92454710. CDK6neg 5' TCCTTG CAGTATCCCAAGCAT 3'; 5'-GGTGAGGTCTCTGGCA TTCAG 3'. For HDAC3, the negative control was an intronic amplicon chr5:141001678-141001852. HDAC3neg 5' GAGT ACCTGTTGGGCCCTG 3'; 5' CCTGGATGTAGGTAA GGGCTAGC-3'. No enrichment with these primers was observed in DDK or BRG1 immunoprecipitates compared to Ctl antibody.

Animal experimentation

Animal experiments were performed in accordance with French law and approved by a local institutional ethical committee (#NCE/2017-283). The animals were maintained in a temperature-controlled facility (22 °C) on a 12-h

light/dark cycle and provided free access to food (standard laboratory chow diet from UAR, Epinay-S/Orge, France). Human MeWo, SKmel28, and A375 melanoma cells, infected with control (LV) or FBXO32-encoding lentiviral vectors, were subcutaneously inoculated into 8-week-old female, immune-deficient, athymic, nude FOXN1tm mice (Harlan Laboratory). The growth tumor curves were determined after measuring the tumor volume (V) using the equation $V = \frac{L \times W^2}{2}$, where L is tumor length and W is tumor width. At the end of the experiment, the mice were euthanized by cervical dislocation, and the tumors were harvested for protein extraction.

Immunofluorescence studies

Short-term culture derived from patient was grown on glass coverslip (2×10^4 cells per point) in 12-well dishes. Cells were then washed, fixed at room temperature for 20 min with 4% paraformaldehyde (PFA, Sigma-Aldrich), and permeabilized by a 10-min treatment with 50 mM NH₄Cl, BSA 3% in PBS followed with 2-min treatment with BSA 3%, 1% Triton X-100 in PBS, before being exposed to anti-FBXO32 or anti-BRG1 antibodies for 1 h at room temperature. Cells were finally incubated with appropriate secondary fluorescent-labeled antibodies (Invitrogen Molecular Probes) for 1 h at room temperature and mounted using Gel/Mount (Biomedica Corp., Foster City, CA). Immunofluorescence was examined and photographed using a Zeiss Axiophot microscope equipped with epifluorescence illumination.

Gene expression profiling

Total RNAs from three different melanoma cell lines (501Mel, SKMel28, and WM9) and one short-term culture treated with control or FBXO32 siRNA were extracted using the RNeasy kit (Qiagen), according to the supplier's recommendations. mRNA expression profiling was performed with 8 × 60 K high-density SurePrint G3 gene expression human Agilent microarray, in accordance with the protocol described by the manufacturer. Microarray data analyses were performed using R (<http://www.r-project.org/>). The quality control was performed using the Bioconductor package ArrayQualityMetrics and custom R scripts. Additional analyses were performed using Bioconductor package Limma. Briefly, data were normalized using the quantile method. Replicated probes were averaged after normalization and control probes were removed. Then we used a linear modeling approach to calculate log ratios, moderated *t*-statistics, and *P*-values. *P*-values were adjusted for multiple testing using the Benjamini and Hochberg method, which controls the false discovery rate.

Statistical analysis

No statistical methods were used to determine sample size. Sample size was determined to be adequate based on the magnitude and consistency of measurable differences between groups. The data are presented as the means ± SD and analyzed using two-sided Student's *t*-test with Prism or Microsoft Excel software. For xenograft studies, sample size was determined using ClinCalc assuming a standard deviation of 30% in the control group and 50% of difference in FBXO32 group ($\alpha = 0.05$, $\beta = 0.1$). No randomization was used, and no blinding was done. The data were analyzed using the non-parametric Mann–Whitney test. The difference between conditions was statistically significant at $p < 0.05$.

Results

MITF controls ubiquitination in melanoma cells

Studying the role of MITF in ubiquitination, in melanoma cells, we observed that MITF silencing, by two different siRNA, led to an inhibition of global ubiquitination in the nuclear fraction of human melanoma SKmel28 and 501Mel cell lines (Fig. 1A). This result indicated that MITF-regulated genes involved in ubiquitination processes. To uncover the mediators of MITF effect on ubiquitination, we interrogated a list of 780 genes (Gene Ontology, AmiGO2) involved in the ubiquitination processes. Among them, we selected those that (i) contained a ChIP-Seq-validated MITF binding site in their promoter [21], (ii) were correlated with MITF expression in the CCLE series of 61 melanoma cells ($\text{Log}(2)\text{FC} > 1$) (<https://portals.broadinstitute.org/ccle/about>), and (iii) were downregulated by siMITF ($\text{log}(2)\text{FC} < -1$).

After applying these stringent filters, three genes reached the threshold (Table 1). TRIM63, which belongs to the TRIPartite Motif protein family [22], and HERC5, a HECT domain E3 ligase, are endowed with a E3 ligase activity [23] and FBXO32, a F-box only protein is an essential component of the SCFs ubiquitin protein ligase complexes [24]. TRIM63 was already identified as a MITF target and was reported to be involved in melanoma cell migration and invasion [25]. We therefore did not pursue the investigation on TRIM63.

Further analysis of the TCGA melanoma cohort showed that HERC5 and FBXO32 expression covaried with MITF (Supplementary Fig. 1C, D); however, they were not correlated significantly with survival of patients with metastatic cutaneous melanoma (Supplementary Fig. 1A, B). Analysis of another cutaneous melanoma cohort (GSE19234) showed that patients with high FBXO32 expression had a decreased survival (Fig. 1B), whereas no significant

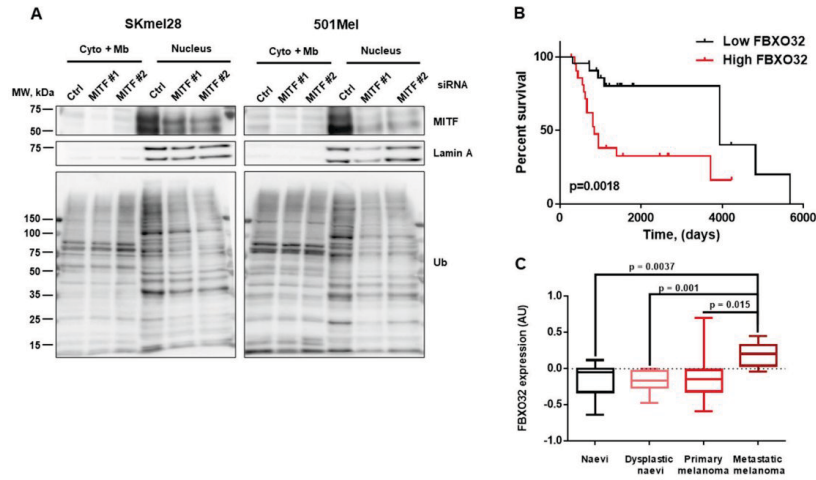


Fig. 1 MITF controls ubiquitination in melanoma cells. **A** Western blot analysis showing the effect of MITF downregulation on ubiquitination in cytoplasmic/membrane and nuclear protein fractions in SKmel28 cells (left panel) and 501Mel cells (right panel). **B** Kaplan–Meier survival curve of cutaneous melanoma patients with

low (black line) or high (red line) expression level of FBXO32 from GSE19234 dataset. **C** FBXO32 expression in human naevi ($n = 18$), dysplastic naevi ($n = 11$), primary melanomas ($n = 23$), and metastatic melanomas ($n = 5$) (GSE12391).

Table 1 List of genes involved in the ubiquitination process that are bound by MITF, correlated with MITF in the CCL6 melanoma cell line panel, and inhibited by siMITF.

Chr no.	Distance to TSS	Max read	Gene name	Gene description	exp	Log FC MITF H/L	siMITF1	siMITF2
Chr 1	-476–89	31/189	TRIM63	Tripartite motif containing 63, E3 ubiquitin protein ligase	6.78	5.27	-4.32	-4.34
Chr 4	-17	41	HERC5	HECT and RLD domain containing E3 ubiquitin protein ligase 5	7.00	2.00	-1.17	-1.07
Chr 8	-96	37	FBXO32	F-box protein 32	6.90	1.12	-1.39	-1.56

association of HERC5 expression with survival (Supplementary Fig. 1E) was observed in the same cohort. Note that MITF expression is also associated with a poor survival in this cohort. This is not the case in the TCGA cohort.

Additional analysis of FBXO32 expression in the GSE12391 cohort, containing different stages of the disease, including nevi, dysplastic nevi, primary, and metastatic melanomas, showed that FBXO32 expression was increased in metastatic melanoma as compared to earlier stages (Fig. 1C).

Taken together these observations prompted us to investigate the role of FBXO32 in melanomas.

FBXO32 is a MITF target

First, we analyzed FBXO32 expression in three melanoma cell lines and four short-term cultures derived from patients’

biopsies in our laboratory. FBXO32 expression was variable and roughly followed the expression of MITF, except for cells isolated from patient 1 that expressed high level of FBXO32 but almost no MITF (Fig. 2A). Of note, these cells, isolated from a patient after treatment with BRAF inhibitor, are resistant to BRAF inhibitors. Then, we showed that adenovirus-forced MITF expression led to an increase in FBXO32 protein expression in both 501MEL and A375 melanoma cell lines (Fig. 2B), while MITF silencing decreased the expression of FBXO32 and DCT, a known transcriptional target of MITF in MeWo and 501Mel cell lines (Fig. 2C). Inhibition of FBXO32 expression ensuing MITF silencing was also verified by qPCR in 501Mel, MeWo, and two short-term melanoma cultures (Supplementary Fig. 2A–E). It should be noted that MITF silencing in cells from patient 1 did not result in a consistent inhibition of FBXO32 expression, further strengthening the

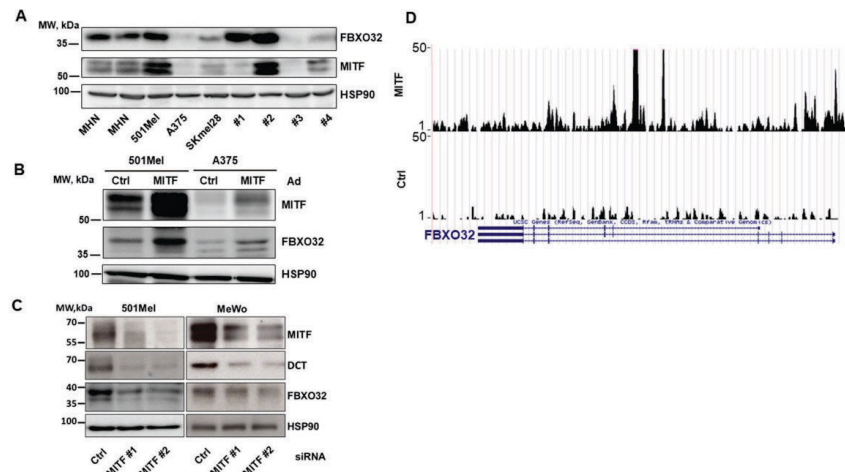


Fig. 2 **FBXO32 is a MITF target.** **A** Western blot analysis of FBXO32 and MITF expression in normal human melanocytes (NHM), A375, 501Mel, SKmel28 cell lines, and in short-term culture of metastatic melanomas isolated from four different patients (1–4). **B** FBXO32 expression in 501Mel and A375 cells after

adenovirus-mediated MITF forced expression. **C** FBXO32 and DCT expression in 501Mel and MeWo cells after siRNA-mediated MITF downregulation. HSP90 expression was probed as loading control. **D** UCSC image capture of the FBXO32 gene from MITF ChIP-Seq experiments [21] shows major MITF-binding sites.

lack of epistatic regulation of FBXO32 by MITF in these cells.

Finally, looking at the MITF ChIP-Seq data from Davidson's lab [21], the UCSC image capture of the FBXO32 gene showed a binding of MITF at the FBXO32 promoter and in intronic region (Fig. 2D). Therefore, our data demonstrate an epistatic relation between MITF and FBXO32, the latter being a direct transcription target of MITF.

FBXO32 controls migration of melanoma cells

In view to explore the biological functions of FBXO32 in melanomas, we studied the effect of FBXO32 silencing or forced expression on the motility of melanoma cells. Using two different siRNA targeting FBXO32, in melanoma cell expressing high endogenous FBXO32 (cells from patient 2), we observed that the inhibition of FBXO32 expression (Fig. 3A) led to a decrease in the migration of melanoma cells in Boyden chambers assays as demonstrated by the pictures of the lower face of the wells (Fig. 3B) and by quantification of three independent experiments (Fig. 3C). Similarly, the migration ability of 501Mel was reduced when FBXO32 expression was downregulated by doxycycline inducible specific shRNA (Supplementary Fig. 3A, B). Furthermore, the effect of FBXO32 silencing on migration cannot be ascribed to an inhibition of proliferation because after 16 h, the time used for migration evaluation, we did

not observe relevant effect on 501Mel and SKmel28 proliferation, while the effect on migration is statistically significant (Supplementary Fig. 3C–J).

Conversely, forced FBXO32 expression using a lentiviral vector (Fig. 3D) stimulated the migration of SKmel28 melanoma cell line (Fig. 3E, F).

Taken together, these data demonstrate that FBXO32 enhances the migration of melanoma cells.

FBXO32 controls proliferation and xenograft tumor development

In short-term culture from patient 1, FBXO32 knockdown by two different siRNA (Fig. 4A) inhibited cell proliferation (Fig. 4B). Conversely, forced expression of FBXO32 in SKmel28 cell line, by lentivirus infection (Fig. 4D), increased the formation of colonies (Fig. 4C). FBXO32-forced expression in 501Mel cell line (Fig. 4E) increased proliferation in vitro (Fig. 4F). FBXO32-forced expression also increased proliferation in A375 (Supplementary Fig. 4A, B) and SKmel28 cell lines expressing low level of endogenous FBXO32 (Supplementary Fig. 4C).

Furthermore, FBXO32-forced expression also favored the growth of MeWo and SKmel28 xenografts in nude mice (Fig. 4G, H). The same observations were made for xenografts with A375 cell line (Supplementary Fig. 4D). The increased expression of FBXO32 in the tumors was verified by western blot (Supplementary Fig. 4E). These data

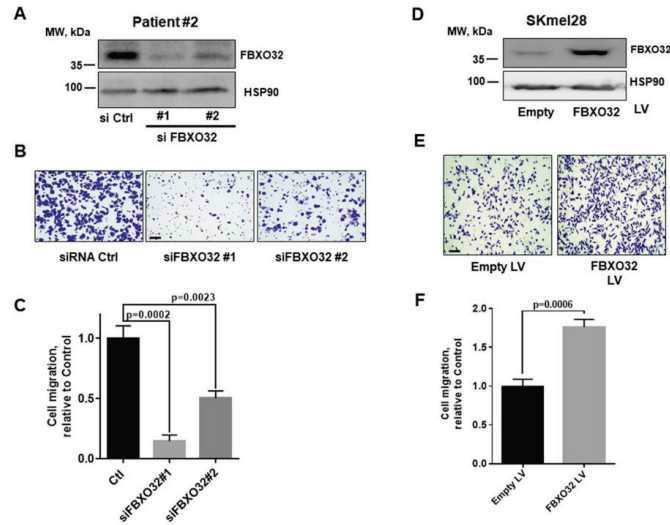


Fig. 3 FBXO32 controls migration of melanoma cells. **A** Western blot analysis of FBXO32 expression after transfection of siRNAs targeting FBXO32 in melanoma cells isolated from patient 2. HSP90 expression was probed as loading control. **B** Representative image of the effects of FBXO32 downregulation on Boyden migration of melanoma cells from patient 2. Bar = 100 μ m. **C** Quantification of patient

2 melanoma cell migration after FBXO32 downregulation (mean ratio \pm SD, $n = 3$). **D** Western blot analysis of FBXO32 in SKmel28 cells after lentivirus-mediated transduction. HSP90 expression was probed as loading control. **E** Effects of FBXO32-forced expression on SKmel28 migration. Bar = 100 μ m. **F** Quantification of SKmel28 migration after FBXO32-forced expression (mean ratio \pm SD, $n = 3$).

indicate that FBXO32 favors the proliferation of melanoma cells, both in vitro and in vivo.

FBXO32 regulates the transcriptional program in melanoma cells

Then, we sought to gain insights on the molecular mechanisms involved in the modification of migration and proliferation induced through FBXO32 expression modulation. To do so, we performed a transcriptomic analysis in three different melanoma cell lines and one short-term culture (patient 2) treated with either control or FBXO32 siRNA. Statistical analysis ($\text{absLog}_2\text{FC} > 0.75$, Adj. p -value < 0.05) identified 331 genes regulated upon FBXO32 knockdown, 216 downregulated, 115 upregulated (Supplementary Table 1). The heat map of the most differentially regulated genes (top 50) is shown (Fig. 5A). Ingenuity pathway analysis revealed that this gene list was associated with an inhibition of cell proliferation and migration (Table 2), in agreement with the proliferation and migration data obtained previously. IPA upstream activators analysis indicated that gene expression changes could result from MITEF, MYC, or TGF β pathway inhibition (Supplementary Table 2). The same analysis also predicted the activation of three microRNAs (mir145, mir124, Let7), p53,

and KDM5B, a histone lysine demethylase, suggesting a link with epigenetics that is strengthened by the upregulation of HDAC3 in FBXO32 depleted cells.

In agreement with the results obtained from gain- and loss-of-function experiments, upon FBXO32 silencing, CDK6 a protein kinase involved in cell proliferation was downregulated and SMAD7, an inhibitor of TGF β signaling linked to cell migration, was upregulated.

Furthermore, western blot analysis in 501Mel cells infected with FBXO32-encoding lentivirus showed an increase in CDK6 expression, while FBXO32 knockdown led to its inhibition (Fig. 5B). Then, Boyden chamber experiments showed that CDK6 inhibition reduced migration in both parental and FBXO32 overexpressing 501Mel cells (Fig. 5C, D). The same observations have been made in A375 cells (Supplementary Fig. 5A, B). CDK6 knockdown also inhibited the proliferation of parental and FBXO32-overexpressing 501Mel and A375 cells (Fig. 5E).

We also validated the effect of FBXO32 on SMAD7 expression, by western blot showing increased SMAD7 level in cells treated with a siRNA to FBXO32 and a decreased SMAD7 level in cells with forced FBXO32 expression (Supplementary Fig. 6A). Furthermore, using TGF β reporter assay, we demonstrated that the inhibition of SMAD7 expression, which was increased upon FBXO32

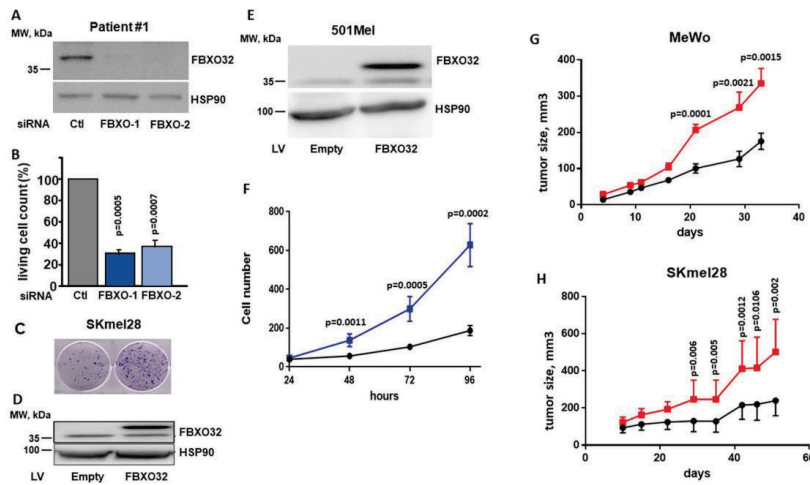


Fig. 4 FBXO32 controls proliferation and xenograft development. **A** Western blot analysis of FBXO32 expression after transfection of siRNAs targeting FBXO32 in melanoma cells isolated from patient 1. HSP90 expression was probed as loading control. **B** Quantification of living cells 72 h after FBXO32 downregulation by siRNAs in melanoma cells from patient 1 (mean ratio \pm SD, $n = 3$). **C** Colony formation assay of parental or FBXO32 overexpressing SKmel28 cells. **D** Western blot analysis of FBXO32 expression after FBXO32-forced expression in SKmel28 cells. HSP90 expression was probed as loading control. **E** Western blot analysis of FBXO32 expression after

lentivirus-mediated FBXO32-forced expression in 501Mel cells. HSP90 expression was probed as loading control. **F** Quantification of 501Mel cell proliferation after empty virus (black line) or FBXO32 encoding virus (blue line) transduction, from 24 to 96 h (mean \pm SD, $n = 6$). **G** Xenograft growth after subcutaneous injection of MeWo cells transduced with empty vector (black line) or FBXO32 encoding virus (red line) (mean \pm SD, $n = 10$). **H** Xenograft growth after subcutaneous injection of SKmel28 cells transduced with empty vector (black line) or FBXO32 encoding virus (red line) (mean \pm SD, $n = 10$).

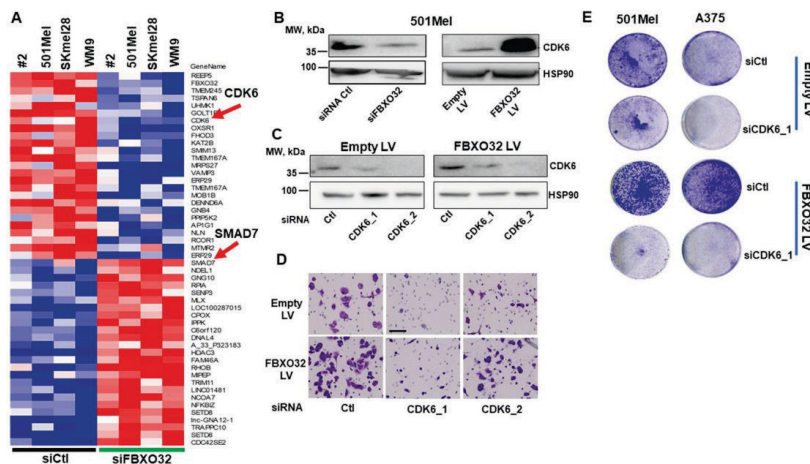


Fig. 5 FBXO32 regulates the transcriptional program in melanoma cells. **A** Heat map showing the top 50 genes significantly affected by FBXO32 knockdown in melanoma cells from patient 2, 501Mel, SKmel28, and WM9 cell lines. **B** Western blot analysis of CDK6 expression after transfection of siRNAs targeting FBXO32 (left panel) or transduction by FBXO32-expressing lentivirus (right panel) in 501Mel cells. HSP90 was probed as loading control. **C** CDK6

expression after siRNAs transfection targeting CDK6 in 501Mel transduced with (right panel) or without (left panel) FBXO32 lentivirus. **D** Representative image of the effect of CDK6 downregulation on migration of 501Mel cells overexpressing (lower panel) or not (upper panel), FBXO32. Bar = 100 μ m. **E** Effect of CDK6 downregulation on colony formation in 501Mel and A375 cells overexpressing, or not, FBXO32.

Table 2 Ingenuity pathway analysis^a of the genes regulated upon FBXO32 silencing.

Diseases or functions annotation	<i>p</i> -value	<i>z</i> -score	Molecules
Proliferation of cells	3.39E-04	-3.66	104
Neoplasia of epithelial tissue	2.71E-04	-2.56	243
Cell proliferation of tumor cell lines	3.71E-03	-2.50	49
Cell proliferation of breast cancer cells	8.20E-03	-2.39	17
Epithelial cancer	4.34E-04	-2.36	241
Formation of cellular protrusions	7.73E-03	-2.35	28
Apoptosis of blood cells	5.98E-03	-2.27	18
Development of neurons	3.00E-04	-2.17	31
Invasion of tumor cell lines	6.19E-03	-2.16	24
Neuritogenesis	3.19E-04	-2.01	25

knockdown, prevented the inhibition of the TGF β pathway in this condition, indicating that SMAD7 is a key player in the inhibition of the TGF β pathway evoked by FBXO32 silencing (Supplementary Fig. 6B, C).

FBXO32 is associated with chromatin remodeling complex at regulated loci

As FBXO32 is not a transcription factor, it remained to understand how it can modulate gene expression. To answer this question, we performed a tandem affinity purification of Myc/DDK tagged FBXO32 expressed in SKmel28 cells. Then, mass spectrometry analysis identified 216 proteins specifically associated with FBXO32 in two independent experiments (Supplementary Table 3). Analysis using David Tools identified enrichment in the GO terms associated with chromosome organization, ribosome biogenesis, RNA processing, and cellular stress (Supplementary Table 4). Consistently, among the FBXO32 partners, we found several members of chromatin remodeling complexes, including SMARCA5 belonging to the ISWI complexes [26], SMARCD1, and SMARCA4 that are associated with BAF/PBAF complexes. SMARCA4 (BRG1) was an attractive candidate to pursue since it was previously described to play a key role in melanoma biology [21]. Moreover, SMARCA4 (as well SMARCD1 and SMARCA5) could make the link between FBXO32 and the transcription machinery.

First, we verified the association of FBXO32 with BRG1 (SMARCA4). Western blot analysis after immunoprecipitation with anti-DDK showed that BRG1 was pulled down with FBXO32 in DDK-tagged FBXO32-expressing SKMEI28 cells, but not in control cells (Fig. 6A). Note that SMARCA5 (BAF60A) was also co-immunoprecipitated with FBXO32. Furthermore, we have also been able to show an interaction between endogenous BRG1 and FBXO32 in 501Mel cells after immunoprecipitation with

anti-BRG1 antibody (Supplementary Fig. 7). Immunofluorescence studies showed a nuclear labeling of FBXO32 that largely overlapped with BRG1 (Fig. 6B).

Then, we hypothesized that FBXO32 interacted with BRG1 and chromatin at loci regulated upon FBXO32 silencing. First, we analyzed BRG1 [21] and H4K4me3 [4] ChIP-Seq data. We observed deposition of active histone marks at CDK6 and HDAC3 promoters, overlapping with BRG1 binding sites (Fig. 6C, D). Therefore, we performed ChIP-qPCR experiments after immunoprecipitation of chromatin either with anti-BRG1 or anti-DDK antibodies, in 501MEL cells expressing or not tagged FBXO32.

Then, qPCR analyses with primers spanning the CDK6 and HDAC3 promoter regions (red bar) showed a strong enrichment in anti-DDK immunoprecipitations from cells expressing tagged FBXO32 compared to parental cells (Fig. 6E, F). After immunoprecipitation with anti-BRG1, we also observed a strong enrichment compared to non-relevant antibody. As expected, there was no significant change between parental and DDK-FBXO32-expressing cells. These data confirm that BRG1 is bound at CDK6 and HDAC3 promoters and demonstrate that FBXO32 interacts with chromatin at loci it regulates.

Discussion

Compelling research works demonstrated the pivotal role of MITF in melanocyte and melanoma through its ability to promote essential biological processes such as differentiation, survival, and proliferation, but also to dampen motility and invasion [19]. This large pleiotropism indicates that MITF impacts and coordinates numerous key molecular pathways, to regulate melanocytes and melanoma homeostasis. Here, we demonstrate that MITF regulates global ubiquitination in melanoma cells, at least in part, through FBXO32. FBXO32 is a phosphorylation-dependent substrate recognition component of SCF E3 ligase complex and was initially identified as a key regulator in muscle homeostasis and heart development [22, 24]. However, the downregulation of FBXO32 upon MITF knockdown cannot totally explain the inhibition of nuclear ubiquitination in MITF-depleted cells. Indeed, overexpression of FBXO32 in MITF knockout cells was not sufficient to rescue the decrease in ubiquitination (data not shown). This is not surprising since MITF also regulated directly TRIM63 and indirectly many other genes involved in ubiquitination process. As no MITF binding was detected in the promoter of these genes, the said genes did not appear in our bioinformatic analysis.

More recently, FBXO32 has been also involved in cancer development and several reports ascribed an anti-

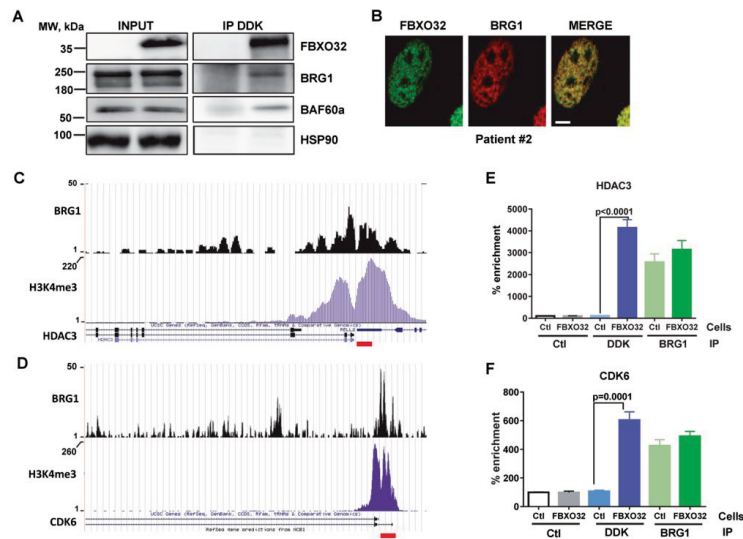


Fig. 6 FBXO32 is associated with chromatin remodeling complex at regulated loci. **A** Co-immunoprecipitation and western blot analysis showing interaction between FBXO32 with BRG1 and BAF60a in SKmel28 transduced with Myc/DDK-tagged FBXO32 vector. **B** Immunofluorescence labeling of FBXO32 (green) and BRG1 (red) in isolated melanoma cells from patient 2. The photos taken by the confocal microscopy show a colocalization of the two proteins in the nucleus. Bar = 5 μm. **C** UCSC capture of HDAC3 locus showing

BRG1-binding site (upper panel) overlapping H3K4me3 active mark (lower panel). **D** UCSC capture of CDK6 locus showing BRG1 binding site (upper panel) overlapping H3K4me3 active mark (lower panel). **E**, **F** ChIP-qPCR analysis in parental and FBXO32 overexpressing 501Mel cells, after immunoprecipitation with DDK antibody. DNA was amplified either with HDAC3 promoter primers (**E**) or CDK6 promoter primers (**F**) (mean ± SD, $n = 3$).

tumorigenic role to FBXO32 [27, 28]. However, in agreement with our data in melanoma, FBXO32 was also shown to favor breast cancer cell xenograft development [29] and analysis of all the TCGA cohorts showed that high levels of FBXO32 were associated with bad prognosis in mesothelioma, kidney renal papillary cell carcinoma, pancreatic adenocarcinoma, and brain lower grade glioma (not shown).

The pro-tumoral function of FBXO32 was confirmed by biological studies demonstrating that FBXO32-forced expression favors proliferation and migration of melanoma cells, while FBXO32 downregulation has opposite effects. Strengthening these observations and its pro-tumorigenic role, FBXO32-forced expression greatly favors xenograft development in nude mice. The mechanisms by which FBXO32 knockdown inhibits cell proliferation is not clear. We observed no apoptosis, a weak G1 arrest, and a faint increase in senescence markers (not shown) after FBXO32 depletion.

At the molecular level, transcriptomic analysis shed light on the molecular cascades affected upon FBXO32 inhibition. FBXO32 regulates genes overlapping with that regulated by MITF, suggesting that FBXO32 might mediate some of the downstream transcriptional effects of MITF. Among the top

upregulated genes, SMAD7 appears to mediate the inhibition of the TGFβ pathway in FBXO32 knockdown cells, in line with previous reports showing that FBXO32 downregulation inhibits the epithelial mesenchymal transition (EMT) induced by TGFβ in human breast epithelial cells [29]. Of note, the increase in the invasive properties is frequently associated with increased EMT, of cancer cells in general [30] and of melanoma cells specifically [31].

In addition, CDK6 belongs to the top downregulated genes upon FBXO32 silencing. CDK6 inhibition mimics the effect of FBXO32 knockdown, indicating that the loss of CDK6 participates to the anti-proliferative and anti-invasive effects of FBXO32 inhibition. The role of CDK6 in both proliferation and invasiveness has been already reported in squamous carcinoma cells [32]. Therefore, the transcriptional rewiring elicited by FBXO32 depletion in melanoma cells predicts an inhibition of proliferation and invasion, in agreement with the results of ours in vitro and in vivo functional studies.

To identify the link between FBXO32 and transcription regulation, we performed a proteomic analysis to identify FBXO32-interacting proteins that unveiled FBXO32 partners functioning in the chromatin remodeling process.

Indeed, we identified ISWI, BAF, and PBAF components associated with FBXO32. As expected, component of the SCF complexes were also identified among FBXO32 partners. Note that FBXO32 was reported to bind and regulate CTBP1 in breast cancer cells [29], but we identified CTBP1 neither in the proteomic analyses nor in classical co-immunoprecipitation experiments (not shown).

Among the BAF components, we focused on SMARCA4, and confirmed its association with FBXO32. However, we have not been able to identify the member of the core BAF/PBAF complex that is ubiquitinated by FBXO32. We therefore concluded that FBXO32 might ubiquitinate an accessory BAF protein that in turn regulates the BAF complex activity. Nevertheless, the direct link between FBXO32, the BAF complex, and transcriptional regulation was further confirmed by ChIP-qPCR experiments showing that FBXO32 together with SMARCA4 interacted with chromatin at HDAC3 and CDK6 genes that are respectively upregulated and downregulated in FBXO32 knockdown cells.

Therefore, we hypothesized that FBXO32 can interact with both activating and repressive complexes. However, according to the proteomic results, the complexes interacting with FBXO32, BAF, PBAF, and NUMAC (containing CARM1) [33] are generally considered as activating complexes. No transcriptional repressors, such as HDAC or REST, which were reported to be associated with SMARCA4, were found in the list of FBXO32 interacting proteins. Nevertheless, it should be noted that in one of the two proteomic analyses, HDAC1 was associated with FBXO32, suggesting an interaction with the SIN3A/HDAC repressive complex [34].

In conclusion, our work establishes the role of MITF as a regulator of the ubiquitination pathway, in melanoma cells, through transcriptional regulation of several genes, among which FBXO32. FBXO32 by interacting with chromatin remodeling complexes containing SMARCA4 regulates the transcriptional repertoire and multiple key biological functions, responsible of melanoma progression and dissemination.

Acknowledgements We thank Alain Mauviel for the gift of the TGFB reporter. We thank Marie Irondele, head of imaging facility, and all the staff of animal facility.

Funding NH was a recipient of ARC fellowship. NE-H was a PhD student of the Labex Signallife program ANR-11 LABEX-0028-01. FS was supported by INCa-10573 to CB and NN by Team ARC grant 2019 to RB. We also thank the "Fond de Dotation de la Société Française de Dermatologie" AO-2019 and the "Ligue Contre le Cancer" N°AAPEAC2019.LCC/STD for their financial supports to BB-dP.

Author contributions NH, FS, and NE-H performed most of the experiments. HH-B and PH performed ubiquitination experiments. SG

and SN performed proliferation and migration experiments. A-SG and DD performed proteomic analyses. GB isolated patient melanoma cells. NN performed bioinformatic analyses. All reviewed and edited the manuscript. BB-dP was involved in conceptualization, funding acquisition, project administration, writing, and editing of manuscript. CB and RB were involved in project conceptualization, funding acquisition, and project administration. They analyzed the data, wrote the original draft, and edited all the versions.

Compliance with ethical standards

Conflict of interest The authors declare that they have no conflict of interest.

Publisher's note Springer Nature remains neutral with regard to jurisdictional claims in published maps and institutional affiliations.

Open Access This article is licensed under a Creative Commons Attribution 4.0 International License, which permits use, sharing, adaptation, distribution and reproduction in any medium or format, as long as you give appropriate credit to the original author(s) and the source, provide a link to the Creative Commons license, and indicate if changes were made. The images or other third party material in this article are included in the article's Creative Commons license, unless indicated otherwise in a credit line to the material. If material is not included in the article's Creative Commons license and your intended use is not permitted by statutory regulation or exceeds the permitted use, you will need to obtain permission directly from the copyright holder. To view a copy of this license, visit <http://creativecommons.org/licenses/by/4.0/>.

References

- Komander D, Rape M. The ubiquitin code. *Annu Rev Biochem.* 2012;81:203–29.
- Senft D, Qi J, Ronai ZA. Ubiquitin ligases in oncogenic transformation and cancer therapy. *Nat Rev Cancer.* 2018;18:69–88.
- Luke JJ, Flaherty KT, Ribas A, Long GV. Targeted agents and immunotherapies: optimizing outcomes in melanoma. *Nat Rev Clin Oncol.* 2017;14:463–82.
- Ohanna M, Cerezo M, Nottet N, Bille K, Didier R, Beranger G, et al. Pivotal role of NAMPT in the switch of melanoma cells toward an invasive and drug-resistant phenotype. *Genes Dev.* 2018;32:448–61.
- Rambow F, Marine JC, Goding CR. Melanoma plasticity and phenotypic diversity: therapeutic barriers and opportunities. *Genes Dev.* 2019;33:1295–318.
- Ma J, Guo W, Li C. Ubiquitination in melanoma pathogenesis and treatment. *Cancer Med.* 2017;6:1362–77.
- Dogrusoz M, Jager MJ. Genetic prognostication in uveal melanoma. *Acta Ophthalmol.* 2018;96:331–47.
- Griewank KG, Muller H, Jackett LA, Emberger M, Moller I, van de Nes JA, et al. SF3B1 and BAP1 mutations in blue nevus-like melanoma. *Mod Pathol.* 2017;30:928–39.
- Aydin IT, Melamed RD, Adams SJ, Castillo-Martin M, Demir A, Bryk D, et al. FBXW7 mutations in melanoma and a new therapeutic paradigm. *J Natl Cancer Inst.* 2014;106:dju107.
- Hu HH, Kannengiesser C, Lesage S, Andre J, Mourah S, Michel L, et al. PARKIN inactivation links Parkinson's disease to melanoma. *J Nat Cancer Inst.* 2016;108:djv340.
- El-Hachem N, Habel N, Naiken T, Bziouche H, Cheli Y, Beranger GE, et al. Uncovering and deciphering the pro-invasive

- role of HACE1 in melanoma cells. *Cell Death Differ.* 2018;25:2010–22.
12. Carreira S, Goodall J, Denat L, Rodriguez M, Nuciforo P, Hoek KS, et al. Mitf regulation of Dia1 controls melanoma proliferation and invasiveness. *Genes Dev.* 2006;20:3426–39.
 13. Cheli Y, Giuliano S, Botton T, Rocchi S, Hofman V, Hofman P, et al. Mitf is the key molecular switch between mouse or human melanoma initiating cells and their differentiated progeny. *Oncogene.* 2011;30:2307–18.
 14. Hoek KS, Eichhoff OM, Schlegel NC, Dobbeling U, Kobert N, Schaerer L, et al. In vivo switching of human melanoma cells between proliferative and invasive states. *Cancer Res.* 2008;68:650–6.
 15. Konieczkowski DJ, Johannessen CM, Abudayyeh O, Kim JW, Cooper ZA, Piris A, et al. A melanoma cell state distinction influences sensitivity to MAPK pathway inhibitors. *Cancer Discov.* 2014;4:816–27.
 16. Muller J, Krijgsman O, Tsoi J, Robert L, Hugo W, Song C, et al. Low MITF/AXL ratio predicts early resistance to multiple targeted drugs in melanoma. *Nat Commun.* 2014;5:5712.
 17. Hugo W, Zaretsky JM, Sun L, Song C, Moreno BH, Hui-Lieskován S, et al. Genomic and transcriptomic features of response to Anti-PD-1 therapy in metastatic melanoma. *Cell.* 2016;165:35–44.
 18. Bertolotto C, Abbe P, Hemesath TJ, Bille K, Fisher DE, Ortonne JP, et al. Microphthalmia gene product as a signal transducer in cAMP-induced differentiation of melanocytes. *J Cell Biol.* 1998;142:827–35.
 19. Goding CR, Arnheiter H. MITF—the first 25 years. *Genes Dev.* 2019;33:983–1007.
 20. Aparicio O, Geisberg JV, Sekinger E, Yang A, Moqtaderi Z, Struhl K. Chromatin immunoprecipitation for determining the association of proteins with specific genomic sequences in vivo. *Curr Protoc Mol Biol.* 2005:Chapter 21:Unit 21–3.
 21. Laurette P, Strub T, Koludrovic D, Keime C, Le Gras S, Seberg H, et al. Transcription factor MITF and remodeller BRG1 define chromatin organisation at regulatory elements in melanoma cells. *eLife.* 2015;4:e06857.
 22. Bodine SC, Baehr LM. Skeletal muscle atrophy and the E3 ubiquitin ligases MuRF1 and MAFbx/atrogin-1. *Am J Physiol Endocrinol Metab.* 2014;307:E469–84.
 23. Sanchez-Tena S, Cubillos-Rojas M, Schneider T, Rosa JL. Functional and pathological relevance of HERC family proteins: a decade later. *Cell Mol Life Sci.* 2016;73:1955–68.
 24. Sukari A, Muqbil I, Mohammad RM, Philip PA, Azmi AS. F-BOX proteins in cancer cachexia and muscle wasting: emerging regulators and therapeutic opportunities. *Semin Cancer Biol.* 2016;36:95–104.
 25. Rambow F, Job B, Petit V, Gesbert F, Delmas V, Seberg H, et al. New functional signatures for understanding melanoma biology from tumor cell lineage-specific analysis. *Cell Rep.* 2015;13:840–53.
 26. Barisic D, Stadler MB, Iurlaro M, Schubeler D. Mammalian ISWI and SWI/SNF selectively mediate binding of distinct transcription factors. *Nature.* 2019;569:136–40.
 27. Zhou H, Liu Y, Zhu R, Ding F, Wan Y, Li Y, et al. FBXO32 suppresses breast cancer tumorigenesis through targeting KLF4 to proteasomal degradation. *Oncogene.* 2017;36:3312–21.
 28. Tanaka N, Kosaka T, Miyazaki Y, Mikami S, Niwa N, Otsuka Y, et al. Acquired platinum resistance involves epithelial to mesenchymal transition through ubiquitin ligase FBXO32 dysregulation. *JCI Insight.* 2016;1:e83654.
 29. Sahu SK, Tiwari N, Pataskar A, Zhuang Y, Borisova M, Diken M, et al. FBXO32 promotes microenvironment underlying epithelial-mesenchymal transition via CtBP1 during tumour metastasis and brain development. *Nat Commun.* 2017;8:1523.
 30. Derynck R, Weinberg RA. EMT and cancer: more than meets the eye. *Dev Cell.* 2019;49:313–6.
 31. Richard G, Dalle S, Monet MA, Ligier M, Boespflug A, Pommier RM, et al. ZEB1-mediated melanoma cell plasticity enhances resistance to MAPK inhibitors. *EMBO Mol Med.* 2016;8:1143–61.
 32. Wang X, Chang K, Gao J, Wei J, Xu G, Xiao L, et al. MicroRNA-504 functions as a tumor suppressor in oral squamous cell carcinoma through inhibiting cell proliferation, migration and invasion by targeting CDK6. *Int J Biochem Cell Biol.* 2020;119:105663.
 33. Trotter KW, Archer TK. The BRG1 transcriptional coregulator. *Nucl Receptor Signal.* 2008;6:e004.
 34. Bansal N, David G, Farias E, Waxman S. Emerging roles of epigenetic regulator Sin3 in cancer. *Adv Cancer Res.* 2016;130:113–35.

1
2
3
4
5
6
7
8
9
10
11
12
13
14
15
16
17
18
19
20
21
22
23
24
25
26
27

SUPPLEMENTAL MATERIALS

FBXO32 links ubiquitination to epigenetic reprogramming of melanoma cells.

Nadia Habel^{1*}, Najla El-Hachem^{1*}, Frédéric Soysouvanh^{1*}, Hanene Hadhiri-Bziouche¹,
Serena Giuliano¹, Sophie Nguyen¹, Pavel Horák¹, Anne-Sophie Gay², Delphine Debayle²,
Nicolas Nottet¹, Guillaume Béranger¹, Brigitte Bressac-de Paillerets⁴, Corine Bertolotto^{1£} and
Robert Ballotti^{1£}

¹Université Nice Côte d'Azur, Inserm U1065, C3M, Nice, France, Team 1, Biology and
pathologies of melanocytes, Equipe labellisée ARC 2019. ²CNRS, Institut de Pharmacologie
Moléculaire et Cellulaire, Sophia Antipolis, France. ⁴Gustave Roussy, Département de
Biopathologie et INSERM U1279, Villejuif, France.

NH, NEH, FS, *equal contribution. CB and RB, £equal contribution. Correspondence should
be addressed to Robert Ballotti: email: ballotti@unice.fr, telephone: +33 4 89 06 43 32

Running title: FBXO32 interacts with BRG1

Declaration of Interests: The authors declare no competing interests

Supplemental table 1. List of the 331 genes regulated by FBXO32 silencing, 216 down-regulated, 115 up-regulated.

<i>Symbol</i>	<i>Expr</i>	<i>Log FC</i>	<i>Adj p-value</i>
<i>REEP5</i>	9.393	-2.546	0.0043
<i>TMEM245</i>	9.671	-2.433	0.0043
<i>FBXO32</i>	8.985	-2.326	0.00311
<i>TSPAN6</i>	9.317	-2.038	0.00591
<i>UHMK1</i>	9.66	-2.037	0.00807
<i>CDK6</i>	10.161	-1.996	0.00976
<i>MRPL17</i>	10.825	-1.949	0.00394
<i>GPD2</i>	8.089	-1.943	0.0208
<i>LAMP2</i>	8.098	-1.93	0.00494
<i>OXSRI</i>	9.633	-1.879	0.00561
<i>ZWINT</i>	9.674	-1.844	0.0043
<i>SLC25A13</i>	10.471	-1.736	0.00311
<i>GOLT1B</i>	8.079	-1.699	0.00591
<i>CHST13</i>	12.644	-1.673	0.0271
<i>SMIM13</i>	9.935	-1.664	0.00623
<i>MRPS27</i>	10.12	-1.651	0.0067
<i>GNB4</i>	11.094	-1.65	0.0075
<i>FHOD3</i>	8.813	-1.629	0.00311
<i>UBE2J1</i>	8.502	-1.558	0.00394
<i>SNX4</i>	9.241	-1.558	0.0067
<i>SLC4A7</i>	6.984	-1.526	0.00774
<i>TMEM167A</i>	9.206	-1.524	0.0043
<i>IVNSIABP</i>	10.681	-1.521	0.00772
<i>GNBI</i>	11.554	-1.506	0.00311
<i>CNOT6</i>	7.158	-1.5	0.00311
<i>DENND6A</i>	9.887	-1.49	0.00311
<i>KAT2B</i>	8.48	-1.466	0.00385
<i>SYPL1</i>	10.634	-1.447	0.0043
<i>ERP29</i>	8.973	-1.438	0.00544
<i>LRRN4CL</i>	7.216	-1.432	0.0145
<i>INSIG1</i>	9.823	-1.426	0.00311
<i>MIGA1</i>	8.703	-1.413	0.00518
<i>STAT6</i>	10.561	-1.411	0.0043
<i>TDG</i>	11.077	-1.369	0.00455
<i>APIG1</i>	9.163	-1.325	0.0043
<i>CCSER2</i>	8.144	-1.306	0.00385
<i>PPP5K2</i>	8.935	-1.303	0.0043
<i>IL13RA1</i>	9.884	-1.302	0.00876
<i>ZDHHC13</i>	7.473	-1.266	0.00989
<i>VAMP3</i>	9.342	-1.264	0.0043
<i>SRXN1</i>	11.34	-1.262	0.0043
<i>JAZF1</i>	8.071	-1.26	0.00867
<i>MOB1B</i>	8.215	-1.258	0.0132
<i>MYO1D</i>	9.21	-1.254	0.00385
<i>RCOR1</i>	8.931	-1.253	0.00311

<i>GRK3</i>	8.838	-1.246	0.00311
<i>ARFGEF1</i>	8.435	-1.233	0.00595
<i>CD44</i>	10.659	-1.231	0.0384
<i>CORO1C</i>	11.348	-1.216	0.00636
<i>ATP6V0A4</i>	9.455	-1.211	0.0134
<i>IPO7</i>	9.177	-1.207	0.0123
<i>FZD6</i>	7.994	-1.2	0.0305
<i>TMEM64</i>	8.243	-1.2	0.00861
<i>ANO6</i>	9.219	-1.185	0.00833
<i>RBMS1</i>	11.685	-1.166	0.00824
<i>SLC22A18</i>	11.681	-1.164	0.0158
<i>FAM78A</i>	8.49	-1.162	0.0132
<i>MEX3C</i>	10.307	-1.157	0.00772
<i>QSOX2</i>	7.874	-1.152	0.0226
<i>TMEM30A</i>	10.792	-1.143	0.0207
<i>GPR19</i>	9.08	-1.133	0.0426
<i>STX3</i>	9.021	-1.131	0.00699
<i>HI-9</i>	10.509	-1.129	0.0132
<i>SLC22A18AS</i>	8.317	-1.128	0.0372
<i>C3orf18</i>	8.033	-1.122	0.0441
<i>CORO2A</i>	8.542	-1.119	0.0305
<i>HNRNPK</i>	11.496	-1.118	0.0089
<i>NLN</i>	7.716	-1.108	0.00867
<i>CCNA2</i>	8.996	-1.105	0.0284
<i>RAP1GDS1</i>	8.076	-1.096	0.0161
<i>EIF5A2</i>	7.86	-1.091	0.0135
<i>PDHX</i>	9.327	-1.091	0.00602
<i>PHTF2</i>	9.494	-1.089	0.0293
<i>SLC25A24</i>	9.261	-1.083	0.00385
<i>PII5</i>	8.582	-1.082	0.0293
<i>ETNK1</i>	8.685	-1.082	0.0228
<i>FBXO28</i>	8.066	-1.076	0.00825
<i>MAD2L1</i>	9.804	-1.076	0.0212
<i>RCHY1</i>	6.516	-1.069	0.0432
<i>MTMR2</i>	7.747	-1.069	0.016
<i>TPCN2</i>	8.32	-1.062	0.00755
<i>NIPA1</i>	8.761	-1.062	0.0145
<i>ASAP2</i>	9.041	-1.06	0.0043
<i>NREP</i>	8.707	-1.058	0.00385
<i>TMEM177</i>	11.32	-1.058	0.0043
<i>CADMI</i>	9.992	-1.051	0.0067
<i>OBSL1</i>	9.524	-1.05	0.013
<i>TFF3</i>	7.335	-1.043	0.0043
<i>DYNLT3</i>	8.802	-1.043	0.0243
<i>PRKCE</i>	7.502	-1.042	0.00824
<i>NAPEPLD</i>	8.324	-1.042	0.0112
<i>RHNO1</i>	8.034	-1.037	0.0481
<i>HIVEP2</i>	8.407	-1.032	0.0117
<i>TMEM173</i>	9.698	-1.032	0.0067
<i>TBCEL</i>	6.594	-1.023	0.0043

<i>CMTM4</i>	9.497	-1.023	0.0115
<i>XPR1</i>	7.436	-1.02	0.0067
<i>GSKIP</i>	10.296	-1.014	0.0179
<i>ZNF264</i>	7.55	-1.008	0.0158
<i>MYL5</i>	7.681	-1.004	0.00755
<i>NUMBL</i>	8.395	-1.003	0.00861
<i>PPCS</i>	9.361	-1.003	0.00867
<i>TBC1D1</i>	6.683	-0.997	0.0043
<i>COMMD2</i>	7.331	-0.99	0.00795
<i>SLC9A8</i>	8.184	-0.98	0.0337
<i>PANK3</i>	9.904	-0.98	0.0145
<i>LOC100130370</i>	7.762	-0.978	0.01
<i>NQO2</i>	10.274	-0.976	0.0239
<i>CDCA7</i>	8.982	-0.974	0.00976
<i>IL17RD</i>	6.508	-0.969	0.0174
<i>PLSCR4</i>	6.612	-0.969	0.0145
<i>ABLIM3</i>	8.097	-0.969	0.00772
<i>MBD2</i>	10.779	-0.968	0.0238
<i>DNAH11</i>	7.121	-0.967	0.00867
<i>GPR137B</i>	11.412	-0.965	0.0441
<i>SPTSSA</i>	9.232	-0.962	0.00772
<i>BTBD7</i>	7.857	-0.961	0.00634
<i>PDHB</i>	11.079	-0.961	0.0151
<i>FMR1</i>	7.221	-0.959	0.00755
<i>CCDC115</i>	10.526	-0.958	0.0103
<i>BLOC1S6</i>	10.657	-0.955	0.0145
<i>WWC3</i>	7.883	-0.953	0.0254
<i>BLMH</i>	9.374	-0.952	0.0395
<i>UCN2</i>	12.039	-0.946	0.0308
<i>GALNT3</i>	7.113	-0.943	0.0267
<i>ID3</i>	11.219	-0.941	0.0239
<i>KLK6</i>	7.013	-0.938	0.0254
<i>HMGCS1</i>	8.624	-0.937	0.039
<i>TMEM187</i>	8.241	-0.931	0.0103
<i>BMP2K</i>	6.79	-0.927	0.00591
<i>ECHDC1</i>	9.736	-0.918	0.0207
<i>TRPM1</i>	6.569	-0.914	0.0484
<i>VEGF</i>	16.752	-0.913	0.0428
<i>TEX30</i>	9.5	-0.91	0.0148
<i>ACSF2</i>	8.471	-0.907	0.00699
<i>CCSAP</i>	7.755	-0.903	0.0147
<i>PHC3</i>	9.347	-0.903	0.00825
<i>MYLK</i>	8.027	-0.899	0.0483
<i>ARHGEF17</i>	9.462	-0.898	0.0112
<i>RHBDL1</i>	9.679	-0.898	0.0444
<i>C20orf194</i>	9.134	-0.897	0.0277
<i>HSDL1</i>	7.394	-0.895	0.00867
<i>CMTR2</i>	6.981	-0.892	0.019
<i>P2RX7</i>	9.667	-0.886	0.027
<i>ID2</i>	8.184	-0.885	0.0228

<i>SLC25A40</i>	6.83	-0.88	0.0319
<i>WDR81</i>	12.054	-0.878	0.00825
<i>GMP</i>	9.072	-0.877	0.0174
<i>CUL4A</i>	10.951	-0.877	0.0394
<i>ATP6VIC1</i>	11.446	-0.875	0.0189
<i>GSEC</i>	7.683	-0.874	0.0305
<i>RBBP4</i>	10.644	-0.874	0.0157
<i>RFC5</i>	11.236	-0.873	0.0481
<i>TPM3</i>	11.287	-0.872	0.0155
<i>RHOQ</i>	7.263	-0.871	0.0288
<i>PPP6C</i>	11.194	-0.871	0.0067
<i>RNF38</i>	9.129	-0.867	0.019
<i>BALAP2</i>	9.387	-0.861	0.0145
<i>MTIL</i>	13.02	-0.856	0.04
<i>BRWD1</i>	7.406	-0.853	0.0067
<i>CASP7</i>	9.407	-0.853	0.0176
<i>KIF23</i>	8.646	-0.852	0.0381
<i>SYNC</i>	7.781	-0.85	0.027
<i>FAM126B</i>	8.071	-0.844	0.018
<i>PFKFB4</i>	10.112	-0.841	0.0161
<i>MAP3K2</i>	8.438	-0.839	0.048
<i>MAGEA10</i>	7.62	-0.837	0.0377
<i>RAB11FIP1</i>	8.148	-0.837	0.0163
<i>MICALL2</i>	10.148	-0.837	0.0337
<i>RHPN2</i>	11.219	-0.837	0.00755
<i>LY96</i>	9.166	-0.834	0.0492
<i>IFFO2</i>	10.15	-0.828	0.0067
<i>SLC19A2</i>	10.668	-0.823	0.0271
<i>MCMBP</i>	10.591	-0.822	0.0186
<i>NSD2</i>	7.711	-0.82	0.0216
<i>SIPA1L2</i>	9.361	-0.816	0.0145
<i>ATP5MC3</i>	15.595	-0.816	0.019
<i>GHDC</i>	8.64	-0.814	0.0193
<i>NAT8L</i>	8.337	-0.812	0.0145
<i>GNPTAB</i>	10.781	-0.812	0.0212
<i>HMBOX1</i>	8.24	-0.811	0.0337
<i>MT1E</i>	11.718	-0.809	0.0384
<i>PDS5B</i>	7.169	-0.806	0.00832
<i>ARHGAP4</i>	13.088	-0.806	0.0426
<i>NT5E</i>	7.08	-0.802	0.0209
<i>FLNA</i>	6.8	-0.8	0.0242
<i>S100B</i>	7.626	-0.8	0.0174
<i>GATAD2A</i>	8.83	-0.799	0.01
<i>NDUFA5</i>	11.304	-0.797	0.00867
<i>SPIN1</i>	8.247	-0.795	0.0134
<i>MT1HL1</i>	12.939	-0.794	0.0441
<i>SMARCD3</i>	10.633	-0.792	0.0341
<i>CHD9</i>	7.881	-0.791	0.0134
<i>C2orf69</i>	8.052	-0.79	0.00867
<i>PIP4K2A</i>	9.862	-0.79	0.019

<i>SLC7A8</i>	6.699	-0.786	0.0117
<i>OVOS2</i>	12.043	-0.785	0.039
<i>TMEM63A</i>	7.393	-0.778	0.0112
<i>YAP1</i>	9.685	-0.776	0.0383
<i>UOCR8</i>	12.912	-0.776	0.018
<i>NRAS</i>	8.849	-0.775	0.0292
<i>TEX19</i>	6.65	-0.77	0.0204
<i>PANX2</i>	7.098	-0.768	0.0126
<i>PPP1R2</i>	7.258	-0.766	0.0165
<i>AHNAK</i>	9.821	-0.766	0.0191
<i>RIDA</i>	8.717	-0.765	0.0461
<i>PLS3</i>	10.52	-0.765	0.0341
<i>SLC6A8</i>	9.952	-0.764	0.027
<i>MPI</i>	10.309	-0.761	0.0233
<i>ABCB6</i>	11.177	-0.761	0.0471
<i>TAF12</i>	10.656	-0.76	0.0301
<i>DDX1</i>	13.36	-0.759	0.027
<i>HSPB8</i>	7.864	-0.755	0.0102
<i>COPS2</i>	10.367	-0.755	0.0135
<i>METAP2</i>	7.887	-0.753	0.0409
<i>ABCC5</i>	10.84	-0.752	0.018
<i>SNHG21</i>	8.25	0.75	0.0228
<i>NFYA</i>	7.996	0.751	0.0187
<i>TGFBR1</i>	6.529	0.752	0.019
<i>RAB11FIP3</i>	9.297	0.752	0.0226
<i>WRAP53</i>	7.175	0.753	0.0238
<i>EIF2S2</i>	7.968	0.756	0.0161
<i>MAFG</i>	11.542	0.757	0.0212
<i>SPOP</i>	8.13	0.774	0.0123
<i>GCSH</i>	12.724	0.774	0.0191
<i>METTL16</i>	10.585	0.776	0.0254
<i>KLF9</i>	10.948	0.779	0.042
<i>PCTP</i>	10.224	0.78	0.0174
<i>DPH3</i>	11.857	0.78	0.0243
<i>WDFY1</i>	9.546	0.784	0.014
<i>SNORA78</i>	12.42	0.786	0.0363
<i>NDST2</i>	9.29	0.789	0.0331
<i>PSMD3</i>	10.888	0.789	0.0089
<i>ACTR3B</i>	8.09	0.79	0.0337
<i>GPRI37</i>	8.453	0.791	0.0434
<i>SMAD7</i>	7.398	0.793	0.00953
<i>BTG1</i>	9.548	0.793	0.0193
<i>IER3</i>	12.605	0.802	0.0463
<i>TSPAN33</i>	8.059	0.805	0.0212
<i>TRAF3IP1</i>	8.788	0.805	0.0395
<i>ALG5</i>	11.703	0.806	0.0366
<i>NDELI</i>	7.474	0.808	0.0193
<i>TXNDC5</i>	11.708	0.817	0.0247
<i>ARL4C</i>	8.601	0.822	0.0187
<i>SAR1A</i>	10.057	0.823	0.0223

<i>C19orf12</i>	10.116	0.823	0.0346
<i>NUP133</i>	6.88	0.825	0.0132
<i>INF2</i>	10.883	0.83	0.0372
<i>CASTOR1</i>	9.082	0.836	0.0161
<i>HOTAIRMI</i>	7.959	0.839	0.0293
<i>CHERP</i>	8.306	0.841	0.00658
<i>TMEM134</i>	9.429	0.843	0.0239
<i>MGAT2</i>	9.805	0.845	0.0112
<i>B4GALT5</i>	11.961	0.845	0.0314
<i>SLC35F5</i>	8.346	0.855	0.0237
<i>LINC00673</i>	8.37	0.86	0.0228
<i>GALNT2</i>	10.335	0.866	0.0208
<i>LOC100287015</i>	7.46	0.868	0.0335
<i>IPPK</i>	7.25	0.869	0.0228
<i>ARHGEF26</i>	8.044	0.875	0.0471
<i>ST6GALNAC1</i>	7.46	0.877	0.0321
<i>C19orf57</i>	8.776	0.877	0.0239
<i>REV3L</i>	9.408	0.877	0.0179
<i>FAM234B</i>	8.542	0.879	0.0165
<i>ASB13</i>	10.209	0.884	0.0285
<i>RPL27A</i>	6.656	0.891	0.019
<i>CCNJ</i>	7.124	0.891	0.0243
<i>MOB3B</i>	8.612	0.891	0.021
<i>ITPRIP</i>	10.655	0.892	0.0152
<i>ADCY9</i>	8.823	0.902	0.0186
<i>DNAL4</i>	7.339	0.907	0.0223
<i>C6orf120</i>	7.46	0.918	0.0368
<i>SPRR2E</i>	8.593	0.918	0.0151
<i>RUNX1</i>	7.407	0.925	0.0293
<i>SPRR2F</i>	8.335	0.929	0.0167
<i>NFKBIA</i>	11.093	0.934	0.0293
<i>R3HDM2</i>	9.22	0.936	0.00625
<i>DANCR</i>	11.845	0.936	0.0419
<i>MINPP1</i>	7.81	0.962	0.0103
<i>PAG1</i>	9.004	0.967	0.0132
<i>CXCL1</i>	8.039	0.982	0.0337
<i>ERVMER34-1</i>	9.149	0.994	0.0228
<i>CALML4</i>	8.98	0.996	0.0102
<i>ILF3-DT</i>	9.896	1.007	0.0104
<i>NUP98</i>	10.526	1.027	0.00455
<i>NUAK1</i>	8.298	1.034	0.0333
<i>NONO</i>	11.755	1.037	0.00564
<i>SPRR2A</i>	8.69	1.042	0.0322
<i>PXN</i>	13.306	1.047	0.0043
<i>C11orf96</i>	12.773	1.068	0.0043
<i>ICK</i>	8.309	1.078	0.0326
<i>HS3ST1</i>	8.326	1.083	0.00867
<i>SNHG19</i>	11.351	1.083	0.0238
<i>LINC01003</i>	8.483	1.088	0.0308
<i>DEXI</i>	11.42	1.095	0.047

<i>CRELD1</i>	7.27	1.099	0.0187
<i>RHOB</i>	9.181	1.099	0.00591
<i>IL6R</i>	7.399	1.1	0.0131
<i>OLIG1</i>	7.775	1.122	0.0174
<i>TENT5A</i>	9.286	1.128	0.0067
<i>TRIM11</i>	7.78	1.13	0.0178
<i>BCL7A</i>	8.61	1.131	0.00595
<i>IP6K2</i>	10.911	1.137	0.0174
<i>LOC730183</i>	8.071	1.141	0.0103
<i>POGLUT2</i>	8.315	1.145	0.0135
<i>SENP3</i>	10.368	1.167	0.00385
<i>LINC01481</i>	7.737	1.179	0.0174
<i>NFKBIZ</i>	7.157	1.182	0.0075
<i>SF3B5</i>	13.496	1.185	0.0172
<i>ARL6IP1</i>	9.419	1.19	0.0167
<i>NAA60</i>	12.394	1.209	0.00684
<i>ONECUT2</i>	7.636	1.218	0.00883
<i>RPLA</i>	10.837	1.218	0.00591
<i>MLX</i>	10.753	1.222	0.00634
<i>AMMECR1L</i>	10.008	1.225	0.0103
<i>PDCD6IPP2</i>	10.791	1.244	0.0197
<i>KMT5A</i>	7.534	1.266	0.00989
<i>SNHG16</i>	13.54	1.272	0.00867
<i>CPOX</i>	10.901	1.28	0.0043
<i>PIK3R2</i>	12.898	1.282	0.0274
<i>GNG10</i>	11.597	1.298	0.0193
<i>C4orf46</i>	7.749	1.308	0.00591
<i>RASD1</i>	7.439	1.315	0.0372
<i>TRAPPC10</i>	7.66	1.317	0.00463
<i>NCALD</i>	7.731	1.365	0.00824
<i>MIPEP</i>	10.483	1.388	0.0247
<i>HDAC3</i>	11.149	1.407	0.00385
<i>SLC7A11</i>	10.248	1.422	0.00311
<i>OPN3</i>	6.79	1.484	0.027
<i>NCOA7</i>	9.149	1.499	0.00636
<i>CDC42SE2</i>	9.375	1.862	0.00385

28
29

Upstream Regulator	Molecule Type	Z-score	p-value
MITF	Transcription regulator	-2.89	1.38E-05
MYC	Transcription regulator	-2.32	2.10E-03
TGFB	Growth factor	-2.14	1.29E-02
PAX7	Transcription regulator	-1.94	2.25E-02
mir-145	Microna	1.98	3.77E-03
TP53	Transcription regulator	2.08	1.06E-02
let-7	Microna	2.38	3.15E-04
KDM5B	Transcription regulator	2.45	1.58E-02
miR-124	Microna	2.69	2.45E-03

30

31 **Supplemental table 2.** IPA® upstream activators analysis of the genes regulated upon FBXO32
32 silencing.
33

Supplemental table 3. List of the peptides identified by mass spectrometry in two independent experiments.

Protein	UNIQUE PEPTIDE EXP1	UNIQUE PEPTIDE EXP2
ACACA	3	1
ACO1	2	4
ACOT9	2	1
AGL	3	1
AIFM2	3	1
AKAP12	2	1
AKAP8	2	4
AP3B1	8	1
APPL1	1	1
ARIH1	1	1
ARMT1	1	1
ASCC3	2	1
ASNS	3	5
ATAD3A	1	5
ATP2B1	1	2
ATXN10	6	3
AUP1	3	1
BICD2	1	5
BRIX1	1	8
C5orf22	2	2
CARM1	1	3
CDK11B	4	1
CDK9	1	2
CEP131	1	12
CKAP5	4	1
CLIP1	1	3
CLPB	1	2
CLPX	2	5
CNOT1	3	1
COPG2	3	1
COPS3	3	1
COPS4	6	7
COPS6	1	3
CPSF1	1	4
CPSF7	4	1
CRNKL1	3	1
CSTF1	2	4
CSTF3	2	3
CTNND1	2	3
CTPS1	3	7
CUL4A	2	3
CUL4B	2	2
DCTN1	1	7
DCTN4	1	6

DDX24	4	9
DEK	5	4
DHCR24	2	1
DHPS	2	4
DKFZp686E1899	8	2
DKFZp686M24262	5	2
DKFZp781N0678	2	4
DNM2	4	7
DPP9	1	4
DYNC1LI1	1	1
EHD4	2	4
EIF2B3	4	1
EIF3M	5	5
ELAC2	2	4
ERAL1	1	3
ERLIN2	2	2
FAF2	3	1
FAM129B	4	10
FAM98A	1	2
FARSA	6	3
FBXO32	2	2
FGFR1OP	3	14
GDI1	3	8
GIGYF2	1	3
GLG1	2	1
GMPPA	2	2
GNA13	3	1
GNAS	4	1
GNL1	3	2
GPKOW	1	3
GTF3C1	1	11
GTPBP10	1	1
GTPBP4	2	12
H2AFY	4	2
hCG_2002731	1	2
hCG_31253	1	9
HELLS	1	2
HERC5	1	1
HGS	2	3
HMCES	1	1
HSPA14	1	1
HSPBP1	3	2
HSPC142	1	2
IDH3B	7	2
IGF2R	3	2
IKBKAP	3	2
ILVBL	1	1
IPO9	2	2
KRR1	3	7
LACTB	2	1

LAS1L	1	9
LBR	2	4
LOC102724159	1	2
LOC51035	2	4
LRWD1	1	1
LTA4H	3	13
LYAR	1	11
MAD1L1	1	2
MAPK3	4	3
MCMBP	1	3
METTL2B	1	1
MGEA5	3	2
MORF4L1	1	1
MPI	1	1
MRI1	1	3
MRPL37	3	1
MRPL39	1	3
MRPS35	3	4
MRPS5	2	6
MRPS9	5	8
MSH2	10	9
MSTO1	1	1
MTHFD1L	5	1
NADK2	5	1
NAE1	1	7
NAGK	2	4
NCAPG	2	1
NCDN	1	1
NCKAP1	4	1
NCLN	4	1
NME7	2	2
NOC4L	1	8
NOP56	3	24
NPLOC4	2	8
NSF	3	2
NSUN4	2	1
NUP107	2	1
NUP155	7	3
NUP37	1	3
NUP88	2	5
NUP98	1	2
OGFR	2	4
OGT	1	2
OSBPL9	1	1
PAF1	1	2
PAK2	3	9
PARVA	2	2
PBEF1	4	8
PC	1	1
PDLIM1	1	8

PDLIM5	1	3
PFKM	6	5
PKN1	1	1
PLAA	2	8
PLEC	2	33
PMPCA	5	4
PMPCB	3	6
PNKP	1	3
POFUT1	3	4
POLR2A	3	4
POP1	5	12
PPM1F	1	2
PPME1	2	7
PPP1R8	1	1
PRIM2	7	2
PRKACA	1	2
PRPSAP1	3	2
PSMC4	8	6
PSMD12	9	7
RCN2	1	3
RECQL	4	9
RPL29	1	2
RRP8	1	3
RSL1D1	2	13
SAMHD1	2	2
SAP30BP	2	1
SDAD1	2	2
SEC23A	1	3
SEC61A1	1	2
SERPINB6	4	5
SMARCA4	4	8
SMARCA5	7	9
SMARCD1	1	2
SMC4	5	5
SMU1	6	4
STT3A	4	1
STT3B	2	2
SUPT6H	1	10
SURF4	1	1
TBCE	1	8
TBR1	1	1
TEX10	1	7
TFG	4	6
TIMM44	4	1
TJP1	2	6
TMEM43	2	1
TOP2A	2	10
TOR1AIP2	1	2
TRIP12	1	14
TRMT1	1	2

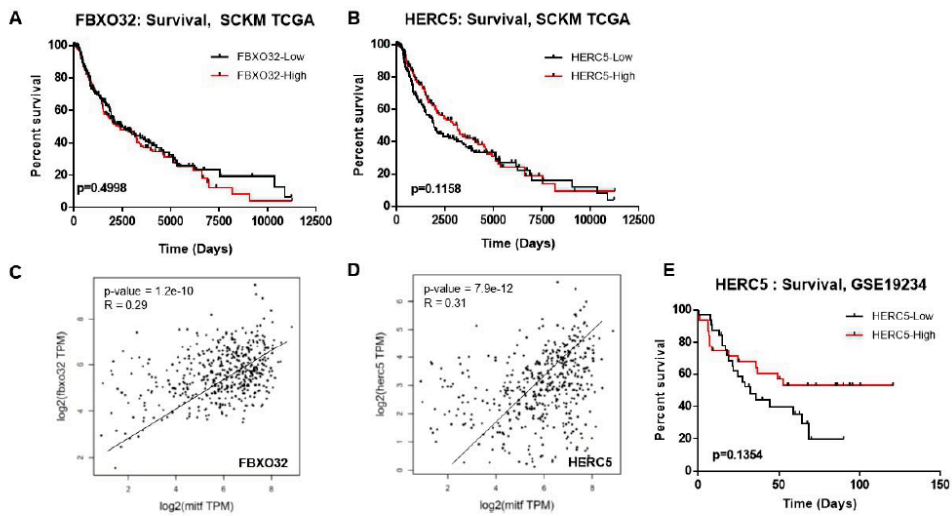
TRMT2A	2	1
TSG101	2	3
TTC4	2	1
TTL12	1	5
TUBA1C	2	4
TUBB2A	3	2
TUBB3	1	5
TUBB6	2	5
TUBGCP3	1	1
U2SURP	1	1
UAP1	1	13
UBE3A	3	7
UCHL5	5	9
UNC45A	4	1
USP10	1	3
USP11	1	4
USP48	1	3
UTP20	2	1
VPS16	1	1
VPS26B	2	1
VTA1	3	3
WDR3	1	1

Category	Term	Genes	Fold Enrichment	Benjamini
Chromatin, Epigenetic	chromosome organization	MORF4L1, MAD1L1, DYNC1L1, NUP98, COPS6, COPS3, COPS4, HCFC1, DEK, TOP1, NCAPG, SMARCD1, PRIM2, H2AFY, NAT10, PRKAA1, NUP37, OGT, LRWD1, TOP2A, TRIP12, HELLS, GNL3, CKAP5, MSH2, LIG1, HMBOX1, CDK9, PKN1, RRP8, LAS1L, NUP155, SMC4, PPM1F, RECQL, PNKP, CUL4A, ASCC3, POLD2, MAPK3, MCMBP, SMARCA5, CLIP1, NUP107, CUL4B, AKAP8, PAF1, CARM1, SMARCA4, SUPT6H	2,78	7,40E-08
	ribosome biogenesis	KRR1, GTPBP4, SDAD1, NOC4L, NUP88, GTPBP10, RRP8, ERAL1, LAS1L, RPL29, RSL1D1, MRPS9, BRX1, WDR3, NAT10, NOP56, LOC102724159, UTP20, GNL1, TEX10, GNL3, NSUN4	4,32	1,48E-05
Ribosome	Ribonucleoprotein complex biogenesis	KRR1, GTPBP4, SDAD1, NOC4L, CRNKL1, NUP88, GTPBP10, CNOT1, ERAL1, LAS1L, RRP8, RPL29, RSL1D1, MRPS9, BRX1, WDR3, CELF2, NAT10, NOP56, LOC102724159, UTP20, GNL1, EIF3M, TEX10, NSUN4, GNL3	3,57	2,17E-05
Cell Cycle	mitotic cell cycle process	DYNC1L1, MAD1L1, NUP98, USP8, CNOT1, TUBGCP3, NUMA1, NCAPG, PRIM2, H2AFY, PRKACA, NUP37, TOP2A, HELLS, TUBB3, CEP131, NUP88, CKAP5, MSH2, LIG1, BIRC6, NUP155, DCTN1, SMC4, NAE1, PSMC4, CUL4A, PSMD12, FGFR1OP, MCMBP, CLIP1, CDK11B, NUP107, CUL4B, AKAP8, CARM1, GIGYF2, SMARCA4, DNM2	2,89	2,94E-06
	mitotic cell cycle	DYNC1L1, MAD1L1, NUP98, USP8, ASNS, CNOT1, TUBGCP3, NUMA1, PAK2, NCAPG, PRIM2, H2AFY, PRKACA, NUP37, TOP2A, HELLS, TUBB3, CEP131, NUP88, CKAP5, MSH2, LIG1, BIRC6, NUP155, DCTN1, SMC4, NAE1, PSMC4, CUL4A, PSMD12, FGFR1OP, MCMBP, CLIP1, CDK11B, NUP107, CUL4B, AKAP8, CARM1, GIGYF2, SMARCA4, DNM2	2,79	3,16E-06
	cell cycle	MAD1L1, DYNC1L1, TSG101, PRKAG1, CNOT1, PAK2, PRIM2, H2AFY, NUP37, PRKACA, TOP2A, TUBB3, DHCR24, GTPBP4, NUP88, LIG1, HERC5, CDK9, RRP8, DCTN1, FGFR1OP, MAPK3, MCMBP, CLIP1, CDK11B, AKAP8, NUP107, CARM1, GIGYF2, SMARCA4, NUP98, USP8, HCFC1, ASNS, TUBGCP3, NUMA1, NCAPG, SH3GLB1, PRKAA1, HELLS, CEP131, MSH2, CKAP5, BIRC6, NUP155, APPL1, SEPT10, SEPT11, SMC4, NAE1, RPS6KA3, PSMC4, PSMD12, CUL4A, CUL4B, DNM2	2,21	8,53E-06
	cell cycle process	DYNC1L1, MAD1L1, NUP98, USP8, TSG101, PRKAG1, CNOT1, TUBGCP3, NUMA1, SH3GLB1, NCAPG, PRIM2, H2AFY, PRKAA1, PRKACA, NUP37, TOP2A, HELLS, TUBB3, DHCR24, CEP131, NUP88, CKAP5, MSH2, LIG1, BIRC6, CDK9, RRP8, NUP155, DCTN1, SMC4, NAE1, PSMD12, PSMC4, CUL4A, FGFR1OP, MCMBP, CLIP1, CDK11B, NUP107, AKAP8, CUL4B, CARM1, GIGYF2, SMARCA4, DNM2	2,23	1,03E-04
	ncRNA metabolic process	ELAC2, PUS1, UBA5, TRMT1, POLR2A, WARS, H2AFY, NAT10, MRPL39, GTF3C1, NSUN4, KRR1, IKBKAP, GTPBP4, MOCS3, NOC4L, CDK9, RRP8, LAS1L, METTL2B, RPL29, RSL1D1, MRPS9, POP1, FARSB, WDR3, FARSA, NOP56, LOC102724159, UTP20, CPSF1, TEX10, SMARCA4	3,81	1,14E-07
RNA	RNA processing	ELAC2, PUS1, CRNKL1, TRMT2A, U2SURP, TRMT1, UBA5, IVNS1ABP, POLR2A, DCPS, HNRNPM, GPKOW, PRKACA, NAT10, NSUN4, KRR1, IKBKAP, GTPBP4, MOCS3, CSTF3, NOC4L, CDK9, LAS1L, RRP8, METTL2B, RPL29, RSL1D1, MRPS9, PPP1R8, CPSF7, POP1, WDR3, CELF2, PAF1, NOP56, LOC102724159, UTP20, CSTF1, CPSF1, TEX10, SUPT6H	2,97	6,33E-07
	ncRNA processing	KRR1, IKBKAP, GTPBP4, MOCS3, ELAC2, NOC4L, PUS1, RRP8, UBA5, TRMT1, LAS1L, METTL2B, RPL29, RSL1D1, MRPS9, POP1, WDR3, NAT10, NOP56, LOC102724159, UTP20, CPSF1, TEX10, NSUN4	3,85	2,21E-05
Cellular Stress	cellular response to stress	ARMT1, MORF4L1, MRPS35, COPS6, CLPB, COPS3, COPS4, DEK, CNOT1, USP10, NUP37, TOP2A, GNL1, EIF2B3, AUP1, NUP88, LIG1, ERLIN2, PKN1, CDK9, RRP8, DCTN1, RSL1D1, PNKP, RECQL, SERPINB6, MRPS9, ASCC3, MAPK3, UCHL5, SMARCA5, NUP107, CARM1, GIGYF2, NUP98, HACD3, UBA5, ASNS, POLR2A, STT3B, SH3GLB1, INPP5F, PRKAA1, SEC61A1, TRIP12, NPLOC4, MSH2, NUP155, RPS6KA3, PSMC4, CUL4A, GSK3A, GFPT1, POLD2, FAF2, CUL4B, DNM2	2,12	2,04E-05

34

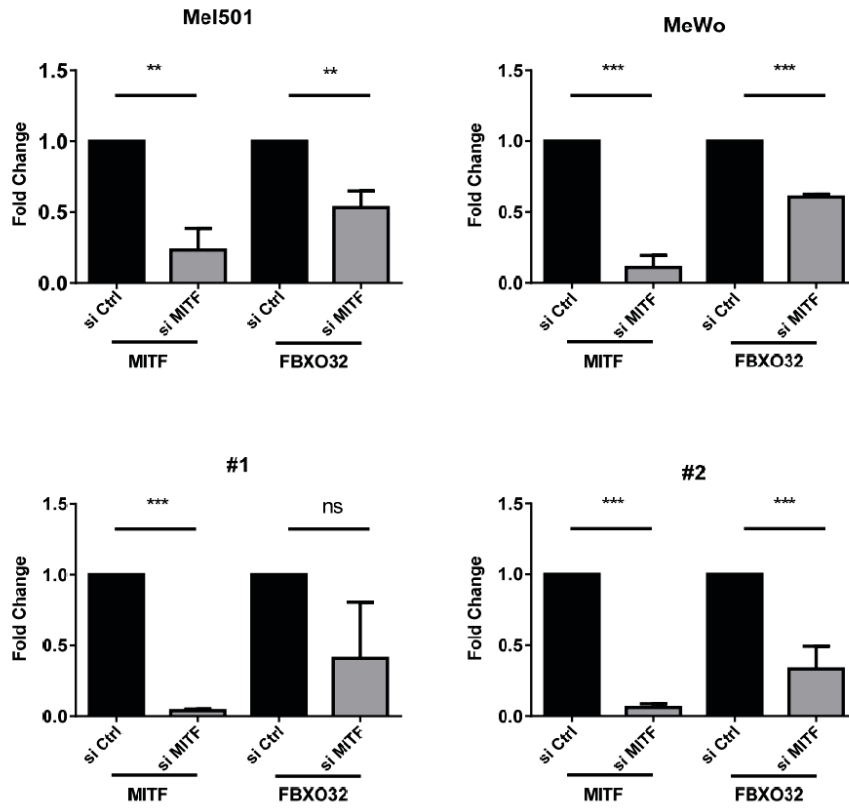
35 **Supplemental table 4.** GO terms enrichment associated with the proteins interacting with
36 FBXO32

37



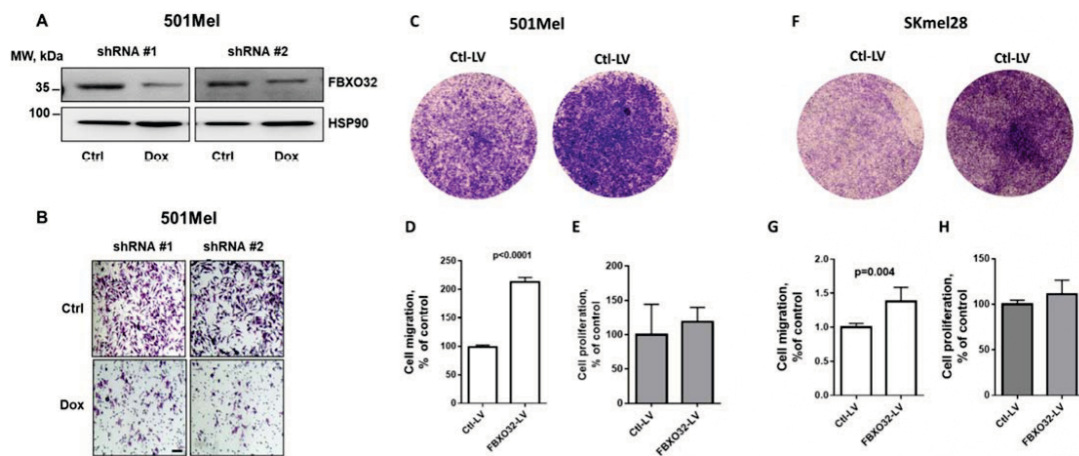
38

39 **Supplemental Figure 1.** (A) Kaplan-Meier survival curve of cutaneous melanoma patients
 40 with low (black line) or high (red line) expression level of FBXO32 from TCGA SKCM dataset.
 41 (B) Survival curve of melanoma patients with low (black line) or high (red line) expression
 42 level of HERC5 from TCGA SCKM dataset. (C) Correlation between MITF and FBXO32
 43 expression in melanoma from TCGA cohort. (D) Correlation between MITF and HERC5
 44 expression in melanoma from TCGA cohort. (E) Survival curve of melanoma patients with low
 45 (black line) or high (red line) expression level of HERC5 from GSE19234 dataset.
 46



47
 48
 49
 50
 51
 52

Supplemental Figure 2. Relative expression of MITF and FBXO32 when MITF is downregulated by siRNA in (A) 501Mel cells, (B) MeWo cells, and (C, D) short-term culture isolated from patients. *: p-value < 0.05, **: p-value < 0.01, ***: p-value < 0.001.



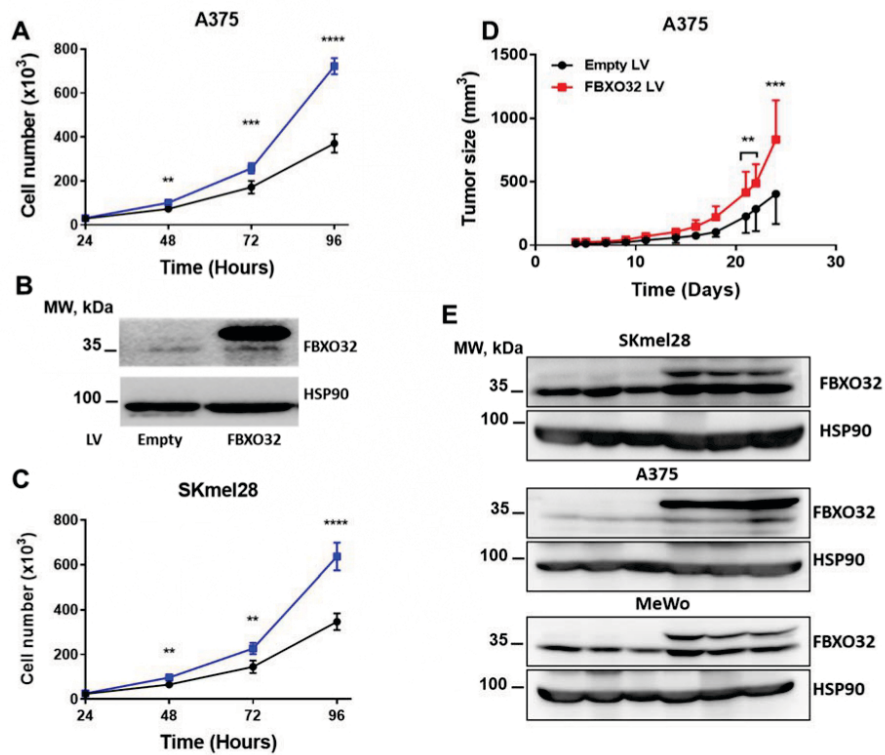
53

54

55 **Supplemental Figure 3.** (A) Expression of FBXO32 in 501Mel after transduction with
 56 doxycycline inducible shRNAs targeting FBXO32. HSP90 was probed as loading control. (B)
 57 Effects of shRNAs-mediated FBXO32 downregulation on migration of 501Mel cells. Bar=100
 58 μm . (C) Expression of FBXO32 in 501Mel after transduction with empty or FBXO32 lentivirus.
 59 HSP90 was probed as loading control. (D, E) Effects of FBXO32 overexpression, on migration
 60 of 501Mel cells (D) representative image, (E) quantification of 3 independent experiments
 61 (Mean \pm SD). (F) Effects of FBXO32 overexpression on proliferation of 501Mel cells. Graph
 62 represent mean \pm SD of 3 independent experiments. (G) Expression of FBXO32 in SKmel28
 63 after transduction with empty or FBXO32 lentivirus. HSP90 was probed as loading control. (D,
 64 E) Effects of FBXO32 overexpression, on migration of SK28mel cells (D) representative
 65 image, (E) quantification of 3 independent experiments (Mean \pm SD). (F) Effects of FBXO32
 66 overexpression on proliferation of SKmel28 cells. Graph represent mean \pm SD of 3
 67 independent experiments.

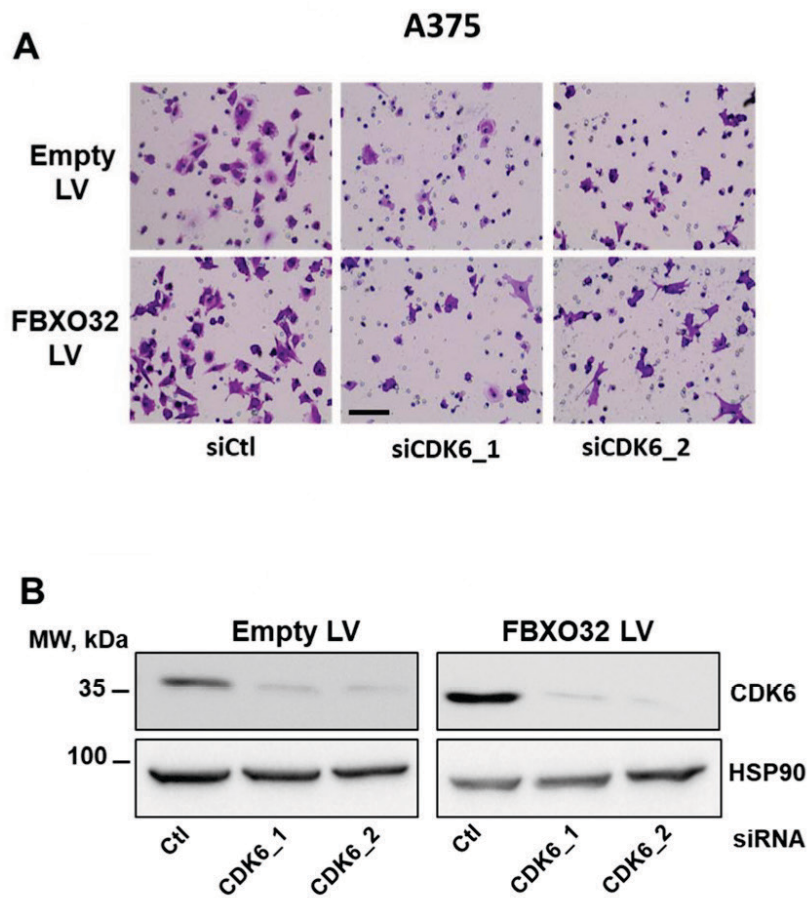
68

69

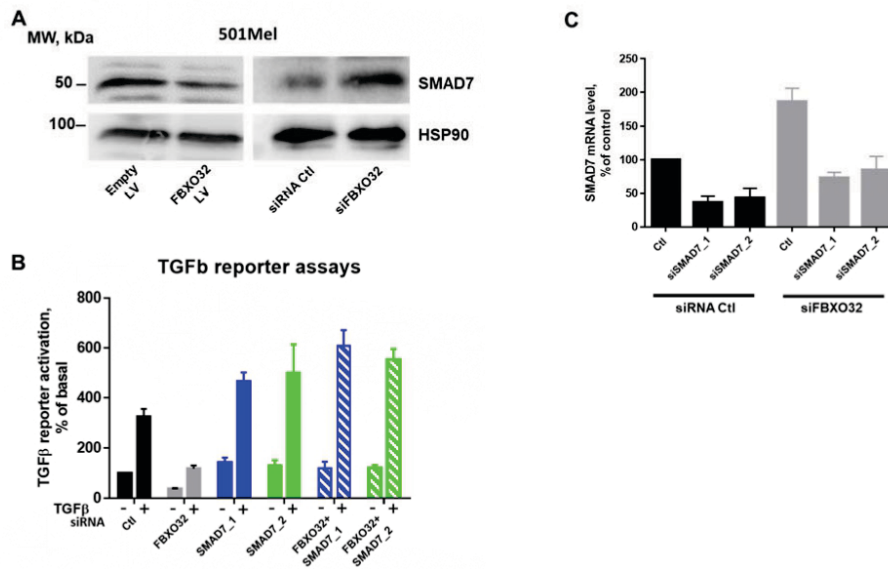


70
71
72
73
74
75
76
77
78
79
80
81

Supplemental Figure 4. (A) Quantification of A375 cells proliferation after empty vector (black line) or FBXO32 virus (blue line) transduction, from 24h to 96h (mean \pm SD, n = 6). (B) Western blot analysis of FBXO32 expression after lentivirus mediated FBXO32 forced expression in A375 cells. HSP90 expression was probed as loading control. (C) Quantification of SKmel28 cells proliferation after empty vector (black line) or FBXO32 (blue line) transduction, from 24h to 96h (mean \pm SD, n = 6). (D) Tumor growth after A375 cells xenografts transduced with empty vector (black line) or FBXO32 (red line) (mean \pm SD, n = 10). (E) Expression of FBXO32 in 6 different tumors after SKmel28, A375 or MeWo cells xenografts. HSP90 was probed as loading control.

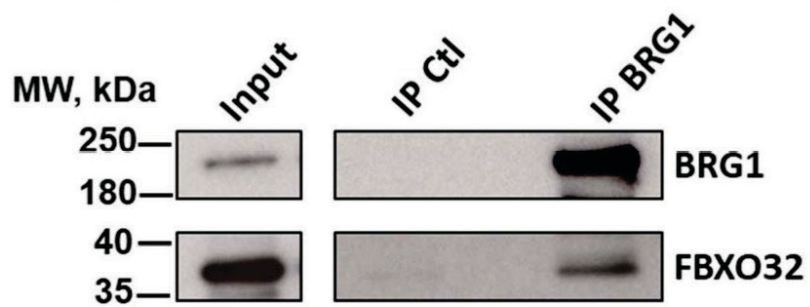


82
 83 **Supplemental Figure 5.** (A) Representative image of the effect of CDK6 downregulation on
 84 migration of A375 overexpressing (lower panel) or not (upper panel) FBXO32. Bar=100 μ m.
 85 (B) Western blot analysis of the expression of CDK6 after siRNAs downregulation in A375
 86 cell with or without FBXO32 forced expression. HSP90 was probed as loading control.
 87
 88



89
 90
 91
 92
 93
 94
 95
 96
 97

Supplemental Figure 6. (A) Western blot analysis of SMAD7 expression after transfection of siRNAs targeting FBXO32 (right panel) or transduction by FBXO32 expressing lentivirus (left panel) in 501Mel cells. HSP90 was probed as loading control. (B) 501Mel were transfected with the TGFβ reporter and the indicated siRNAs. When indicated cell were incubated to TGFβ (5nM, for 18h). TGFβ reporter activity was calculated as % of basal activity (mean ± SD, n = 3). (C) qPCR analysis of SMAD7 expression in the different conditions as in B.



98
99

100 **Supplemental Figure 7.** Co-immunoprecipitation and western blot analysis showing
 101 interaction between FBXO32 with BRG1 in 501Mel cells. Western blot with anti-BRG1 and
 102 anti-FBXO32 in total extract (Input), in immune-precipitates with control (IP Ctl) or BRG1 (IP
 103 BRG1) antibodies.

Význam aberantně aktivované dráhy Hedgehog/Gli pro nádorovou progresi

Importance of Aberrantly Activated Hedgehog/Gli Pathway in Tumour Progression

Kreisingerová K., Ondrušová L., Horák, P., Vachtenheim, J.

Ústav lékařské biochemie a laboratorní diagnostiky, 1. LF UK a VFN Praha

Souhrn

Východiska: Nádorová onemocnění jsou druhou nejčastější příčinou úmrtí v České republice. Léčba tohoto typu onemocnění je pro pacienty velmi náročná a její úspěšnost je často limitovaná kvůli častým relapsům. Navíc se mohou objevit metastázy, nejčastěji v plicích a játrech, které zhoršují pacientovu prognózu na přežití. Signální dráha Hedgehog (Hh) je jednou z významných signalizačních kaskád, které ovlivňují rozvoj a následné udržování mnoha typů nádorů. Její aberantní signalizace pomáhá buňkám uniknout apoptóze, narušuje energetický metabolismus buněk, má vliv na proces epiteliálně-mezenchymálního přechodu, pomáhá nádorovým buňkám uniknout imunitnímu systému, udržuje nádorové kmenové buňky a podílí se na tvorbě metastáz. Role signální dráhy Hh v rozvoji, udržování a progresi nádorů je intenzivně studovaná. Bylo vyvinuto několik typů inhibitorů této signální dráhy. Nejvíce studované byly inhibitory receptoru Smoothened, ale vzhledem k často vznikající rezistenci se nyní dostává do popředí výzkum dalších skupin inhibitorů, které cílí mimo receptor Smoothened. Zdá se, že tyto inhibitory by mohly pomoci překonat rezistenci inhibicí přímých efektorů dráhy, tj. transkripčních faktorů Gli, nezávisle na membránové signalizaci. Tyto nové léky dávají naději pacientům, u kterých v současné době léčba selhává. **Cíl:** Tento souhrnný článek se snaží shrnout poznatky o roli signální dráhy Hh v rozvoji nádorů a popisuje některé zásadní pokroky ve vývoji cílených inhibitorů této dráhy.

Klíčová slova

apoptóza – epiteliálně-mezenchymální přechod – metastázy – chemorezistence – cílená molekulární terapie – signální dráha Hedgehog – nádorové kmenové buňky

Summary

Background: Cancer is the second most common cause of death in the Czech Republic. The treatment of this disease is very exhausting for the patients and the treatment has often limited success only. The disease often relapses after a period of remission. Moreover, metastases often appear in lungs, liver or other organs and worsen patient's prognosis and probability of survival. The Hedgehog (Hh) signaling pathway is one of the important pathways that affects initiation and maintenance of various types of tumours. When aberrantly activated, Hh signaling pathway helps cells escape apoptosis, disturbs cell energy metabolism, influences the process of epithelial-mesenchymal transition, helps to escape immune system, maintains cancer stem cells and supports metastasis. The role of Hh signaling cascade in tumour initiation, maintenance and progression is intensively studied. Several types of inhibitors of this pathway were developed. The most intensively studied were inhibitors of the receptor Smoothened. Due to commonly occurring resistance, the research of other groups of inhibitors is in the centre of interest. These new drugs do not target receptor Smoothened but proteins standing downstream of Smoothened (inhibition of final Gli transcription factors). The drugs could give new hope to patients whose treatment fails. **Purpose:** This review summarizes the findings about the role of Hh signaling pathway in tumour development and describes the progress in the development of targeted inhibitors of this pathway.

Key words

apoptosis – epithelial-mesenchymal transition – metastasis – drug resistance – molecular targeted therapy – Hedgehog signaling pathway – cancer stem cells

Práce byla podpořena institucionálním projektem Univerzity Karlovy PROGRES Q25.

This work was supported by the institutional project of Charles University PROGRES Q25.

Autoři deklarují, že v souvislosti s předmětem studie nemají žádné komerční zájmy.

The authors declare they have no potential conflicts of interest concerning drugs, products, or services used in the study.

Redakční rada potvrzuje, že rukopis práce splnil ICMJE kritéria pro publikace zaslané do biomedicínských časopisů.

The Editorial Board declares that the manuscript met the ICMJE recommendation for biomedical papers.



Mgr. Kateřina Kreisingerová

Ústav lékařské biochemie

a laboratorní diagnostiky

1. LF UK a VFN

Kateřinská 32

121 08 Praha 2

e-mail: katerina.vlckova@lf1.cuni.cz

Obdrženo/Submitted: 28. 10. 2019

Přijato/Accepted: 24. 2. 2020

doi: 10.14735/amko2020177

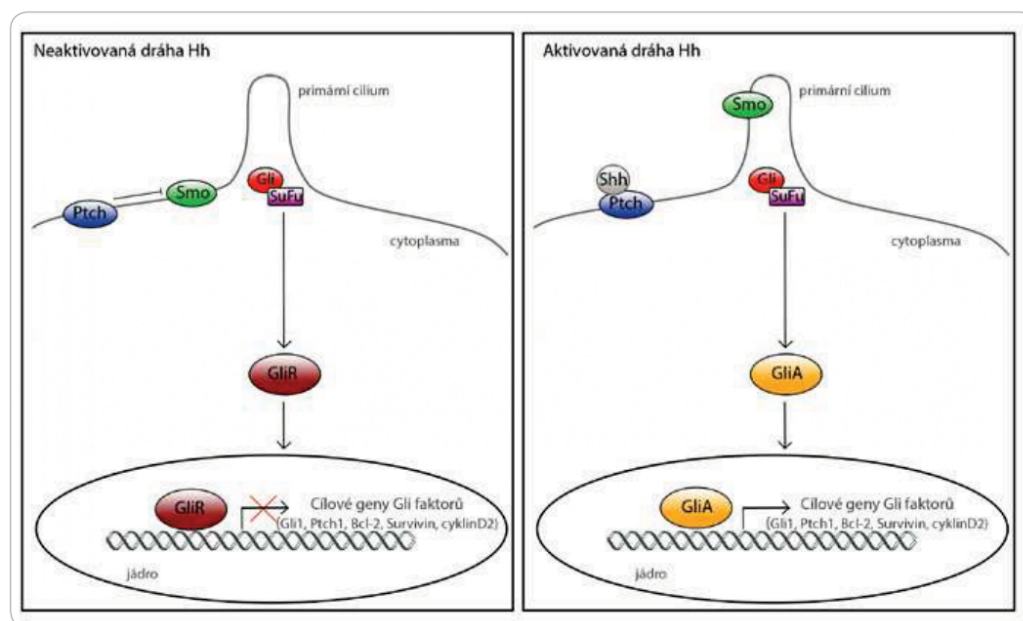
Úvod

Signální dráha Hedgehog (Hh)/Gli je evolučně velmi konzervovaná od *Drosophily* po člověka. Poprvé byla popsána v roce 1980, kdy Nüsslein-Volhard a Wieschaus provedli velký screening mutací, které měnily vývoj tělního plánu larev octomilky [1]. Od té doby je tato dráha předmětem intenzivního výzkumu a ukázalo se, že hraje zásadní roli v embryonálním vývoji, ve kterém ovlivňuje diferenciaci buněk, proliferaci a polarizaci tkání. Hh signalizace je důležitá ve vývoji mozečku, mužského reprodukčního traktu, kostí, střeva nebo neurální trubice [2]. V dospělosti je aktivita dráhy ve většině tkání velmi nízká, ale je důležitá pro udržování kmenových buněk a je součástí reparace a regenerace tkání [3–5]. Aberantní aktivace dráhy Hh byla nalezena u mnoha typů nádorů, vede k rozvoji metastáz a podílí se na rezistenci k chemoterapii [6].

Signální dráha Hedgehog a aktivace transkripčních faktorů Gli

Signální dráha je aktivována navázáním ligandu na transmembránový receptor Patched (Ptch). Byly identifikovány tři různé ligandy, které aktivují dráhu Hh. Jsou to Sonic Hedgehog (Shh), Desert Hedgehog (Dhh) a Indian Hedgehog (Ihh). Tyto ligandy mají v embryonálním vývoji různou tkáňovou expresi. Všechny tři ligandy se mohou vázat na receptor Ptch a tím spustit Hh signalizaci [7]. Pokud nedojde k navázání ligandu, neaktivovaný receptor Ptch blokuje receptor Smoothened (Smo). Tím je signalizace inaktivovaná a transkripční faktory Gli 1–3 neaktivují transkripci cílových proonkogenních genů. Pokud ligand aktivuje Ptch, dojde k uvolnění blokáce receptoru Smo a ten se dostává na povrch primárního cilia a následně ovlivňuje cytoplazmatický komplex slo-

žený z proteinů Suppression of Fused (SuFu), Gli a dalších proteinů. Následně dochází k uvolnění proteinů Gli z komplexu, vzniku jejich aktivních forem a tím aktivaci signální dráhy Hh. Gli proteiny jsou zinc-fingerové transkripční faktory. Nyní jsou známy 3 varianty těchto proteinů. Gli1 je aktivátor dráhy Hh, váže se na promotory cílových genů a tím spouští jejich transkripci. Gli2 je také považovaný především za aktivátor transkripce, nicméně má i represorovou doménu a může se jako represor chovat. Protein Gli3 může být aktivátorem nebo represorem dráhy Hh, záleží na buněčném kontextu. Aktivace dráhy Hh má za následek spuštění transkripce cílových genů. Těmi jsou v první řadě komponenty dráhy Hh (*Gli1*, *Ptch1*, *Ptch2*, *Hhip*), dále regulátory buněčného cyklu (*CCDN2*, *CCNE1*, *cyklinD2*), regulátory apoptózy (*BCL-2*, *survivin*, *PAX6*), geny epiteliálně-mezenchymálního přechodu (epithe-



Obr. 1. Signální dráha Hedgehog (Hh).

V nepřítomnosti Hh ligandu receptor Patched (Ptch) blokuje receptor Smoothened (Smo) a z proteinového komplexu, tvořeného proteiny Gli, SuFu a dalšími, se uvolňuje represorová forma Gli proteinů. Represorové Gli proteiny blokuji transkripci cílových genů dráhy Hh. Po aktivaci receptoru Ptch ligandem dráhy Hh (v tomto případě Shh), dochází k translokaci receptoru Smo na povrch primárního cilia, následně dojde k uvolnění proteinového Gli/SuFu komplexu, ze kterého se uvolňují aktivní formy Gli faktorů. Po jejich translokaci do jádra aktivují transkripci cílových genů dráhy Hh.

lial-mesenchymal transition – EMT) *ZEB1*, *ZEB2*, *Twist2* [7–10] a mnoho dalších, převážně proonkogenních genů (obr. 1).

K aktivaci Gli faktorů však může dojít i nekanonicky. To znamená, že Gli faktory jsou přímo aktivovány proteiny z jiných signálních drah a procesu aktivace se v tomto případě neúčastní upstream receptory dráhy Hh, tj. Ptch a Smo. Nekanonická signalizace je častá především u maligních onemocnění. Většina signálních drah, které nekanonicky aktivují Gli faktory, jsou stejně jako dráha Hh významné pro rozvoj malignit a porozumění jejich propojení je tedy zcela zásadní. Pozitivní regulační vliv na transkripční aktivitu Gli má například dráha KRAS-MEK-ERK u buněk karcinomu žaludku [11]. Podobně bylo prokázáno, že Ras-MEK/AKT stimuluje transkripční aktivitu Gli1 u melanomu [12]. Dalším důležitým faktorem, který ovlivňuje Gli faktory, je růstový transformující faktor beta (TGF-β), který je důležitý během embryonálního vývoje a při udržování homeostázy dospělých tkání. TGF-β je zásadní pro expresi Gli a pro proliferaci cyklopa-min-rezistentních buněk karcinomu slivivky [13]. Analýza *Gli2* promotoru prokázala, že SMAD3 a β-*katenin* se vážou na *Gli2* promotor v odpovědi na TGF-β, a *Gli2* se proto dá považovat za přímý transkripční cíl TGF-β [14]. Důležitá signální dráha PI3K-AKT-mTOR, která se účastní mnoha buněčných procesů, také dokáže nekanonicky ovlivňovat aktivaci Gli. PI3K brání proteazomové degradaci Gli2 a usnadňuje tak aktivaci Gli2 a jeho translokaci do jádra [15]. Bylo popsáno mnoho dalších proteinů, které ovlivňují Gli faktory, patří mezi ně proteinkináza C, DYRK1 a DYRK2 kinázy nebo 5'-adenosinmonofosfát-aktivovaná proteinkináza (AMPK) [16,17]. Je jasné, že nekanonická signalizace je u nádorových onemocnění stejně důležitá jako signalizace kanonická, oba dva typy se v nádorech často vyskytují společně. Výzkum léčby nádorových onemocnění by měl tedy směřovat ke kombinované terapii, která bude blokovat jak klasickou dráhu Hh, tak samotné Gli faktory, případně jejich další spouštěče.

Role Hh v nádorové progresi

Je zřejmé, že dráha Hh je významná při rozvoji mnoha typů nádorů. Zásadní vliv hraje dráha Hh v rozvoji meduloblastomu [18], bazaliomu [19], karcinomu pankreatu [20] nebo karcinomu plic [21]. U mnoha dalších typů tumorů tato dráha přispívá k rozvoji nádorové progresi. Téměř všechny zásadní změny, které vedou k progresi nádorů, jsou nějak ovlivňovány dráhou Hh. K těmto významným případům patří například uniknutí programované buněčné smrti, ovlivnění činnosti telomerázy, angiogeneze, narušení energetického metabolismu buněk, EMT, uniknutí imunitnímu systému, ovlivnění genomové stability nebo ovlivnění schopnosti tvořit metastázy a udržování viability nádorových kmenových buněk. V dalším textu jsou blíže popsány některé tyto případy, u kterých je význam dráhy Hh zcela zřejmý a prokázáný.

Apoptóza

Apoptóza neboli programovaná buněčná smrt je proces, který řídí auto-destrukci buněk, které jsou natolik poškozené, že na ně nestačí reparační mechanismy buňky. Narušení procesu apoptózy ovlivňuje homeostázu buněk a následně i tkání a je považováno za silně proonkogenní činitel. Ukazuje se, že signální dráha Hh je významným regulátorem apoptózy. Hh signalizace ovlivňuje expresi některých proapoptotických i antiapoptotických proteinů a tím určuje, zda buňka vstoupí do apoptózy, nebo ne. Dvě vědecké skupiny v roce 2004 současně prokázaly, že antiapoptotický protein BCL2 je přímým transkripčním cílem Gli faktorů. Jejich výsledky se lišily tím, že jedna skupina určila za hlavní regulátor BCL2 protein Gli1 [22], zatímco druhá považovala za regulátor genu BCL2 transkripční faktor Gli2 [23]. V roce 2011 byl další antiapoptotický protein XIAP označen jako transkripční cíl faktoru Gli2 [24]. Zvýšení hladiny antiapoptotického proteinu survivinu v nádorových buňkách bylo také připsáno signální dráze Hh [10]. Vysoká exprese survivinu byla v nádorových buňkách snížena pomocí inhibitoru GANT61, což je specifický inhibitor faktorů Gli. Za hlavní mediátor

expresy byl v této studii označen faktor Gli2, který aktivoval expresi survivinu mnohem více než Gli1. V jiné nedávné studii autoři prokázali, že Hh neovlivňuje jen antiapoptotické proteiny, ale také proteiny proapoptotické. U buněk TP53-mutovaného rhabdomyosarkomu a meduloblastomu autoři ukázali, že snížení exprese proteinu Gli1 zvyšuje expresi proapoptotického proteinu Noxa. Podle této studie Gli1 reprimuje protein Noxa pravděpodobně přes early growth response protein 1 (EGR1) [25]. Nejznámější nádorový supresor p53 je také ovlivňován dráhou Hh. Signalizace Hh aktivuje ubikvitin ligázu Mdm2, která ubikvitinuje právě protein p53, čímž snižuje množství akumulovaného proteinu p53 v buňkách [26]. Na cholangiocarcinomových buňkách bylo ukázáno, že Hh signalizace také dokáže ovlivnit, jak konkrétně bude apoptóza probíhat, zda vnější apoptotickou cestou, nebo vnitřní (mitochondriální) cestou. Hh reguluje expresi XIAP proteinu (viz výše), který reprimuje vnější apoptotickou dráhu. Zablokování Hh signalizace vede ke snížení exprese XIAP proteinu a tím se v buňkách opět může aktivovat vnější apoptotická dráha [24]. Ze stavu současného poznání můžeme vyvodit, že dráha Hh narušuje rovnováhu apoptotických signálů v nádorových buňkách a vychyluje ji směrem k potlačení apoptózy. Tímto Hh signalizace velmi přispívá k iniciaci nádorového bujení a k dalšímu růstu již rozvinutých nádorů.

EMT a schopnost nádorů metastazovat

Epiteliálně-mezenchymální přechod (EMT) je buněčný mechanismus, který je velmi důležitý v průběhu embryonálního vývoje a během reparace tkání. Epiteliální fenotyp buněk se v procesu EMT mění na fenotyp mezenchymový. EMT významně ovlivňuje vývojové dráhy Wnt, Notch a Hedgehog (Hh). Proces EMT je také velmi důležitý během rozvoje nádorového bujení, umožňuje buňkám primárního nádoru uvolnit se do krve nebo lymfy a následně se usadit ve vzdálených orgánech s úplně jiným prostředím, než jaké bylo v primárním nádoru. Během procesu EMT dochází ke snížení adhezivity buněk, ke ztrátě bu-

něčné polarity a získání invazivních a migračních vlastností [27]. Pro indukci EMT stačí v buňce aktivovat několik faktorů, jako například ZEB1 a ZEB2, LEF-1, Snail1 a Snail2 (Slug).

Během procesu EMT dochází ke snížení nebo úplnému vymizení exprese E-cadherinu, který je běžnou adhezivní molekulou v buňkách. Dále se zvyšuje exprese mezenchymálních markerů, jakými jsou vimentin, N-cadherin a fibronektin [28]. U většiny typů nádorových buněk již byla prokázána souvislost mezi dráhou Hh a EMT a migračními schopnostmi buněk. Přímý vliv Hh/Gli dráhy na EMT byl prokázán v klinické studii zkoumající pacientky s karcinomem prsu, kde vysoké hladiny Shh/Gli1 korelovaly s vysokou expresí proteinů Snail1 a vimentinu a s nízkou expresí E-cadherinu. V pokusech na buněčných kulturách pak zablokování faktorů Gli1 a Gli2 pomocí specifického inhibitoru GANT61 vedlo ke snížení invazivity a migrace buněk [29]. Podobné jsou výsledky klinické studie zabývající se karcinomem jícnu. Aberantní exprese Gli1 a Gli2 korelovala se sníženou expresí E-cadherinu a zvýšenou expresí proteinů Snail1, Slug, N-cadherinu a vimentinu. Inhibice Gli faktorů i v tomto případě snížila mobilitu a invazivitu buněk [30]. U pankreatických nádorových buněk podobných kmenovým buňkám (cancer stem-like cells – CSLC) dráha Hh ovlivňuje EMT a další invazivní vlastnosti. Inhibice Hh signalizace Smo (knockdown receptoru Smo) snížila až inhibovala proces EMT, invazivitu, chemorezistenci, plicní metastázy a tumorigenezí pankreatických CSLC [31]. Zdá se, že Gli1 nemá u pankreatických buněk vliv na iniciaci EMT, ale podporuje EMT indukovanou TGF- β 1 a epidermálním růstovým faktorem (epidermal growth factor – EGF) [32]. TGF- β 1 podobně zvyšuje expresi Gli u nemalobuněčného karcinomu plic a tím přispívá k rozvoji EMT [33].

Role Hh signalizace v procesu EMT a ve schopnosti buněk metastazovat je méně jasná u nádorů prsu. Podle studie publikované v roce 2017 se zdá, že nemetastazují buňky, které prošly procesem EMT, ale buňky z okolí těch, které procesem EMT prošly. Migrační schopnosti těchto buněk se pravděpodobně

zvyšují díky parakrinní aktivaci faktorů Gli [34]. Hh signalizace také zvyšuje migrační schopnosti a invazivitu nádorových buněk tím, že aktivuje AKT dráhu a následně aktivuje matrix metaloproteinázy. Matrix metaloproteináza 9 (MMP-9) je takto upregulovaná například u karcinomu žaludku [35], u dlaždicového karcinomu dutiny ústní [36] a společně s matrix metaloproteinázou 2 (MMP-2) je zvýšená u buněk hepatocelulárního karcinomu [37].

Nádorové kmenové buňky

Za nádorové kmenové buňky (cancer stem cells, CSC) je považována malá frakce nádorových buněk, která získala vlastnosti podobné kmenovým buňkám. Především jde o schopnost sebeobnovy buněk, které jsou považovány za jakési „jádro“ nádoru. CSC jsou také rezistentní vůči chemoterapii a rekrutují se z nich metastatické buňky. Obecně se tedy předpokládá, že tyto buňky jsou zodpovědné za udržování a rozvoj nádorů a také za rezistenci vůči protinádorové léčbě [38]. CSC mají aberantně aktivované různé signální dráhy, které během normálního vývoje hrají důležitou roli v embryonálním vývoji a při diferenciaci buněk. Není tedy překvapivé, že dráha Hh je považována za jednu z klíčových cest pro rozvoj a udržení vlastností nádorových kmenových buněk [39]. Předpokládá se, že Hh mimo jiné aktivuje expresi genů, které jsou považovány za markery kmenovosti buněk. Jeden z těchto genů, transkripční faktor Nanog, je přímým transkripčním cílem signální dráhy Hh [40]. Hh signalizace dále ovlivňuje i další markery kmenových buněk: SOX2, Bmi1 a OCT4 [41,42]. Role Hh v udržování CSC byla popsána u mnoha typů nádorů, např. u akutní a chronické myeloidní leukemie, mnohočetného myelomu, karcinomu prsu nebo gliomu [43,44].

Cílená terapie

Vzhledem ke stále lepšímu poznání prostředí nádorů, procesů iniciace, progresu a metastazování nádorů se také rozvíjí oblast cílené léčby nádorů. V posledních letech bylo připraveno mnoho nízkomolekulárních inhibitorů jednotlivých komponentů dráhy Hh. Jako první byl z rostliny *Veratrum Californicum* izolován

inhibitor cyklopamin, který způsobuje závažné vývojové abnormality u zvířat. V roce 1998 bylo prokázáno, že tento alkaloid inhibuje Hh signalizaci přímým navázáním na receptor Smo [45]. Další zkoumání však ukázalo, že cyklopamin má poměrně nízkou účinnost, a navíc jej nelze užívat perorálně. Další zkoumání brzy přineslo účinnější deriváty cyklopaminu, například sonidegib (erismodegib, LDE-225), saridegib (patidegib, IPI-926) a vismodegib (GDC-0449). Dva inhibitory Smo byly schváleny americkým Úřadem pro kontrolu potravin a léčiv (Food and Drug Administration – FDA) i Evropskou lékovou agenturou (European Medicines Agency – EMA) pro léčbu bazaliomu. Prvním z nich je vismodegib. Byl schválen FDA v roce 2012 pro léčbu metastatického bazaliomu [46]. V roce 2013 pak byl schválen také EMA. Od té doby proběhlo několik dalších klinických studií, které studovaly vliv vismodegibu u dalších typů nádorů. U žádné však výsledky nedopadly tak dobře jako u bazaliomu. Vismodegib se například testoval jako monoterapie u pacientů s metastatickým kastrocně rezistentním karcinomem prostaty; testovaná léčba však neprokázala výraznou klinickou aktivitu vismodegibu [47]. V dalších studiích byl vismodegib použit jako součást kombinované terapie. Například u pacientů s metastatickou formou kolorektálního karcinomu byl vismodegib podáván v kombinaci s bevacizumabem a chemoterapií. Vliv tohoto typu léčby na prodloužení pacientova života se však v této studii signifikantně neprokázal [48]. Další klinické studie stále probíhají nebo jsou ve fázi hledání vhodných pacientů [49]. Druhým inhibitorem Smo, který je schválený FDA a EMA je sonidegib [50]. Oba úřady jej schválily v roce 2015 k léčbě lokálně pokročilého bazaliomu, který není vhodný k chirurgické léčbě nebo radioterapii. Další inhibitor Smo patidegib (saridegib) měl slibné výsledky ve fázi II klinických zkoušek a nyní začíná fázi III klinických zkoušek, kdy preparát bude podáván ve formě 2% gelu k lokální aplikaci. Testovací léčba je určena pro pacienty s Gorlinovým syndromem, který způsobuje chronickou formu bazaliomu. Léčba patidegibem má za cíl snížit celkový počet bazaliomů, což by mělo vést

ke snížení počtu nutných operací. V současné době je tato studie ve fázi hledání pacientů, kteří se zúčastní klinické zkoušky [51]. Zatím posledním inhibitory Smo schváleným FDA je glasdegib. Byl schválen v roce 2018 k léčbě nově diagnostikované akutní myeloidní leukemie u pacientů ≥ 75 let nebo u pacientů, u kterých je vyloučena intenzivní indukční chemoterapie. Léčba glasdegibem je doprovázena podáváním nízkých dávek cytarabinu [52]. Další inhibitory Smo je celá řada a jsou intenzivně studovány; patří mezi ně například taladegib nebo itrakonazol, což je látka s protiplísňovými vlastnostmi. Problémem však je, že v mnoha nádorech je receptor Smo mutovaný a výše zmíněné Smo inhibitory jsou tedy méně účinné nebo neúčinné. Neúčinnost Smo inhibitorů i při nemutovaném Smo je lehce vysvětlitelná tím, že dráha Hh může být velmi často aktivována nekanonicky jinými signálními cestami a nepotřebuje tedy upstream signální podněty. Tento problém se nyní obchází použitím inhibitorů jiných komponent dráhy Hh. Například inhibitor robotnikinin se váže na extracelulární Shh a blokuje tak Shh signalizaci [53]. Shh také blokuje protilátky 5E1, 3H8 a 6D7 (MED1-5307) [54]. Další skupinou jsou inhibitory Gli faktorů. Nízkomolekulární inhibitory GANT58 a GANT61 zabraňují vazbě Gli proteinů na DNA v jádře a tak blokuje jejich transkripční aktivitu [55]. Tyto inhibitory zatím nejsou používány v klinických studiích, nicméně jsou intenzivně zkoumány *in vitro*, popř. *in vivo* studiích se slibnými výsledky. Prokázalo se, že mnoho typů nádorových buněk je senzitivních ke GANT61 *in vitro* a že GANT61 tyto buňky zabíjí procesem apoptózy [56–58]. V další studii GANT61 v kombinaci s obatoclaem (inhibitor rodiny proteinů BCL2) působil velmi slibně na buňky maligního melanomu [59]. Mezi Gli inhibitory patří také oxid arsenitý, látka schválená FDA pro léčbu akutní promyelotické leukemie [60].

Léková rezistence

Problémem cílené léčby nádorů je, že během ní často vzniká *de novo* získaná rezistence k danému typu léčby. V pří-

padě dráhy Hh se nyní řeší především rezistence vůči inhibitorům Smo, která snižuje možnosti léčby i eradikace CSC [61]. Na významu získávají inhibitory Smo, které mají jiný mechanismus účinku než cyklopamin a jeho deriváty a jiné běžné inhibitory Smo. Například itrakonazol je považován za inhibitor Smo, nicméně neblokuje přímo molekulu Smo, ale zabraňuje kumulaci Smo v primárním cilium. Kumulace a aktivace Smo v primárním cilium je zásadní krok v Hh signalizaci; narušení tohoto procesu má za následek přerušování signalizační dráhy [62]. Itrakonazol (inhibitor Smo) a oxid arsenitý (inhibitor Gli), ať každý zvlášť, nebo v kombinaci, inhibují růst medulloblastomu a bazaliomu u myši *in vivo* a prodlužují život myši s medulloblastomem s mutovaným Smo, který je rezistentní vůči léčbě [63]. Další důležitou kategorií jsou inhibitory „downstream“ od Smo, které jsou nyní předmětem intenzivního zkoumání. Inhibitor Gli faktorů GANT61 má slibné výsledky *in vitro* i *in vivo* studiích, nicméně zatím neprobíhá žádná klinická studie.

Na druhou stranu léčba Hh inhibitory může zvýšit citlivost buněk/tumorů rezistentních vůči určitému typu léčby, například vůči radioterapii. U buněk karcinomu prostaty GANT61 zvýšil citlivost rezistentních buněk vůči radioterapii jak *in vitro*, tak *in vivo*. U myšičího modelu *in vivo* se citlivost k nové léčbě projevila snížením nádorového růstu a byla spojená se sníženou proliferací a zvýšenou apoptózou [64]. Podobně je u lidského glioblastomu častá snížená citlivost nádoru vůči léčbě chemoterapeutikem temozolomidem. Poté, co byly buňky gliomu vystaveny působení GANT61, reagovaly zvýšením citlivosti k temozolomidu [65]. V další studii bylo prokázáno, že Hh signalizace chrání buňky hepatocelulárního karcinomu před účinkem ionizační radioterapie; umlčení dráhy Hh pomocí protilátky proti Shh a pomocí Gli1 siRNA zvrátilo tento jev a buňky byly následně k terapii citlivé [66]. Jako další příklad lze uvést studie kastročně rezistentního karcinomu prostaty, kdy kombinace umlčení fosfolipázy Cc a inhibice Gli faktorů pomocí GANT61 vedla ke zvýšení citlivosti buněk vůči enzalutamidu, který je jedním z mála účinných léků na tento typ karcinomu [67].

Závěr

Z výše popsaného souhrnu je zřejmé, že výzkum signální dráhy Hh od jejího popsaní v roce 1980 pokračuje poměrně rychle. Dráha Hh je zásadní pro správný embryonální vývoj. I když se zdá, že základní kostra signální dráhy je dobře prozkoumaná, stále chybí některé důležité informace o jejím fungování. Není například známý přesný mechanismus, jakým Ptch blokuje receptor Smo. Informace o propojení Hh signalizace s jinými signálními dráhami, popř. informace o aktivaci Hh komponent pomocí jiných signálních drah určitě není kompletní a na tomto poli může dojít k mnoha průlomovým objevům. Aberantní aktivace dráhy Hh je spojená s rozvojem různých typů nádorů. Poznatky o tom, že dráha Hh je velice důležitá v iniciaci, růstu, rozvoji i udržení nádorového bujení, následoval úspěšný vývoj cílených Hh inhibitorů. Problematická je ovšem nízká účinnost mnohých z nich, přítomnost závažných nežádoucích účinků nebo vznikající rezistence k dané léčbě. Hh inhibitory jsou stále testovány v různých preklinických i klinických studiích, většinou se jedná o inhibitory receptoru Smo. Snad se brzy objeví další klinické studie testující např. léčbu pomocí specifických inhibitorů faktorů Gli. Můžeme doufat, že některé z klinických studií přinesou takové výsledky, které umožní uvedení alespoň některých inhibitorů do klinické praxe a výrazně zlepšit nové možnosti léčby onkologických pacientů.

Literatura

1. Nüsslein-Volhard C, Wieschaus E. Mutations affecting segment number and polarity in *Drosophila*. *Nature* 1980; 287(5785): 795–801. doi: 10.1038/287795a0.
2. Ingham PW, McMahon AP. Hedgehog signaling in animal development: paradigms and principles. *Genes Dev* 2001; 15(23): 3059–3087. doi: 10.1101/gad.938601.
3. Machold R, Hayashi S, Rutlin M et al. Sonic hedgehog is required for progenitor cell maintenance in telencephalic stem cell niches. *Neuron* 2003; 39(6): 937–950. doi: 10.1016/s0896-6273(03)00561-0.
4. Lowry WE, Richter L, Yachechko R et al. Generation of human induced pluripotent stem cells from dermal fibroblasts. *Proc Natl Acad Sci U S A* 2008; 105(8): 2883–2888. doi: 10.1073/pnas.0711983105.
5. Watkins DN, Berman DM, Burkholder SG et al. Hedgehog signaling within airway epithelial progenitors and in small-cell lung cancer. *Nature* 2003; 422(6929): 313–317. doi: 10.1038/nature01493.
6. Hanna A, Shevde LA. Hedgehog signaling: modulation of cancer properties and tumor microenvironment. *Mol Cancer* 2016; 15: 24. doi: 10.1186/s12943-016-0509-3.

60. Beauchamp EM, Ringer L, Bulut G et al. Arsenic trioxide inhibits human cancer cell growth and tumor development in mice by blocking Hedgehog/GLI pathway. *J Clin Invest* 2011; 121(1): 148–160. doi: 10.1172/JCI42874.
61. Peer E, Tesanovic S, Aberger F. Next-generation Hedgehog/GLI pathway inhibitors for cancer therapy. *Cancers (Basel)* 2019; 11(4): 538. doi: 10.3390/cancers11040538.
62. Kim J, Tang JY, Gong R et al. Itraconazole, a commonly used antifungal that inhibits Hedgehog pathway activity and cancer growth. *Cancer Cell* 2010; 17(4): 388–399. doi: 10.1016/j.ccr.2010.02.027.
63. Kim J, Aftab BT, Tang JY et al. Itraconazole and arsenic trioxide inhibit Hedgehog pathway activation and tumor growth associated with acquired resistance to smoothened antagonists. *Cancer Cell* 2013; 23(1): 23–34. doi: 10.1016/j.ccr.2012.11.017.
64. Gonnissen A, Isebaert S, McKee CM et al. The hedgehog inhibitor GANT61 sensitizes prostate cancer cells to ionizing radiation both in vitro and in vivo. *Oncotarget* 2016; 7(51): 84286–84298. doi: 10.18632/oncotarget.12483.
65. Li J, Cai J, Zhao S et al. GANT61, a GLI inhibitor, sensitizes glioma cells to the temozolomide treatment. *J Exp Clin Cancer Res* 2016; 35(1): 184. doi: 10.1186/s13046-016-0463-3.
66. Chen YJ, Lin CP, Hsu ML et al. Sonic Hedgehog signaling protects human hepatocellular carcinoma cells against ionizing radiation in an autocrine manner. *Int J Radiat Oncol Biol Phys* 2011; 80(3): 851–859. doi: 10.1016/j.ijrobp.2011.01.003.
67. Sun W, Li L, Du Z et al. Combination of phospholipase C α knockdown with GANT61 sensitizes castration-resistant prostate cancer cells to enzalutamide by suppressing the androgen receptor signaling pathway. *Oncol Rep* 2019; 41(5): 2689–2702. doi: 10.3892/or.2019.7054.

Informace z České onkologické společnosti

Zápis ze schůze výboru České onkologické společnosti konané 12. 5. 2020 ve FN Motol v Praze naleznete na www.linkos.cz.

DISCUSSION OF RESULTS

In this doctoral thesis, I aim to elucidate the contribution of HH pathway to the phenotype exhibited by tumors. I disclose findings of newly discovered gene targeted by HH and of the rate of expression of components of HH pathway upon introduction of its inhibitors. The general role of HH pathway in melanomas is also discussed. Given the widespread disruption of this pathway across various tumor types, we examine its impact on several cellular processes, including cell growth, the transition from epithelial to mesenchymal states, metastasis, cell death, and notably, the sustenance of CSC populations. The focal point of our study are melanomas; therefore, melanoma cell lines were used as a model to conduct the experiments on, however some other tumor cell lines were also used in elucidating the effect of HH inhibitors.

In the first paper “**The Hedgehog/GLI signaling pathway activates transcription of Slug (Snail2) in melanoma cells**”, we proved, for the first time, that HH signaling pathway directly targets C2H2-type zinc-finger transcription factor Slug. This protein is a member of the Snail superfamily of zinc finger transcription factors, and it modulates both basal and activator dependent transcription (Ganesan et al., 2015). In osteoblasts, it upregulates transcriptional activity of RUNX2 and downregulates the expression of SOX9 (Lambertini et al., 2009), it binds to CXCL12 promoter through E-box regions, and it facilitates osteoblast maturation (Piva et al., 2010). It plays a role in migration of neural crest cells and participates in facilitating RAF-1-mediated transcriptional repression of the TJ protein (Ganesan et al., 2015). It also binds to E2-box-containing silencer and in concert with CTBP1 and HDAC1 represses BRCA2 in breast cells (Tripathi et al. 2005). Further E-box elements are targeted to regulate E-Cadherin/CDH1 expression. Slug silences expression of ITGA3 in epidermal keratinocytes and regulates their proliferation and cell adhesion abilities by acting on ITGB1 and ITGB4 (Wu et al., 2020).

Slug stimulates BSG expression via E-box2 binding during TGF β 1-mediated EMT in hepatocytes and furthermore, during TWIST-mediated EMT, Slug contributes to the pro-invasive and metastatic phenotype (Naber et al., 2013).

The discovery of regulation of Slug expression is fundamental regarding further cancer research as Slug is aberrantly over-expressed in wide variety of tumors and only a limited amount of research has been dedicated to deciphering of its regulation (Li et al., 2015).

In this paper, we demonstrate that elements of Hedgehog signaling pathway, namely GLI transcription factors are entangled in the Slug gene expression regulation and suggest that Slug is a subject of HH-mediated transcriptional regulation. Even though Slug promoter lacks the GLI full consensus sequence GACCACCCA, originally determined by Kinzler and Vogelstein (1990), we identified more than 80 potential GLI binding sites (page 58). However, these binding sites all comprise at least one and up to three mismatches, but it is known that these sites also bind the GLI factors and can act in transcriptional activation. This was demonstrated before by Winklemayr et al. (2010), where multiple deviations from the consensus sequence within the binding site do not abolish binding and trans-acting GLI activity.

The response of this promoter to varying levels of GLI transcription factors was analyzed. Its full length (-5216+112) was shortened in multiple ways to produce 5 different excerpts. It was discovered that the middle part of the promoter (-4635-2092) is the most active fragment of the promoter as its removal from the full length resulted in decreased luciferase expression (the “Dmiddle” construct). When being the only portion used for the reporter construct, it yields the most increased expression response with approximately 3-fold uptick compared to the full length. The upstream fragment (-5216-4635) displayed an inhibitory contribution as its deletion led to increased luciferase activity. The proximal promoter (-2092+112), when used by itself, showed increased luciferase expression despite harboring only two 2-nucleotide mismatches. Since its activity was considerable (1,5-fold increase), this version of the promoter was selected for subsequent experiments.

The activity of the promoter was examined to find out that said activity is reduced by exposure to cyclopamine (SMO inhibitor) and GANT61 (GLI1 and GLI2 inhibitor). This was a common theme for all three of the observed cell lines – 501Mel, SK-MEL-5 and SK-MEL-28. We observed consistent inhibitions reaching a 40-60% decrease in luciferase expression. The promoter-reporter assays also showed an increase in promoter activity upon lipofection of GLI1, GLI2 and GLI3 expression plasmids, with GLI2 increasing the activity to the largest extent (page 59). Functionality of this mean of promotion of luciferase expression was verified for GLI-responsive promoter containing 12 canonical GLI binding sites, whose activity was upregulated at least 80-fold (GLI3), and almost 800-fold (Δ GLI2 – a truncated version of GLI2 lacking the N-terminal repressor domain). These findings were compared to GLI expression plasmids lipofection alongside pGL3-basic empty control promoter, whose activity remained constant in presence of any of the GLI transcription factors variants. The same approach was employed for another known GLI-responsive promoter – the PATCHED promoter, as well as for three versions of the Slug promoter – the full-length, the Dmiddle and the proximal

promoter. In all these instances, the Δ GLI2 expression vector induced the strongest increase of promoter activity. Also, in concordance with initial luciferase promoter experiment, the Dmiddle promoter version exhibited the lowest response to presence of GLI transcription factors. For all these samples, a parallel one, introducing GANT61 was prepared. We observed a consistent decrease in promoter activity with western blot confirming that the levels of GLI proteins were the same for all the samples. This led us to believe that the Slug promoter activity is governed predominantly by GLI2, but this control can be abolished by introduction of GANT61.

To investigate how this regulatory activity translates itself to actual mRNA levels in cell cytoplasm, we decided to perform RT-qPCR analysis of 6 cell lines (501Mel, SK-MEL-2, SK-MEL-3, SK-MEL-5, SK-MEL-28, MALME3M, MeWo and Hbl) harvested prior and after GANT61 exposure. We observed a coherent decrease of Slug mRNA levels in all 6 melanoma cell lines. A 20-hour exposure to 20 μ M concentration of GANT61 provoked a decrease within 40-60 % interval across the cell panel.

To further support the argument of embedding HH pathway into regulation of Slug transcription factor expression a chromatin immunoprecipitation was performed. The proximal portion of the promoter, containing two binding sites of two mismatches and 29 binding sites of three mismatches was selected as it displayed appreciable activity during promoter-reporter assays. The 2kb DNA excerpt was divided into 4 shorter regions (A representing the -2108 to -1766 portion, B containing -1769 to -1163 nucleotides, C spanning from -1182 to -490 and D comprised of -509 to +112 nucleotides) of which each was precipitated with antibodies against all three versions of GLI transcription factors alongside positive and negative control (anti-acetylated histone H3 and nonimmune IgG, respectively). This analysis revealed that the GLI transcription factors do, indeed, bind to the Slug promoter, albeit distributed disproportionately within this portion of the promoter. While GLI1 and GLI2 were found to bind subsections A, C and D, GLI3 showed binding to different subsections – namely A, B and C. GLI1 binding was the most notable on C fragment, slightly less intense on A fragment and significantly less intense on D fragment. Meanwhile, GLI2 was bound the most to the D fragment, which also contains the transcription initiation site, binding to A fragment was notably lower and to the C fragment significantly lower. Contrasting binding profile of GLI3 was manifested by comparable and sound binding to the B and C fragments and less significant binding to the A fragment. The findings further advocate intercalation of the GLI transcription factors into Slug regulatory concert, even though they suggest its higher level of complexity, which will require further research to decode properly.

Performing the western blot assay, we verified the regulatory influence of HH pathway on Slug protein levels. GANT61 exposure led to Slug protein levels decreased consistently across a panel of 8 melanoma cell lines. This finding was further supported by immunofluorescence staining performed on GANT61-treated melanoma cells. Western blot also revealed GANT61-induced decline of other known regulators of EMT, such as E- and N-cadherins, vimentin, Zeb1 and Zeb2 in six of the cell lines. Alteration was reported also for CSC markers Klf4 and ALDH1A1. Klf4 expression was reduced in SK-MEL-5, SK-MEL-28 and MeWo, while ALDH1A1 slightly increased in 501Mel, MeWo, SK-MEL-5 and SK-MEL-28. Lastly, Brn2, a known repressor of MITF activity decreased in five of six observed cell lines, hinting that its expression is at least partly regulated by HH signaling.

In regard with this finding, we decided to design a set of promoter-reporter assays based on parallel co-transfection of Slug gene promoter with either MITF, or MITF-Vp16 expression plasmids into 501Mel cell. MITF-Vp16 differs from its wild-type counterpart in its N-terminal domain. While wild-type possesses the AD N-terminal domain, MITF-Vp16 has the hyperactive Vp16 AD N-terminal domain, which has higher affinity as a *trans*-acting factor. This transcriptional regulation has been observed in *Xenopus laevis* (Kumasaka et al., 2005) and melanocytes (Sánchez-Martín, 2002), however no research has been conducted on melanoma cells. We found out that the wild-type MITF had no effect on Slug promoter activity, but its hyperactive form increased it approximately 2-fold. Contrarily, the melastatin promoter, which is a documented MITF target (Miller et al., 2004) was impacted by both MITF and MITF-Vp16. The melastatin promoter activity was found out to be 4 and 10 times higher compared to control, respectively. To further investigate this potential dependency another set of co-transfection experiments was designed. This time, MITF expression vectors were introduced into cells equipped with anti-MITF shRNA, whose transcription is triggered by doxycycline in a dose dependent manner. What we observed was that upon doxycycline introduction there was a drop of MITF protein levels, but not those of Slug protein. Contrarily, the intercellular concentration of a known MITF target – livin (also called ML-IAP) was mimicking decreasing levels of MITF. No other measured protein was affected by doxycycline treatment, seemingly implying that Slug is expressed independently of MITF in human melanoma cells.

To gain more knowledge about the relation of expression patterns of MITF, GLI2 and Slug, sections of normal skin, nevus and melanoma metastasis were stained immunohistochemically. The normal skin was found to be relatively abundant in GLI2 and Slug (scored 2-3), however only limited number of (albeit strongly) MITF-positive (score 4)

melanocytes was present. In nevus, GLI2 and Slug were stained to a lesser level (both score 2, with Slug sporadically score 3). MITF was once again found strongly positive (score 4), but this time in much larger number of cells. Epidermal keratinocytes were MITF negative (score 0). In metastatic melanoma approximately a half of the cells was GLI2 and Slug positive (score 2-4) with Slug being overall more abundant of the two. MITF staining revealed that only a small number of cells is MITF positive. It was also established that cells which were previously found to contain GLI2 and/or Slug were MITF negative, or only very slightly positive (score 0-1). This is in accordance with previous results stating that invasive and metastatic cells are either low MITF, or MITF negative (Sánchez-Martín et al., 2003). It is noteworthy that all three proteins were localized in the nuclei, yet immunohistological staining demonstrated clear association of Slug presence with that of GLI2, but not MITF, supporting our earlier findings of positive regulation of Slug expression by GLI2, but no clear dependency of Slug on MITF in melanoma cells.

In the following paper “**Widespread Expression of Hedgehog Pathway components in a large panel of Human Tumor Cells and Inhibition of Tumor Growth by GANT61: Implications for cancer therapy**”, we subjected a grand total of 56 cell lines of various origins (53 cancer cell lines and 3 non-cancerous control cell lines) to western blot analysis (page 74) to investigate the ubiquitous presence of HH components. The intracellular levels of SHH, PTCH1, SMO, SUFU, GLI1, GLI2, GLI3, Survivin and BCL-2 were assessed.

Our large-scale screening revealed that the primary components of the HH pathway are universally expressed across all tumor cell lines. This suggests a pervasive role of the HH pathway in these cells. The GLI effector transcription factors were also abundant, and they were found in virtually all the cell lines. Their presence was observed even in cases when some of the upstream components of the cascade were missing. This is to be accounted to non-canonical HH activation and other kinds of signaling crosstalk. (Pietrobono et al, 2019). In G-401 and NCI H446 lines, GLI1 levels were notably low, but GLI2 was abundantly expressed. This indicates a potential compensatory mechanism where one GLI protein may offset the low expression of another. Other cell lines showed a reverse pattern, with low GLI2 but sufficient GLI1 (e.g., RPMI-7951, Calu-1). This variation in GLI expression across different cell lines might reflect the diverse regulatory mechanisms of the HH pathway in different tumor types. Expression profiles of BCL2 and survivin, two proteins whose genes are regulated by HH, were also analyzed. It was determined that BCL2 was present in 41 cell lines (including the control ones) out of the 56 and survivin was expressed in all cancer cell lines, but not in control cell

lines IMR-90 and WI-38 (human fibroblasts). The universal presence of survivin in all tumor cell lines, and the ability of transfected GLI2 to induce survivin expression in normal cells (IMR90), highlights the critical role of HH signaling in both tumor and normal cell survival. BCL-2's varied expression, independent of tumor type, further emphasizes the diverse regulatory mechanisms in different cancers.

It was then analyzed how the cell lines would respond to GANT61 treatment through proliferation assay. Certain cells (SK-MEL-3, U-2 OS, MeWo, SK-N-MC, H196) were completely eradicated by GANT61 treatment, indicating high sensitivity to this inhibitor. (page 75). Another group, including Saos-2, SK-N-SH, G-401, and BxPC-3, exhibited only partial sensitivity under the experimental conditions. A significant portion of the cell lines, including A549, Calu-1, A-201, Hep-G2, and three pancreatic cancer cell lines (MIA PaCa-2, PANC-1, PA-TU-8902), showed no sensitivity to GANT61. The pancreatic tumors demonstrated surprising resistance to GANT61, contradicting previous reports that highlighted their sensitivity to HH signaling blockage. This being said, PANC-1, a pancreatic cancer cell line that was formerly described as GANT61 and cyclophosphamide resistant, turned out to be affected by GANT61 in combination with rapamycin. This synchronal inhibition of HH and mTOR reduced cell viability and sphere formation. Consistent with expectations, melanomas were sensitive to GANT61. Your previous tests on melanoma cells confirmed this variable effectiveness, and the combination with obatoclox (a BCL-2 family inhibitor) showed enhanced efficacy, indicating synthetic lethality in several melanoma lines. The most sensitive cell line was SK-MEL-3, whereas two osteosarcomas, one SCLC, and the G-401 line were less responsive, showing sensitivity only at a later stage (day 9). Two neuroblastoma cell lines also responded to GANT61, but others like A-204, Hep-G2, NSCLCs, and most pancreatic cell lines, with the slight exception of BxPC-3, did not show any sensitivity. It was notable that, except for the highly sensitive SK-MEL-3 line, all other cells responded only to a higher concentration of 20 μ M GANT61, showing no response to a 10 μ M concentration. This suggests a potential dose-dependent effect of GANT61 on tumor cells.

We then shifted our focus on TUNEL apoptotic assay that verified, that GANT61, indeed, causes apoptosis in melanoma cells. Based on existing literature (Huang et al. 2014), GANT61 is known to induce apoptosis in cells. Our objective was to confirm if this mechanism was at play in the eradication of tumor cells in response to GANT61 treatment. A massive apoptotic rate was observed along with apoptotic nuclei found in cell cultures upon GANT61 introduction. We chose two GANT61-sensitive tumor cell lines, SK-MEL-3 and SK-MEL-5, for our experiments. This selection was based on their demonstrated sensitivity to GANT61 in

previous assays (as shown in Figure 2 and Figure S1). Our previous data (Vlčková et al., 2016) concurred with results obtained using a slightly different subset of melanoma cells by Faiao-Flores et al. (2017) with equal induction of apoptosis by GANT61. This data further supports the anti-apoptotic nature of HH signaling in melanoma. However, more extensive research in this domain is needed as recent research identifies MITF as a key regulator of the pro- and anti-apoptotic and balance. (Hu et al., 2021; Estrada et al., 2022). Links between MITF and anti-apoptotic proteins BCL2 and BIRC7 have been documented (McGill et al., 2002).

Next, we utilized a 12xGLI-luciferase reporter along with a reference plasmid, co-transfected into several cell lines. This system was designed to measure the activity of GLI-responsive promoters, which are indicative of the HH pathway activation. The chosen cell lines varied in their response to GANT61 in proliferation assays, ranging from sensitive to non-responsive. This cell line showed extensive inhibition of reporter activity by both cyclopamine and GANT61, aligning with its sensitivity in proliferation assays. These cells also exhibited inhibited reporter activity, but to a lesser extent. The response of these cell lines in proliferation assays was diverse: U-2 OS cells were eradicated from day 5, G-401 cells showed diminished proliferation only on day 9, and A-204 cells were resistant. Cell Lines Like PANC-1, PA-TU-8902, MIA-PaCa-2, A-549, and Hep-G2: These cell lines showed insignificant inhibition of reporter activity by GANT61 or cyclopamine. They also exhibited complete resistance in the proliferation assays. The reporter activity closely mirrored the sensitivity of the cells to GANT61, with some exceptions. For instance, A-204 cells were marginally inhibited by cyclopamine (due to very low standard deviation) and were resistant to GANT61 in proliferation assays. Your results indicate a correlation between the sensitivity of cell lines to HH inhibitors in the reporter assay and their responsiveness in proliferation assays over a longer duration. Reporter assays indicated a correlation between HH signaling inhibition and reduced cell proliferation. This suggests that HH signaling plays a role in preventing apoptosis in more than half of all tumor cell lines. In conclusion, HH signaling is crucial in preventing apoptosis in specific cancer types, highlighting its significance in cancer biology and therapy.

Our data detail the protein mass of selected constituents of HH signaling pathway in 56 cell lines. It was confirmed that GANT61 causes apoptosis in melanoma cells in accordance with former research that identified HH signaling as an influence on overall anti-apoptotic phenotype of melanoma cells.

Our next study “**Inducibly decreased MITF levels do not affect proliferation and phenotype switching but reduce differentiation of melanoma cells**” discusses the complex role of the Microphthalmia-associated transcription factor (MITF) in melanoma, particularly in relation to EMT, cell proliferation, and invasiveness. MITF is a lineage-specific transcription factor from the MiT-TFE family that regulates expression of factors involved in cell death, DNA replication, repair, mitosis, microRNA production, membrane trafficking, mitochondrial metabolism, and much more (Cheli Y. et al., 2010). MITF, as the master regulator of melanoma biogenesis, coordinates a range of cellular functions in melanocytes and melanomas, including survival, differentiation, proliferation, invasion, senescence, metabolism, and DNA damage repair (Liu et al., 2022). In the experimental part, we used doxycycline (DOX)-based inducible lentiviral system (Tet-on system) to control expression of MITF protein to elucidate what role does it play in melanoma phenotype switching. Specific aberrances in MITF production are linked to cancer, melanoma development, proliferation, survival, differentiation invasion and metastasis.

Data (Carreira et al., 2006, Hoek and Goding, 2010) suggest that there are (at least) two intrinsically distinct populations of cells in melanoma differing in intracellular MITF concentration. The so-called rheostat model of MITF activity, suggests that high-MITF cells exhibit high differentiation rate coupled with increased proliferation but low invasion. An vice versa, low MITF activity is associated with reduced proliferation, dedifferentiation, but heightened invasion. The activity of MITF depends on post-translational protein modifications, which vary within tumors and between primary and metastatic melanomas. This indicates the need for careful identification of melanomas that may be amenable to MITF targeting. Our aim was to analyze this phenomenon in six melanoma cell lines with inducibly regulated MITF levels. 501Mel, Malme 3M, MeWo, SK-MEL-3, SK-MEL-5 and SK-MEL-28 lines were selected because of their average-to-high basal level of MITF. Upscaling of DOX concentration (0-1 µg/ml) was negatively correlated with MITF expression. We observed a massive decrease in MITF production. (page 88).

As MITF is often an interlink on a figurative intersection of various cell cycle signals, we expected its depletion will impact either the proliferation rate, invasion, or migration of treated cells, but we observed no such thing. Lowering of MITF expression was reflected in a slight decrease in proliferation rate, often observable only after prolonged exposure. More intriguing data, however, was collected by expanding 15 prospering clones from SK-MEL-5 and SK-MEL-28 lineages while keeping them in DOX media. After a 4–5-week cultivation, ten of the cell lines were proliferating in an unaffected way, while of the remaining five, two clones’

proliferation was limited to about 85 % compared to the control and three clones were limited to approximately 25 %. The discrete quantification of proliferation rate that cells exhibit suggest that within a seemingly homologous cell culture there is a heterogeneity at a single cell level. We then extended the research by measuring proliferation rate and MITF levels in six native melanoma cell lines. There was no correlation found between the two measurables. DOR and SK-MEL-2 had the lowest and second lowest amount of MITF respectively, yet they stand on the opposing ends of proliferation rate ranking. SK-MEL-2 proliferated the slowest and DOR the fastest. These findings are in discord with the rheostat model which proclaims that proliferation rate and MITF expression are tightly linked (Carreira et al., 2006; Hoek and Goding, 2010). Our data indicate that MITF levels do not determine the proliferation rate.

Further we analyzed the role of MITF in invasion and migration. Again, no direct correlation between MITF levels and the measurables was found (page 92). In most cases, the difference between DOX treated cells and control ones in invasiveness and migration was barely measurable, once more disagreeing with the rheostat model.

Since varying amounts of MITF in the cell are not reflected in its proliferation rate, we decided to determine what is. We analyzed transcription activity of known targets of MITF signaling – melastatin and tyrosinase. We saw a consistent dip in amounts of both mRNAs (page 93), across all the six cell lines upon DOX exposure. Subsequently, protein mass of these and other MITF-influenced factors was measured (page 90). The experiment was divided into three subparts – proteins not directly connected to EMT-like process, proteins associated with EMT-like process and stem cell markers. Of the proteins that are not linked to the EMT-like process, we observed variation in amounts of AXL, BRN2, livin and p27. Levels of p27, AXL and BRN2 increased. p27 increased in all the cell lines, while AXL in MeWo cells and BRN2 in 501Mel, SK-MEL-3 and SK-MEL-28. The negative correlation between MITF and p27 levels was documented before (Carreira et al., 2006) as was for the case of AXL (Sensi et al., 2011). The amount of livin found in cells diminished, mimicking the decreasing trend of MITF levels in all cell lines, which is consistent with previous research (Dynek et al., 2008).

Of the EMT-like related proteins, a mild reduction of singular factor was observed in multiple cell lines. These factors were E-cadherin (in MeWo cells), Snail (Malme 3M) and Zeb1 (SK-MEL-5). Only N-cadherin was slightly upregulated (SK-MEL-28). We conclude that MITF lowering does not alter EMT-like characteristics of the cells. This finding, once again, positions us in a discord with the rheostat theory that states that low MITF cells exhibit increased invasiveness and by proxy an enhanced capability to undergo EMT.

As for the stem cell markers, only production of Sox2 was altered, as it increased in MeWo, SK-MEL-5 and SK-MEL-28. SOX2 is a transcription factor that governs maintaining pluripotency of undifferentiated embryonic stem cells and its aberrant regulation is associated with epithelial hyperplasia, squamous cell carcinoma, forms of colorectal cancer and tumorigenicity of melanoma-initiating cells. It is interesting to see an appearance of Sox2 mass with decreasing MITF levels as inverted dependency was reported *in vitro* (Cimadamore et al., 2012).

Our data do not indicate that decreasing levels of MITF are manifested by variation in proliferation rate, invasion, migration or EMT. Which puts the rheostat model to question. The limitations of the rheostat theory were reported in the past (Seberg et al., 2017; Vachtenheim and Ondrušová, 2015). Our results were reviewed by Goding and Arnheiter (2019). Prof. Colin Goding, whose research laid base for the rheostat model, approved of our results. Another proposed theory states that the actual effect MITF exercises on cellular processes is coded in a space-temporal concert with other factors, rather than in its expression rate (Wellbrock and Arozarena, 2015). These mutually excluding theories are a glaring sign that more extensive research needs to be done in this domain.

To further deepen my knowledge on MITF function in melanoma cells, I applied for and received a scholarship that allowed me to join the research group of professor Ballotti in Centre méditerranéen de médecine moléculaire in Nice, France. Professor Ballotti was kind enough to harbor me for three months while working on his project of identifying novel way of MITF influencing ubiquitination in melanoma cells. In the publication **“FBXO32 links ubiquitination to epigenetic reprogramming in melanoma cells”** we show that levels of FBXO32, a component of the SCF E3 ubiquitin ligase complex, are directly regulated by MITF. Preliminary experiments showed that silencing of MITF results in overall reduction of ubiquitination rate in nuclei of SK-MEL-28 and 501Mel (page 107). This was further accentuated in TCGA melanoma cohort analysis that showed that levels of not only FBXO32 (Terragni et al., 2011), but also of HER5 were tightly correlated to MITF expression. In the GSE12391 cohort, which is comprised of various stages of melanoma progression (including nevi, dysplastic nevi, primary and metastatic melanomas) metastatic melanomas exhibit an increased expression of MITF compared to their earlier stages (page 107).

We used three cell lines (501Mel, SK-MEL-28 and A375) and four short-term cultures derived from patients' biopsies to relate the expression rates of MITF and FBXO32. These roughly followed each other's trend except for culture derived from patient 1. Patient 1

underwent a BRAF inhibitor-based treatment and arisen culture was immediately displaying BRAF inhibitor resistance. This was also the only culture in which MITF silencing did not result in a consistent inhibition of FBXO32 expression, suggesting an absence of epistatic regulation of FBXO32 by MITF. Subsequently, examination of ChIP-Seq data from Dr. Davidson's lab (UCSC) revealed MITF binding at the FBXO32 promoter and in an intronic region, which implies that FBXO32 is a transcriptional target of MITF. This also alludes to the existence of an epistatic relationship between MITF and FBXO32 in melanoma cells, with FBXO32 being a direct transcriptional target of MITF.

To determine the contribution of FBXO32 to the overall phenotype, we observed the outcomes of FBXO32 silencing using siRNA and FBXO32 lentiviral vector-induced forced expression. Our data show that lowering of FBXO32 levels is associated with reduced migration in cells with high baseline expression (501Mel, patient 2) and inhibited proliferation (patient 1). Conversely, cells that do not maintain high FBXO32 levels respond to its forced expression by augmented rates of migration (A375, SK-MEL-28), colony formation capabilities (SK-MEL-28) and proliferation (501Mel, SK-MEL-28, A375) *in vitro* (page 110). These results were later confirmed by inserting xenografts in nude mice. Here, using two different siRNAs to knock down FBXO32 expression led to inhibited cell proliferation, and conversely, boosting of FBXO32 expression (verified by western blot) resulted in favorable growth of SK-MEL-28, A375 and MeWo xenografts. These combined data clearly indicate that FBXO32 enhances the migration of melanoma cells. The ability of FBXO32 to influence cell motility suggests that FBXO32 promotes the proliferation of melanoma cells, both *in vitro* and *in vivo*. This indicates a significant role for FBXO32 in melanoma progression, potentially contributing to tumor growth and metastasis.

Subsequent transcriptomic analysis in 501Mel, SK-MEL-28, A375 and patient 2 cultures revealed that over 300 genes responded to FBXO32 knockdown, of which the most upregulated ones are associated with an inhibition of cell proliferation and migration. The changes in gene expression could result from the inhibition of the MITF, MYC, or TGF β pathways. Additionally, the activation of three microRNAs (mir145, mir124, Let7), p53, and KDM5B (a histone lysine demethylase) was predicted, suggesting a potential link with epigenetic regulation as these molecules are known to play significant roles in epigenetic regulation. MicroRNAs modulate gene expression post-transcriptionally, while KDM5B alters chromatin structure through histone demethylation, impacting gene expression. The increased expression of histone deacetylase HDAC3 in FBXO32 depleted cells supports the argument of an epigenetic mechanism. HDACs are crucial in modifying chromatin structure and thus

regulating gene expression. The changes in the expression of epigenetic modifiers like KDM5B and HDAC3, along with microRNAs, suggest that FBXO32 might influence melanoma cell proliferation and migration through epigenetic pathways. These modifications can alter the expression of genes involved in these critical cellular processes. The alterations in microRNA expression and histone modification enzymes imply that FBXO32 knockdown could lead to a broader reprogramming of gene expression in melanoma cells. This reprogramming could be responsible for the observed changes in cell proliferation and migration. Next, increased CDK6 expression was observed in 501Mel cells with forced FBXO32 expression, while its inhibition occurred with FBXO32 knockdown. CDK6 inhibition reduced migration in both parental and FBXO32 overexpressing 501Mel and A375 cells, as well as inhibited their proliferation. Also, p53, KDM5B and HDAC3 were increased in production, further linking FBXO32 function to epigenetic machinery. We then designed an experiment based on inhibiting CDK6, which led to reduction of migration and proliferation in both parental and FBXO32-depleted 501Mel and A375 cells (page 110). Finally, we showed that SMAD7 levels are negatively correlated to FBXO32 levels. FBXO32 knockdown leads to heightened levels of SMAD7, which in turn inhibits the TGF β signaling pathway. Inhibition of SMAD7 expression restores TGF β signaling in this scenario.

All these results suggested that FBXO32 directly impacts expression of various genes, despite not being a transcription factor. To shed light onto molecular means that are employed to regulate the gene expression, we performed a tandem affinity purification of Myc/DDK tagged FBXO32 from SK-MEL-28. Subsequent mass spectrometry identified 216 proteins that bind to FBXO32. These proteins were linked to chromatin remodeling, chromosome organization, ribosome biogenesis, RNA processing and cellular stress response. Especially representatives of chromatin remodeling complex, namely SMARCA4 (also called BRG1), SMARCA5 and SMARCD1 were of our interest as they could link FBXO32 to the transcription machinery. SMARCA4 was found in FBXO32 co-immunoprecipitate pull-down in 501Mel cells and FBXO32-overexpressing SK-MEL-28 cells. Immunofluorescence assay further advocated this interaction as nuclear labeling of FBXO32 and SMARCA4 were largely mutually overlapping. Analysis of SMARCA4 ChIP-Seq data revealed a correlation between the SMARCA4 binding sites within CDK6 and HDAC3 promoters and active histone marks. This discovery inspired us to perform a ChIP-qPCR using DNA obtained from 501Mel cells using anti-SMARCA4, or anti-DDK antibodies. We found out that CDK6 and HDAC3 promoter regions are being pulled down with SMARCA4 and thus confirmed that it is the enabler of FBXO32-mediated transcriptional regulation.

In conclusion, this thesis has significantly advanced our understanding of HHs role in the maintenance of CSC subpopulations. CSCs represent a fascinating realm of future discoveries given by the inherent difficulty in detecting them. Still, once detected, CSCs, known for their elusive nature and resistance to conventional therapies, present a significant challenge in cancer treatment. The similarities between CSCs and iPSCs, particularly in their pluripotency and self-renewal capabilities, add another layer of complexity to this study. These parallels not only deepen our understanding of stem cell biology but also enhance our ability to identify and target CSCs, which, like iPSCs, are notoriously difficult to detect and isolate.

The findings of this research underscore how the HH pathway can be a critical tool in targeting these hard-to-detect CSCs. The findings presented herein not only clarify the mechanistic aspects of the HH involvement in CSC regulation but also highlight its potential as a therapeutic target in cancer treatment. The implications of these discoveries are particularly poignant in the context of developing more effective and targeted cancer therapies.

While this research has made strides in elucidating the complexities of CSC maintenance via the HH pathway, it also opens new avenues for exploration, especially in terms of overcoming resistance to current treatments and further understanding the interplay between CSCs and their microenvironments. This study, therefore, lays a crucial foundation for future research in oncology, paving the way for more nuanced and effective approaches to cancer treatment. By shedding light on the mechanisms through which the HH pathway regulates CSCs, this study not only enhances our understanding of CSC maintenance but also opens potential strategies for their detection and eradication. These revelations have substantial implications for the development of more effective cancer therapies, specifically tailored to target CSCs. While advancing our comprehension of the intricate dynamics of CSC biology, this thesis also highlights the need for continued research into the HH pathway's potential in overcoming the obstacles posed by CSCs in cancer treatment, thereby setting a promising direction for future oncological breakthroughs.

By elucidating the intricate relationship between the HH pathway and CSC maintenance, and drawing comparisons with iPSCs, this work paves the way for novel approaches in cancer therapy, especially in strategies aimed at CSC identification and eradication. This study, therefore, contributes significantly to the field of oncology, proposing new research directions for overcoming the challenges posed by CSCs in cancer treatment, and opens promising avenues for future exploration in the intersecting realms of stem cell and cancer research.

V CONCLUSIONS

GLI transcription factors are the effector element of the intricate signaling interplay assuring a proper embryonic development. As such, when aberrantly activated in adulthood, the same GLI transcription factors become detrimental by sparking cancer initiation and subsequent progression. Data gathered for this doctoral thesis provide a link between HH signaling pathway and its newly documented transcriptional target - Slug gene - and a brief insight to regulation of its transcription by other selected *trans*-acting factors.

- Our data imply that an important regulator of EMT and embryonic neural development, Slug transcription factor, which is associated with tumors' propensity to metastasis and poor prognosis for cancer patients is directly regulated by HH signaling pathway. It has been clearly proven that Slug is a transcriptional target of GLI transcription factors and notably GLI2.
- We confirmed that all the main constituents of the HH signaling pathway are being produced in virtually all of cancer cell lines that were analyzed (56 cell lines in total), leading us to a conclusion that HH signaling pathway is aberrantly activated in cancers regardless of its origin and as such contributes to the CSC phenomenon.
- We found that GANT61, a known inhibitor of GLI1 and GLI2 transcription factors, reduces intracellular levels of Slug protein in melanoma significantly.
- We also aimed to elucidate how varying levels of MITF influence actual phenotype of melanoma cells. Conclusions drawn from our data, put us in opposition to the "rheostat" model, a theory which states that proliferation rate, migration and invasiveness are all regulated by presence, or absence of MITF. What we observed was that these parameters remained invariant to decreasing MITF levels. On the other hand, we gathered data that establish a link between MITF and seemingly unrelated, yet essential process – protein ubiquitination in melanoma.

VI REFERENCES

- Al-Mamun, M., Kaiissar Mannoor, Cao, J., Qadri, F., & Song, X. (2018). SOX2 in cancer stemness: tumor malignancy and therapeutic potentials. *Journal of Molecular Cell Biology*, *12*(2), 85–98. <https://doi.org/10.1093/jmcb/mjy080>
- Alshaer, W., Hervé Hillaireau, Vergnaud-Gauduchon, J., Ismail, S. I., & Fattal, E. (2014). Functionalizing Liposomes with anti-CD44 Aptamer for Selective Targeting of Cancer Cells. *Bioconjugate Chemistry*, *26*(7), 1307–1313. <https://doi.org/10.1021/bc5004313>
- Baker, M. (2009). Cancer stem cells resemble healthy stem cells, resist chemotherapy. *Nature Reports*. <https://doi.org/10.1038/stemcells.2009.110>
- Balzeau, J., Menezes, M. R., Cao, S., & Hagan, J. P. (2017). The LIN28/let-7 Pathway in Cancer. *Frontiers in Genetics*, *8*. <https://doi.org/10.3389/fgene.2017.00031>
- Bao, B., Ahmad, A., Azmi, A. S., Ali, S., & Sarkar, F. H. (2013). Overview of Cancer Stem Cells (CSCs) and Mechanisms of Their Regulation: Implications for Cancer Therapy. *Current Protocols in Pharmacology*, *61*(1). <https://doi.org/10.1002/0471141755.ph1425s61>
- Barakat, M. T., Humke, E. W., & Scott, M. P. (2010). Learning from Jekyll to control Hyde: Hedgehog signaling in development and cancer. *Trends in Molecular Medicine*, *16*(8), 337–348. <https://doi.org/10.1016/j.molmed.2010.05.003>
- Barati, M., Akhondi, M., Narges Sabahi Mousavi, Newsha Haghparast, Ghodsi, A., Hossein Baharvand, Ebrahimi, M., & Hassani, S.-N. (2021). Pluripotent Stem Cells: Cancer Study, Therapy, and Vaccination. *Stem Cell Reviews and Reports*, *17*(6), 1975–1992. <https://doi.org/10.1007/s12015-021-10199-7>
- Bausch, D., Fritz, S., Bolm, L., Wellner, U. F., Fernández-del-Castillo, C., Warshaw, A. L., Thayer, S. P., & Liss, A. S. (2020). Hedgehog signaling promotes angiogenesis directly and indirectly in pancreatic cancer. *Angiogenesis*, *23*(3), 479–492. <https://doi.org/10.1007/s10456-020-09725-x>
- Beck, B., & Cédric Blanpain. (2013). Unravelling cancer stem cell potential. *Nature Reviews Cancer*, *13*(10), 727–738. <https://doi.org/10.1038/nrc3597>
- Begicevic, R.-R., & Falasca, M. (2017). ABC Transporters in Cancer Stem Cells: Beyond Chemoresistance. *International Journal of Molecular Sciences*, *18*(11), 2362–2362. <https://doi.org/10.3390/ijms18112362>
- Berabez, N., Durand, S., & Mathieu Gabut. (2019). Post-transcriptional regulations of cancer stem cell homeostasis. *Current Opinion in Oncology*, *31*(2), 100–107. <https://doi.org/10.1097/cco.0000000000000503>
- Bisht, S., Nigam, M., Kunjwal, S. S., Sergey Plygun, Abhay Prakash Mishra, & Javad Sharifi-Rad. (2022). Cancer Stem Cells: From an Insight into the Basics to Recent Advances and Therapeutic Targeting. *Stem Cells International*, *2022*, 1–28.

<https://doi.org/10.1155/2022/9653244>

- Bley, N., Hmedat, A., Müller, S., Rolnik, R., Rausch, A., Lederer, M., & Hüttelmaier, S. (2021). Musashi-1—A Stemness RBP for Cancer Therapy? *Biology*, *10*(5), 407–407. <https://doi.org/10.3390/biology10050407>
- Bonnet, D., & Dick, J. E. (1997). Human acute myeloid leukemia is organized as a hierarchy that originates from a primitive hematopoietic cell. *Nature Medicine*, *3*(7), 730–737. <https://doi.org/10.1038/nm0797-730>
- Brewer, B. G., Mitchell, R. A., Amir Harandi, & Eaton, J. W. (2009). Embryonic vaccines against cancer: An early history. *Experimental and Molecular Pathology*, *86*(3), 192–197. <https://doi.org/10.1016/j.yexmp.2008.12.002>
- Bryl, R., Oliwia Piwocka, Kawka, E., Mozdziak, P., Kempisty, B., & Agnieszka Knopik-Skrocka. (2022). Cancer Stem Cells—The Insight into Non-Coding RNAs. *Cells*, *11*(22), 3699–3699. <https://doi.org/10.3390/cells11223699>
- Bubna, A. K. (2015). Vorinostat-An overview. *Indian Journal of Dermatology*, *60*(4), 419–419. <https://doi.org/10.4103/0019-5154.160511>
- Bürglin, T. R. (2008). The Hedgehog protein family. *GenomeBiology.com (London. Print)*, *9*(11), 241–241. <https://doi.org/10.1186/gb-2008-9-11-241>
- Cabarcas, S. M., Mathews, L. A., & Farrar, W. L. (2011). The cancer stem cell niche—there goes the neighborhood? *International Journal of Cancer*, *129*(10), 2315–2327. <https://doi.org/10.1002/ijc.26312>
- Caras, I. W. (2020). Two cancer stem cell-targeted therapies in clinical trials as viewed from the standpoint of the cancer stem cell model. *Stem Cells Translational Medicine*, *9*(8), 821–826. <https://doi.org/10.1002/sctm.19-0424>
- Carballo, G. B., Honorato, J., Pinto, G., & Leite, C. (2018). A highlight on Sonic hedgehog pathway. *Cell Communication and Signaling*, *16*(1). <https://doi.org/10.1186/s12964-018-0220-7>
- Carpenter, R. L., & Ray, H. (2019). Safety and Tolerability of Sonic Hedgehog Pathway Inhibitors in Cancer. *Drug Safety*, *42*(2), 263–279. <https://doi.org/10.1007/s40264-018-0777-5>
- Carreira, S., Goodall, J., Denat, L., Rodríguez, M., Paolo Nuciforo, Hoek, K. S., Alessandro Testori, Larue, L., & Goding, C. R. (2006). Mitf regulation of Dial1 controls melanoma proliferation and invasiveness. *Genes & Development*, *20*(24), 3426–3439. <https://doi.org/10.1101/gad.406406>
- Carvalho, L. S., Nélio Gonçalves, Fonseca, N. A., & João Nuno Moreira. (2021). Cancer Stem Cells and Nucleolin as Drivers of Carcinogenesis. *Pharmaceuticals*, *14*(1), 60–60. <https://doi.org/10.3390/ph14010060>
- Castelli, V., Giordano, A., Benedetti, E., Giansanti, F., Quintiliani, M., Cimini, A., & d’Angelo, M. (2021). The Great Escape: The Power of Cancer Stem Cells to Evade Programmed

- Cell Death. *Cancers*, 13(2), 328–328. <https://doi.org/10.3390/cancers13020328>
- Chagastelles, P. C., & Nardi, N. B. (2011). Biology of stem cells: an overview. *Kidney International Supplements*, 1(3), 63–67. <https://doi.org/10.1038/kisup.2011.15>
- Chatterjee, D., Parmeswaran Diagaradjane, & Krishnan, S. (2011). Nanoparticle-mediated hyperthermia in cancer therapy. *Therapeutic Delivery*, 2(8), 1001–1014. <https://doi.org/10.4155/tde.11.72>
- Cheli, Y., Mickaël Ohanna, Ballotti, R., & Bertolotto, C. (2010). Fifteen-year quest for microphthalmia-associated transcription factor target genes. *Pigment Cell & Melanoma Research*, 23(1), 27–40. <https://doi.org/10.1111/j.1755-148x.2009.00653.x>
- Chen, C., Zhao, S., Karnad, A. B., & Freeman, J. W. (2018). The biology and role of CD44 in cancer progression: therapeutic implications. *Journal of Hematology & Oncology*, 11(1). <https://doi.org/10.1186/s13045-018-0605-5>
- Chen, Z., Huang, J., Feng, Y., Li, Z., & Jiang, Y. (2021). Profiling of specific long non-coding RNA signatures identifies ST8SIA6-AS1 AS a novel target for breast cancer. *The Journal of Gene Medicine*, 23(2). <https://doi.org/10.1002/jgm.3286>
- Cheng, E. M., Tsarovsky, N., Sondel, P. M., & Rakhmilevich, A. L. (2022). Interleukin-12 as an in situ cancer vaccine component: a review. *Cancer Immunology, Immunotherapy*, 71(9), 2057–2065. <https://doi.org/10.1007/s00262-022-03144-1>
- Cimadamore, F., Shah, M., Amador-Arjona, A., Enma Navarro-Peran, Chen, C., Huang, C.-T., & Terskikh, A. V. (2012). SOX2 modulates levels of MITF in normal human melanocytes, and melanoma lines in vitro. *Pigment Cell & Melanoma Research*, 25(4), 533–536. <https://doi.org/10.1111/j.1755-148x.2012.01012.x>
- Clark, D. W., & Komaraiah Palle. (2016). Aldehyde dehydrogenases in cancer stem cells: potential as therapeutic targets. *Annals of Translational Medicine*, 4(24), 518–518. <https://doi.org/10.21037/atm.2016.11.82>
- Clarke, M. F., Dick, J. E., Dirks, P. B., Eaves, C. J., Jamieson, C., D. Leanne Jones, Visvader, J. E., Weissman, I. L., & Wahl, G. M. (2006). Cancer Stem Cells—Perspectives on Current Status and Future Directions: AACR Workshop on Cancer Stem Cells. *Cancer Research*, 66(19), 9339–9344. <https://doi.org/10.1158/0008-5472.can-06-3126>
- Cochrane, C. R., Szczepny, A., Watkins, N., & Cain, J. E. (2015). Hedgehog Signaling in the Maintenance of Cancer Stem Cells. *Cancers*, 7(3), 1554–1585. <https://doi.org/10.3390/cancers7030851>
- Dayanc, B. E., Beachy, S. H., Ostberg, J. R., & Repasky, E. A. (2008). Dissecting the role of hyperthermia in natural killer cell mediated anti-tumor responses. *International Journal of Hyperthermia*, 24(1), 41–56. <https://doi.org/10.1080/02656730701858297>
- Didiášová, M., Schaefer, L., & Małgorzata Wygrecka. (2018). Targeting GLI Transcription Factors in Cancer. *Molecules*, 23(5), 1003–1003. <https://doi.org/10.3390/molecules23051003>

- Dietrich, A. M., E. Tánzos, Wolfgang Vanscheidt, Schöpf, E., & Simon, J. C. (1997). High CD44 surface expression on primary tumours of malignant melanoma correlates with increased metastatic risk and reduced survival. *European Journal of Cancer*, *33*(6), 926–930. [https://doi.org/10.1016/s0959-8049\(96\)00512-6](https://doi.org/10.1016/s0959-8049(96)00512-6)
- Ding, X., Wu, J., & Jiang, C. (2010). ABCG2: A potential marker of stem cells and novel target in stem cell and cancer therapy. *Life Sciences*, *86*(17-18), 631–637. <https://doi.org/10.1016/j.lfs.2010.02.012>
- Divisato, G., Piscitelli, S., Elia, M., Cascone, E., & Parisi, S. (2021). MicroRNAs and Stem-like Properties: The Complex Regulation Underlying Stemness Maintenance and Cancer Development. *Biomolecules*, *11*(8), 1074–1074. <https://doi.org/10.3390/biom11081074>
- Dragu, D. (2015). Therapies targeting cancer stem cells: Current trends and future challenges. *World Journal of Stem Cells*, *7*(9), 1185–1185. <https://doi.org/10.4252/wjsc.v7.i9.1185>
- Dragu, D. L. (2015). Therapies targeting cancer stem cells: Current trends and future challenges. *World Journal of Stem Cells*, *7*(9), 1185–1185. <https://doi.org/10.4252/wjsc.v7.i9.1185>
- Dusek, C. O., & M. Kyle Hadden. (2020). Targeting the GLI family of transcription factors for the development of anti-cancer drugs. *Expert Opinion on Drug Discovery*, *16*(3), 289–302. <https://doi.org/10.1080/17460441.2021.1832078>
- Dynek, J. N., Li, S., Liu, J., Jiping Zha, Fairbrother, W. J., & Vucic, D. (2008). Microphthalmia-Associated Transcription Factor Is a Critical Transcriptional Regulator of Melanoma Inhibitor of Apoptosis in Melanomas. *Cancer Research*, *68*(9), 3124–3132. <https://doi.org/10.1158/0008-5472.can-07-6622>
- Ebrahimie, E., Rahimirad, S., Mohammadreza Tahsili, & Manijeh Mohammadi-Dehcheshmeh. (2021). Alternative RNA splicing in stem cells and cancer stem cells: Importance of transcript-based expression analysis. *World Journal of Stem Cells*, *13*(10), 1394–1416. <https://doi.org/10.4252/wjsc.v13.i10.1394>
- Edwards, P. C., Ruggiero, S. L., Fantasia, J. E., Burakoff, R. P., Moorji, S. M., E. Paric, Razzano, P., Grande, D., & Mason, J. (2004). Sonic hedgehog gene-enhanced tissue engineering for bone regeneration. *Gene Therapy*, *12*(1), 75–86. <https://doi.org/10.1038/sj.gt.3302386>
- Ertaş, Y. N., Keyvan Abedi-Dorcheh, Akbari, A., & Jabbari, E. (2021). Nanoparticles for Targeted Drug Delivery to Cancer Stem Cells: A Review of Recent Advances. *Nanomaterials*, *11*(7), 1755–1755. <https://doi.org/10.3390/nano11071755>
- Estrada, C., Mirabal-Ortega, L., Méry, L., Florent Dingli, Besse, L., Cédric Messaoudi, Loew, D., Celio Pouponnot, Bertolotto, C., Alain Eychène, & Druillenec, S. (2022). MITF activity is regulated by a direct interaction with RAF proteins in melanoma cells. *Communications Biology*, *5*(1). <https://doi.org/10.1038/s42003-022-03049-w>
- Eun, K., Seok Won Ham, & Kim, H. (2017). Cancer stem cell heterogeneity: origin and new

- perspectives on CSC targeting. *Journal of Biochemistry and Molecular Biology*, 50(3), 117–125. <https://doi.org/10.5483/bmbrep.2017.50.3.222>
- Evans, S. S., Repasky, E. A., & Fisher, D. (2015). Fever and the thermal regulation of immunity: the immune system feels the heat. *Nature Reviews Immunology*, 15(6), 335–349. <https://doi.org/10.1038/nri3843>
- Faião-Flores, F., Débora Kristina Alves-Fernandes, Paula Comune Pennacchi, Sandri, S., Vicente, A. A., Cristovam Scapulatempo-Neto, de, V., Reis, R. L., Chauhan, J., Goding, C. R., Keiran S.M. Smalley, & Silvyia Stuchi Maria-Engler. (2017). Targeting the hedgehog transcription factors GLI1 and GLI2 restores sensitivity to vemurafenib-resistant human melanoma cells. *Oncogene*, 36(13), 1849–1861. <https://doi.org/10.1038/onc.2016.348>
- Fendrich, V., Waldmann, J., Farzad Esni, Ramaswamy, A., Mullendore, M., Buchholz, M., Maitra, A., & Feldmann, G. (2007). Snail and Sonic Hedgehog activation in neuroendocrine tumors of the ileum. *Endocrine-Related Cancer*, 14(3), 865–874. <https://doi.org/10.1677/erc-07-0108>
- Foroozandeh, P., & Azlan Abdul Aziz. (2018). Insight into Cellular Uptake and Intracellular Trafficking of Nanoparticles. *Nanoscale Research Letters*, 13(1). <https://doi.org/10.1186/s11671-018-2728-6>
- French, R., & Siim Pauklin. (2020). Epigenetic regulation of cancer stem cell formation and maintenance. *International Journal of Cancer*, 148(12), 2884–2897. <https://doi.org/10.1002/ijc.33398>
- Gąbka-Buszek, A., Kwiatkowska-Borowczyk, E., Jankowski, J., Anna Karolina Kozłowska, & Mackiewicz, A. (2020). Novel Genetic Melanoma Vaccines Based on Induced Pluripotent Stem Cells or Melanosphere-Derived Stem-Like Cells Display High Efficacy in a murine Tumor Rejection Model. *Vaccines*, 8(2), 147–147. <https://doi.org/10.3390/vaccines8020147>
- Ganesan, R., Mallets, E. R., & Julián Gómez-Cambronero. (2015). The transcription factors Slug (SNAI2) and Snail (SNAI1) regulate phospholipase D (PLD) promoter in opposite ways towards cancer cell invasion. *Molecular Oncology*, 10(5), 663–676. <https://doi.org/10.1016/j.molonc.2015.12.006>
- Ghorbani, Z., Heidari, M., Mojtaba Jafarinaia, Rohani, M., & Akbari, A. (2023). Transcriptional Regulation of the Colorectal Cancer Stem Cell Markers, Nanog and Oct4, Induced by a Thermodynamic-Based Therapy Approach. *Iranian Journal of Public Health*. <https://doi.org/10.18502/ijph.v52i4.12458>
- Giammona, A., Crivaro, E., & Stecca, B. (2023). Emerging Roles of Hedgehog Signaling in Cancer Immunity. *International Journal of Molecular Sciences*, 24(2), 1321–1321. <https://doi.org/10.3390/ijms24021321>
- Gires, O., Klein, C. A., & Baeuerle, P. A. (2009). On the abundance of EpCAM on cancer stem cells. *Nature Reviews Cancer*, 9(2), 143–143. <https://doi.org/10.1038/nrc2499-c1>

- Glumac, P. M., & LeBeau, A. M. (2018). The role of CD133 in cancer: a concise review. *Clinical and Translational Medicine*, 7(1). <https://doi.org/10.1186/s40169-018-0198-1>
- Goding, C. R., & Heinz Arnheiter. (2019). MITF—the first 25 years. *Genes & Development*, 33(15-16), 983–1007. <https://doi.org/10.1101/gad.324657.119>
- Gong, S., Li, Q., Jeter, C., Fan, Q., Tang, D. G., & Liu, B. (2015). Regulation of NANOG in cancer cells. *Molecular Carcinogenesis*, 54(9), 679–687. <https://doi.org/10.1002/mc.22340>
- Greaves, M., & Maley, C. C. (2012). Clonal evolution in cancer. *Nature*, 481(7381), 306–313. <https://doi.org/10.1038/nature10762>
- Guo, X., & Wang, X.-F. (2008). Signaling cross-talk between TGF- β /BMP and other pathways. *Cell Research*, 19(1), 71–88. <https://doi.org/10.1038/cr.2008.302>
- Hashemi, F., Mahdieh Razmi, Fatemeh Tajik, & Zahra Madjd. (2022, December 27). *Efficacy of Whole Cancer Stem Cell-Based Vaccines: A Systematic Review of Preclinical and Clinical Studies*. ResearchGate; Oxford University Press. https://www.researchgate.net/publication/366620120_Efficacy_of_Whole_Cancer_Stem_Cell-Based_Vaccines_A_Systematic_Review_of_Preclinical_and_Clinical_Studies
- He, J., Shi, J., Zhang, K., Xue, J., Li, J., Yang, J., Chen, J., Wei, J., Ren, H., & Liu, X. (2017). Sox2 inhibits Wnt- β -catenin signaling and metastatic potency of cisplatin-resistant lung adenocarcinoma cells. *Molecular Medicine Reports*, 15(4), 1693–1701. <https://doi.org/10.3892/mmr.2017.6170>
- Heussler, H. (2003). Sonic hedgehog. *Journal of Clinical Pathology-Molecular Pathology*, 56(>3), 129–131. <https://doi.org/10.1136/mp.56.3.129>
- Hicks, M. R., & Pyle, A. D. (2023). The emergence of the stem cell niche. *Trends in Cell Biology*, 33(2), 112–123. <https://doi.org/10.1016/j.tcb.2022.07.003>
- Hoek, K. S., & Goding, C. R. (2010). Cancer stem cells versus phenotype-switching in melanoma. *Pigment Cell & Melanoma Research*, 23(6), 746–759. <https://doi.org/10.1111/j.1755-148x.2010.00757.x>
- Hong, S. (2017). RNA Binding Protein as an Emerging Therapeutic Target for Cancer Prevention and Treatment. *Journal of Cancer Prevention*, 22(4), 203–210. <https://doi.org/10.15430/jcp.2017.22.4.203>
- Horák, P., Kateřina Kreisingerová, Jiří Réda, Lubica Ondrušová, Balko, J., Jiri Vachtenheim, Žáková, P., & J Vachtenheim. (2023). The Hedgehog/GLI signaling pathway activates transcription of Slug (Snail2) in melanoma cells. *Oncology Reports*, 49(4). <https://doi.org/10.3892/or.2023.8512>
- Hu, S., Bai, S., Dai, Y., Yang, N., Li, J., Zhang, X., Wang, F., Zhao, B., Bao, G., Chen, Y., & Wu, X. (2021). Deubiquitination of MITF-M Regulates Melanocytes Proliferation and Apoptosis. *Frontiers in Molecular Biosciences*, 8. <https://doi.org/10.3389/fmolb.2021.692724>

- Huang, L., Walter, V., Hayes, D. N., & Onaitis, M. W. (2014). Hedgehog–GLI Signaling Inhibition Suppresses Tumor Growth in Squamous Lung Cancer. *Clinical Cancer Research*, 20(6), 1566–1575. <https://doi.org/10.1158/1078-0432.ccr-13-2195>
- Huang, W., Hu, H., Zhang, Q., Wang, N., Yang, X., & Guo, A. (2020). Genome-Wide DNA Methylation Enhances Stemness in the Mechanical Selection of Tumor-Repopulating Cells. *Frontiers in Bioengineering and Biotechnology*, 8. <https://doi.org/10.3389/fbioe.2020.00088>
- Hyman, J. M., Firestone, A. J., Heine, V. M., Zhao, Y., Ocasio, C. A., Han, K., Sun, M., Rack, P. D., Sinha, S., Wu, J., Solow-Cordero, D. E., Jen, J., Rowitch, D. H., & Chen, J. (2009). Small-molecule inhibitors reveal multiple strategies for Hedgehog pathway blockade. *Proceedings of the National Academy of Sciences of the United States of America*, 106(33), 14132–14137. <https://doi.org/10.1073/pnas.0907134106>
- Ignatova, T. N., Kukekov, V. G., Laywell, E. D., Oleg Suslov, Vrionis, F. D., & Steindler, D. A. (2002). Human cortical glial tumors contain neural stem-like cells expressing astroglial and neuronal markers in vitro. *Glia*, 39(3), 193–206. <https://doi.org/10.1002/glia.10094>
- Ingham, P. W. (2022). Hedgehog signaling. *Current Topics in Developmental Biology*, 1–58. <https://doi.org/10.1016/bs.ctdb.2022.04.003>
- Islam, S. S., Mokhtari, R. B., Noman, A. S., Uddin, M., Rahman, M. Z., Azadi, M. A., A. Zlotta, van, H. Yeger, & Farhat, W. A. (2015). Sonic hedgehog (Shh) signaling promotes tumorigenicity and stemness via activation of epithelial-to-mesenchymal transition (EMT) in bladder cancer. *Molecular Carcinogenesis*, 55(5), 537–551. <https://doi.org/10.1002/mc.22300>
- Izadpanah, A., Niloufar Mohammadkhani, Masoudnia, M., Mahsa Ghasemzad, Arefeh Saeedian, Mehdizadeh, H., Mansour Poorebrahim, & Ebrahimi, M. (2023). Update on immune-based therapy strategies targeting cancer stem cells. *Cancer Medicine*, 12(18), 18960–18980. <https://doi.org/10.1002/cam4.6520>
- Jaiswal, S., Jamieson, C., Pang, W. W., Park, C. Y., Chao, M. P., Ravindra Majeti, Traver, D., Nico van Rooijen, & Weissman, I. L. (2009). CD47 Is Upregulated on Circulating Hematopoietic Stem Cells and Leukemia Cells to Avoid Phagocytosis. *Cell*, 138(2), 271–285. <https://doi.org/10.1016/j.cell.2009.05.046>
- Jalili, A., Mertz, K. D., Romanov, J., Wagner, C., Kalthoff, F., Stuetz, A., Gaurav Pathria, Gschaidner, M., Stingl, G., & Wagner, S. N. (2013). NVP-LDE225, a Potent and Selective SMOOTHENED Antagonist Reduces Melanoma Growth In Vitro and In Vivo. *PLOS ONE*, 8(7), e69064–e69064. <https://doi.org/10.1371/journal.pone.0069064>
- Jia, Y., Wang, Y., & Xie, J. (2015). The Hedgehog pathway: role in cell differentiation, polarity and proliferation. *Archives of Toxicology*, 89(2), 179–191. <https://doi.org/10.1007/s00204-014-1433-1>
- Jiang, Q., Crews, L. A., Holm, F., & Jamieson, M. (2017). RNA editing-dependent epitranscriptome diversity in cancer stem cells. *Nature Reviews Cancer*, 17(6), 381–

392. <https://doi.org/10.1038/nrc.2017.23>
- Jin, X., Jin, X., Ji Eun Jung, Beck, S. J., & Kim, H. (2013). Cell surface Nestin is a biomarker for glioma stem cells. *Biochemical and Biophysical Research Communications*, 433(4), 496–501. <https://doi.org/10.1016/j.bbrc.2013.03.021>
- Jordan, C. T., Guzman, M. L., & Noble, M. (2006). Cancer Stem Cells. *The New England Journal of Medicine*, 355(12), 1253–1261. <https://doi.org/10.1056/nejmra061808>
- Kang, D., Lee, Y., & Lee, J. (2020). RNA-Binding Proteins in Cancer: Functional and Therapeutic Perspectives. *Cancers*, 12(9), 2699–2699. <https://doi.org/10.3390/cancers12092699>
- Katoh, M. (2019). Genomic testing, tumor microenvironment and targeted therapy of Hedgehog-related human cancers. *Clinical Science*, 133(8), 953–970. <https://doi.org/10.1042/cs20180845>
- Kaur, S., Cicalese, K. V., Rajdeep Bannerjee, & Roberts, D. A. (2020). Preclinical and clinical development of therapeutic antibodies targeting functions of CD47 in the tumor microenvironment. *Antibody Therapeutics*, 3(3), 179–192. <https://doi.org/10.1093/abt/tbaa017>
- Kenney, A. M., & Rowitch, D. H. (2000). Sonic hedgehog Promotes G₁ Cyclin Expression and Sustained Cell Cycle Progression in Mammalian Neuronal Precursors. *Molecular and Cellular Biology*, 20(23), 9055–9067. <https://doi.org/10.1128/mcb.20.23.9055-9067.2000>
- Khales, S. A., Mozaffari-Jovin, S., Geerts, D., & Mohammad Reza Abbaszadegan. (2022). TWIST1 activates cancer stem cell marker genes to promote epithelial-mesenchymal transition and tumorigenesis in esophageal squamous cell carcinoma. *BMC Cancer*, 22(1). <https://doi.org/10.1186/s12885-022-10252-9>
- Kinzler, K. W., & Vogelstein, B. (1990). The GLI gene encodes a nuclear protein which binds specific sequences in the human genome. *Molecular and Cellular Biology*, 10(2), 634–642. <https://doi.org/10.1128/mcb.10.2.634>
- Klein, S. P., Nguyen, D. C., Bhakta, V., Wong, D. A., Chang, V. Y., Davidson, T. B., & Martinez-Agosto, J. A. (2019). Mutations in the sonic hedgehog pathway cause macrocephaly-associated conditions due to crosstalk to the PI3K/AKT/mTOR pathway. *American Journal of Medical Genetics - Part A*, 179(12), 2517–2531. <https://doi.org/10.1002/ajmg.a.61368>
- Kreso, A., & Dick, J. E. (2014). Evolution of the Cancer Stem Cell Model. *Cell Stem Cell*, 14(3), 275–291. <https://doi.org/10.1016/j.stem.2014.02.006>
- Kumar, V., Mohit Vashishta, Kong, L., Wu, X., Lu, J. J., Guha, C., & Dwarakanath, B. S. (2021). The Role of Notch, Hedgehog, and Wnt Signaling Pathways in the Resistance of Tumors to Anticancer Therapies. *Frontiers in Cell and Developmental Biology*, 9. <https://doi.org/10.3389/fcell.2021.650772>
- Kumasaka, M. Y., Sato, S., Yajima, I., Goding, C. R., & Yamamoto, H. (2005). Regulation of

- melanoblast and retinal pigment epithelium development by *Xenopus laevis* Mitf. *Developmental Dynamics*, 234(3), 523–534. <https://doi.org/10.1002/dvdy.20505>
- Lambertini, E., Lisignoli, G., Torreggiani, E., Manferdini, C., Gabusi, E., Franceschetti, T., Letizia Penolazzi, Gambari, R., Facchini, A., & Piva, R. (2009). Slug gene expression supports human osteoblast maturation. *Cellular and Molecular Life Sciences*, 66(22), 3641–3653. <https://doi.org/10.1007/s00018-009-0149-5>
- Larsen, L. J., & Lisbeth Birk Møller. (2020). Crosstalk of Hedgehog and mTORC1 Pathways. *Cells*, 9(10), 2316–2316. <https://doi.org/10.3390/cells9102316>
- Leone, K., Poggiana, C., & Zamarchi, R. (2018). The Interplay between Circulating Tumor Cells and the Immune System: From Immune Escape to Cancer Immunotherapy. *Diagnostics*, 8(3), 59–59. <https://doi.org/10.3390/diagnostics8030059>
- Li, W. J., Wang, Y., Liu, R., Kasinski, A. L., Shen, H., Slack, F. J., & Tang, D. G. (2021). MicroRNA-34a: Potent Tumor Suppressor, Cancer Stem Cell Inhibitor, and Potential Anticancer Therapeutic. *Frontiers in Cell and Developmental Biology*, 9. <https://doi.org/10.3389/fcell.2021.640587>
- Li, Y., Wu, Y., Abbatiello, T. C., Wu, W., Ju Ri Kim, Sarkissyan, M., Suren Sarkissyan, Chung, S., Yahya Elshimali, & Vadgama, J. V. (2015). Slug contributes to cancer progression by direct regulation of ER α signaling pathway. *International Journal of Oncology*, 46(4), 1461–1472. <https://doi.org/10.3892/ijo.2015.2878>
- Lian, S., Xie, R., Ye, Y., Xie, X., Li, S., Lu, Y., Li, B., Cheng, Y., Katanaev, V. L., & Jia, L. (2019). Simultaneous blocking of CD47 and PD-L1 increases innate and adaptive cancer immune responses and cytokine release. *EBioMedicine*, 42, 281–295. <https://doi.org/10.1016/j.ebiom.2019.03.018>
- Lian, S., Xie, X., Lu, Y., & Jia, L. (2019). Checkpoint CD47 Function On Tumor Metastasis And Immune Therapy. *OncoTargets and Therapy*, Volume 12, 9105–9114. <https://doi.org/10.2147/ott.s220196>
- Liao, C., Wang, Q., An, J., Chen, J., Li, X., Qian, L., Xiao, L., Guan, X., & Liu, J. (2022). CD44 Glycosylation as a Therapeutic Target in Oncology. *Frontiers in Oncology*, 12. <https://doi.org/10.3389/fonc.2022.883831>
- Liu, F., Feng, X., Shang Ling Zhu, Huang, H., Ying Di Chen, Pan, Y., June, R. R., Song Guo Zheng, & Huang, J. (2018). Sonic Hedgehog Signaling Pathway Mediates Proliferation and Migration of Fibroblast-Like Synoviocytes in Rheumatoid Arthritis via MAPK/ERK Signaling Pathway. *Frontiers in Immunology*, 9. <https://doi.org/10.3389/fimmu.2018.02847>
- Liu, J., Fu, M., Wang, M., Wan, D., Wei, Y., & Wei, X. (2022). Cancer vaccines as promising immuno-therapeutics: platforms and current progress. *Journal of Hematology & Oncology*, 15(1). <https://doi.org/10.1186/s13045-022-01247-x>
- Lu, Y., Futtner, C. R., Rock, J. R., Xu, X., Whitworth, W. R., Brigid L.M. Hogan, & Onaitis, M. W. (2010). Evidence That SOX2 Overexpression Is Oncogenic in the Lung. *PLOS*

- ONE*, 5(6), e11022–e11022. <https://doi.org/10.1371/journal.pone.0011022>
- Lu, Y., Zhu, Y., Deng, S., Chen, Y., Li, W., Sun, J., & Xu, X. (2021). Targeting the Sonic Hedgehog Pathway to Suppress the Expression of the Cancer Stem Cell (CSC)—Related Transcription Factors and CSC-Driven Thyroid Tumor Growth. *Cancers*, 13(3), 418–418. <https://doi.org/10.3390/cancers13030418>
- Luo, X., Shen, Y., Huang, W., Bao, Y., Mo, J., Yao, L., & Yuan, L. (2023). Blocking CD47-SIRP α Signal Axis as Promising Immunotherapy in Ovarian Cancer. *Cancer Control*, 30, 107327482311597-107327482311597. <https://doi.org/10.1177/10732748231159706>
- Lynch, M. D., Massimiliano Cariati, & Purushotham, A. D. (2006). Breast cancer, stem cells and prospects for therapy. *Breast Cancer Research*, 8(3). <https://doi.org/10.1186/bcr1513>
- Ma, Y., Shen, N., Wicha, M. S., & Luo, M. (2021). The Roles of the Let-7 Family of MicroRNAs in the Regulation of Cancer Stemness. *Cells*, 10(9), 2415–2415. <https://doi.org/10.3390/cells10092415>
- Macas, J., Ku, M.-C., Nern, C., Xu, Y., H. Bühler, Remke, M., Synowitz, M., Franz, K., Seifert, V., Plate, K. H., Helmut Kettenmann, Rainer Glaß, & Momma, S. (2014). Generation of Neuronal Progenitor Cells in Response to Tumors in the Human Brain. *Stem Cells*, 32(1), 244–257. <https://doi.org/10.1002/stem.1581>
- Malekshah, O. M., Chen, X., Alireza Nomani, Sarkar, S., & Hatefi, A. (2016). Enzyme/Prodrug Systems for Cancer Gene Therapy. *Current Pharmacology Reports*, 2(6), 299–308. <https://doi.org/10.1007/s40495-016-0073-y>
- Martens, M. H., Doenja M J Lambregts, Kluza, E., & Regina. (2014). Tumor Response to Treatment: Prediction and Assessment. *Current Radiology Reports*, 2(9). <https://doi.org/10.1007/s40134-014-0062-z>
- Martinez-Cruzado, L., Tornín, J., Santos, L., Rodríguez, A., García-Castro, J., Morís, F., & René Rodríguez. (2016). Aldh1 Expression and Activity Increase During Tumor Evolution in Sarcoma Cancer Stem Cell Populations. *Scientific Reports*, 6(1). <https://doi.org/10.1038/srep27878>
- May, C. D., Sphyris, N., Evans, K. W., Werden, S. J., Guo, W., & Mani, S. A. (2011). Epithelial-mesenchymal transition and cancer stem cells: a dangerously dynamic duo in breast cancer progression. *Breast Cancer Research*, 13(1). <https://doi.org/10.1186/bcr2789>
- McGill, G., Horstmann, M., Widlund, H. R., Du, J., Motyckova, G., Nishimura, E. K., Lin, Y.-L., Ramaswamy, S., Avery, W., Ding, H., Jordan, S. A., Jackson, I. J., Korsmeyer, S. J., Golub, T. R., & Fisher, D. E. (2002). Bcl2 Regulation by the Melanocyte Master Regulator Mitf Modulates Lineage Survival and Melanoma Cell Viability. *Cell*, 109(6), 707–718. [https://doi.org/10.1016/s0092-8674\(02\)00762-6](https://doi.org/10.1016/s0092-8674(02)00762-6)
- Metz, J., Geritz, S., Meszéna, G., Jacobs, F., & Van Heerwaarden, J. (1995). *Adaptive*

Dynamics: A Geometrical Study of the Consequences of Nearly Faithful Reproduction.
https://warwick.ac.uk/fac/sci/sbdtc/msc/ch927/notes/metz_et_al_adaptive_dynamics.pdf

- Miller, A. J., Du, J., Rowan, S., Hershey, C. L., Widlund, H. R., & Fisher, D. E. (2004). Transcriptional Regulation of the Melanoma Prognostic Marker Melastatin (TRPM1) by MITF in Melanocytes and Melanoma. *Cancer Research*, *64*(2), 509–516. <https://doi.org/10.1158/0008-5472.can-03-2440>
- Monk, M., & Holding, C. (2001). Human embryonic genes re-expressed in cancer cells. *Oncogene*, *20*(56), 8085–8091. <https://doi.org/10.1038/sj.onc.1205088>
- Monroe, M. M., Anderson, E., Clayburgh, D., & Wong, M. H. (2011). Cancer Stem Cells in Head and Neck Squamous Cell Carcinoma. *Journal of Oncology*, *2011*, 1–8. <https://doi.org/10.1155/2011/762780>
- Naber, H., Drabsch, Y., B. Ewa Snaar-Jagalska, Peter ten Dijke, & Theo van Laar. (2013). Snail and Slug, key regulators of TGF- β -induced EMT, are sufficient for the induction of single-cell invasion. *Biochemical and Biophysical Research Communications*, *435*(1), 58–63. <https://doi.org/10.1016/j.bbrc.2013.04.037>
- Neradil, J., & Veselská, R. (2015). Nestin as a marker of cancer stem cells. *Cancer Science*, *106*(7), 803–811. <https://doi.org/10.1111/cas.12691>
- Neumann, C. J. (2005). Hedgehogs as Negative Regulators of the Cell Cycle. *Cell Cycle*, *4*(9), 1139–1140. <https://doi.org/10.4161/cc.4.9.1999>
- Newman, R., McHugh, J., & Turner, M. (2015). RNA binding proteins as regulators of immune cell biology. *Clinical and Experimental Immunology*, *183*(1), 37–49. <https://doi.org/10.1111/cei.12684>
- Nie, Y., Fu, G., & Leng, Y. (2023). Nuclear Delivery of Nanoparticle-Based Drug Delivery Systems by Nuclear Localization Signals. *Cells*, *12*(12), 1637–1637. <https://doi.org/10.3390/cells12121637>
- Ning, N., Pan, Q., Zheng, F., Seagal Teitz-Tennenbaum, Egenti, M., Yet, J., Li, M., Christophe Ginestier, Wicha, M. S., Moyer, J. S., Mark E.P. Prince, Xu, Y., Xiao Lian Zhang, Huang, S., Chang, A. E., & Li, Q. (2012). Cancer Stem Cell Vaccination Confers Significant Antitumor Immunity. *Cancer Research*, *72*(7), 1853–1864. <https://doi.org/10.1158/0008-5472.can-11-1400>
- Nouri, F. S., Wang, X., & Hatefi, A. (2015). Genetically engineered theranostic mesenchymal stem cells for the evaluation of the anticancer efficacy of enzyme/prodrug systems. *Journal of Controlled Release*, *200*, 179–187. <https://doi.org/10.1016/j.jconrel.2015.01.003>
- O'Reilly, K. E., Eleazar, Segura, M. F., Friedman, E. B., Poliseno, L., Sung Won Han, Zhong, J., Zavadil, J., Pavlick, A. C., Hernando, E., & Osman, I. (2013). Hedgehog Pathway Blockade Inhibits Melanoma Cell Growth in Vitro and in Vivo. *Pharmaceuticals*, *6*(11), 1429–1450. <https://doi.org/10.3390/ph6111429>

- Oskarsson, T., Batlle, E., & Massagué, J. (2014). Metastatic Stem Cells: Sources, Niches, and Vital Pathways. *Cell Stem Cell*, *14*(3), 306–321. <https://doi.org/10.1016/j.stem.2014.02.002>
- Ouyang, X., Telli, M. L., & Wu, J. C. (2019). Induced Pluripotent Stem Cell-Based Cancer Vaccines. *Frontiers in Immunology*, *10*. <https://doi.org/10.3389/fimmu.2019.01510>
- Phi, L. T., Ita Novita Sari, Yang, Y., Lee, S., Jun, N., Kwang Seock Kim, Yun Kyung Lee, & Hyog Young Kwon. (2018). Cancer Stem Cells (CSCs) in Drug Resistance and their Therapeutic Implications in Cancer Treatment. *Stem Cells International*, *2018*, 1–16. <https://doi.org/10.1155/2018/5416923>
- Piccioni, A., Gaetani, E., Palladino, M., Gatto, I., Smith, R. C., Neri, V., Marcantoni, M., Igor Giarretta, Silver, M., Straino, S., Capogrossi, M. C., Landolfi, R., & Pola, R. (2014). Sonic hedgehog gene therapy increases the ability of the dystrophic skeletal muscle to regenerate after injury. *Gene Therapy*, *21*(4), 413–421. <https://doi.org/10.1038/gt.2014.13>
- Pietrobono, S., Gagliardi, S., & Stecca, B. (2019). Non-canonical Hedgehog Signaling Pathway in Cancer: Activation of GLI Transcription Factors Beyond Smoothed. *Frontiers in Genetics*, *10*. <https://doi.org/10.3389/fgene.2019.00556>
- Piva, R., Manferdini, C., Elisabetta Lambertini, & Lisignoli, G. (2010, December). *Slug contributes to the regulation of CXCL12 expression in human osteoblasts*. https://www.researchgate.net/publication/49706569_Slug_contributes_to_the_regulation_of_CXCL12_expression_in_human_osteoblasts
- Plaks, V., Kong, N., & Werb, Z. (2015). The Cancer Stem Cell Niche: How Essential Is the Niche in Regulating Stemness of Tumor Cells? *Cell Stem Cell*, *16*(3), 225–238. <https://doi.org/10.1016/j.stem.2015.02.015>
- Poręba, M. (2020). Protease-activated prodrugs: strategies, challenges, and future directions. *The FEBS Journal*, *287*(10), 1936–1969. <https://doi.org/10.1111/febs.15227>
- Rajaraman, R., Guernsey, D. L., Murali Rajaraman, & Rajaraman, S. R. (2006). *Cancer Cell International*, *6*(1), 25–25. <https://doi.org/10.1186/1475-2867-6-25>
- Roy, S., Subhashree Kumaravel, Sharma, A., Duran, C. L., Bayless, K. J., & Chakraborty, S. (2020). Hypoxic tumor microenvironment: Implications for cancer therapy. *Experimental Biology and Medicine*, *245*(13), 1073–1086. <https://doi.org/10.1177/1535370220934038>
- Ruan, Z., Yang, X., & Cheng, W. (2018). OCT4 accelerates tumorigenesis through activating JAK/STAT signaling in ovarian cancer side population cells. *Cancer Management and Research*, *Volume 11*, 389–399. <https://doi.org/10.2147/cmar.s180418>
- Safa, A. R. (2022). Drug and apoptosis resistance in cancer stem cells (CSCs): A puzzle with many pieces. *Cancer Drug Resistance*, *5*(4), 850–872. <https://doi.org/10.20517/cdr.2022.20>
- Sánchez-Martín, M., Arancha Rodríguez-García, Jesús Pérez-Losada, Sagrera, A., Read, A. F.,

- & Sánchez-García, I. (2002). SLUG (SNAI2) deletions in patients with Waardenburg disease. *Human Molecular Genetics*, *11*(25), 3231–3236. <https://doi.org/10.1093/hmg/11.25.3231>
- Sánchez-Martín, M., Jesús Pérez-Losada, Arancha Rodríguez-García, Belén González-Sánchez, Korf, B. R., Wolfgang Küster, Moss, C., Spritz, R. A., & Sánchez-García, I. (2003). Deletion of the SLUG (*SNAI2*) gene results in human piebaldism. *American Journal of Medical Genetics*, *122A*(2), 125–132. <https://doi.org/10.1002/ajmg.a.20345>
- Sasaki, N., Toshiyuki Ishiwata, Hasegawa, F., Masaki Michishita, Kawai, H., Matsuda, Y., Arai, T., Ishikawa, N., Aida, J., Kaiyo Takubo, & Toyoda, M. (2018). Stemness and anti-cancer drug resistance in ATP-binding cassette subfamily G member 2 highly expressed pancreatic cancer is induced in 3D culture conditions. *Cancer Science*, *109*(4), 1135–1146. <https://doi.org/10.1111/cas.13533>
- Schultz, C. W., Ranjan Preet, Dhir, T., Dixon, D. A., & Brody, J. R. (2020). Understanding and targeting the disease-related RNA binding protein human antigen R (HuR). *WIREs RNA*, *11*(3). <https://doi.org/10.1002/wrna.1581>
- Seberg, H., Eric Van Otterloo, & Cornell, R. F. (2017). Beyond MITF : Multiple transcription factors directly regulate the cellular phenotype in melanocytes and melanoma. *Pigment Cell & Melanoma Research*, *30*(5), 454–466. <https://doi.org/10.1111/pcmr.12611>
- Sensi, M., Catani, M., Castellano, G., Nicolini, G., Federica Alciato, Gabrina Tragni, Giuseppina De Santis, Bersani, I., GC Avanzi, Tomassetti, A., & Canevari, S. (2011). Human Cutaneous Melanomas Lacking MITF and Melanocyte Differentiation Antigens Express a Functional Axl Receptor Kinase. *Journal of Investigative Dermatology*, *131*(12), 2448–2457. <https://doi.org/10.1038/jid.2011.218>
- Shackleton, M., Quintana, E., Fearon, E. R., & Morrison, S. J. (2009). *Heterogeneity in Cancer: Cancer Stem Cells versus Clonal Evolution*. *138*(5), 822–829. <https://doi.org/10.1016/j.cell.2009.08.017>
- Shamsoon, K., Hiraki, D., Yoshida, K., Kiyofumi Takabatake, Hiroaki Takebe, Kenji Yokozeki, Horie, N., Fujita, N., Nisrina Ekayani Nasrun, Tatsuo Okui, Hitoshi Nagatsuka, Yoshihiro Abiko, Akihiro Hosoya, Saito, T., & Shimo, T. (2023). The Role of Hedgehog Signaling in the Melanoma Tumor Bone Microenvironment. *International Journal of Molecular Sciences*, *24*(10), 8862–8862. <https://doi.org/10.3390/ijms24108862>
- Sharifi-Rad, J., Quispe, C., Jayanta Kumar Patra, Yengkhom Disco Singh, Manasa Kumar Panda, Das, G., Charles Oluwaseun Adetunji, Olugbenga Samuel Michael, Oksana Sytar, Polito, L., Jelena Živković, Natália Cruz-Martins, Klimek-Szczykutowicz, M., Ekiert, H., Muhammad Iqbal Choudhary, Seyed Abdulmajid Ayatollahi, Bekzat Tynybekov, Farzad Kobarfard, Ana Covilca Muntean, & Ioana Grozea. (2021). Paclitaxel: Application in Modern Oncology and Nanomedicine-Based Cancer Therapy. *Oxidative Medicine and Cellular Longevity*, *2021*, 1–24. <https://doi.org/10.1155/2021/3687700>

- Sheikh, S., Ernst, D., & Keating, A. (2021). Prodrugs and prodrug-activated systems in gene therapy. *Molecular Therapy*, 29(5), 1716–1728. <https://doi.org/10.1016/j.ymthe.2021.04.006>
- Sigafoos, A. N., Paradise, B. D., & Fernandez-Zapico, M. E. (2021). Hedgehog/GLI Signaling Pathway: Transduction, Regulation, and Implications for Disease. *Cancers*, 13(14), 3410–3410. <https://doi.org/10.3390/cancers13143410>
- Skitzki, J. J., Repasky, E. A., & Evans, S. S. (2009). Hyperthermia as an immunotherapy strategy for cancer. *Current Opinion in Investigational Drugs (London, England : 2000)*, 10(6), 550–558. <https://www.ncbi.nlm.nih.gov/pmc/articles/PMC2828267/>
- Sneddon, J. B., & Werb, Z. (2007). Location, Location, Location: The Cancer Stem Cell Niche. *Cell Stem Cell*, 1(6), 607–611. <https://doi.org/10.1016/j.stem.2007.11.009>
- Sottocornola, R., & Cristina Lo Celso. (2012). Dormancy in the stem cell niche. *Stem Cell Research & Therapy*, 3(2). <https://doi.org/10.1186/scrt101>
- Stetler, R. A., Gan, Y., Zhang, W., Anthony Kian-Fong Liou, Gao, Y., Cao, G., & Chen, J. (2010). Heat shock proteins: Cellular and molecular mechanisms in the central nervous system. *Progress in Neurobiology*, 92(2), 184–211. <https://doi.org/10.1016/j.pneurobio.2010.05.002>
- Sun, J., Luo, Q., Liu, L., & Song, G. (2016). Liver cancer stem cell markers: Progression and therapeutic implications. *World Journal of Gastroenterology*, 22(13), 3547–3547. <https://doi.org/10.3748/wjg.v22.i13.3547>
- Takabatake, K., Shimo, T., Murakami, J., Anqi, C., Kawai, H., Yoshida, S., May Wathone Oo, Omori, H., Shintaro Sukegawa, Hidetsugu Tsujigiwa, Nakano, K., & Hitoshi Nagatsuka. (2019). The Role of Sonic Hedgehog Signaling in the Tumor Microenvironment of Oral Squamous Cell Carcinoma. *International Journal of Molecular Sciences*, 20(22), 5779–5779. <https://doi.org/10.3390/ijms20225779>
- Tang, M., J. Carlos Villaescusa, Sarah Xinwei Luo, Guitarte, C., Lei, S., Miyamoto, Y., Makoto Mark Taketo, Arenas, E., & Huang, E. J. (2010). Interactions of Wnt/ -Catenin Signaling and Sonic Hedgehog Regulate the Neurogenesis of Ventral Midbrain Dopamine Neurons. *The Journal of Neuroscience*, 30(27), 9280–9291. <https://doi.org/10.1523/jneurosci.0860-10.2010>
- Tang, S.-N., Fu, J., Nall, D., Rodova, M., Shankar, S., & Srivastava, R. K. (2011). Inhibition of sonic hedgehog pathway and pluripotency maintaining factors regulate human pancreatic cancer stem cell characteristics. *International Journal of Cancer*, 131(1), 30–40. <https://doi.org/10.1002/ijc.26323>
- Terragni, J., Nayak, G., Banerjee, S., Medrano, J.-L., Graham, J. G., Brennan, J. F., Sepulveda, S., & Cooper, G. M. (2011). The E-box Binding Factors Max/Mnt, MITF, and USF1 Act Coordinately with FoxO to Regulate Expression of Proapoptotic and Cell Cycle Control Genes by Phosphatidylinositol 3-Kinase/Akt/Glycogen Synthase Kinase 3 Signaling. *Journal of Biological Chemistry*, 286(42), 36215–36227. <https://doi.org/10.1074/jbc.m111.246116>

- Thankamony, A. P., Saxena, K., Murali, R., Mohit Kumar Jolly, & Nair, R. (2020). Cancer Stem Cell Plasticity – A Deadly Deal. *Frontiers in Molecular Biosciences*, 7. <https://doi.org/10.3389/fmolb.2020.00079>
- Toh, T. B., Lim, J., & Edward Kai-Hua Chow. (2017). Epigenetics in cancer stem cells. *Molecular Cancer*, 16(1). <https://doi.org/10.1186/s12943-017-0596-9>
- Toledo-Guzmán, M. E., Miguel Ibañez Hernández, Gómez-Gallegos, Á. A., & Ortiz-Sánchez, E. (2019). ALDH as a Stem Cell Marker in Solid Tumors. *Current Stem Cell Research & Therapy*, 14(5), 375–388. <https://doi.org/10.2174/1574888x13666180810120012>
- Tripathi, M. K., Misra, S., Khedkar, S. V., Hamilton, N., Irvin-Wilson, C. V., Sharan, C., Sealy, L., & Chaudhuri, G. (2005). Regulation of BRCA2 Gene Expression by the SLUG Repressor Protein in Human Breast Cells. *Journal of Biological Chemistry*, 280(17), 17163–17171. <https://doi.org/10.1074/jbc.m501375200>
- Vachtenheim, J., & Lubica Ondrušová. (2015). Microphthalmia-associated transcription factor expression levels in melanoma cells contribute to cell invasion and proliferation. *Experimental Dermatology*, 24(7), 481–484. <https://doi.org/10.1111/exd.12724>
- Valent, P., Sadovnik, I., Gregor Eisenwort, Bauer, K., Herrmann, H., Gleixner, K. V., Schulenburg, A., Rabitsch, W., Sperr, W. R., & Wolf, D. (2019). Immunotherapy-Based Targeting and Elimination of Leukemic Stem Cells in AML and CML. *International Journal of Molecular Sciences*, 20(17), 4233–4233. <https://doi.org/10.3390/ijms20174233>
- Vlčková, K., Jiri Réda, Lubica Ondrušová, Krayem, M., Ghanem Elias Ghanem, & Jiri Vachtenheim. (2016). GLI inhibitor GANT61 kills melanoma cells and acts in synergy with obatoclox. *International Journal of Oncology*, 49(3), 953–960. <https://doi.org/10.3892/ijo.2016.3596>
- Völker-Albert, M., Bronkhorst, A. J., Holdenrieder, S., & Imhof, A. (2020). Histone Modifications in Stem Cell Development and Their Clinical Implications. *Stem Cell Reports*, 15(6), 1196–1205. <https://doi.org/10.1016/j.stemcr.2020.11.002>
- Walcher, L., Kistenmacher, A.-K., Suo, H., Reni Kitte, Dluczek, S., Strauß, A., André-René Blaudszun, Tetyana Yevsa, Stephan, F., & Uta Kossatz-Boehlert. (2020). Cancer Stem Cells—Origins and Biomarkers: Perspectives for Targeted Personalized Therapies. *Frontiers in Immunology*, 11. <https://doi.org/10.3389/fimmu.2020.01280>
- Wang, E. C., & Wang, A. Z. (2013). Nanoparticles and their applications in cell and molecular biology. *Integrative Biology*, 6(1), 9–26. <https://doi.org/10.1039/c3ib40165k>
- Wang, J., Liu, X., Li, P., Wang, J., Yu, S., Zhong, X., Zhen Xing Gao, Yang, J., Jiang, Y., Zhou, X., & GengYang. (2022). Long noncoding RNA HOTAIR regulates the stemness of breast cancer cells via activation of the NF-κB signaling pathway. *Journal of Biological Chemistry*, 298(12), 102630–102630. <https://doi.org/10.1016/j.jbc.2022.102630>
- Wang, L., Zuo, X., Xie, K., & Wei, D. (2017). The Role of CD44 and Cancer Stem Cells. *Methods in Molecular Biology*, 31–42. https://doi.org/10.1007/978-1-4939-7401-6_3

- Wang, W., Quan, Y., Fu, Q., Liu, Y., Liang, Y., Wu, J., Yang, G., Luo, C., Ouyang, Q., & Wang, Y. (2014). Dynamics between Cancer Cell Subpopulations Reveals a Model Coordinating with Both Hierarchical and Stochastic Concepts. *PLOS ONE*, *9*(1), e84654–e84654. <https://doi.org/10.1371/journal.pone.0084654>
- Wang, Y., & Tong, M. (2023). Protein Posttranslational Modification in Stemness Remodeling and Its Emerging Role as a Novel Therapeutic Target in Gastrointestinal Cancers. *International Journal of Molecular Sciences*, *24*(11), 9173–9173. <https://doi.org/10.3390/ijms24119173>
- Wang, Z., Fei, X., Dai, X., Chen, H., Tian, H., Wang, A., Dong, J., & Huang, Q. (2015). Differentiation of Glioma Stem Cells and Progenitor Cells into Local Host Cell-Like Cells: A Study Based on Choroidcarcinoma Differentiation of Choroid Plexus of GFP Transgenic Nude Mouse. *Cancer Biotherapy and Radiopharmaceuticals*, *30*(5), 225–232. <https://doi.org/10.1089/cbr.2014.1722>
- Wei, Z., Zhou, Y., Wang, R., Wang, J., & Chen, Z. (2022). Aptamers as Smart Ligands for Targeted Drug Delivery in Cancer Therapy. *Pharmaceutics*, *14*(12), 2561–2561. <https://doi.org/10.3390/pharmaceutics14122561>
- Wellbrock, C., & Imanol Arozarena. (2015). Microphthalmia-associated transcription factor in melanoma development andMAP-kinase pathway targeted therapy. *Pigment Cell & Melanoma Research*, *28*(4), 390–406. <https://doi.org/10.1111/pcmr.12370>
- Weng, J., Han, X., Liu, K., Yang, J., Wei, S., Zhang, Y., Zeng, F., Yang, L., Shen, L., & Gao, Y. (2019). CD44 3'-Untranslated Region Functions as a Competing Endogenous RNA to Enhance NK Sensitivity of Liver Cancer Stem Cell by Regulating ULBP2 Expression. *International Journal of Biological Sciences*, *15*(8), 1664–1675. <https://doi.org/10.7150/ijbs.35216>
- Wicha, M. S., Liu, S., & Dontu, G. (2006). Cancer Stem Cells: An Old Idea—A Paradigm Shift. *Cancer Research*, *66*(4), 1883–1890. <https://doi.org/10.1158/0008-5472.can-05-3153>
- Willingham, S. B., Jens Peter Volkmer, Gentles, A. J., Sahoo, D., Piero Dalerba, Mitra, S., Wang, J., Contreras-Trujillo, H., Martin, R. K., Cohen, J. D., Lovelace, P., Scheeren, F. A., Chao, M. P., Weiskopf, K., Tang, C., Anne Kathrin Volkmer, Naik, T. J., Storm, T. A., Mosley, A., & Edris, B. (2012). The CD47-signal regulatory protein alpha (SIRPα) interaction is a therapeutic target for human solid tumors. *Proceedings of the National Academy of Sciences of the United States of America*, *109*(17), 6662–6667. <https://doi.org/10.1073/pnas.1121623109>
- Winklmayr, M., Schmid, C., Laner-Plamberger, S., Kaser, A., Aberger, F., Eichberger, T., & Anna-Maria Frischauf. (2010). Non-consensus GLI binding sites in Hedgehog target gene regulation. *BMC Molecular Biology*, *11*(1). <https://doi.org/10.1186/1471-2199-11-2>
- Witt, A. E., Lee, C. W., Lee, T. I., Azzam, D. J., Wang, B., Corrado Caslini, Fabio Petrocca, Grosso, J., Jones, M., Cohick, E., Gropper, A. B., Claes Wahlestedt, Richardson, A. L., Ramin Shiekhattar, Young, R. A., & Ince, T. A. (2016). Identification of a cancer stem

- cell-specific function for the histone deacetylases, HDAC1 and HDAC7, in breast and ovarian cancer. *Oncogene*, 36(12), 1707–1720. <https://doi.org/10.1038/onc.2016.337>
- Wu, A., Zhang, S., Liu, J., Huang, Y., Deng, W., Shu, G., & Yin, G. (2020). Integrated Analysis of Prognostic and Immune Associated Integrin Family in Ovarian Cancer. *Frontiers in Genetics*, 11. <https://doi.org/10.3389/fgene.2020.00705>
- Wu, X., Li Shu Zhang, Toombs, J. E., Yi Chun Kuo, Piazza, J. T., Rubina Tuladhar, Barrett, Q., Chih Wei Fan, Zhang, X., Walensky, L. D., Kool, M., Cheng, S. Y., Brekken, R. A., Opferman, J. T., Green, D. R., Tudor Moldoveanu, & Lum, L. (2017). Extra-mitochondrial prosurvival BCL-2 proteins regulate gene transcription by inhibiting the SUFU tumour suppressor. *Nature Cell Biology*, 19(10), 1226–1236. <https://doi.org/10.1038/ncb3616>
- Yamashita, T., Honda, M., Nakamoto, Y., Baba, M., Kouki Nio, Hara, Y., Zeng, S., Hayashi, T., Kondo, M., Hajime Takatori, Yamashita, T., Eishiro Mizukoshi, Ikeda, H., Zen, Y., Takamura, H., Xin Wei Wang, & Kaneko, S. (2013). Discrete nature of EpCAM⁺ and CD90⁺ cancer stem cells in human hepatocellular carcinoma. *Hepatology*, 57(4), 1484–1497. <https://doi.org/10.1002/hep.26168>
- Yang, Y., Li, X., Wang, T., Guo, Q., Xi, T., & Zheng, L. (2020). Emerging agents that target signaling pathways in cancer stem cells. *Journal of Hematology & Oncology*, 13(1). <https://doi.org/10.1186/s13045-020-00901-6>
- Yoon, C., Jun Lü, Yi, B. C., Chang, K. C., M. Celeste Simon, Ryeom, S., & Yoon, S. S. (2021). PI3K/Akt pathway and Nanog maintain cancer stem cells in sarcomas. *Oncogenesis*, 10(1). <https://doi.org/10.1038/s41389-020-00300-z>
- Yun, Z., & Lin, Q. (2013). Hypoxia and Regulation of Cancer Cell Stemness. *Advances in Experimental Medicine and Biology*, 41–53. https://doi.org/10.1007/978-1-4614-5915-6_2
- Zeng, Z., Fu, M., Hu, Y., Wei, Y., Wei, X., & Luo, M. (2023). Regulation and signaling pathways in cancer stem cells: implications for targeted therapy for cancer. *Molecular Cancer*, 22(1). <https://doi.org/10.1186/s12943-023-01877-w>
- Zhang, J., Kale, V., & Chen, M. (2014). Gene-Directed Enzyme Prodrug Therapy. *The AAPS Journal*, 17(1), 102–110. <https://doi.org/10.1208/s12248-014-9675-7>
- Zhang, Q., Han, Z., Zhu, Y., Chen, J., & Li, W. (2020). The Role and Specific Mechanism of OCT4 in Cancer Stem Cells: A Review. *International Journal of Stem Cells*, 13(3), 312–325. <https://doi.org/10.15283/ijsc20097>
- Zhang, W., Sui, Y., Ni, J., & Yang, T. (2016). Insights into the *Nanog* gene: A propeller for stemness in primitive stem cells. *International Journal of Biological Sciences*, 12(11), 1372–1381. <https://doi.org/10.7150/ijbs.16349>
- Zhao, W., Li, Y., & Zhang, X. (2017). Stemness-related markers in cancer. *Cancer Translational Medicine*, 3(3), 87–87. https://doi.org/10.4103/ctm.ctm_69_16
- Zhao, Z., Lu, P., Zhang, H., Xu, H., Gao, N., Li, M., & Liu, C. (2014). Nestin positively

regulates the Wnt/ β -catenin pathway and the proliferation, survival and invasiveness of breast cancer stem cells. *Breast Cancer Research*, 16(4). <https://doi.org/10.1186/s13058-014-0408-8>

Zhu, Q., Liang, P., Chu, C., Zhang, A., & Zhou, W. (2022). Protein sumoylation in normal and cancer stem cells. *Frontiers in Molecular Biosciences*, 9. <https://doi.org/10.3389/fmolb.2022.1095142>

Zhu, X., Chen, H., Gao, C., Zhang, X., Jiang, J., Zhang, Y., Fang, J., Zhao, F., & Chen, Z. (2020). Energy metabolism in cancer stem cells. *World Journal of Stem Cells*, 12(6), 448–461. <https://doi.org/10.4252/wjsc.v12.i6.448>

VII APPENDIX

PERMISSIONS TO REPRINT PUBLICATIONS

Publication I:

Horák, P., Kreisingerová, K., Réda, J., Ondrušová, L., Balko, J., Vachtenheim Jr., J., Žáková, P. & Vachtenheim J. (2023) **The Hedgehog/GLI signaling pathway activates transcription of Slug (Snail2) in melanoma cells.** *Oncology reports*, 49(75).

Oncology Reports - Spandidos Publications <or@spandidos-publications.com>
to me

May 19, 2023, 9:38 AM

Dear Author,

Thank you for your inquiry and for your interest in our Journals.

Permission is hereby granted for the reproduction of the below mentioned manuscript, for the purpose outlined in your message.

The original work should be cited.

Please do not hesitate to contact us for anything further.

Yours sincerely,
Spandidos Publications

From: Pavel Horák [mailto:ppavel.hhorak@gmail.com]

Sent: Wednesday, May 17, 2023 9:44 PM

To: contact@spandidos-publications.com

Subject: Permission to reprint (article 290065)

Dear Spandidos Support Team!

Our group recently published the article: *The Hedgehog/GLI signaling pathway activates transcription of Slug (Snail2) in melanoma cells* in *Oncology reports* (Reference: 290065).

Now I am kindly asking you for permission to reprint this article in my doctoral thesis. The permission would surely help me to defend my thesis as this article is basically the output of my research.

The thesis will be submitted to 1st Faculty of Medicine of the Charles University, Prague and will be freely accessible in the university on-line depository.

Kind regards,

Pavel Horák, MSc.

Publication II:

Réda, J., Vachtenheim, J., Vlčková, K., **Horák, P.**, & Ondrušová, L. (2018). **Widespread expression of hedgehog pathway components in a large panel of human tumor cells and inhibition of tumor growth by GANT61: Implications for cancer therapy.** *International Journal of Molecular Sciences*, 19(9).

publisher@mdpi.com
to me

Fri, May 19, 2023, 4:55 PM

Dear Pavel,

Thank you for your email.

No special permission is required to reuse or reprint all or part of an article published by MDPI, including figures and tables. For articles published under an open access Creative Common CC BY license, any part of the article may be reused without permission, provided that the original article is clearly cited. Reuse of an article does not imply endorsement by the authors or MDPI.

Please Note: Some articles (especially Reviews) may contain figures, tables or text taken from other publications, for which MDPI does not hold the copyright or the right to re-license the published material. Please note that you should speak with the original copyright holder (usually the original publisher or authors), to enquire about whether or not this material can be re-used.

For further information, please visit: <https://www.mdpi.com/openaccess>.

Please let us know if you have any further questions!

Kind regards,

Megan Moeschlin
Administrative Assistant

MDPI AG
St. Alban-Anlage 66
4052 Basel, Switzerland
<https://www.mdpi.com/>

From: noreply@mdpi.com <noreply@mdpi.com>

Sent: Wednesday, 17 May 2023 21:03

To: reprints@mdpi.com

Subject: MDPI Contact Form: Permission to reprint article (Widespread expression of hedgehog pathway components in a large panel of human tumor cells and inhibition of tumor growth by GANT61: Implications for cancer therapy)

Dear all,

The following message has been sent to you from the [mdpi.com](https://www.mdpi.com) contact form.

Received: 17 May 2023

Creator: Pavel Horak

Email: ppavel.hhorak@gmail.com

Query: Article reprints

Dear MDPI support Team!

Our group has published article titled Widespread expression of hedgehog pathway components in a large panel of human tumor cells and inhibition of tumor growth by GANT61: Implications for cancer therapy (doi: 10.3390/ijms19092682.).

Now I am kindly asking you for permission to reprint this article in my doctoral thesis. The permission would surely help me to defend my thesis as this article is one of the cornerstones of the output of my doctoral research.

The thesis will be submitted to 1st Faculty of Medicine of the Charles University, Prague and will be freely accessible in the university on-line depository.

Kind regards,

Pavel Horák, MSc.

Publication III:

Vlčková, K., Vachtenheim, J., Réda, J., **Horák, P.**, & Ondrušová, L. (2018). **Inducibly decreased MITF levels do not affect proliferation and phenotype switching but reduce differentiation of melanoma cells.** *Journal of Cellular and Molecular Medicine*, 22(4).

This publication was published in International Journal of Molecular Sciences and is an open access article distributed under the terms and conditions of the Creative Commons Attribution(CC BY) license (<https://creativecommons.org/licenses/by/4.0/>), which allows to copy and redistribute the material in any medium or format.

©2018 by the authors. Licensee MDPI, Basel, Switzerland.

The publication is available online at: <https://www.mdpi.com/1422-0067/19/9/2682>

I declare that no changes were made in the material.

Publication IV:

Habel, N., El-Hachem, N., Soysouvanh, Hadhiri-Bziouche, Giuliano, S., Nguyen, **Horak, P.**, Gay, A.S., Debayle, D., Nottet, N., Beranger, G., Paillerets, B.B., Bertolotto, C. & Ballotti, R. (2021). **FBXO32 links ubiquitination to epigenetic reprogramming of melanoma cells.** *Cell Death and Differentiation* 28:1837–1848

Journalpermissions <journalpermissions@springernature.com>
to me

Thu, May 18, 2023,
12:32 PM

Dear Pavel,

Thank you for your recent email. Springer Nature journal authors may reuse their article's Version of Record, in whole or in part, in their own thesis without any additional permission required, provided the original publication is properly cited and includes the following acknowledgement "Reproduced with permission from Springer Nature". This includes the right to make a copy of your thesis available in your academic institution's repository, or other repository required by your awarding institution. For more information please visit see our FAQs [here](#).

If your awarding institution requires formal permission, please locate your article on either [nature.com](#) or [link.springer.com](#). At the end of the article page you will find the 'Reprints and Permissions' link; clicking on this will redirect you to our CCC RightsLink service where you may input the details of your request. **Please ensure you select "reuse in a thesis/dissertation" as your type of use, and to tick the box that asks whether you are the author.**

During the process, you will need to set up an account with RightsLink. You will be able to use your RightsLink account in the future to request permissions from Springer Nature and from other participating publishers. RightsLink will also email you confirmation of your request with a link to your printable licence.

If you have any further questions, please do not hesitate to get in touch.

Kind Regards,

Elise

Elise Lagden

Permissions Executive

SpringerNature

The Campus, 4 Crinan Street, London N1 9XW, United Kingdom

T: [+442078434596](tel:+442078434596)

E elise.lagden@springernature.com

<http://www.nature.com>

<http://www.springernature.com>

From: Pavel Horák <ppavel.hhorak@gmail.com>

Sent: 17 May 2023 20:19

To: Journalpermissions <Journalpermissions@springernature.com>

Subject: Permission to reprint (Paper #CDD-20-0834RR)

[External - Use Caution]

Dear Cell Death and Differentiation regulatory Team!

Our group has published the article: *FBXO32 links ubiquitination to epigenetic reprogramming of melanoma cells* in your journal. (doi: 10.1038/s41418-020-00710-x)

Now I am kindly asking you for permission to reprint this article in my doctoral thesis. The permission would surely help me to defend my thesis as this article is one of the cornerstones of the output of my doctoral research.

The thesis will be submitted to 1st Faculty of Medicine of the Charles University, Prague and will be freely accessible in the university on-line depository.

Kind regards,

Pavel Horák, MSc.

Publication V:

Kreisingerová K, Ondrušová L., Horák P, Vachtenheim J. (2020) **Význam aberantně aktivované dráhy Hedgehog/Gli pro nádorovou progresi.** *Klinická Onkologie*, 33(3):177-183.

Vuk Fait <faitvuk@me.com>
to me

Tue, Feb 6, 6:53 PM

Translate to English

Dobrý den,

publikované práce jsou v současnosti pravidelnou součástí disertací na není zapotřebí se obávat jejich přetisknutí do disertační práce - nejedná se o neoprávněné šíření.

Tedy, pochopitelně práci kopii použijte, je pochopitelně nutno., aby bylo zcela jasno, v jakém časopise jste publikoval.

S pozdravem V. Fait

Začátek přeposílané zprávy:

Od: "Ing. Petra Polsen" <petra.polsen@carecomm.cz>

Předmět: Re: **Žádost o povolení otištění článku v Disertační práci**

Datum: 5. února 2024 v 12:34:28 SEČ

Komu: Pavel Horák <ppavel.hhorak@gmail.com>

Kopie: Vuk Fait <faitvuk@me.com>

Vážený pane magistře,
děkuji za Vaši zprávu.

Záležitost předávám doc. Faitovi, který je kompetentní v této záležitosti rozhodnout.

Se srdečným pozdravem,

Petra Polsen

Od: Pavel Horák <ppavel.hhorak@gmail.com>

Odesláno: pondělí 5. února 2024 10:22

Komu: Ing. Petra Polsen <petra.polsen@carecomm.cz>

Předmět: Žádost o povolení otištění článku v Disertační práci

Vážená paní Polsen,

jsem spoluautorem článku "Význam aberantně aktivované dráhy Hedgehog/GLI pro nádorovou progresi", publikovaném v časopise *Klinická Onkologie* (DOI: [10.14735/amko2020177](https://doi.org/10.14735/amko2020177)). V současné době dokončuji práci na své Disertační práci a rád bych se Vás dotázal, zda mohu tento článek ve své práci otisknout?

Práce bude vydaná pod záštitou 1. Lékařské Fakulty Univerzity Karlovy a bude přístupná v online repozitáři UK.

Kontakt na Vás jsem našel na stránkách časopisu v sekci "instrukce pro autory". Pokud by však bylo vhodné v této záležitosti kontaktovat někoho jiného, mohla byste mi, prosím, doporučit odpovědnou osobu?

S přáním příjemného zbytku dne,

Pavel Horák